Report Title:

Coal/Polymer Coprocessing with Efficient Use of Hydrogen

Report Type: FINAL	Reporting Period Start Date: 09/01/96 End Date: 08/31/00
Principal Author(s): Dr. Linda J. Broadbelt, Matthew J. De Witt and Hsi-Wu Wong	
Report Issue Date: 09/30/00	DOE Award No.: DE-FG22-96PC96204

Submitting Organization(s)

Name & Address

Northwestern University
2145 Sheridan Road
Department of Chemical Engineering
Evanston, IL 60208

(1)

(2)

(3)

(4)

(5)

Disclaimer

Abstract

The final project period was devoted to investigating the binary mixture pyrolysis of polypropylene and polystyrene. Their interactions were assessed in order to provide a baseline for experiments with multicomponent mixtures of polymers with coal. Pyrolysis of polypropylene, polystyrene and their binary mixture was investigated at temperatures of 350°C and 420°C with reaction times from 1 to 180 minutes. Two different loadings, 10 mg and 20 mg, were studied for neat polypropylene and polystyrene to assess the effect of total pressure on product yields and selectivities. For neat pyrolysis of polypropylene, total conversion was much higher at 420°C, and no significant effect of loading on the total conversion was observed. Four classes of products, alkanes, alkenes, dienes, and aromatic compounds, were observed, and their distribution was explained by a typical free radical mechanism. For neat polystyrene pyrolysis, conversion reached approximately 75% at 350°C, while at 420°C the conversion reached a maximum around 90% at 10 minutes and decreased at longer times because of condensation reactions. The selectivities to major products were slightly different for the two different loadings due to the effect of total reaction pressure on secondary reactions. For binary mixture pyrolysis, the overall conversion was higher than the average of the two neat cases. The conversion of polystyrene remained the same, but a significant enhancement in the polypropylene conversion was observed. This suggests that the less reactive polypropylene was initiated by polystyrene-derived radicals. These results are summarized in detail in an attached manuscript that is currently in preparation. The other results obtained during the lifetime of this grant are documented in the set of attached manuscripts.

Table Of Contents

I. Executive Summary

In this project period, the binary mixture pyrolysis of polypropylene and polypropylene was investigated. These experiments provided baseline information to which the reactions of multicomponent mixtures of polymers with coal model compounds and coal could be compared. The conversion of polypropylene was enhanced in the presence of polystyrene with little change in product selectivities, suggesting that polystyrene-derived radicals initiated the decomposition of polypropylene through hydrogen transfer. This enhancement was similar to that we observed earlier for reactions of polyethylene and polyethylene model compounds with a coal model compound. In all these systems, modeling work predicted that the rate of hydrogen abstraction from the more intractable component is less favorable than self-hydrogen abstraction by the more reactive component. This body of work suggests that phase behavior and physical effects leading to inhomogeneities in local concentration may govern interactions between multicomponents.

II. Introduction

Inadequacies of current recovery and disposal methods for mixed plastic wastes drive the exploration of viable strategies for plastics resource recovery. The combination of diminishing landfill space and increasing usage of plastic products poses a significant dilemma, since current recovery methods are costly and ill-suited to handle contaminants. Coprocessing of polymeric waste with other materials may provide potential solutions to the deficiencies of current resource recovery methods, including unfavorable process economics. By incorporating plastic waste as a minor feed into an existing process, variations in supply and composition could be mediated, permitting continuous operation. One attractive option is the coprocessing of polymeric waste with coal under direct liquefaction conditions, allowing for simultaneous conversion of both feedstocks into high-valued products. Catalyst-directed coliquefaction of coal and polymeric materials not only has attractive environmental implications but also has the potential to enhance the economic viability of traditional liquefaction processes. By exploiting the higher H/C ratio of the polymeric material and using it as a hydrogen source, the overall process demand for molecular hydrogen and hydrogen donor solvents may be reduced. However, polymeric waste is inherently a mixture of different types of plastics. Therefore, it is beneficial to investigate not only reactions of single component polymers with coal and coal mimics but also to examine the reactions of multicomponent polymer feeds. As detailed in the attached manuscripts, the project has used both experiments and modeling to help understand the interactions between coal and multicomponent mixtures of polymers.

III. Methodology

Our experimental methodology centered on using well-defined polymeric feedstocks, polymeric model compounds and coal mimics and obtaining detailed product information. The experimental approach is detailed in the attached manuscripts:

De Witt, M.J. and Broadbelt, L.J., "Binary Interactions Between Tetradecane and 4-(1-Naphthylmethyl) Bibenzyl During Low and High Pressure Pyrolysis", *Energy & Fuels*, **1999**, *13*(5), 969-983.

De Witt, M.J. and Broadbelt, L.J., "Binary Interactions Between High Density Polyethylene and 4-(1-Naphthylmethyl) Bibenzyl During Low Pressure Pyrolysis", *Energy & Fuels*, **1999**, *14(2)*, 448-458.

Wong, H.-W. and Broadbelt, L.J., "Tertiary Resource Recovery from Waste Polymers: Polypropylene and Polystyrene", in preparation for *Ind. Eng. Chem. Res.*, **2000**.

De Witt, M.J. and Broadbelt, L.J., "Coprocessing of Polymeric Waste with Coal: Reaction of Polyethylene and Coal Model Compounds", Preprints of the American Chemical Society, Division of Fuel Chemistry, **1997**, *42*(1), 38-42.

Wong, H.-W., Kruse, T.M., Woo, O.S. and Broadbelt, L.J., "Tertiary Resource Recovery from Waste Polymers via Pyrolysis: Polypropylene", Preprints of the American Chemical Society, Division of Fuel Chemistry, **2000**.

Our modeling work was based on development of algorithms for computer generation of reaction mechanisms. By building detailed kinetic mechanisms of model components, we were able to understand the nature of the interactions between polymers and coal mimics. Our modeling methodology is described in the attached manuscripts:

De Witt, M.J., Dooling, D.J. and Broadbelt, L.J., "Computer Generation of Reaction Mechanisms Using Quantitative Rate Information: Application to Long-Chain Hydrocarbon Pyrolysis", *Ind. Eng. Chem. Res.*, **2000**, *39(7)*, 2228-2237.

De Witt, M.J., Dooling, D.J. and Broadbelt, L.J., "Application of Computer Generation of Reaction Mechanisms Using Quantitative Rate Information to Hydrocarbon Pyrolysis", Preprints of the American Chemical Society, Division of Fuel Chemistry, **1999**, *44*(3), 476-478.

De Witt, M.J., Dooling, D.J. and Broadbelt, L.J., "Computer Generation of Reaction Mechanisms Using Quantitative Rate Information: Application to Long-Chain Hydrocarbon Pyrolysis", Proceedings of the American Institute of Chemical Engineers, Houston, TX, **1999**.

IV. Results and Discussion

All experimental results are presented and discussed in the following manuscripts which are attached:

De Witt, M.J. and Broadbelt, L.J., "Binary Interactions Between Tetradecane and 4-(1-Naphthylmethyl) Bibenzyl During Low and High Pressure Pyrolysis", *Energy & Fuels*, **1999**, *13*(5), 969-983.

De Witt, M.J. and Broadbelt, L.J., "Binary Interactions Between High Density Polyethylene and 4-(1-Naphthylmethyl) Bibenzyl During Low Pressure Pyrolysis", *Energy & Fuels*, **1999**, *14(2)*, 448-458.

Wong, H.-W. and Broadbelt, L.J., "Tertiary Resource Recovery from Waste Polymers: Polypropylene and Polystyrene", in preparation for *Ind. Eng. Chem. Res.*, **2000**.

De Witt, M.J. and Broadbelt, L.J., "Coprocessing of Polymeric Waste with Coal: Reaction of Polyethylene and Coal Model Compounds", Preprints of the American Chemical Society, Division of Fuel Chemistry, **1997**, *42*(1), 38-42.

Wong, H.-W., Kruse, T.M., Woo, O.S. and Broadbelt, L.J., "Tertiary Resource Recovery from Waste Polymers via Pyrolysis: Polypropylene", Preprints of the American Chemical Society, Division of Fuel Chemistry, **2000**.

All modeling results obtained during the period of this grant are summarized in the Ph.D. dissertation of Matthew J. De Witt, "Elucidation of the Primary Reaction Pathways and Degradation Mechanism During Coprocessing of Polymeric Waste with Coal", 1999, and the following manuscripts that are attached:

De Witt, M.J., Dooling, D.J. and Broadbelt, L.J., "Computer Generation of Reaction Mechanisms Using Quantitative Rate Information: Application to Long-Chain Hydrocarbon Pyrolysis", *Ind. Eng. Chem. Res.*, **2000**, *39(7)*, 2228-2237.

De Witt, M.J., Dooling, D.J. and Broadbelt, L.J., "Application of Computer Generation of Reaction Mechanisms Using Quantitative Rate Information to Hydrocarbon Pyrolysis", Preprints of the American Chemical Society, Division of Fuel Chemistry, **1999**, *44*(3), 476-478.

De Witt, M.J., Dooling, D.J. and Broadbelt, L.J., "Computer Generation of Reaction Mechanisms Using Quantitative Rate Information: Application to Long-Chain Hydrocarbon Pyrolysis", Proceedings of the American Institute of Chemical Engineers, Houston, TX, **1999**.

V. Conclusions

Recent investigations have demonstrated the feasibility of coprocessing of coal with polymers. In our work, feedstock interactions were unraveled using model compound mimics of both coal and polyethylene. Interactions in a binary mixture of polymers representative of mixed plastic waste were investigated. Both experiments and modeling work were carried out, and the major conclusions from each phase of our study are summarized here.

In binary mixtures of tetradecane and 4-(1-naphthylmethyl) bibenzyl (NBBM), the conversion of tetradecane increased while the selectivity to primary products of NBBM pyrolysis was enhanced. These observations were attributed to the stabilization of NBBM-derived radicals through hydrogen abstraction from tetradecane in the gas phase, which in turn increased the rate of tetradecane conversion. At low pressures, the initial loading of each reactant and the overall loadings were found to affect both the conversion of tetradecane and the overall product distribution during coprocessing. As the NBBM to tetradecane ratio was raised, only a slight difference in reactant conversions was observed, but there were significant changes in product selectivities. NBBM showed increased selectivity towards secondary products, while n-alkanes were formed in higher yields for tetradecane degradation. The higher proportion of NBBM resulted in an increase of self-interactions, which resulted in a larger quantity of retrograde condensation reactions. The higher loadings of NBBM also yielded larger tetradecane-derived radical populations within the system, leading to a shift in the products towards longer paraffins. The increase in high molecular weight paraffin yields was attributed to a relative reduction of repeated unimolecular radical transformations with increasing reactant loadings. Increasing the initial charge of both reactants resulted in a significant enhancement of tetradecane reactivity. The primary product yields from NBBM were essentially identical when compared to the reactions conducted with the same reactant ratio but lower total loading. However, the values were higher than those observed for the reactions conducted with a larger ratio of NBBM to tetradecane. These effects on conversions and selectivities were attributed to an increase in both tetradecane-NBBM and tetradecane-tetradecane reactions at higher concentrations.

As the overall system pressure was increased, small changes in the relative rates of competing reaction pathways for NBBM and tetradecane decomposition were observed. For neat pyrolysis of tetradecane at high pressures of an inert gas, the yield of normal paraffins was increased at the expense of lighter hydrocarbons and α-olefins. These observations were attributed to enhancement in the rate of bimolecular reactions for tetradecane-derived radicals due to the ability of high concentrations of inert molecules to facilitate energy transfer and to promote "cage" effects. With respect to neat NBBM-derived products, there was an increase in toluene formation at high pressures. It is likely that this occurred mainly through recombination of radical species of NBBM and 1-methyl-4-(1-naphthylmethyl)benzene, or radical addition of a 1-methyl-4-(1-naphthylmethyl)benzene radical to 1-(2-phenylethenyl)-4-(1-naphthylmethyl)benzene, and subsequent cleavage of a benzyl radical. The rates for these reactions were enhanced at high pressures due to the phase behavior of the system. For binary mixture reactions at high pressures,

the favorable interactions observed at low pressures were still realized, with only slight enhancement of paraffin yields and constant yields of toluene being observed.

Binary mixture reactions employing HDPE and NBBM demonstrated that the feedstock synergism that was observed during reactions with tetradecane and NBBM was still obtained. There was an increase in selectivity to primary products of the coal model compound with a significant reduction in the formation of secondary and tertiary products. The major difference in the product trends for reactions with the polymer, though, was that there was initially a minimal enhancement or inhibition in the formation of primary products of NBBM, depending upon reactant loadings, followed by subsequent enhancement. This observation, in addition to the reduced selectivity to secondary and tertiary products of NBBM as compared to the model compound studies, was primarily due to the differences in the phase behavior in the reaction system during coprocessing with HDPE. In this study, the high proportion of HDPE in the liquid phase induced diffusion limitations in the system which resulted in a slight reduction in the rate of NBBM degradation, but also minimized NBBM self-reactions by promoting reactions with the surrounding polymer. However, the HDPE-NBBM interactions initially led to alternative reaction pathways for the coal-derived radicals to form products which could not be identified and quantified. These products eventually underwent degradation themselves, though, resulting in significantly enhanced selectivities for primary products at longer reaction times. Therefore, the increase in selectivity to primary NBBM products observed during previous studies was still realized, but as an added benefit, there was a significant reduction in the formation of NBBM ipso-substitution products.

The effects of coprocessing on the HDPE-derived product yields were similar to those observed during studies employing tetradecane, where a significant increase in the yields of high molecular weight paraffins at the expense of the full range of α-olefins was observed. The changes were more marked for reactions with the polymer, though, which were attributed to the occurrence of additional bimolecular reactions in the liquid phase which resulted in the formation of *n*-alkanes and consumption of α-olefins. Increasing the relative loadings of the components only slightly altered the product selectivities for NBBM but resulted in enhanced yields of longer alkanes at the expense of α-olefins. These observations were consistent with increasing the overall polymer loading during neat pyrolysis.

Overall, the degradation mechanisms of HDPE and tetradecane are similar for both neat pyrolysis and reaction in the presence of NBBM. By employing the information obtained from previous model compound studies, it was possible to deconvolute the complicated feedstock interactions and identify the relevant reaction pathways during reactions employing the polymer. Therefore, the model compound reactions that were previously carried out provided valuable insight and guidance when reactions with a more complicated feedstock were performed.

To complement the experimental studies, a mechanistic model of low pressure tetradecane pyrolysis was constructed using algorithms for automated model construction and a rate-based generation criterion. Novel modifications were made to the core algorithmic components in this work to improve and broaden the rate-based approach. The major alterations were the use of time rather than conversion as the controlling iteration and termination variable, the new definition for the characteristic rate of change in the system, and the use of thermodynamic data to impose thermodynamic consistency between forward and reverse reactions. For the investigation of low pressure tetradecane pyrolysis, the rate-based model construction was successfully employed to produce a compact model with essential chemical detail. Once constructed, the model was able to accurately fit experimental data from two different reaction temperatures with no adjustment to the activation energies for any reactions. Only frequency factors were permitted to vary, and the final optimized values were consistent with literature values for each respective reaction family. Once rate parameters were determined, the mechanistic model was able to accurately predict reactant conversions and product yields for varying reaction conditions with no adjustments to the optimized

rate parameters. Both relative trends and the actual values were predicted correctly over a wide range of reactant conversions and initial reactant loadings.

The pyrolysis of polystyrene and polypropylene, neat and in binary mixtures, was investigated. The total conversion of polypropylene during pyrolysis at 420°C in a batch reactor reached around 60%, whereas at 350°C it reached around 2.5%. Four kinds of products were observed during polypropylene pyrolysis – alkanes, alkenes, dienes, and aromatic compounds. The product distribution also showed that most alkenes appeared in the form of C_{3n}, alkanes in the form of C_{3n-1}, and dienes in the form of C_{3n-2}. This product distribution can be explained by the typical free radical mechanism. Polystyrene degraded in 10 minutes at 420°C, and condensation products were observed at longer times. At 350°C, the conversion of polystyrene pyrolysis reached around 75%. During binary pyrolysis of the two polymers, the overall conversion was higher than the average of the neat cases at both temperatures. The conversion of polystyrene in binary reactions was similar to that of the neat cases. However, the conversion of polypropylene in binary reactions was enhanced by the presence of polystyrene.

VI. Manuscripts, Presentations and Publications

De Witt, M.J. and Broadbelt, L.J., "Binary Interactions Between Tetradecane and 4-(1-Naphthylmethyl) Bibenzyl During Low and High Pressure Pyrolysis", *Energy & Fuels*, **1999**, *13*(5), 969-983. (attached)

De Witt, M.J. and Broadbelt, L.J., "Binary Interactions Between High Density Polyethylene and 4-(1-Naphthylmethyl) Bibenzyl During Low Pressure Pyrolysis", *Energy & Fuels*, **1999**, *14(2)*, 448-458. (attached)

De Witt, M.J., Dooling, D.J. and Broadbelt, L.J., "Computer Generation of Reaction Mechanisms Using Quantitative Rate Information: Application to Long-Chain Hydrocarbon Pyrolysis", *Ind. Eng. Chem. Res.*, **2000**, *39(7)*, 2228-2237. (attached)

Broadbelt, L.J., "Catalytic Resource Recovery From Waste Polymers", Invited review article, *Catalysis*, Vol. 14, Royal Society of Chemistry, **1999,** 110-147. (attached)

Wong, H.-W. and Broadbelt, L.J., "Tertiary Resource Recovery from Waste Polymers: Polypropylene and Polystyrene", in preparation for *Ind. Eng. Chem. Res.*, **2000**. (attached)

De Witt, M.J. and Broadbelt, L.J., "Coprocessing of Polymeric Waste with Coal: Reaction of Polyethylene and Coal Model Compounds", Preprints of the American Chemical Society, Division of Fuel Chemistry, **1997**, *42*(1), 38-42. (attached)

De Witt, M.J., Dooling, D.J. and Broadbelt, L.J., "Application of Computer Generation of Reaction Mechanisms Using Quantitative Rate Information to Hydrocarbon Pyrolysis", Preprints of the American Chemical Society, Division of Fuel Chemistry, **1999**, *44*(3), 476-478. (attached)

De Witt, M.J., Dooling, D.J. and Broadbelt, L.J., "Computer Generation of Reaction Mechanisms Using Quantitative Rate Information: Application to Long-Chain Hydrocarbon Pyrolysis", Proceedings of the American Institute of Chemical Engineers, Houston, TX, **1999**. (attached)

Wong, H.-W., Kruse, T.M., Woo, O.S. and Broadbelt, L.J., "Tertiary Resource Recovery from Waste Polymers via Pyrolysis: Polypropylene", Preprints of the American Chemical Society, Division of Fuel Chemistry, **2000**. (attached)

L.J. Broadbelt, "Polymer Resource Recovery Through Coprocessing", Catalysis Club of Chicago, Spring Symposium, Evanston, IL, April 2, 1997.

L.J. Broadbelt, "Polymer Resource Recovery Through Coprocessing", Environmental Health Engineering Seminar Series, Northwestern University, Evanston, IL, April 23, 1997.

L.J. Broadbelt, "Polymer Resource Recovery Through Coprocessing", Department of Chemical Engineering, The Ohio State University, Columbus, OH, May 29, 1997.

L.J. Broadbelt, "Polymer Resource Recovery Through Coprocessing", Department of Chemical Engineering, North Carolina State University, Raleigh, NC, October 27, 1997.

L.J. Broadbelt, "Recent Developments in Computer Generation of Reaction Mechanisms", UOP Workshop on Complex Reaction Kinetics, UOP, Des Plaines, IL, March 6, 1998.

L.J. Broadbelt, "Polymer Resource Recovery: Thermal and Catalytic Chemistry", Engelhard Corporation, Iselin, NJ, April 29, 1998.

L.J. Broadbelt, "Understanding Degradation of Polymers Through Experiments and Mechanistic Modeling", SC Johnson Polymer, Racine, WI, April 15, 1999.

L.J. Broadbelt, "Understanding Complex Degradation Chemistry of Polymers Through Experiment and Mechanistic Modeling", Engineering Foundation Conference on Polymer Reaction Engineering VI, Palm Coast, FL, March 20,, 2000.

L.J. Broadbelt, "Tertiary Resource Recovery from Waste Polymers", Department of Chemical Engineering, Tufts University, forthcoming in December, 2000.

De Witt, M.J., Woo, O.S., and Broadbelt, L.J. "Catalytic Degradation of Waste Polymers: Reaction of Polystyrene and Polyethylene Model Compounds over Acid Catalysts", poster presentation at AIChE Annual Meeting, Chicago, IL, November, 1996.

De Witt, M.J. (speaker) and Broadbelt, L.J. "Coprocessing of Polymeric Waste with Coal: Reaction of Polyethylene and Coal Model Compounds", Annual Meeting of the American Chemical Society, Division of Fuel Chemistry, San Francisco, CA, April, 1997.

De Witt, M.J. and Broadbelt, L.J. "Coprocessing of Polymeric Waste with Coal: Reaction of Polyethylene and Coal Model Compounds", poster presentation at Annual Meeting of the American Chemical Society, Division of Fuel Chemistry, San Francisco, CA, April, 1997.

De Witt, M.J. and Broadbelt, L.J. "Coprocessing of Polymeric Waste with Coal: Reaction of Polyethylene and Coal Model Compounds", poster presentation at American Institute of Chemical Engineers Chicago Local Section Meeting, Chicago, IL, April, 1998.

De Witt, M.J. and Broadbelt, L.J. "Coprocessing of Polymeric Waste with Coal: Reaction of Polyethylene and Coal Model Compounds", poster presentation at Catalysis Club of Chicago Spring Symposium, Chicago, IL, May, 1998.

De Witt, M.J. (speaker) and Broadbelt, L.J. "Coprocessing of Polymeric Waste with Coal: Reaction of Polyethylene and Coal Model Compounds", AIChE Annual Meeting, T1002, Miami Beach, FL, November, 1998.

Broadbelt, L.J. (speaker), De Witt, M.J. and Dooling, D.J. "Computer Generation of Reaction Mechanisms Using Quantitative Rate Information", AIChE Spring Meeting, Houston, TX, March, 1999.

De Witt, M.J., Dooling, D.J. and Broadbelt, L.J. "Computer Generation of Reaction Mechanisms Using Quantitative Rate Information", poster presentation at American Institute of Chemical Engineers Chicago Local Section Meeting, Chicago, IL, April, 1999.

Broadbelt, L.J. (speaker), De Witt, M.J. and Dooling, D.J., "Application of Computer Generation of Reaction Mechanisms Using Quantitative Rate Information to Hydrocarbon Pyrolysis", Symposium on Chemistry of Reactive Intermediates and Modeling in Hydrocarbon Conversion, American Chemical Society National Meeting, New Orleans, August, 1999.

Broadbelt, L.J., De Witt, M.J. and Dooling, D.J., "Application of Computer Generation of Reaction Mechanisms Using Quantitative Rate Information to Hydrocarbon Pyrolysis", poster presentation at Sci-Mix Poster Session, American Chemical Society National Meeting, New Orleans, August, 1999.

De Witt, M.J., Dooling, D.J. (speaker) and Broadbelt, L.J. "Computer Generation of Reaction Mechanisms Using Quantitative Rate Information", AIChE Annual Meeting, Dallas, TX, November, 1999.

Broadbelt, L.J., Wong, H.-W., Kruse, T.M. and Woo, O.S. "Tertiary Resource Recovery from Waste Polymers via Pyrolysis", American Chemical Society National Meeting, Washington, D.C., August, 2000.

Wong, H.-W. (speaker), Kruse, T.M. and Broadbelt, L.J. "Tertiary Resource Recovery from Waste Polymers via Pyrolysis", AIChE Annual Meeting, Los Angeles, CA, November, 2000.

Binary Interactions Between Tetradecane and 4-(1-Naphthylmethyl) Bibenzyl During Low and High Pressure Pyrolysis

Matthew J. De Witt and Linda J. Broadbelt*
Department of Chemical Engineering
Northwestern University
Evanston, Illinois 60208-3120

Abstract

Low and high pressure pyrolysis experiments employing tetradecane and 4-(1-naphthylmethyl)bibenzyl (NBBM) as model compounds for polyethylene and coal, respectively, were conducted at 420°C at different reactant loadings both neat and in binary mixtures. These reaction sets demonstrated that when reacted in binary mixtures, the conversion of tetradecane increased while the selectivities to primary products of NBBM were enhanced in the gas phase. Variation of the relative concentrations of the components revealed that the effect was indeed a chemical one and not simply a result of dilution. As the polymer mimic to coal model compound ratio increased, there was a decrease in self-interactions of NBBM with minimal changes in the degradation products of tetradecane. Increasing the overall reaction pressure in the system through addition of an inert gas from atmospheric pressure to 2360 psig resulted in small decreases in reactant conversions and altered product distributions only slightly. Overall, the experiments carried out demonstrated that favorable interactions exist in the gas phase during coprocessing, and primary reaction pathways and mechanisms governing the interactions between the feedstocks were elucidated.

Introduction

Alternatives for the disposal of used plastic products are being sought as public concern for the environment has escalated in recent years. As the number of landfills closing each year exceeds

the number being opened, disposal through landfilling is becoming a less viable option.[1] Since approximately 80% of the municipal solid waste stream (MSW) is landfilled, this will have a dramatic impact on the disposal of used products.[2] A significant portion of the MSW, approximately 18% by volume, is comprised of plastic products.[2] The US alone produces 60 billion pounds of polymers annually, and their production is projected to increase.[3] The public has responded to the growing use of plastics by pressuring industry and government to promote recycling as a means of extending the useful lifetime of plastic products. Incineration, i.e., energy recovery through burning, is simple yet viewed adversely by the public. Alternative recycling approaches in which mixed plastics are ground, melted and then reshaped result in a loss of material strength and are therefore not widely applied.[4]

Another strategy for plastics resource recovery is tertiary recycling, a method in which the polymers are broken down into their corresponding monomers or into petrochemicals and fuels. Tertiary recycling strategies include coprocessing of polymeric waste with other materials to potentially enhance reactivity and product selectivities through synergistic effects. One option for coprocessing is to react polymeric waste with coal under direct liquefaction conditions.[5-7] Coprocessing of polymeric waste with coal may provide for simultaneous conversion of both feedstocks into high-valued fuels and chemicals.

Although the viability of coprocessing of polymeric waste with coal has been demonstrated,[5-7] the complexity of real feedstocks obscures the nature of the interactions among them and makes it difficult to unravel the underlying reaction pathways, kinetics, and mechanism. The development of processes for coprocessing would benefit from greater fundamental understanding of constituent interactions. In order to begin to obtain this information which can aid in process optimization, a series of experiments using model compounds for coal and polyethylene, a voluminous component of polymeric waste, has been carried out. Neat and binary mixture

pyrolysis reactions both at low and high pressures were a logical starting point since they provide valuable thermal baseline information to which experiments with additional components may be compared. Results from thermal degradation studies which have been conducted over a broad range of pressures and reactant loadings will be discussed.

Experimental

In order to obtain information about underlying reaction pathways, kinetics, and mechanism without the complicating effects of the macrostructure, experiments were performed using model compounds for both coal and high density polyethylene, a voluminous component of mixed plastic waste. To mimic the structure of coal, 4-(1-naphthylmethyl)bibenzyl (NBBM) (MW=322) was used. NBBM contains both condensed and isolated aromatic species connected by short alkyl chains. An added feature is that it contains five different aromatic-aliphatic or aliphatic-aliphatic carbon-carbon bonds. Successful predictions of the relevant primary products for real systems using NBBM confirmed the adequacy of this model compound, and thus, it was employed in this study.[8-11] The structure of NBBM with the main chain carbon-carbon bonds labeled A-E is depicted in Figure 1. Although numerous hydrocarbons may serve as appropriate model compounds for high density polyethylene, tetradecane, $C_{14}H_{30}$ (MW=198), was chosen as an appropriate compromise in reactant size.

The model compound experiments were conducted at both low and high pressures to span the range of relevant processing conditions. Low pressure batch pyrolyses of these model compounds were conducted in 3.1 ml pyrex ampoules (Wheaton). High pressure reactions were conducted in batch reactors constructed from 316 stainless steel. The reactors were fitted with glass sleeves in order to minimize wall interactions, which resulted in an effective reactor volume of 8.25 ml. A two-way ball valve was attached to the reactor in order to trap product gases for analysis by gas chromatography.

For both low and high pressure experiments, reactions were carried out in an isothermal (±1 °C) fluidized sand bath. For the low pressure pyrolyses, the ampoules were charged with the appropriate amount of reactant, purged with argon, and flame sealed. Pyrolyses were conducted at 420°C with reaction times ranging from 5-150 minutes. Upon completion of the reaction period, the ampoules were removed from the sand bath and were placed into a room temperature sand bath to cool. Each reaction time was at minimum duplicated and in some cases, three replicates were performed.

Gaseous products were collected using a sampling system of a known volume of 18.1 ml and quantified using an HP 5890 GC equipped with a thermal conductivity detector (TCD) employing a 6 ft stainless steel Porapak Q column (Supelco). The liquid and solid reaction products were extracted from the ampoules using 5 ml of methylene chloride, and an external standard (biphenyl) was added. Product identification and quantification, which enabled reactant conversions and product yields to be determined, were achieved using an HP 6890 GC/MS and HP 6890 GC equipped with a flame ionization detector (FID), respectively, each employing a Hewlett Packard 30 m crosslinked 5%-diphenyl-95%-dimethylsiloxane capillary column. The yield values were then used to calculate selectivity values for each product, which were defined as the ratio of the moles of the species formed to the moles of reactant converted.

For quantification of gaseous products, response factors for toluene and α-olefins and paraffins of carbon numbers of one to six were determined by using gaseous standards for each species. For liquid and solid products, response factors based on the external standard, biphenyl, were measured for representative species, while those for the remaining species were estimated using interpolation between these values. For linear hydrocarbons, calibration was performed using hexane, octane, and tetradecane. For species derived from the coal model compound, response factors were calculated for benzene, toluene, 1-naphthylphenylmethane, and NBBM.

At low reaction times, mass balances greater than 99% were obtained for all reaction sets. However, the mass balances diminished with increased reactant loading and extent of reaction, depending upon the reactants employed. For neat tetradecane pyrolysis, mass balances were greater than 94% for all data sets. The yields of n-pentane and 1-pentene are low since masking by the solvent caused difficulty in quantifying the liquid fraction of these species. The overall mass balance for neat NBBM pyrolysis reached a minimum of 91% at the highest conversion. Mass balances for binary mixture reactions at varying reaction times were consistent with the trends observed during the neat reactions. The reproducibility for the majority of reaction sets in this study was better than ±1% and at maximum ±3%. Therefore, the error bars for all figures presented in this paper are on the order of the symbol size used.

For the high pressure experiments, the reactor was filled with the appropriate amount of reactant and pressurized to 2500 psig with nitrogen in order to ensure a leak-free seal was obtained. The reactors were then purged with 1000 psig of nitrogen five times prior to reaction in order to completely exclude oxygen. The reactors were pressurized to 1000 psig (cold) with nitrogen, and thermal degradation was conducted at 420°C for 20-150 minutes. Upon completion of the reaction time, the reactor was immersed in a room temperature sand bath to quench the reaction. Gaseous products were collected using a sampling system of known volume of 345 ml. Liquid and solid products were extracted by washing the glass liner and reactor with a total of 15 ml of methylene chloride. Product analysis was conducted using the same methods described for the low pressure experiments. Mass balances observed during high pressure reactions were slightly higher than those obtained at low pressures.

Results and Discussion

Low Pressure Reactions. Neat and binary mixture batch pyrolysis reactions of tetradecane and NBBM were conducted at low pressures. Neat reactions were conducted to identify the controlling degradation mechanism for each reactant and to provide baseline information for subsequent binary mixture reactions. Comparison of these reaction sets permitted the identification of the underlying feedstock interactions during coprocessing. The effects of altering both the initial reactant ratio and the overall reactant loading on the conversions and product selectivities were also addressed for binary mixture reactions. Representative experimental data from the various reaction sets are summarized in Tables 1-3. Results and discussion of these reaction sets are reported in the following sections.

*Neat Tetradecane Pyrolysis***.** Low pressure neat pyrolysis of tetradecane was conducted with initial loadings ranging from 6.2 to 27.8 mg (1.01×10^{-2} to 4.53×10^{-2} M). Simulation of the phase behavior for the reaction conditions in these studies was performed using the software package HYSIS employing the Peng-Robinson equation of state. These results indicated that at low pressures, all species were in the gas phase during tetradecane pyrolysis. A plot of conversion versus time for the different concentrations is provided in Figure 2. Overall, the tetradecane conversion increased as the reactant loading was increased. For the reaction conditions studied, the dependence of the degradation rate on concentration was most pronounced at low loadings, as the rate became relatively insensitive to reactant loading at higher concentrations. This behavior is indicative of an overall reaction order that is a function of concentration and approaches first order kinetics at higher concentrations. At the lowest reactant concentration, the best fit of the overall reaction order using the integral method was 1.75.

Detailed product analysis revealed that α-olefins and paraffins with carbon numbers from 1 to 5 were major products of tetradecane pyrolysis at all concentrations studied. The highest molar product selectivities at all initial concentrations were observed for propylene and ethane, which had approximately equal values. These remained relatively constant throughout the range of reaction

times studied and were independent of the initial reactant loading, with an average value of approximately 0.38±0.05. The alkene which had the second highest selectivity was ethylene, and its yield as a function of conversion is plotted in Figure 3. As revealed in Figure 3, its yield was a decreasing function of initial reactant concentration, and its selectivity also decreased with increasing conversion and reactant concentration. The selectivity achieved a maximum of 0.45±0.02 at the lowest conversion and the lowest reactant loading, and the minimum selectivity of 0.20±0.02 was observed at the highest conversion for the highest reactant loading. The selectivities of 1-butene and 1-pentene were lower than that of ethylene but remained relatively constant with both conversion and reactant loading at values of approximately 0.17±0.02 and 0.12±0.02, respectively.

Paraffins in the C_3-C_5 range were all formed with lower selectivities than their corresponding alkene. Propane, butane, and pentane all showed increases in yield and selectivity with increasing initial concentration. The yield of butane is plotted as a function of conversion in Figure 4 and is representative of this behavior. Methane displayed the opposite trend, decreasing with increasing reactant loadings. The trends for C_4 and C_5 paraffins as a function of carbon number were similar to those observed for the corresponding α-olefins, i.e., a decrease in yield with increasing carbon number. However, the reduction in yield as carbon number increased was much more marked for the paraffins than for α-olefins. These trends were even more evident when alkanes and alkenes in the range of carbon numbers from 7 to 12 were examined. There was a significantly higher alkene to alkane ratio for the liquid products than for the gaseous products, with α-olefins predominating at the higher carbon numbers. The selectivity of α-olefins for the higher carbon numbers was relatively independent of reactant concentration. The yields of the corresponding paraffins, however, showed significant increases with increasing conversion and reactant loading, and the selectivities increased as the initial reactant loading was raised. These trends are shown for 1-undecene and n-undecane in Figure 5.

Overall, the product distributions were consistent with those reported previously for long-chain paraffin pyrolysis conducted at moderate temperatures and low pressures.[12-16] As discussed in detail in these studies, thermolysis of long n-alkanes under mild conditions leads to high yields of gaseous products and α-olefins, with minor yields of n-alkanes smaller than the parent species. The pyrolytic degradation occurs through a combination of unimolecular and bimolecular free-radical reactions, with the relative rates depending upon the reaction temperature and substrate pressure. In particular, the controlling reaction mechanism can be rationalized by using a combination of the Rice-Herzfeld and Rice-Kossiakoff mechanisms, which are represented in Figure 6.[12-14] The decomposition is initiated by carbon-carbon bond fission along the main chain to form two primary radicals. These primary radicals can then propagate through three main types of reactions: β-scission, intermolecular hydrogen abstraction, and intramolecular hydrogen abstraction. Isomerization through intramolecular hydrogen abstraction forms secondary radicals, which can undergo the same types of propagation reactions. If the secondary radical undergoes a β-scission, an α-olefin and a smaller primary radical are formed, and the primary radical can then undergo similar reactions until the resulting species is too small to further decompose. The high yields of terminal olefins and gaseous species, with smaller proportions of n-alkanes, observed in our work and the literature suggest that the dominant mode of propagation is isomerization of primary radicals followed by β-scission of secondary radicals. For the experimental studies presented in this paper, preliminary detailed kinetic modeling has been carried out and reveals that these mechanistic ideas are able to capture the experimental trends observed.[17]

The trends observed as a function of the initial reactant loading for the gaseous species can be explained by considering the reaction pathways leading to the formation of these products and the impact of changes in total concentration on the relative rates of these pathways. The most striking trend observed was the decrease in the selectivity to ethylene with increasing reaction time and reactant concentration. This behavior can be rationalized by noting that the formation of ethylene occurs primarily through a unimolecular reaction, a β-scission reaction of a primary radical

to form ethylene and a smaller primary radical. As reaction time and the initial reactant concentration increase, bimolecular reactions become more competitive with unimolecular reactions due to the increase in substrate concentrations. These bimolecular reactions lead to a reduction in the rate of formation of ethylene since there is a corresponding decrease in the relative population of primary radicals in the system. In addition, ethylene degradation rates are higher due to increased addition reactions. The increase in bimolecular reactions also results in a reduction in the number of sequential isomerization/β-scission steps higher molecular weight radicals undergo. Consequently, there is an increase in the yields of long-chain alkanes at the expense of smaller species. This idea will be discussed further when the n-paraffin product trends with increasing reactant loadings are discussed.

The increase in the selectivities of gaseous n-alkanes at higher initial reactant concentrations can be explained by noting that secondary thermal cracking can occur as the number of intermolecular reactions increases, which would lead to an increase in the quantity of precursors for the formation of the gaseous species. In addition, as the proportion of bimolecular reactions increases, there is a higher probability that a primary radical will be capped and become stable rather than undergo further degradation via unimolecular reactions.

The observed decrease in selectivity of α-olefins for carbon numbers greater than seven as reaction time increases can be rationalized by noting that these species undergo secondary reactions at longer reaction times. Reactions including initiation (primarily at the allylic position which ultimately results in the formation of propylene), intermolecular hydrogen abstraction, and radical addition reactions will lead to the disappearance of the longer alkenes. The formation rate of the olefins will also be reduced with increasing conversion, since there will be fewer precursors available for their formation.

As mentioned above, the increase in long paraffin yields with increasing conversion and loading can be explained using mechanistic arguments. By employing mechanistic modeling, it has been possible to estimate the effect of reactant concentration and conversion on the concentration of radicals in the system.[17] It has been shown that although the total radical concentration increases with increasing reactant loading, the relative radical yields (the ratio of the total sum of radicals to the initial reactant loading) show the opposite trend. The reduction in the total normalized radical population as reactant concentration increases is predominantly due to reduction in yields of low molecular weight radical species. This suggests that the ability of higher molecular weight radicals to undergo sequential isomerization/β-scission steps is diminished when hydrogen abstraction is a competing pathway with an enhanced rate. The increase in the alkane to alkene ratio and the reduction in small molecule yields, e.g., ethylene, are both consistent with this idea.

Neat NBBM Pyrolysis. Neat pyrolysis of NBBM provided the baseline to which subsequent binary experiments were compared. Although NBBM is primarily in the liquid phase at the reaction conditions employed, rudimentary experiments with a U-tube reactor configuration revealed non-negligible amounts of NBBM in the vapor phase. Accordingly, predictions of the phase behavior for the system using the same methodology described in the previous section indicated that approximately 98.4% of NBBM was in the liquid phase under reaction conditions. The major and minor products that were identified and quantified during NBBM pyrolysis are shown in Figure 7. Two of the major products from pyrolysis of NBBM were toluene and 1-methyl-4-(1-naphthylmethyl)benzene, each observed with a selectivity of greater than 0.28 at all reaction times studied. The other major product was 1-(2-phenylethenyl)-4-(1-naphthylmethyl)benzene, with an initial selectivity of approximately 0.37±0.01, which decreased linearly with reaction time to 0.12±0.01 at 150 minutes.

Minor selectivities were observed for a number of products from NBBM pyrolysis, the selectivity of which either increased or decreased with increasing reaction time. Two minor

products, 4-methylbibenzyl and 1-(4-methylbenzyl)-4-(1-naphthylmethyl)benzene, were observed with initial selectivities of 0.055±0.001 and 0.070±0.001, respectively. Each of these showed a reduction in selectivity as reaction time progressed, which is one possible indicator of subsequent decomposition reactions. Other minor products included 1,4-(bi-1-naphthylmethyl)benzene, 1-naphthylphenylmethane, naphthalene, 1-methylnaphthalene, 1-benzyl-4-(1-naphthylmethyl) benzene, 1-methyl-4-(2-phenylethenyl)benzene, p-xylene and bibenzyl which showed increased selectivities with reaction time. The selectivities to these species, which accounted for 7-10% of the total product spectra at low conversions, are depicted in Figure 8.

Mechanistic interpretation using the ideas put forth by Walter et al.[11] for pyrolysis of NBBM in the presence of high pressure of an inert gas successfully accounted for the observed product spectra from neat pyrolysis at low pressures in our study. The major exception, though, was the appearance of 1-(2-phenylethenyl)-4-(1-naphthylmethyl)benzene in our study, which was not observed by Walter et al.[11] As Walter et al.[11] reported, the formation of high yields of toluene and 1-methyl-4-(1-naphthylmethyl)benzene is consistent with the proposed mechanism involving fission of the bibenzyl linkage (bond D) in NBBM. This is the weakest bond in the molecule, since the radicals which are formed can be stabilized by the adjacent phenyl rings and will thus undergo homolysis most readily.[18-20] Initially, these radicals are stabilized through hydrogen abstraction from the bibenzyl linkage or the -CH_2- unit linking the naphthyl and center phenyl moieties of other NBBM molecules. Although the carbon-hydrogen bond strengths for these two sites are comparable (88 kcal/mol versus 84 kcal/mol)[21], the majority of the chemistry controlling product formation occurs at the bibenzyl linkage. The radical which is formed through hydrogen abstraction at the -CH_2- unit would not likely undergo β-scission or disproportionation and therefore predominantly acts as a site for hydrogen shuttling. Furthermore, products resulting from recombination of this radical were not observed, suggesting that steric hindrance precludes it or cleavage is likely.

Once a radical is formed on the bibenzyl linkage of NBBM, it can undergo various reaction pathways to form 1-(2-phenylethenyl)-4-(1-naphthylmethyl)benzene, a product not reported by Walter et al.[11] The formation of the unsaturated species in this study can be explained through analogy to explanations for the formation of stilbene during pyrolysis of 1,2-diphenylethane (1,2-DPE).[18-20,22] During 1,2-DPE pyrolysis, Miller and Stein[18] showed that once a radical is formed on the bibenzyl linkage, stilbene can be formed through two major and one minor pathway. Disproportionation of 1,2-DPE radicals directly forms stilbene, and recombination of two 1,2-DPE radicals, when followed by a hydrogen abstraction to form a radical which decomposes rapidly by β-scission, indirectly forms stilbene. The minor stilbene formation pathway is through β-scission of a hydrogen atom from a 1,2-DPE radical. It is likely that the formation of 1-(2-phenylethenyl)-4-(1-naphthylmethyl)benzene in our study occurs through analogous reaction pathways. However, it is assumed that the disproportionation and recombination reactions can occur with any radical in the system.

In addition to the aforementioned reaction pathways, free radical ipso-substitution reactions were also important routes for NBBM conversion and the formation of several minor products. Our observations were consistent with the free radical ipso-substitution scheme as proposed by Walter et al.[11] An example of this type of reaction pathway is the addition of a benzyl radical to the 1-naphthyl position of a NBBM molecule followed by a β-scission of this intermediate to form 1-naphthylphenylmethane. This was shown to be a relevant minor reaction pathway in this study. Likewise, various radical attacks at the phenyl ring at bond C can explain the appearance of 1-(4-methylbenzyl)-4-(1-naphthylmethyl)benzene, 1,4-(bi-1-naphthylmethyl)benzene, and 1-benzyl-4-(1-naphthylmethyl)benzene. Overall, the main reaction families for NBBM pyrolysis are bond homolysis, hydrogen abstraction, radical ipso-substitution, β-scission, and radical disproportionation and recombination reactions.[11]

Binary Mixture Pyrolysis. Reactions of binary mixtures of tetradecane and NBBM at low pressures revealed interactions between the reactants and synergistic effects. Reactions were conducted varying both the initial reactant ratio and the overall reactant loading. As observed in Figure 9, the conversion of tetradecane was significantly enhanced for all of the reactions which were conducted in the presence of NBBM. The pseudo-first order rate constants for tetradecane degradation increased from 3.6×10^{-5} s^{-1} for the 6.2 mg loading to 6.3×10^{-5} s^{-1} and 6.9×10^{-5} s^{-1} in the presence of 10.0 and 20.0 mg of NBBM, respectively, and from 5.2×10^{-5} s^{-1} to 8.6×10^{-5} s^{-1} for the 12.3 mg loading with the addition of 20.0 mg of NBBM. These increases were rationalized in terms of kinetic coupling.[23] The internal carbon-carbon bonds of tetradecane have a higher bond dissociation energy (90 kcal mol^{-1}) than that of the bibenzyl bond in NBBM (60 kcal mol^{-1}).[20] This has the potential to increase the quantity of radicals in the system with respect to the neat tetradecane experiments at a particular reaction time. The NBBM-derived radicals can competitively abstract hydrogen from the secondary carbons of tetradecane, forming a tetradecane-derived radical and converting a tetradecane molecule, enhancing its conversion. Once formed, these tetradecane-derived radicals undergo decomposition reactions similar to those observed during neat pyrolysis.

Although analogous rate constants measured in the gas phase and reaction path degeneracy suggest that hydrogen abstraction at benzylic sites is slightly faster than aliphatic sites,[22] phase behavior favors hydrogen abstraction from tetradecane. During coprocessing, there are reactions occurring in both the gas and the liquid phases. Phase behavior predictions indicated that during binary mixture reactions at the highest reactant loadings, approximately 97.4% of NBBM and 4.1% of tetradecane were in the liquid phase. When NBBM homolytically cleaves, the smaller (primarily benzyl) radicals are able to partition into the gas phase; during neat reactions, there are few viable reaction pathways in the gas phase due to the low vapor fraction of NBBM. When these species enter the gas phase during binary mixture reactions, though, they will encounter high relative concentrations of tetradecane, which will favor NBBM-tetradecane interactions. Once a tetradecane radical is formed, it will follow a degradation mechanism very similar to that observed during neat

pyrolysis due to the relative high concentrations of tetradecane in the gas phase. Overall, this will result in an increase in tetradecane reactivity since initiation to form tetradecane radicals through hydrogen abstraction will occur more readily than carbon-carbon bond fission.

Both the initial charge of each reactant and the overall reactant loading strongly influenced reactant conversions and product selectivities during coprocessing. The conversion of tetradecane was most dramatically affected by both of these factors during the binary experiments. In order to quantify the effect of increasing the initial NBBM to tetradecane ratio, the Bin(1:1) and Bin(1:2) reactions were compared. As the loading of NBBM was increased, the rate of conversion of tetradecane was enhanced. This result is consistent with an increase in the effective radical concentration in the system with a higher loading of NBBM, which in turn increases the conversion of the polymer mimic. The rate enhancement observed during neat pyrolysis for tetradecane as the loading was increased is also observed when NBBM is present. The rate of conversion of tetradecane was enhanced at a constant NBBM loading, as the rate was higher for the Bin(2:2) than for Bin(1:2). However, a reduction in conversion was observed at long reaction times. The highest rate of conversion was obtained when both factors contributed to the disappearance of tetradecane, as the Bin(2:2) showed the largest rate of conversion. As the total reactant concentration increases, the rate of bimolecular reactions increases. The rate of hydrogen abstraction from tetradecane by NBBM-derived radicals increases with increasing concentrations, thus increasing the rate of tetradecane degradation further. Therefore, increasing both the molar ratio of NBBM to tetradecane and the total molar concentration results in an enhancement of the polymer model compound reactivity.

Although changes in concentration influenced the major products of NBBM, the conversion of NBBM was not strongly affected as shown in Figure 10. As discussed previously, the degradation of the coal model compound primarily occurs through the thermolysis of bond D. As described above, the radicals afforded will react selectively with tetradecane rather than with other

NBBM molecules if they diffuse into the gas phase, and therefore, the consumption of NBBM associated with self-interactions through hydrogen abstraction will be diminished. During the neat NBBM studies, the gas phase radicals, which primarily consist of benzyl and to a lesser extent the complimentary radical formed during homolytic fission of bond D, can undergo recombination reactions to reform NBBM. During coprocessing, however, the radicals evolved from bond D scission that interact with tetradecane will not have the opportunity to recombine to form NBBM. The data suggest that a balance is achieved between these two effects and consequently, the conversion of NBBM is essentially unchanged.

The overall mechanisms for degradation of tetradecane and NBBM were similar for the neat and binary mixture experiments, but some differences in product selectivities were observed as a result of binary interactions. As with the variations in tetradecane conversions, these differences also depended upon both the overall reactant concentration and the relative amount of NBBM in the system. The effect of coprocessing NBBM and tetradecane at low concentrations on tetradecane-derived products can be observed by comparing the C_{14}-6.2 and Bin(1:1) experimental results. Although there was a significant increase in the polymer model compound reactivity, there were only small changes in the tetradecane-derived product spectra. The ethylene and methane selectivities displayed the most significant differences with the addition of NBBM. The dependence of the selectivity of ethylene as a function of concentration and the addition of the NBBM co-reactant is shown in Figure 11. In addition to the reduced formation of ethylene and methane, the yields of α-olefins also decreased while the selectivities of longer paraffins increased. As previously described, these trends are consistent with those observed as the initial concentration of tetradecane in the neat experiments was raised, and the changes are consistent with a reduction in repeated unimolecular degradation steps of higher molecular weight radicals.

With the addition of tetradecane, the selectivity to NBBM-derived primary products significantly increased. Since abstraction of hydrogen from tetradecane is favored due to phase

behavior, NBBM radicals are capped and stable before undergoing secondary reactions. This effect on the overall product yields can be discerned from Figures 12 and 13. The radicals which are formed from cleavage of the bibenzyl bond in NBBM will abstract hydrogen from tetradecane with higher selectivity and afford higher yields of toluene and its compliment. This behavior is also illustrated by the trends observed for the selectivity of 1-(2-phenylethenyl)-4-(1-naphthylmethyl)benzene, the species produced as NBBM-derived radicals are capped during neat pyrolysis, which is shown in Figure 14. The selectivity to this species decreases with the addition of tetradecane at longer reaction times. This observation, coupled with the increased selectivities for primary products of NBBM, indicates that NBBM-derived radicals are abstracting hydrogen from tetradecane rather than from NBBM. These favorable interactions between feedstocks are even more apparent in the selectivity trends of other NBBM-derived products, such as 1-naphthylphenylmethane, a product formed through secondary reactions. Since the benzyl radicals that would lead to formation of 1-naphthylphenylmethane via ipso-substitution are shuttled away from NBBM with the addition of tetradecane, its selectivity decreases.

As the loading of NBBM was increased at a constant tetradecane loading, there was a decrease in selectivity towards α-olefins and gaseous hydrocarbons, and an increase towards paraffins of carbon numbers greater than seven. As stated above, this behavior can be explained by noting that there is reduction in the ability of tetradecane-derived radicals to undergo repeated unimolecular transformations under these reaction conditions.

Increasing the molar loading of tetradecane while keeping the coal model compound loading constant resulted in little change in the tetradecane-derived product distributions. The differences in conversion of tetradecane in the Bin(1:2) and Bin(2:2) reaction sets are similar to those for the C_{14}-6.2 and C_{14}-12.3 experiments, indicating that the primary role of NBBM under such conditions is to enhance the rate of initiation but not to alter the subsequent decomposition pathways of

tetradecane. Therefore, the nature of the tetradecane interactions is similar during the binary reactions to those observed during neat reactions as suggested by the comparable product slates.

It has been shown that during low pressure co-reaction of coal and polymer model compounds, favorable interactions between reactants exist. The conversion of tetradecane increased while the selectivity to primary products of NBBM pyrolysis was enhanced. These observations were attributed to the stabilization of NBBM-derived radicals through hydrogen abstraction from tetradecane which in turn, increases the rate of tetradecane conversion. The relative concentrations of each reactant also affected the tetradecane conversion and selectivity towards primary products of NBBM. Increasing both the NBBM to tetradecane ratios and the overall reactant loading resulted in an increase of interactions between NBBM and its derivatives and an enhancement of tetradecane degradation.

High Pressure Reactions. A series of high pressure reactions was conducted to determine the influence of overall system pressure on the reaction mechanism and kinetics. The same total reactant molar concentrations used during the low pressure sets were employed when possible, but it was necessary to perform some reactions with increased concentrations due to analytical limitations. Representative experimental data from the various reaction sets are shown in Tables 1-3. Results and discussion of the neat and binary mixture experiments in the presence of an inert gas at high pressure are reported in the following sections.

Neat Tetradecane Pyrolysis. High pressure pyrolysis experiments of tetradecane were conducted using the methods described in the experimental section with reactant loadings varying between 16.5 and 53.2 mg. The reaction set C_{14}-16.5 will not be included in this discussion since it was not possible to fully quantify n-alkanes due to the low reactant loading and the amount of solvent required for extraction. Therefore, discussion will focus on the C_{14}-32.7 and C_{14}-53.2 reaction sets and comparison of the results to their low pressure counterparts, C_{14}-12.3 and C_{14}-20, respectively.

It should be noted that the high pressures for the reactions discussed in the following sections are due to the inert gas, not an increase in the quantity of substrate charged to the system. Furthermore, simulation of the phase behavior for the reaction conditions employed indicated that tetradecane was exclusively in the gas phase during reaction. Therefore, the reaction sets that will be discussed are not analogous to the high pressure liquid phase pyrolysis of long-chain paraffins described to some extent in the literature.[24-27] Few studies on the effects of increasing inert pressure on gas phase long-chain hydrocarbon pyrolysis have been carried out; thus there is little information available in the literature from which to draw comparisons.[28,29]

Comparison of tetradecane conversion as a function of reactant concentration and total reaction pressure is shown in Figure 15. The conversion is relatively insensitive to the reaction conditions for low reaction times, but the conversion for the reactions at high pressure diminished at longer times. The high pressure experiments yielded products similar to the low pressure neat pyrolysis reactions, with α-olefins and n-alkanes as the primary products. However, the observed selectivities for products from the two pressure regimes were different, particularly for the n-alkanes and light hydrocarbons. In addition, methane was not observed during the high pressure reactions.

Of the light hydrocarbons, ethylene, ethane, and propylene displayed the most notable differences in their product selectivities. The selectivities of each of these were significantly reduced for the high pressure reactions, with the C_{14}-53.2 reaction set having the lowest values. For n-alkanes larger than butane, the high pressure reactions resulted in notably higher yields than those observed in the low pressure pyrolyses. The α-olefin selectivities followed similar trends for both sets of reactions, with the olefins of higher carbon numbers (>8) showing higher selectivities during the low pressure experiments.

Although the detailed mechanistic modeling study currently in progress will be used to interpret the differences between the low and high pressure reactions, initial mechanistic speculation

can be put forth to explain these trends. At higher total pressures in which a high concentration of inert molecules is present, the rate of bimolecular reactions can be enhanced substantially due to two effects: the ability of third bodies to dissipate the energy of the reactants and the effect of increasing pressure to promote "cage" effects.[30] Third bodies can substantially improve rates of exothermic reactions, particularly recombination reactions, by dissipating the energy of the reactants that is released during reaction.[30] In addition to dissipating the energy evolved during reaction, high concentrations of inert gas lead to an enhancement in bimolecular reactions due to the ability to increase the frequency of collisions of reacting species by reducing their ability to migrate away from each other.[30,31] The observations in our studies at high pressures are similar to the "cage" effects described during liquid phase reactions, which would be the limiting case at extremely high pressures.[19,31] The combination of the two effects would explain the absence of methane and reduced yields of light hydrocarbons for the high pressure reactions. Radical precursors which could potentially lead to the formation of light hydrocarbons will undergo bimolecular reactions with higher frequency. The combination of these species with themselves, other radicals, and molecular species would lead to increased yields of n-alkanes of higher carbon numbers and reduced selectivities to longer α-olefins. The observation that the reactant conversion is not significantly affected by reaction pressure can be explained by noting that although recombination rates would be enhanced, bimolecular propagation reactions, which lead to the conversion of tetradecane, increase.

For the reactions carried out at high pressure, the dependence of the product spectra on increasing the initial tetradecane loading is the same as that observed at low pressure. As the reactant loading was raised, the selectivity to light hydrocarbons and long α-olefins declined, while the yields of n-alkanes increased. It should be noted, though, that the magnitude of the selectivity differences was larger for the high pressure reaction. These trends can again be rationalized in terms of a relative decrease in repeated unimolecular radical transformations with increasing reactant

loadings, in addition to the contributions of inert molecules to bimolecular reaction rates at high pressure.

Neat NBBM Pyrolysis. Neat high pressure pyrolysis of NBBM was performed to provide a comparison to low pressure experiments and to serve as a baseline for subsequent high pressure experiments with binary mixtures. Phase simulations revealed that the percent of NBBM in the vapor phase increased at higher total pressures to a value of approximately 12% for these reaction conditions. The phase behavior with respect to increasing system pressure goes against intuition, in which one would expect high molecular weight species to more selectively partition into the liquid phase. However, the increase in system pressure is due to the addition of an inert gas, not the addition of reactant. Therefore, even though the vapor pressure of NBBM is quite low and thus its partial pressure in the vapor phase is also low, the total number of moles of NBBM in the gas phase to establish thermodynamic equilibrium is not insignificant and increases as the total pressure increases.

The overall conversion for NBBM, which is consistent with values reported by Walter et al.[11] for similar reaction conditions, was reduced during the high pressure experiments compared to the low pressure reaction sets, as shown in Figure 16. Two of the major products formed during high pressure pyrolysis were toluene and 1-methyl-4-(1-naphthylmethyl)benzene, which were produced from fission of the bibenzyl bond in NBBM and subsequent hydrogen abstraction. The other major product formed was 1-(2-phenylethenyl)-4-(1-naphthylmethyl)benzene. Minor selectivities were observed for a number of species, all of which were reported above for low pressure NBBM pyrolysis.

Although the major and minor reaction products observed during NBBM degradation were the same for both high pressure and low pressure pyrolyses, there were significant differences in product yields between the two sets of experiments. The most notable differences in the observed

yields were for the three major products. The yields of the bond D product pair were almost equivalent during the low pressure experiments but were clearly significantly different for the high pressure reactions, as shown in Figure 17. Toluene showed an increase in yield for the high pressure reactions, while 1-methyl-4-(1-naphthylmethyl)benzene showed diminishing yields. The selectivity to 1-(2-phenylethenyl)-4-(1-naphthylmethyl)benzene was also reduced during the high pressure reactions compared to the low pressure runs. The yields of the minor products were essentially unchanged with the exception of 1-(4-methylbenzyl)-4-(1-naphthylmethyl)benzene, 4-methylbibenzyl, and naphthalene, which showed slightly higher yields during the high pressure reactions.

The reduction of NBBM conversion can be rationalized by taking into account the phase behavior at high pressures and the ability of inert molecules to facilitate bimolecular reactions. Since the vapor fraction of NBBM increases at high pressure, this also implies that the majority of the NBBM-derived radicals, which have higher vapor pressures than the parent compound, will also be in even higher proportion in the gas phase. Accordingly, the concentration of 1-methyl-4-(1-naphthylmethyl)benzene radicals in the gas phase will be significantly enhanced with high concentrations of inert gas. Without the availability of high concentrations of NBBM as in the low pressure reactions, hydrogen abstraction reaction rates will diminish and recombination rates, mediated by inert molecules, will become more likely. This scenario, along with increased recombination of benzyl and 1-methyl-4-(1-naphthylmethyl)benzene radicals, explains the decreased conversion of NBBM, which is consumed to a lesser extent by hydrogen abstraction. This also explains the decrease in the selectivities to 1-methyl-4-(1-naphthylmethyl)benzene and 1-(2-phenylethenyl)-4-(1-naphthylmethyl)benzene, since both of which rely on a hydrogen abstraction step for their formation.

Although the same logic would imply that the selectivity to toluene should also decrease, postulating an additional reaction pathway for its formation helps to resolve this conflict. Initially,

in order to explain the increase in toluene yields, an overall phenyl ring balance was calculated. The balances for the low and high pressure reaction sets were essentially equivalent, indicating that toluene was being formed at the expense of 1-methyl-4-(1-naphthylmethyl)benzene and 1-(2-phenylethenyl)-4-(1-naphthylmethyl)benzene. Under the scenario presented in the previous paragraph, two reaction types in the gas phase that would be enhanced at high pressures are radical recombination and radical addition. As stated above, the higher overall inert pressures result in both increased rates of bimolecular reactions and higher proportions of larger molecular weight species in the gas phase. One particular reaction pathway which will be enhanced at high pressures is the recombination of a 1-methyl-4-(1-naphthylmethyl)benzene radical and a radical on the ethyl linkage of NBBM. The product of this recombination reaction possesses a tertiary carbon, providing a center for facile bond fission, and a benzyl radical which would ultimately result in the formation of toluene could be easily released. These ideas are captured in Figure 18 and comprise a viable reaction pathway for the increased selectivity to toluene with a concomitant reduction in the yields of 1-methyl-4-(1-naphthylmethyl)benzene and 1-(2-phenylethenyl)-4-(1-naphthylmethyl) benzene. In addition to recombination reactions, radical addition is also enhanced. Addition of a 1-methyl-4-(1-naphthylmethyl)benzene radical to the alkene present in the highest yield, 1-(2-phenylethenyl)-4-(1-naphthylmethyl)benzene, can ultimately form the intermediate species shown in Figure 18, and a benzyl radical may be released as discussed above. This type of radical addition would lead to a further enhancement in the selectivity of toluene at the expense of the other major products.

Additional experimental evidence supported the hypothesis that recombination reactions of NBBM-derived species were favored as a result of vapor-liquid partitioning at high pressure. Comparison between high and low pressure reaction sets revealed that there was a decrease in the sum of the naphthyl moieties for the high pressure reactions. In addition, there was a larger quantity of higher molecular species as evidenced by an increase in products with longer chromatographic retention times. It was not possible to identify all of these high molecular weight compounds that eluted at times greater than NBBM, but through mass spectrometry it was possible

to identify 4,4´-(bi-1-naphthylmethyl)bibenzyl, a product formed through either radical recombination or the radical addition pathway presented in the previous paragraph. The difference in naphthyl ring balances is attributed to the increase in the yields of high molecular weight products which were not quantified, which result from reaction mechanisms similar to the one presented in Figure 18. The selectivity of bibenzyl, a minor product formed during NBBM pyrolysis, remained relatively constant during the high pressure experiments. This can be rationalized by noting that although the rate of recombination is enhanced at high pressures, the concentration of radicals other than benzyl radicals in the gas phase significantly increases. These effects result in minimal changes in the observed bibenzyl yields.

With the exceptions discussed above, the reaction pathways and mechanism for the neat pyrolysis of NBBM are similar for both high and low pressure reaction conditions, as evidenced by the similar product yields. Overall, the only significant difference is that higher molecular weight species are more selectively partitioned into the vapor phase at high pressures, which leads to an increase in recombination and radical addition reactions. These reactions result in increased yields of toluene at the expense of 1-methyl-4-(1-naphthylmethyl)benzene and 1-(2-phenylethenyl)-4-(1-naphthylmethyl)benzene primarily.

Binary Mixture Pyrolysis. Pyrolysis of binary mixtures of tetradecane and NBBM at high pressures showed interactions between the reactants and synergistic effects similar to those observed during the low pressure experiments. Phase behavior predictions indicated that during binary mixture reactions at the highest reactant loadings, approximately 87.5% of NBBM and 1.2% of tetradecane were in the liquid phase. As observed in Figure 19, the conversion of tetradecane was once again significantly enhanced for all of the reactions which were conducted in the presence of NBBM. For the high pressure reactions, the pseudo-first order rate constant for tetradecane degradation increased from 4.2×10^{-5} s^{-1} to 1.0×10^{-4} s^{-1} for the 32.7 mg loadings, which corresponded to the same molar concentration as 12.3 mg loadings for the low pressure reactions.

The reactivity of NBBM was relatively unaffected during coprocessing, which is consistent with observations from low pressure experiments, indicating that the primary degradation mechanism for NBBM remained unchanged.

The changes in the trends for tetradecane-derived products during binary mixture reactions at high pressures were similar to those observed during the low pressure reaction sets. During coprocessing, the yields of light hydrocarbons and α-olefins diminished while the selectivity to longer paraffins increased. As was the case at low pressures, upon initiation of an NBBM molecule, the radicals which are formed will selectively abstract hydrogen from a tetradecane molecule, initiating a tetradecane radical. Once initiated, these species will undergo degradation mechanisms similar to those observed during neat reactions.

The effect of increasing the overall tetradecane loading at a constant NBBM loading was investigated by comparing the Bin(2:2) HP and Bin(3.2:2) HP reaction sets. The product selectivities for the α-olefins were relatively unaffected as the reactant ratio changed. However, there was a more significant increase in paraffin selectivities with increased loadings of the polymer mimic at high pressures than there was at low pressures. This increase was a result of both the increase in the relative amount of tetradecane radicals and the facilitation of bimolecular reactions at high inert pressures.

The alterations to the degradation mechanism for NBBM during coprocessing at high pressures were similar to those observed for reactions at reduced pressures. As tetradecane was introduced, there was a decrease in secondary and tertiary reactions, with an increase in the yield of 1-methyl-4-(1-naphthylmethyl)benzene. The relative selectivity of toluene, however, remained nearly constant. The former observations were attributed to the stabilization of NBBM-derived radicals through abstraction of readily available hydrogen from tetradecane molecules, which also resulted in enhanced tetradecane reactivities. The relatively constant value of toluene selectivity

during coprocessing can be explained by considering how the relative reaction rates of competing mechanistic steps change during coprocessing. The rate of recombination of NBBM-derived intermediates diminishes as evidenced by the reduced yields of NBBM-derived secondary and tertiary products. In particular, the increased yields of 1-methyl-4-(1-naphthylmethyl)benzene indicate that the recombination mechanism between an NBBM radical and 1-methyl-4-(1-naphthylmethyl)benzene radicals discussed above for neat NBBM pyrolysis at high pressure is lowered. Therefore, there will be a decrease in the formation of toluene from this pathway. However, the yield of toluene through favorable interactions with the polymer mimic is increased due to stabilization of benzyl radicals by tetradecane before they can undergo further reactions. It is suggested that these two effects balance each other for binary mixtures at high pressures, resulting in relatively constant yields of toluene.

The result of increasing the ratio of the polymer mimic to the coal model compound on NBBM-derived products was the same as that observed at low pressures. As the tetradecane loading increased at a constant NBBM concentration, the selectivity to products formed through self-interactions of NBBM decreased. With a higher concentration of tetradecane, there is an increased proportion of reactions between NBBM and tetradecane-derived molecules and intermediates, which leads to the altered distributions of NBBM-derived products. This is consistent with the behavior at low pressures and is illustrated for 1-(2-phenylethenyl)-4-(1-naphthylmethyl)benzene in Figure 20 as a representative example at high pressure, indicating that NBBM-derived radicals selectively react with tetradecane.

Coprocessing of tetradecane and NBBM at high pressures resulted in favorable interactions similar to those observed for reactions conducted at low pressures. The reactivity of tetradecane was significantly enhanced, while the degradation pathways for NBBM remained relatively unaffected. The only significant differences in the trends of the product spectra were that increased yields of longer paraffins were observed and a relatively constant selectivity to toluene was obtained

during coprocessing at high pressures. Overall, comparison of the experiments conducted at low and high pressures demonstrated that coprocessing provides similar and favorable interactions in both pressure regimes.

Conclusions

Recent investigations have demonstrated the feasibility of coprocessing of coal with polymers. In this study, feedstock interactions were observed using model compounds of both coal and polyethylene. In binary mixtures, the conversion of tetradecane increased while the selectivity to primary products of NBBM pyrolysis was enhanced. These observations were attributed to the stabilization of NBBM-derived radicals through hydrogen abstraction from tetradecane in the gas phase, which in turn increased the rate of tetradecane conversion.

At low pressures, the initial loading of each reactant and the overall loadings were found to affect both the conversion of tetradecane and the overall product distribution during coprocessing. As the NBBM to tetradecane ratio was raised, only a slight difference in reactant conversions was observed, but there were significant changes in product selectivities. NBBM showed increased selectivity towards secondary products, while n-alkanes were formed in higher yields for tetradecane degradation. The higher proportion of NBBM resulted in an increase of self-interactions, which resulted in a larger quantity of retrograde condensation reactions. The higher loadings of NBBM also yielded larger tetradecane-derived radical populations within the system, leading to a shift in the products towards longer paraffins. The increase in high molecular weight paraffin yields was attributed to a relative reduction of repeated unimolecular radical transformations with increasing reactant loadings. Increasing the initial charge of both reactants resulted in a significant enhancement of tetradecane reactivity. The primary product yields from NBBM were essentially identical when compared to the reactions conducted with the same reactant ratio but lower total loading. However, the values were higher than those observed for the reactions

conducted with a larger ratio of NBBM to tetradecane. These effects on conversions and selectivities were attributed to an increase in both tetradecane-NBBM and tetradecane-tetradecane reactions at higher concentrations.

As the overall system pressure was increased, small changes in the relative rates of competing reaction pathways for NBBM and tetradecane decomposition were observed. For neat pyrolysis of tetradecane at high pressures of an inert gas, the yield of normal paraffins was increased at the expense of lighter hydrocarbons and α-olefins. These observations were attributed to enhancement in the rate of bimolecular reactions for tetradecane-derived radicals due to the ability of high concentrations of inert molecules to facilitate energy transfer and to promote "cage" effects. With respect to neat NBBM-derived products, there was an increase in toluene formation at high pressures. It is likely that this occurred mainly through recombination of radical species of NBBM and 1-methyl-4-(1-naphthylmethyl)benzene, or radical addition of a 1-methyl-4-(1-naphthylmethyl)benzene radical to 1-(2-phenylethenyl)-4-(1-naphthylmethyl)benzene, and subsequent cleavage of a benzyl radical. The rates for these reactions were enhanced at high pressures due to the phase behavior of the system. For binary mixture reactions at high pressures, the favorable interactions observed at low pressures were still realized, with only slight enhancement of paraffin yields and constant yields of toluene being observed.

Acknowledgment. The authors are grateful for financial support from the United States Department of Energy, Grant DE-FG22-96-PC96204. The authors would also like to thank Naresh Shah and Gerald Huffman from the University of Kentucky and Dady Dadyburjor from West Virginia University for their insightful comments and help in designing a high pressure delivery system. Undergraduates Mike Dennis and Daniel Prekup are also acknowledged for conducting some of the low pressure tetradecane pyrolysis experiments.

References

(1) Pett, R. A.; Golovoy, A.; Labana, S. S., In *Plastics, Rubber, and Paper Recycling: A Pragmatic Approach* ; Rader, C. P., Baldwin, S. D., Cornell, D. D., Sadler, G. D., Stockel, R. F., Eds.; American Chemical Society: Washington, DC, 1995; Vol. 609, pp 47.

(2) Rowatt, R. J., *Chemtech,* **1993**, *23(1)*, 56-60.

(3) Mackey, G., In *Plastics, Rubber, and Paper Recycling: A Pragmatic Approach* ; Rader, C. P., Baldwin, S. D., Cornell, D. D., Sadler, G. D., Stockel, R. F., Eds.; American Chemical Society: Washington, DC, 1995; Vol. 609, pp 161.

(4) Holmes, H., *Garbage,* **1991**, *(January/February)*, 23.

(5) Taghei, M.; Feng, Z.; Huggins, F.; Huffman, G. R., *Energy Fuels,* **1994**, *8*, 1228-1232.

(6) Joo, H. K.; Curtis, C. W., *Energy Fuels,* **1997**, *11(4)*, 801-812.

(7) Rothenberger, K. S.; Cugini, A. V.; Thompson, R. L.; Ciocco, M. V., *Energy Fuels,* **1997**, *11(4)*, 849-855.

(8) Farcasiu, M.; Smith, C., *Energy Fuels,* **1991**, *5(1)*, 83-87.

(9) Matson, D. W.; Linehan, J. C.; Darab, J. G.; Buehler, M. F., *Energy Fuels,* **1994**, *8*, 10-18.

(10) Tang, Y.; Curtis, C. W., *Energy Fuels,* **1994**, *8*, 63.

(11) Walter, T. D.; Casey, S. M.; Klein, M. T.; Foley, H. C., *Cat. Today,* **1994**, *19*, 367-380.

(12) Rice, F. O., *J. Am. Chem. Soc.,* **1933**, *55*, 3035-3040.

(13) Rice, F. O.; Herzfeld, K. F., *J. Am. Chem. Soc.,* **1934**, *56*, 284-289.

(14) Kossiakoff, A.; Rice, F. O., *J. Am. Chem. Soc.,* **1943**, *65*, 590-595.

(15) Voge, H. H.; Good, G. M., *J. Am. Chem. Soc.,* **1949**, *71*, 593-597.

(16) Mushrush, G. W.; Hazlett, R. N., *Ind. Eng. Chem. Fund.,* **1984**, *23*, 288-294.

(17) De Witt, M. J.; Dooling, D. J.; Broadbelt, L. J., *in preparation*.

(18) Miller, R. E.; Stein, S. E., *J. Phys. Chem.,* **1981**, *85*, 580-589.

(19) Stein, S. E.; Robaugh, D. A.; Alfieri, A. D.; Miller, R. E., *J. Am. Chem. Soc.,* **1982**, *104*, 6567-6570.

(20) Poutsma, M. L., *Energy Fuels,* **1990**, *4(2)*, 113-131.

(21) McMillen, D. F.; Golden, D. M., *Ann. Rev. Phys. Chem.,* **1982**, *33*, 493-532.

(22) Poutsma, M. L.; Dyer, C. W., *J. Org. Chem.,* **1982**, *47*, 4903-4914.

(23) LaMarca, C.; Libanati, C.; Klein, M. T., *Chem. Eng. Sci.,* **1990**, *45(8)*, 2059-2065.

(24) Fabuss, B. M.; Smith, J. O.; Lait, R. I.; Borsanyi, A. S.; Satterfield, C. N., *Ind. Eng. Proc. Des. & Dev.,* **1962**, *1*, 293-299.

(25) Fabuss, B. M.; Smith, J. O.; Satterfield, C. N., *Adv. Petr. Chem. Refin.,* **1964**, *9*, 158-201.

(26) Song, C.; Lai, W. C.; Schobert, H. H., *Ind. Eng. Chem. Res.,* **1994**, *33*, 534-547.

(27) Khorasheh, F.; Gray, M. R., *Ind. Eng. Chem. Res.,* **1993**, *32*, 1853-1863.

(28) Safarik, I.; Strausz, O. P., *Res. Chem. Inter.,* **1996**, *22(3)*, 275-314.

(29) Rebick, C., In *Pyrolysis: Theory and Industrial Practice* ; Albright, L. F., Crynes, B. L., Corcoran, W. H., Eds.; Academic Press, Inc.: New York, 1983; Vol. , pp 69-86.

(30) Moore, J. W.; Pearson, R. G. *Kinetics and Mechanism*; John Wiley & Sons, Inc; New York, 1981.

(31) Kochi, J. K. *Free Radicals*; John Wiley & Sons, Inc.; New York, 1973.

Table 1: Representative Experimental Data for Neat Tetradecane Pyrolysis Conducted at Low and High Pressure

Reaction Set	6.2	6.2	12.3	12.3	20	20	27.8	27.8	32.7-HP	32.7-HP	53.2-HP	53.2-HP
Reaction Time (min)	40	120	40	120	40	120	40	120	40	120	40	120
Pressure [a]	LP	LP	LP	LP	LP	LP	LP	LP	HP	HP	HP	HP
$C_{14}H_{30}$ Loading (mg)	6.4	6.2	12.3	12.2	19.7	20.2	27.6	27.7	32.5	32.8	53.0	52.8
$C_{14}H_{30}$ Conversion	0.10	0.24	0.11	0.32	0.11	0.32	0.14	0.35	0.11	0.29	0.12	0.30
Product Yield (x10 ^{2}) [b]												
methane	2.55	6.98	2.46	6.98	2.23	6.60	1.97	5.78	0.00	0.00	0.00	0.00
ethylene	4.04	9.77	3.92	9.33	3.58	8.00	3.05	6.35	1.73	4.95	1.41	4.28
ethane	4.05	10.27	4.61	12.14	4.89	12.64	4.61	11.69	2.71	7.09	2.44	7.55
propylene	3.43	10.00	4.21	12.60	4.75	13.32	4.56	12.30	2.79	8.14	2.64	8.92
propane	1.49	4.36	2.47	7.10	3.33	8.87	3.54	9.22	1.98	5.10	2.25	6.26
1-butene	1.71	4.59	2.04	5.66	2.35	6.03	2.24	5.77	1.71	4.39	1.53	4.70
n-butane	0.18	1.34	0.73	2.58	1.17	3.68	1.34	4.22	1.13	2.67	1.17	3.71
1-pentene	1.22	3.18	1.45	3.92	1.66	4.04	1.50	3.80	1.28	3.89	1.30	3.91
n-pentane	0.05	0.45	0.11	0.95	0.42	1.45	0.49	1.71	0.29	1.54	0.68	2.10
1-hexene	1.43	3.12	1.73	4.13	2.43	5.21	2.53	5.39	2.08	4.80	1.98	5.26
n-hexane	0.00	0.00	0.00	0.18	0.16	0.42	0.28	0.71	0.29	0.74	0.28	1.45
1-heptene	0.82	1.80	1.18	2.68	1.78	3.62	1.67	3.35	1.48	2.94	1.42	3.39
n-heptane	0.00	0.00	0.00	0.26	0.20	0.57	0.25	0.69	0.39	0.71	0.52	1.13
1-octene	0.93	2.16	1.22	2.84	1.51	2.99	1.54	3.02	1.23	2.02	1.11	2.60
n-octane	0.00	0.00	0.00	0.25	0.08	0.42	0.19	0.57	0.19	0.47	0.35	0.76
1-nonene	0.96	2.07	1.08	2.49	1.30	2.51	1.38	2.60	0.87	1.43	0.95	1.86
n-nonane	0.00	0.00	0.00	0.21	0.00	0.34	0.15	0.47	0.20	0.27	0.27	0.54
1-decene	0.94	1.91	1.03	2.29	1.22	2.27	1.28	2.31	0.88	1.43	0.95	1.74
n-decane	0.00	0.04	0.00	0.07	0.11	0.28	0.15	0.38	0.15	0.24	0.27	0.48
1-undecene	0.82	1.65	0.90	1.93	1.04	1.93	1.08	1.93	0.79	1.31	0.85	1.55
n-undecane	0.00	0.09	0.00	0.15	0.09	0.25	0.14	0.33	0.17	0.25	0.26	0.46
1-dodecene	0.79	1.54	0.86	1.75	0.97	1.78	1.00	1.75	0.75	1.25	0.81	1.45
n-dodecane	0.00	0.00	0.00	0.00	0.00	0.05	0.04	0.08	0.00	0.05	0.04	0.10
1-tridecene	0.18	0.36	0.19	0.40	0.21	0.40	0.22	0.40	0.18	0.29	0.19	0.34
n-tridecane	0.00	0.00	0.00	0.00	0.00	0.00	0.03	0.04	0.00	0.00	0.02	0.05

(a) LP : Low pressure, HP : High pressure. (b) Product yield defined as: (moles species i formed)/(initial moles tetradecane).

Table 2: Representative Experimental Data for Tetradecane-Derived Products During Binary Mixture Pyrolysis

Reaction Set	(1:1) [c]	(1:1)	(1:2)	(1:2)	(2:2)	(2:2)	(2:2)-HP	(2:2)-HP	(3.2:2)-HP	(3.2:2)-HP
Reaction Time (min)	40	120	40	120	40	120	40	120	40	120
Pressure [a]	LP	LP	LP	LP	LP	LP	HP	HP	HP	HP
$C_{14}H_{30}$ Loading (mg)	6.1	6.4	6.4	6.3	12.2	12.2	32.5	32.7	53.0	53.0
$C_{14}H_{30}$ Conversion	0.19	0.38	0.22	0.42	0.26	0.48	0.23	0.44	0.24	0.47
NBBM Loading (mg)	10.1	9.9	19.9	19.9	20.0	20.0	53.0	53.1	53.0	53.1
Product Yield (x10 ^{2}) [b]										
methane	3.95	9.86	3.99	9.88	3.92	9.99	0.00	0.00	0.00	0.00
ethylene	6.01	11.48	5.83	9.89	5.39	9.09	2.86	6.61	2.52	5.34
ethane	7.65	17.40	7.72	17.35	8.17	18.67	5.08	12.53	5.07	12.59
propylene	6.99	16.49	6.67	14.90	7.76	16.60	4.95	11.26	4.97	11.78
propane	4.32	10.38	4.31	10.67	5.63	13.28	4.05	9.14	4.42	10.96
1-butene	3.49	7.17	3.40	6.49	3.75	7.14	2.84	5.80	2.86	5.81
n-butane	1.51	4.31	1.61	4.81	2.21	6.39	2.45	5.72	2.78	7.02
1-pentene	2.48	4.82	2.40	4.28	2.51	4.72	2.41	4.75	2.40	4.71
n-pentane	0.84	1.79	0.71	2.18	0.89	2.89	1.54	3.64	1.77	4.54
1-hexene	2.69	5.53	3.27	5.23	3.58	6.09	3.33	5.53	3.52	5.64
n-hexane	0.00	0.84	0.43	1.13	0.57	1.80	1.20	2.67	1.54	3.53
1-heptene	1.64	3.36	1.85	2.85	2.22	3.41	1.94	2.94	2.16	3.31
n-heptane	0.00	0.56	0.28	0.79	0.35	1.18	0.92	1.84	1.18	2.67
1-octene	1.73	3.15	1.75	2.58	1.92	2.90	1.61	2.18	1.84	2.40
n-octane	0.00	0.53	0.25	0.92	0.35	1.13	0.82	1.59	1.04	2.09
1-nonene	1.65	2.72	1.52	2.15	1.81	2.33	1.22	1.38	1.38	1.56
n-nonane	0.00	0.00	0.23	0.70	0.32	0.93	0.61	0.99	0.83	1.48
1-decene	1.56	2.48	1.35	1.89	1.56	1.98	1.17	1.32	1.30	1.45
n-decane	0.00	0.40	0.19	0.63	0.26	0.80	0.57	0.88	0.75	1.31
1-undecene	1.29	1.97	1.12	1.42	1.31	1.49	1.02	1.12	1.11	1.20
n-undecane	0.00	0.37	0.19	0.50	0.24	0.65	0.56	0.76	0.71	1.15
1-dodecene	1.22	1.77	1.03	1.22	1.19	1.29	0.96	1.03	1.03	1.10
n-dodecane	0.00	0.00	0.05	0.19	0.06	0.24	0.13	0.29	0.13	0.28
1-tridecene	0.26	0.39	0.24	0.28	0.27	0.26	0.21	0.25	0.24	0.28
n-tridecane	0.00	0.00	0.00	0.10	0.00	0.12	0.06	0.17	0.08	0.22

(a) LP : Low pressure, HP : High pressure. (b) Product yield defined as: (moles species i formed)/(initial moles tetradecane).
(c) (a:b) denotes ratio of a moles of tetradecane to b moles of NBBM loaded, referenced to 1.0E-2 M of NBBM corresponding to a value of b = 1.

Table 3: Representative Experimental Data for NBBM-Derived Products During Low and High Pressure Pyrolysis

Reaction Set	N-20	N-20	N-53.2	N-53.2	(1:1) [d]	(1:1)	(1:2)	(1:2)	(2:2)	(2:2)	(2:2)-HP	(2:2)-HP	(3.2:2)-HP	(3.2:2)-HP
Reaction Time (min)	40	120	40	120	40	120	40	120	40	120	40	120	40	120
Pressure [a]	LP	LP	HP	HP	LP	LP	LP	LP	LP	LP	HP	HP	HP	HP
NBBM Loading (mg)	20.3	20.3	53.0	52.9	10.1	9.9	19.9	19.9	20.0	20.0	53.0	53.1	53.0	53.1
NBBM Conversion	0.23	0.65	0.16	0.51	0.26	0.61	0.23	0.61	0.24	0.61	0.15	0.50	0.21	0.51
$C_{14}H_{30}$ Loading (mg)	0.0	0.0	0.0	0.0	6.1	6.4	6.4	6.3	12.2	12.2	32.5	32.7	53.0	53.0
Product Yield (x10 ^{2}) [b]														
toluene	7.58	23.14	6.51	23.80	10.16	27.50	8.95	25.29	9.07	26.73	6.28	22.76	7.86	23.91
ethylbenzene	0.00	0.41	0.00	0.23	0.00	0.65	0.05	0.77	0.17	1.16	0.14	0.84	0.25	1.15
p-xylene	0.00	1.12	0.00	0.51	0.00	1.21	0.07	1.33	0.18	1.63	0.11	1.09	0.17	1.38
naphthalene	0.23	1.18	0.17	0.95	0.20	1.21	0.25	1.59	0.33	2.25	0.26	1.99	0.29	2.13
1-methylnaphthalene	0.26	1.52	0.17	0.89	0.31	1.42	0.31	1.48	0.34	1.57	0.26	1.08	0.33	1.19
bibenzyl	0.09	0.41	0.06	0.31	0.00	0.27	0.08	0.32	0.08	0.28	0.04	0.23	0.04	0.21
4-methylbibenzyl	1.10	3.22	0.82	2.85	1.15	2.82	1.25	3.57	1.34	4.05	1.16	3.82	1.37	3.99
1-methyl-4-(2-phenylethenyl)-benzene	0.09	0.98	0.06	0.53	0.00	0.73	0.10	0.68	0.10	0.51	0.07	0.35	0.09	0.30
1-naphthylphenyl methane	0.81	4.24	0.52	2.79	0.72	2.55	0.78	3.15	0.71	2.54	0.46	1.90	0.50	1.57
1-methyl-4-(1-*A*)benzene [c]	7.63	19.75	4.70	12.55	9.76	25.06	8.78	22.02	9.01	23.34	5.43	15.09	6.34	16.27
1-benzyl-4-(1-*A*)benzene	0.33	2.74	0.17	1.78	0.26	1.37	0.28	1.91	0.29	1.55	0.17	1.27	0.18	0.94
1-(4-methylbenzyl)-4-(1-*A*)benzene	1.37	2.95	1.28	3.18	0.89	1.79	1.33	2.77	1.25	2.58	1.23	2.85	1.21	2.41
1-(2-phenylethenyl)-4-(1-*A*)benzene	7.18	11.17	4.26	9.47	7.67	7.73	6.86	7.12	6.34	4.63	4.31	4.88	4.24	3.63
1,4-(bi-1-*A*)benzene	0.83	4.11	0.34	3.15	0.70	2.14	0.76	2.84	0.68	2.16	0.36	2.01	0.35	1.44

(a) LP : Low pressure, HP : High pressure. (b) Product yield defined as: (moles species i formed)/(initial moles NBBM). (c) Symbol *A* denotes (naphthylmethyl).
(d) (a:b) denotes ratio of *a* moles of tetradecane to *b* moles of NBBM loaded, referenced to 1.0E-2 M of NBBM corresponding to a value of *b* = 1.

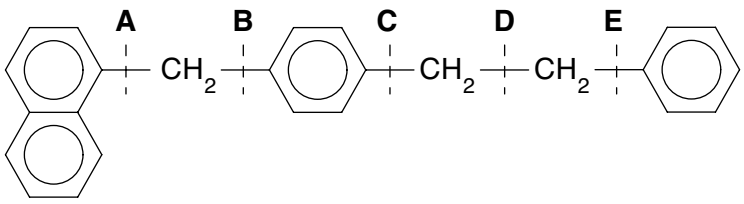

Figure 1: Structure of coal model compound 4-(1-naphthylmethyl)bibenzyl.

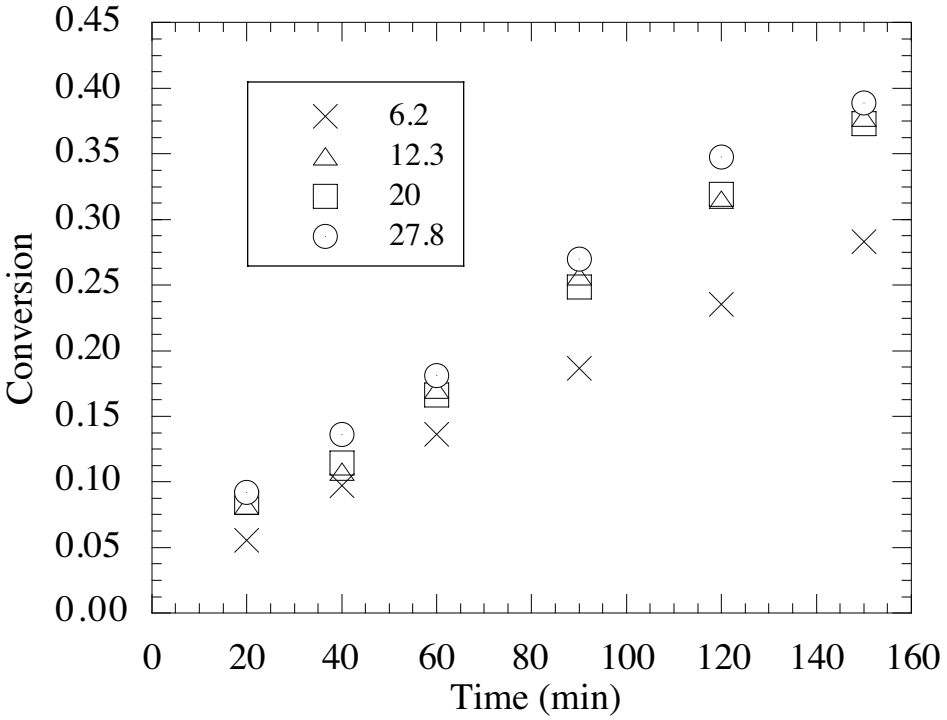

Figure 2: Comparison of neat tetradecane conversion as a function of reactant loading for low pressure pyrolysis experiments.

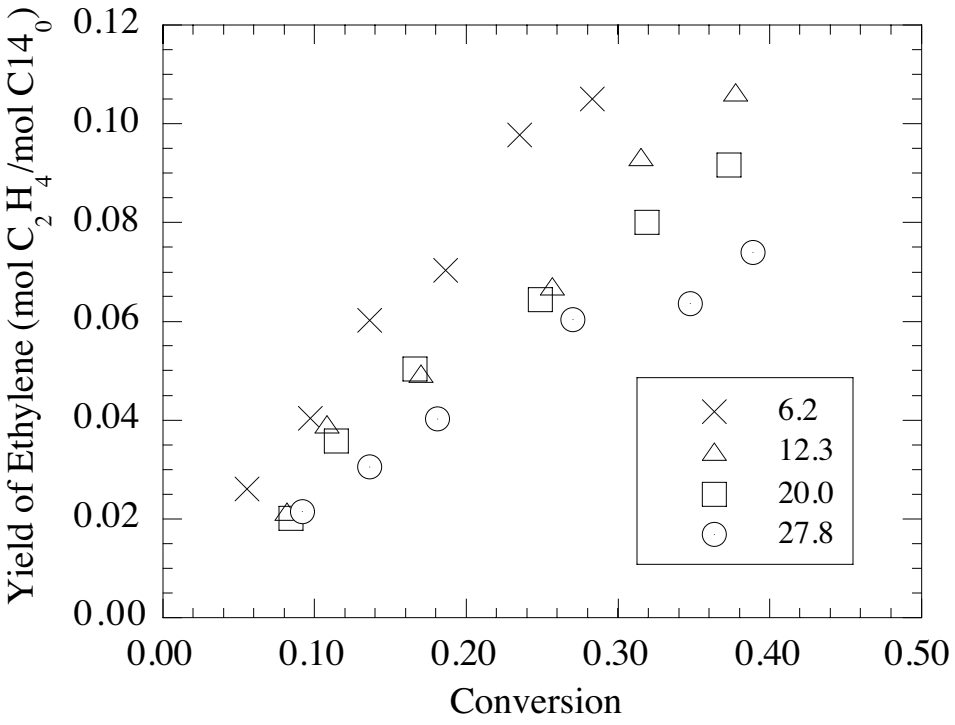

Figure 3: Comparison of ethylene yield as a function of reactant loading and conversion for neat pyrolysis of tetradecane at low pressures.

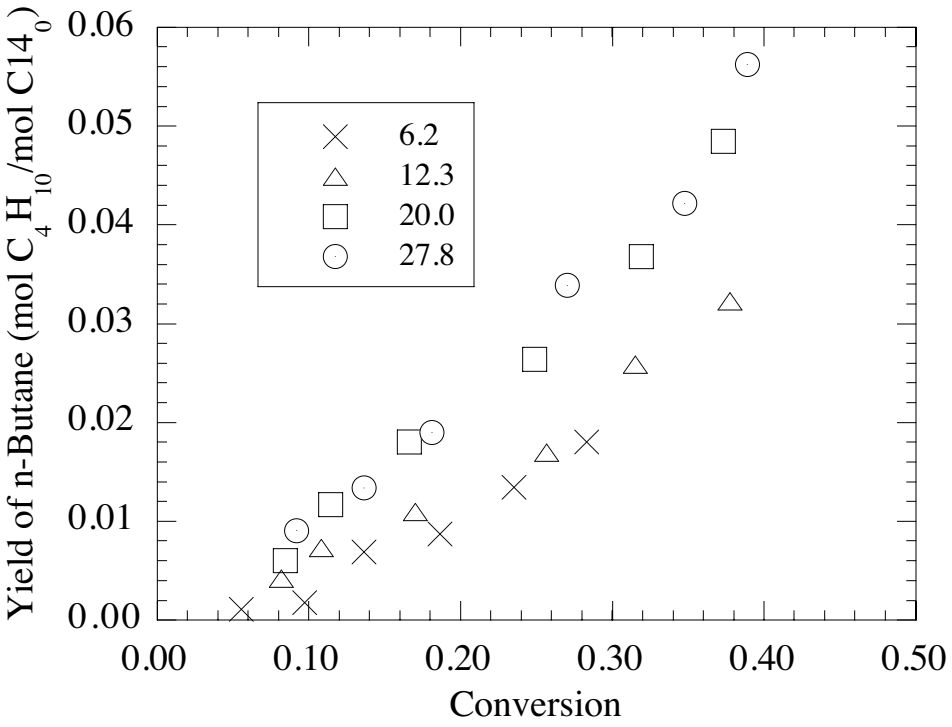

Figure 4: Comparison of n-butane yield as a function of reactant loading and conversion for neat pyrolysis of tetradecane at low pressures.

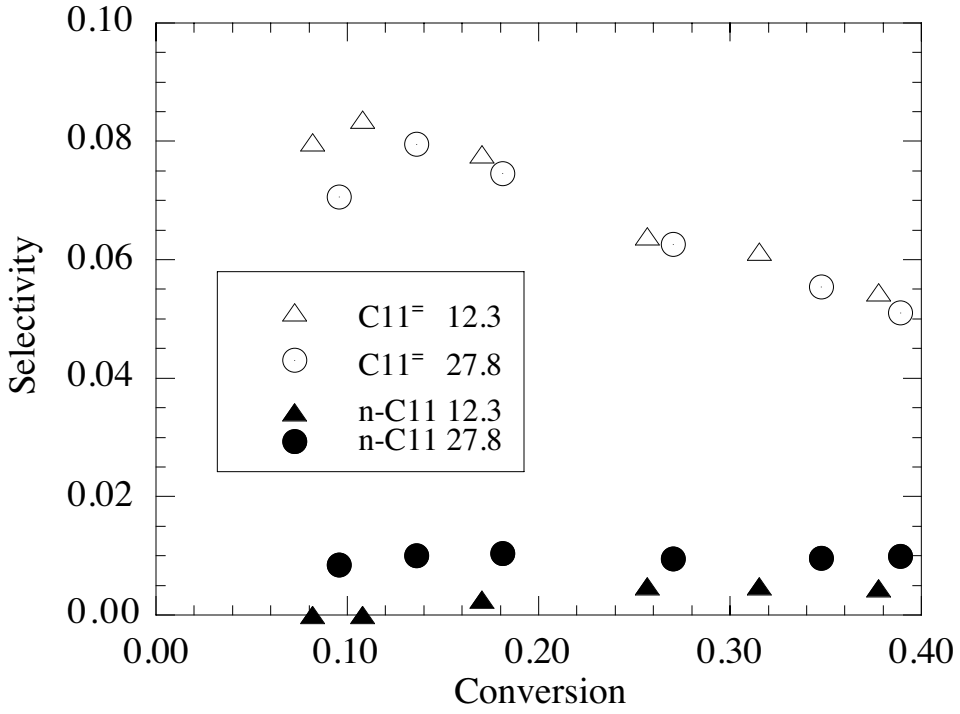

Figure 5: Comparison of 1-undecene and n-undecane selectivities as a function of reactant loading and conversion for neat pyrolysis of tetradecane at low pressures.

Initiation

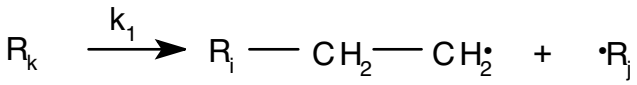

Propagation

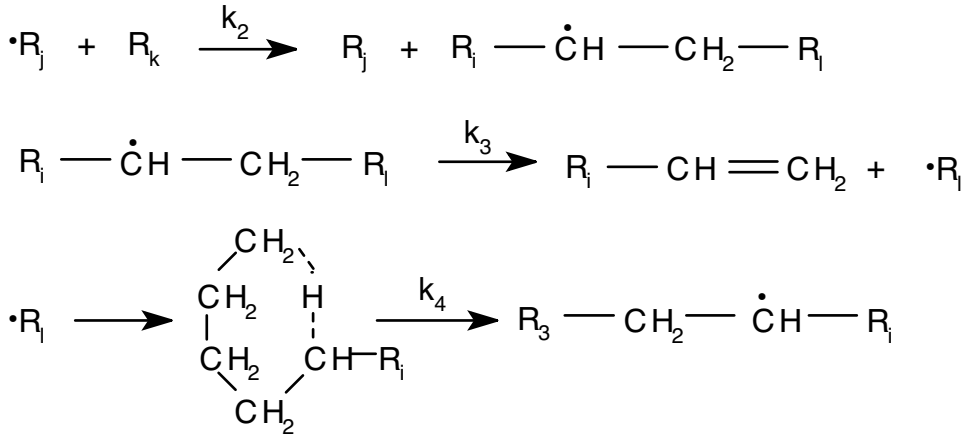

Termination

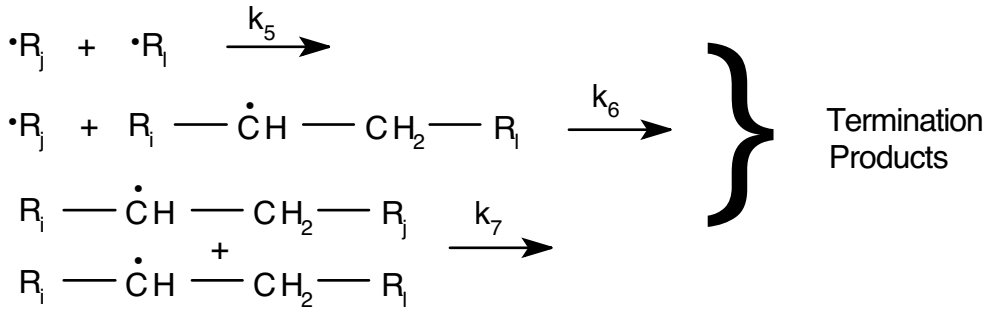

Figure 6: Proposed mechanism for pyrolysis of tetradecane.[12-14]

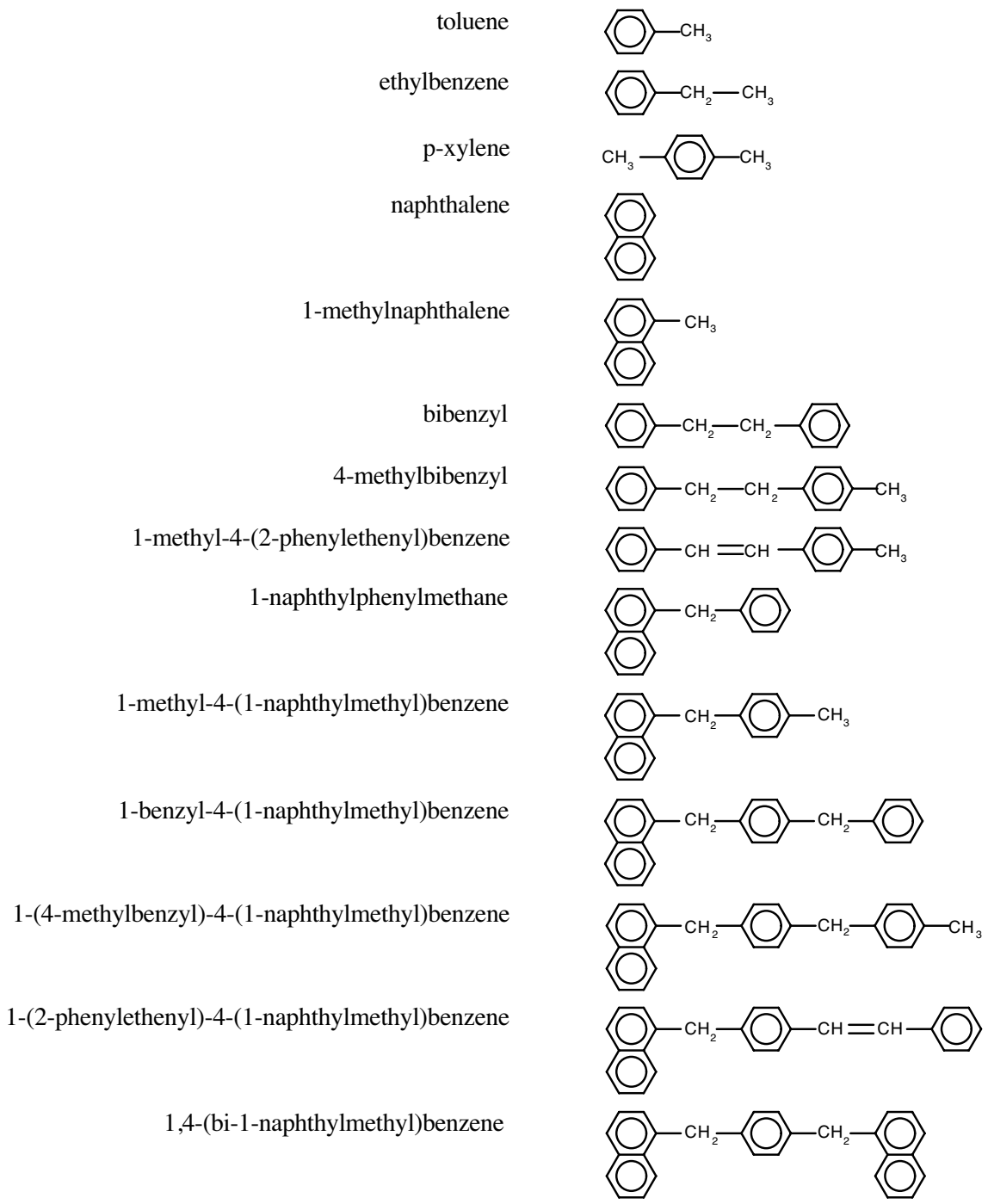

Figure 7: Major and minor products observed during NBBM pyrolysis at 420°C.

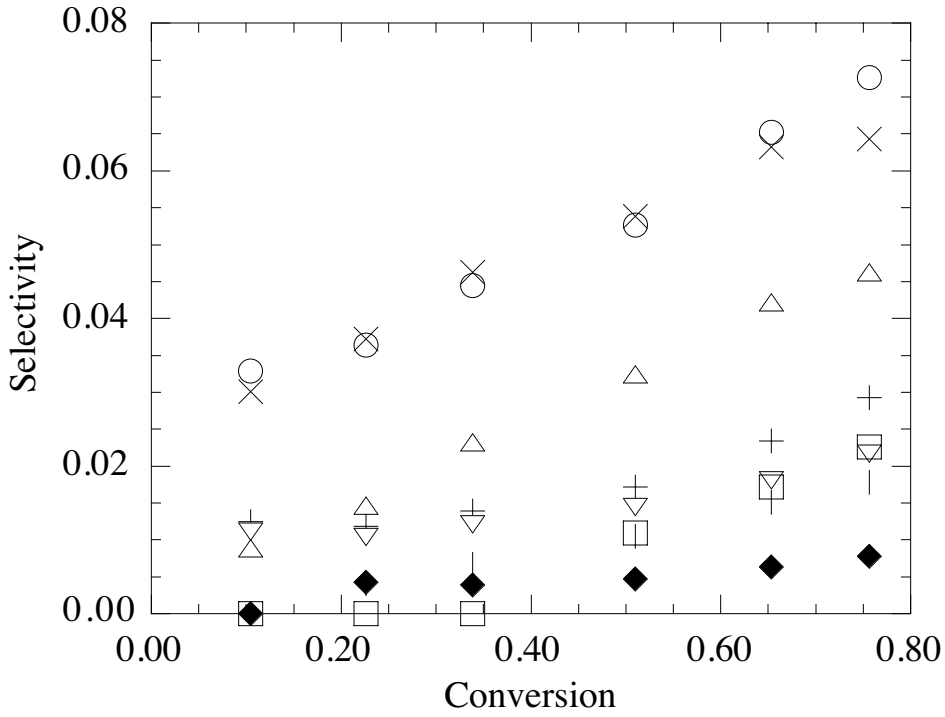

Figure 8: Comparison of selectivities for 1-napthylphenylmethane (O), 1,4-(bi-1-naphthylmethyl)benzene (X), 1-benzyl-4-(1-naphthylmethyl)benzene (Δ), 1-methylnaphthalene (+), naphthalene (∇), p-xylene (□), 1-methyl-4-(2-phenylethenyl) benzene (l), and bibenzyl(♦) as a function of conversion for neat NBBM pyrolysis.

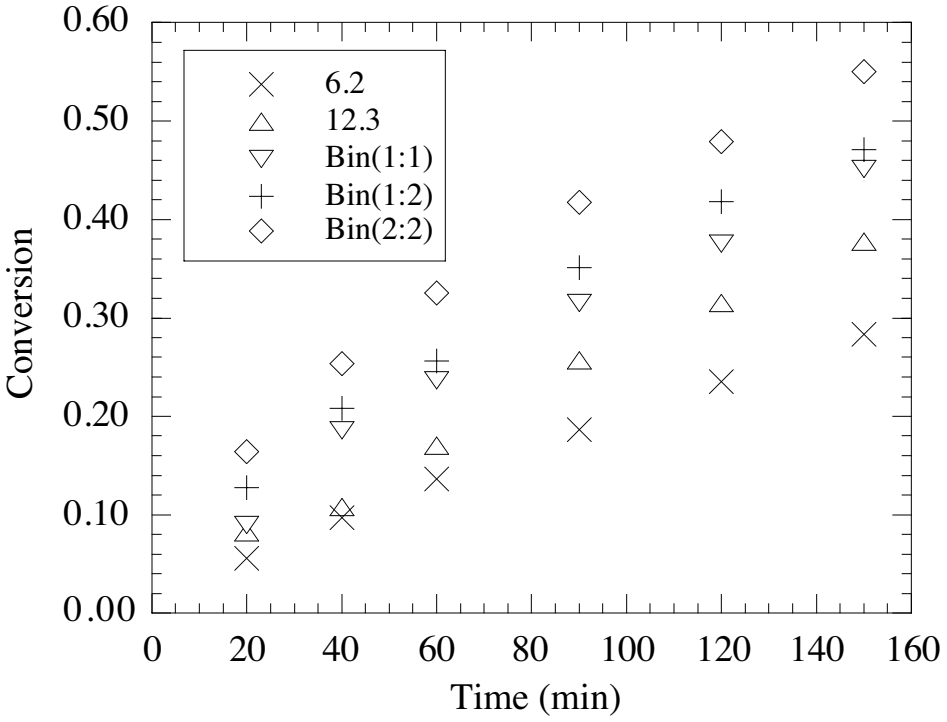

Figure 9: Comparison of tetradecane conversions as a function of reactant loading during binary reactions for low pressure reaction sets.

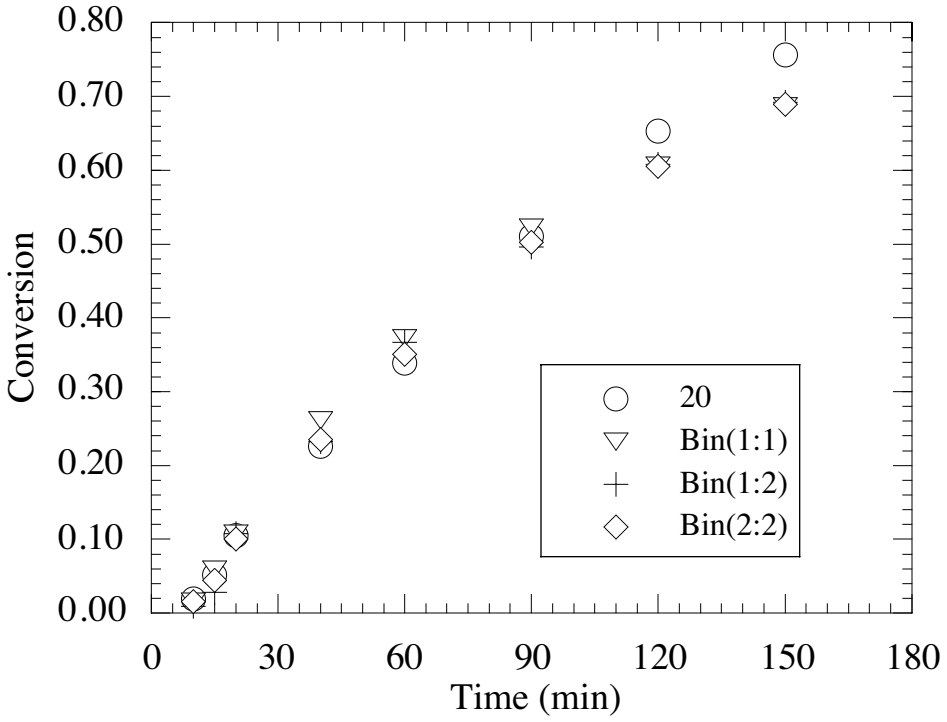

Figure 10: Comparison of conversion of NBBM as a function of reactant loading during binary reactions for low pressure reaction sets.

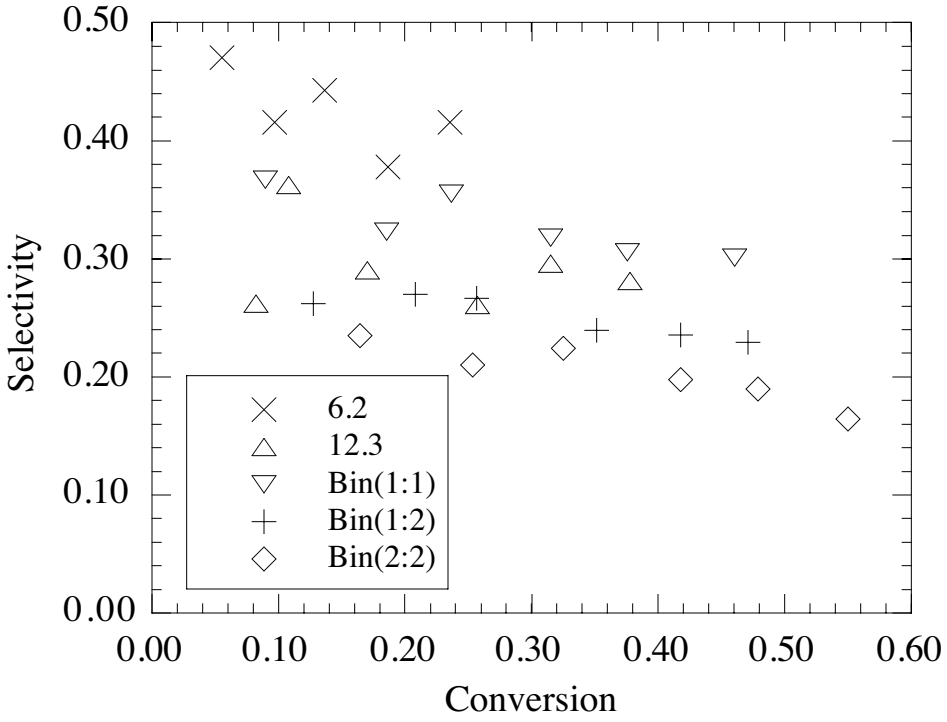

Figure 11: Comparison of ethylene selectivity as a function of conversion and reactant loadings for low pressure reaction sets.

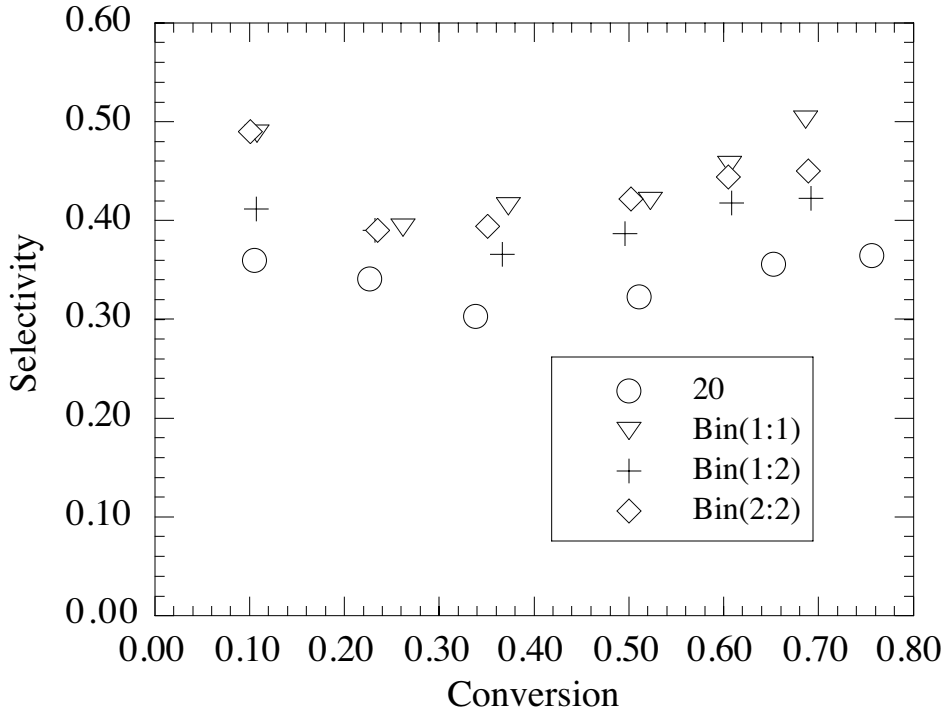

Figure 12: Comparison of toluene selectivity as a function of reactant loading and conversion for low pressure reaction sets.

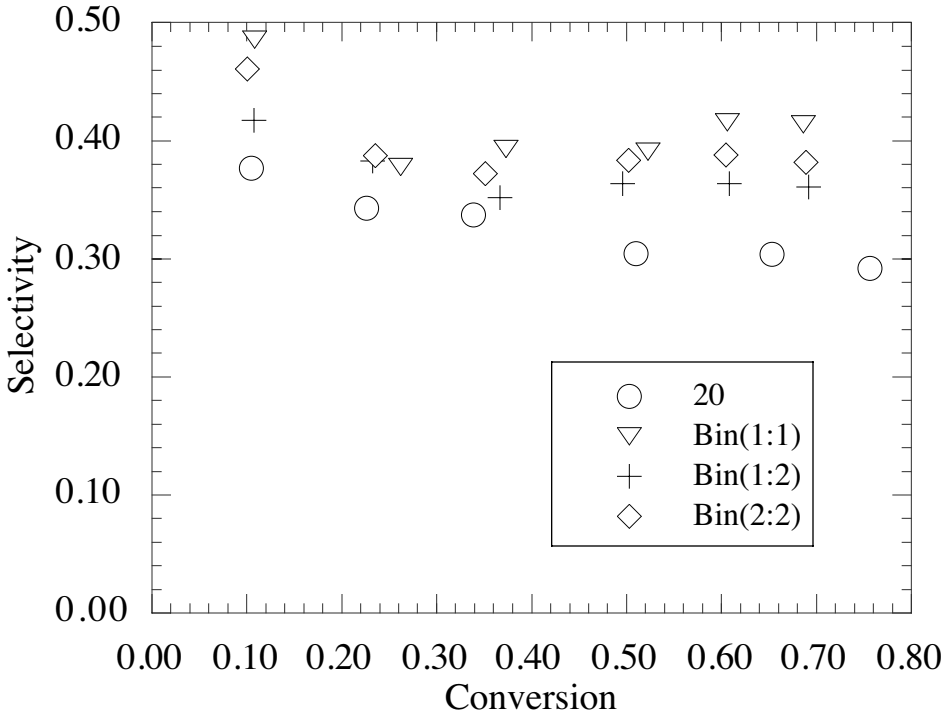

Figure 13: Comparison of 1-methyl-4-(1-naphthylmethyl)benzene as a function of reactant loading and conversion for low pressure reaction sets.

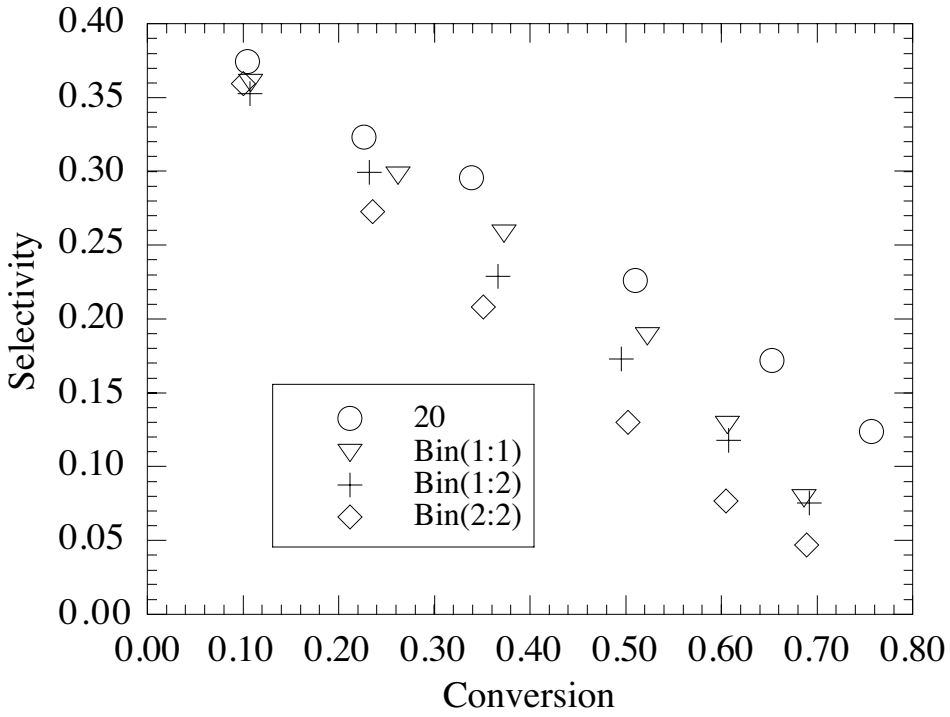

Figure 14: Comparison of selectivities of 1-(2-phenylethenyl)-4-(1-naphthylmethyl)benzene as a function of reactant loading and conversion for low pressure reaction sets.

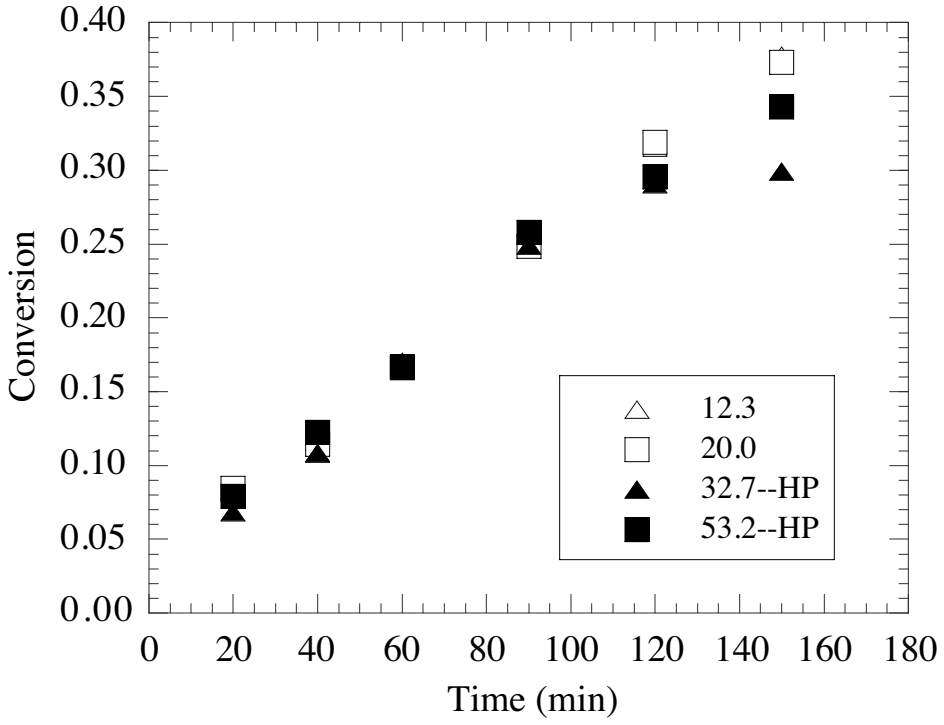

Figure 15: Comparison of conversions for neat tetradecane pyrolyses as a function of reactant concentration and reaction pressure.

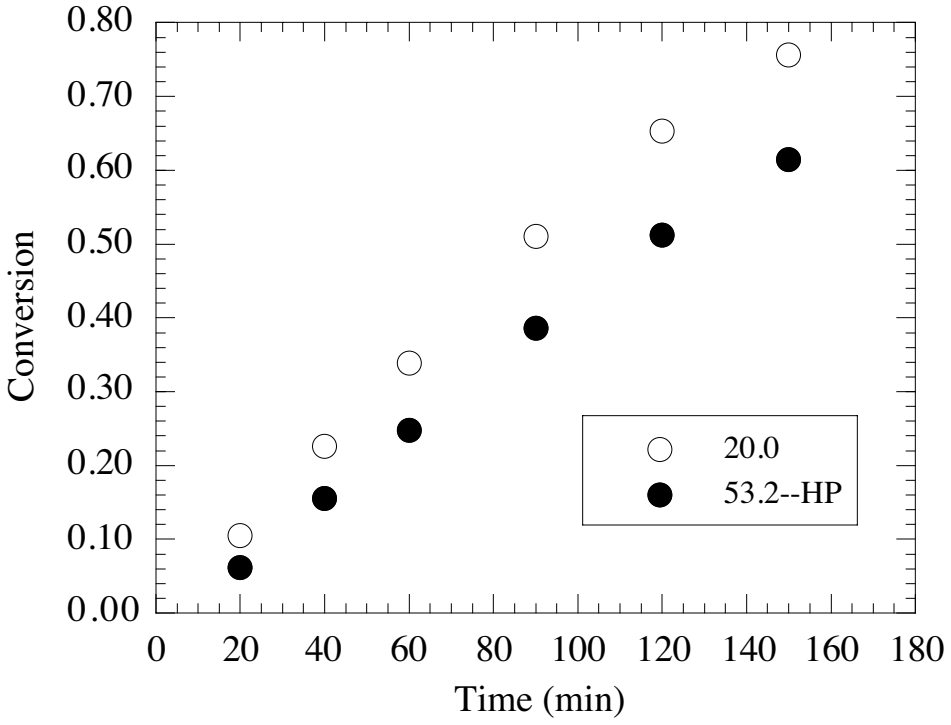

Figure 16: Comparison of NBBM conversion for low and high pressure neat pyrolysis reactions.

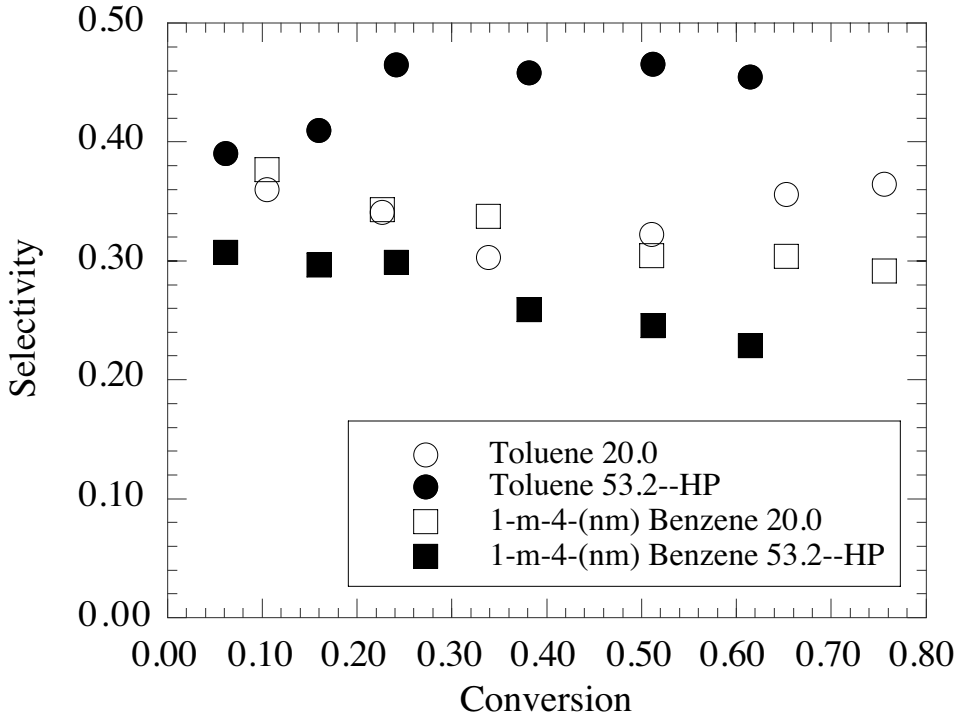

Figure 17: Comparison of toluene and 1-methyl-4-(1-naphthylmethyl)benzene selectivities for neat NBBM pyrolysis as a function of reaction pressure and conversion.

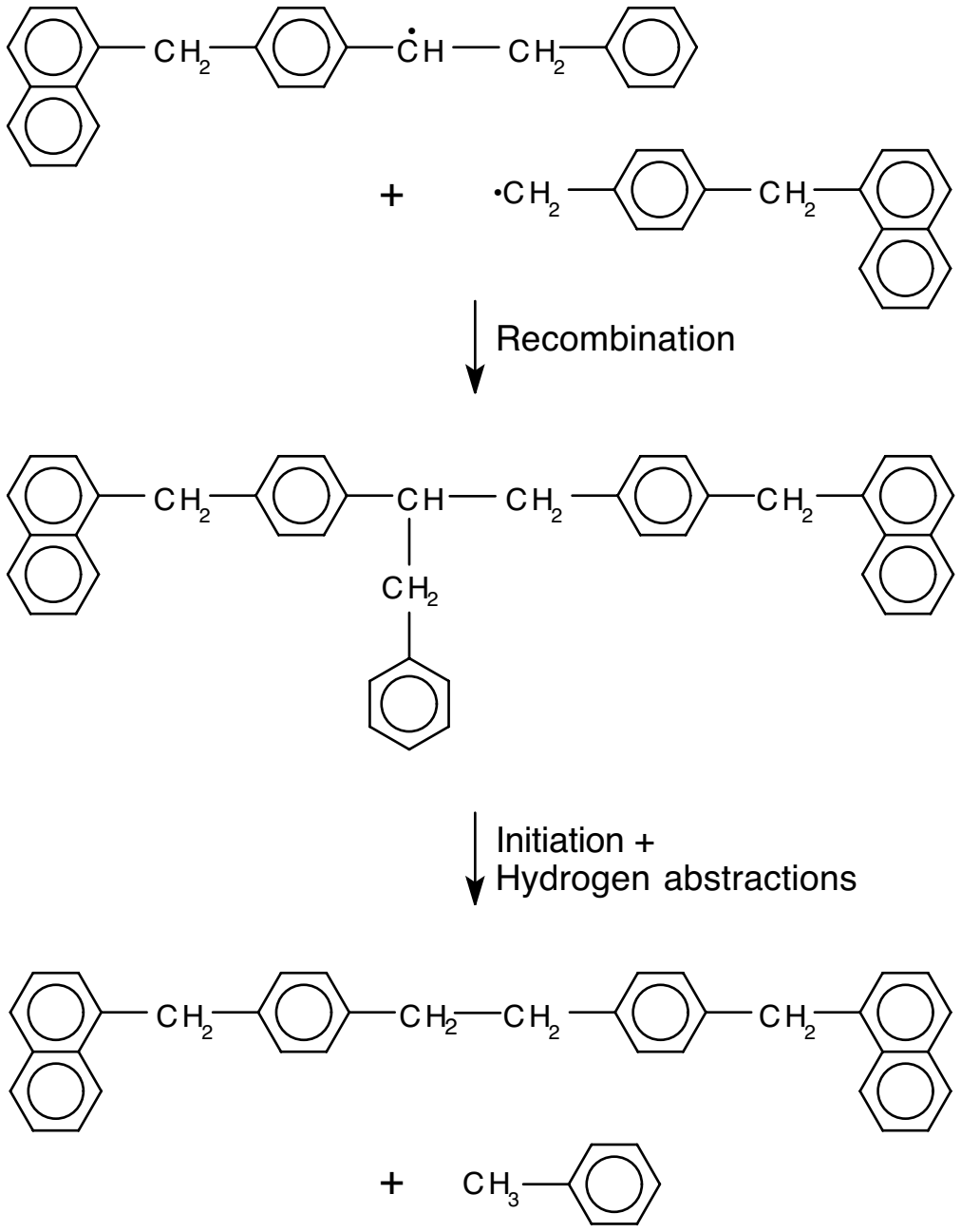

Figure 18: Proposed mechanistic scheme for the formation of toluene at the expense of 1-methyl-4-(1-naphthylmethyl)benzene and 1-(2-phenylethenyl)-4-(1-naphthylmethyl)benzene at high pressures.

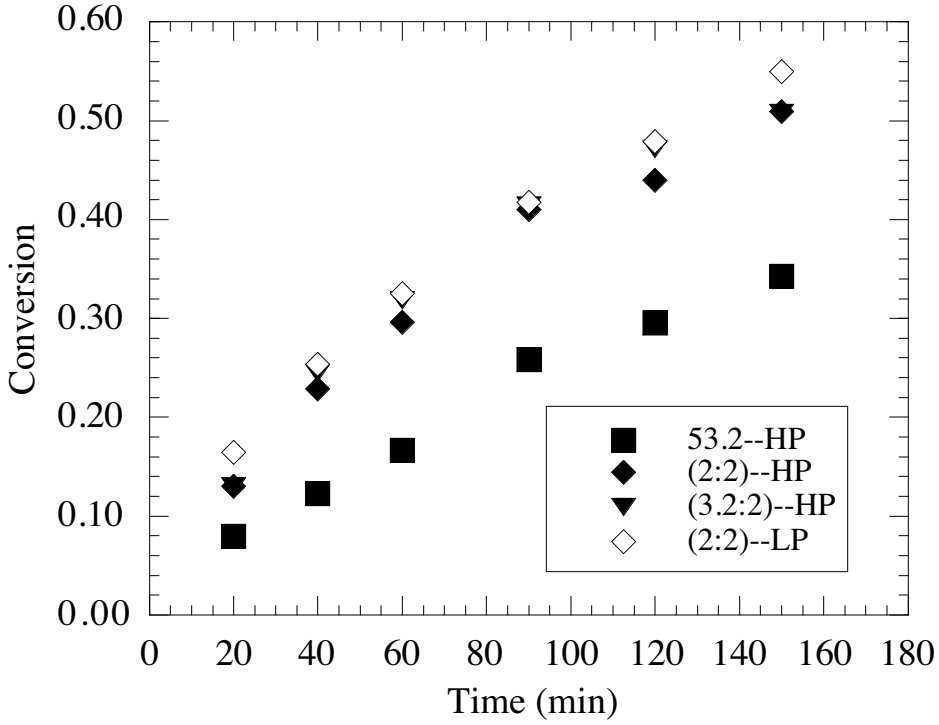

Figure 19: Comparison of tetradecane conversions for binary mixture reactions conducted at low and high pressures.

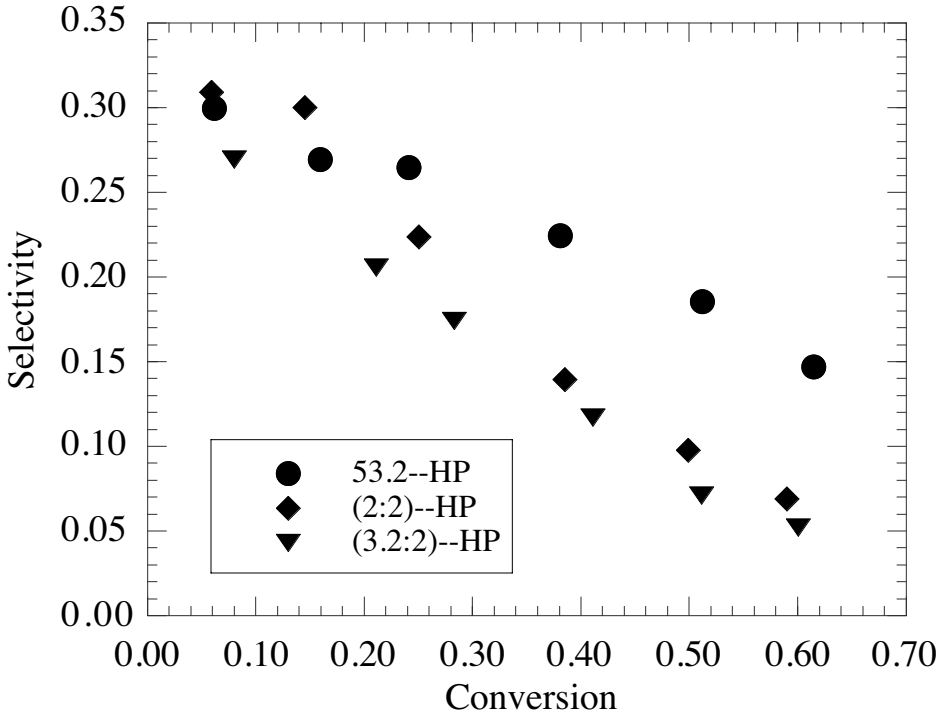

Figure 20: Comparison of 1-(2-phenylethenyl)-4-(1-naphthylmethyl)benzene selectivities as a function of reactant loadings and conversion at high pressures.

Binary Interactions Between High Density Polyethylene and 4-(1-Naphthylmethyl)Bibenzyl During Low Pressure Pyrolysis

Matthew J. De Witt and Linda J. Broadbelt*
Department of Chemical Engineering
Northwestern University
Evanston, Illinois 60208-3120

Abstract

Low pressure pyrolysis experiments employing a high molecular weight polymer and a model compound for coal were conducted to address the effect of phase behavior on the overall degradation mechanism and reaction pathways during coprocessing. Thermal degradation of high density polyethylene (HDPE) and 4-(1-naphthylmethyl)bibenzyl (NBBM) was conducted at 420°C at different reactant loadings, both neat and in binary mixtures. During binary mixture experiments, there was an enhancement in the selectivities to primary products of NBBM at longer reaction times, with a significant reduction in the formation of secondary and tertiary products. These favorable interactions occurred because the polymer induced diffusion limitations in the system compared to neat NBBM pyrolysis, which minimized NBBM self-interactions and promoted reactions with the surrounding polymer. The degradation pathways of HDPE during binary mixture experiments were similar to those during neat reactions, with slight changes to the product yields that were consistent with increasing the overall reactant loading during neat pyrolysis. Variation of the relative reactant loadings indicated that the favorable feedstock interactions were still realized with only slight alterations in the product slate for NBBM and increased yields of saturated species derived from HDPE. Overall, the experiments carried out demonstrated that favorable interactions exist in both the liquid and gas phases during

coprocessing, and primary reaction pathways and the mechanism governing the interactions between the feedstocks were elucidated.

Introduction

The growing abundance of mixed plastic waste and diminishing landfill space in the United States are driving the exploration of new strategies for viable plastics resource recovery. Post-consumer plastic is a major contributor to the municipal solid waste stream, comprising approximately 18% by volume.[1] Disposal through landfilling is becoming a less viable option, however, as the number of landfills closing each year exceeds the number being opened.[2] This poses a significant dilemma because there appears to be no immediate decrease in the usage of plastic products; in fact, due to their versatility, their usage will most likely increase. Current recovery methods suffer from a number of inadequacies, which range from costly separation to the removal of impurities and contaminants. As a result, products manufactured from recycled polymers are of lower quality and higher cost than those produced from the corresponding virgin resins.[3] Therefore, new methods for the recovery of spent plastics must be developed.

A strategy for plastics resource recovery that is currently gaining momentum is tertiary recycling, a method in which the polymers are broken down into their corresponding monomers or into petrochemicals and fuels. However, variations in the supply and composition of the waste plastics and unfavorable economics have restricted the widespread application of this technology. These problems can be minimized, though, by coprocessing polymeric waste with other materials for which a process has already been developed. By incorporating plastics as a co-feed to an existing process, variations in supply and composition can be mediated, allowing for continuous operation. One option is to coprocess plastic waste with coal under direct

liquefaction conditions,[4-6] which may provide for simultaneous conversion of both feedstocks into high-valued fuels and chemicals. Although the viability of coprocessing of plastic waste with coal has been demonstrated,[4-6] the nature of the interactions between the feedstocks is unclear. Process development for these technologies would benefit from a greater understanding of the underlying reaction pathways, kinetics, and mechanism during coprocessing. In order to begin to obtain this information, studies have been conducted in our laboratory using a combination of both model compounds and real feedstocks.

Previous studies employing model compounds for coal and polyethylene demonstrated that favorable interactions exist during binary reactions.[7] It was shown that the selectivities to primary products of the coal model compound were significantly enhanced in the presence of the polymer mimic (tetradecane), which also resulted in increased reactivity of the polymer model compound. These experiments provided substantial insight into the reaction pathways and mechanism controlling the degradation of these species, both neat and in binary mixtures. In the work described here, we have conducted reactions of a high molecular weight reactant, high density polyethylene (HDPE) with $M_w \approx 125{,}000$, neat and in the presence of the coal model compound, 4-(1-naphthylmethyl)bibenzyl (NBBM). The fundamental information obtained from the previous study using model compounds for both reactants was used to help deconvolute the complicated interactions when a real feedstock is used and to understand the effect of phase behavior on the overall degradation mechanism and reaction pathways. The following sections will describe the experimental protocol that was employed and the results obtained for the HDPE/NBBM studies, and these results will be discussed and compared to the experiments with model compounds.

Experimental

Neat and binary mixture experiments were conducted employing high density polyethylene (HDPE) and 4-(1-naphthylmethyl)bibenzyl (NBBM). The reactions were conducted at 420°C in 3.1 mL pyrex ampules for 30-240 minutes. The HDPE was obtained from Aldrich Chemical ($M_w \approx 125{,}000$) in pellet form. It was necessary to melt and cut the HDPE pellets at 120±5°C to obtain samples of appropriate weight; however, the melting conditions were mild enough that no degradation was observed. NBBM has been used repeatedly as a model compound for coal and has successfully predicted the relevant primary products for real systems.[8-11] It contains both condensed and isolated aromatic ring structures joined by short alkyl chains, as well as five different aromatic-aliphatic or aliphatic-aliphatic carbon-carbon bonds. The structure of NBBM is depicted in Figure 1. The ampules were initially charged with the appropriate amount of reactant(s), purged with argon, and then sealed using a propane/oxygen torch. Three sets of neat HDPE experiments, using loadings of 12.3, 20.0 and 27.8 mg, respectively, were conducted. For binary mixture reactions, both the total initial reactant loading and overall reactant ratio were varied. Specific reactant loadings are shown in Tables 1-3. Upon completion of sample preparation, the ampules were placed in an isothermal (±1°C) fluidized sand bath at the specified reaction temperature for a predetermined amount of time. At the end of the reaction period, the ampules were cooled in a room temperature fluidized sand bath. Each reaction time was at minimum duplicated, and in some cases, up to five replicates were performed.

Overall gaseous product yields were obtained employing the same methodology as used for the low pressure model compound studies described previously.[7] Once gas analysis was performed, extraction was carried out by placing the ampules in 14 mL vials, adding

approximately 7 mL of cyclohexane (HPLC-grade) and 20 mg of an external standard (biphenyl), and capping the vials. Cyclohexane was chosen as the solvent since a large range of products could be extracted, but the highest molecular weight compound solubilized could still be analyzed using gas chromatography. Extraction was conducted for a minimum of 12 hours, with occasional manual agitation of the vials. Quantitative analysis through a series of extractions using different solvent volumes for different lengths of time revealed that this protocol was sufficient to completely extract products of carbon numbers less than 24 and partially extract up to carbon number 35. The extracted liquid and solid products were identified and quantified using gas chromatography and mass spectrometry as described for the model compound experiments.[7] The percent conversion of HDPE for this study, X_{HDPE}, was determined using the equation:

$$X_{HDPE} = \frac{W_{g+e}}{W_i} \quad x \quad 100 \qquad (1)$$

where W_i is the initial weight loading of HDPE, and W_{g+e} is the weight of the gaseous and extracted liquid and solid products which were quantified. This same relationship was used to calculate the conversion of HDPE in binary mixture experiments, where W_{g+e} was restricted to products derived from HDPE only. It should be noted that there were extracted liquid and solid products that could not be identified due to low relative yields, and these species were not included in the calculation of X_{HDPE}. In addition, products for carbon numbers C_6 and C_7 could not be fully quantified due to the presence of these species as an impurity in the extraction solvent, and *n*-pentane and 1-pentene yields are believed to be low since there was difficulty in quantifying the liquid fraction of these species. For binary mixture reactions, products of carbon number C_{21} could not be fully quantified because chromatographic peaks for these species were

merged with a peak of a species derived from the coal mimic. The conversion of NBBM was calculated by monitoring its disappearance:

$$X_{NBBM} = \frac{N_{NBBM,o} - N_{NBBM}}{N_{NBBM,o}} \qquad (2)$$

where $N_{NBBM,o}$ is the initial number of moles of NBBM and N_{NBBM} is the number of moles remaining at a given reaction time.

Results and Discussion

Neat Pyrolysis of High Density Polyethylene (HDPE)

The three sets of pyrolysis experiments, using loadings of 12.3, 20.0, and 27.8 mg, respectively, were conducted to provide comparison to reactions using tetradecane and to provide baseline information to which subsequent binary mixture reactions could be compared. Because it was only possible to track the evolution of low molecular weight products from HDPE in detail, a true measure of the polymer conversion was not obtained, and therefore, selectivity values were not used for interpreting the experiments with the polymer. Instead, comparison of reaction products at different reactant loadings was conducted using normalized molar yields, which were defined as the number of moles of product *i* divided by the corresponding moles of reactant charge based on the initial number average molecular weight of HDPE. Representative product yields for neat HDPE pyrolysis are summarized in Table 1. The reproducibility of calculated yield values for the shortest reaction times was ±7%, which decreased with increasing reaction time to ±2% at 240 minutes.

The primary products observed during HDPE pyrolysis were linear hydrocarbons, consisting of α-olefins and *n*-alkanes, which is consistent with results from the literature.[12] Minor yields of internal olefins were found only at reaction times greater than 120 minutes.

These products are similar to those found during tetradecane pyrolysis conducted in our laboratory,[7] indicating that the feedstocks decompose via similar free-radical mechanisms. Light gaseous hydrocarbons and high molecular weight α-olefins were initially found in the highest yields for all reaction sets, and their yields increased with reaction time. The yields of paraffins for carbon numbers greater than C_{10} increased at a faster rate than the corresponding α-olefins. The two products formed in the highest yields for all of the reaction times and reactant loadings studied were ethane and propylene. The trends observed for the *n*-alkanes and α-olefins with respect to reaction time were similar to those observed during our previous studies employing tetradecane.[7]

During the pyrolytic degradation of HDPE, initiation occurs through the fission of a main chain carbon-carbon bond to form two primary radicals. These radicals then propagate through three main types of reactions: intermolecular hydrogen abstraction, intramolecular hydrogen abstraction, and β-scission. Termination occurs through either recombination or disproportionation. These reaction types are consistent with those postulated to occur during low pressure hydrocarbon pyrolysis.[13-15] However, the pyrolysis of HDPE is complicated by the fact that reactions are occurring in both the liquid and the gas phase. The liquid phase is primarily composed of high molecular weight hydrocarbons, while the gas phase consists of low molecular weight species which have diffused from the liquid phase. In the liquid phase, bimolecular reactions involving the polymer, such as intermolecular hydrogen abstraction, will be favored over unimolecular decomposition due to the high concentrations of substrate.[16,17] Unimolecular pathways will initially predominate in the gas phase, but as reaction time proceeds and the concentration of hydrocarbons increases, bimolecular reactions will become more competitive. During HDPE pyrolysis, the two phase system leads to higher relative ratios of *n*-alkanes to α-

olefins than observed during gas-phase tetradecane pyrolysis since saturated hydrocarbons are primarily formed through intermolecular hydrogen abstraction.

The normalized yields of both *n*-alkanes and α-olefins for carbon numbers greater than C_8 were initially found to be very similar. However, there were significant changes in the respective yields as reaction time increased. The yields of lower molecular weight α-olefins of carbon numbers C_8-C_{24} increased more significantly at longer reaction times. Representative trends are shown in Figures 2 and 3 as a function of reaction time and carbon number for the 20 mg reactions. The increased yields of shorter hydrocarbons are observed because these species are more stable than longer compounds due to the lower number of possible sites for main chain cleavage or hydrogen abstraction. In addition, smaller α-olefins can be produced as longer species undergo further degradation.

The *n*-alkanes also showed an increased selectivity towards smaller products as reaction time increased, due to the same reasons discussed in the previous paragraph for α-olefins. However, there was also a marked increase in yields of high molecular weight paraffins. In particular, the yields of *n*-alkanes of carbon numbers C_{20}-C_{24} showed significant growth with reaction time, which is contrary to the behavior for the α-olefins of the same carbon numbers. The α-olefins of these carbon numbers formed at a slightly slower rate than the paraffins and had relatively constant yields for reaction times greater than 90 minutes. The trends for the saturated product yields are presented in Figures 4 and 5 for the 20 mg experiments. The increase in the yields of the full range of *n*-alkanes occurs because the saturated species are primarily formed through hydrogen abstraction reactions, which predominate in the liquid phase and also in the gaseous phase at longer reaction times. As a result, the α-olefin to *n*-alkane ratio became smaller

with increasing reaction time since the paraffins continue to form at increased rates as the olefins undergo further degradation.

As was observed during tetradecane pyrolysis, the initial reactant loading affected the final product distributions obtained during thermal degradation of HDPE. For low molecular weight hydrocarbons (C_1-C_5), the trends observed as a function of initial reactant loading were similar to those observed during studies employing tetradecane in our laboratory.[7] In general, there was a reduction in the formation of methane, ethane and olefins with increasing reactant loading. The yields of propane, butane and pentane were relatively constant with reactant loading.

The yields of longer terminal olefins also decreased as the reactant loading was increased. An example of this trend is shown in Figure 6 where the yield of 1-eicosene ($C_{20}H_{40}$) is plotted as a function of reaction time and reactant loading. The highest yields for 1-eicosene were observed for the 12.3 mg loading experiments, with decreasing yields for increased loadings. The yields of high molecular weight *n*-alkanes, however, followed the opposite trend than that for the α-olefins, increasing with increased reactant loadings. Although higher reactant loadings do not affect the liquid phase concentration, these observations can be attributed to an increase in bimolecular reactions in the gas phase due to higher concentrations as reaction evolves, which is the same effect observed during neat tetradecane pyrolysis.[7] For thermal degradation of both tetradecane and HDPE, the α-olefin to *n*-alkane ratio was found to decrease with increasing reactant loading for all carbon numbers. This trend is shown for the degradation of HDPE in Figure 7 using the ratio of 1-octadecene to *n*-octadecane as a representative example.

Overall, the pyrolysis of HDPE resulted in the same major types of products as those observed during tetradecane pyrolysis, and the relative primary product yields and trends were

similar during tetradecane and HDPE pyrolysis. This indicated that these species degrade via similar reaction mechanisms and that tetradecane is an adequate model compound for identifying the dominant reaction families and in particular, helping to understand the gas phase transformations of HDPE degradation products.

Coprocessing of NBBM with HDPE

Binary mixture reactions using HDPE and NBBM were conducted to probe binary interactions between the reactants, and the results were compared to the model compound studies to determine the effects of phase behavior on reactant conversions and product yields. Both the initial reactant ratio and the overall reactant loading were varied as summarized in Tables 2 and 3. The same experimental procedure used during neat HDPE pyrolysis was employed. Product trends for species derived from HDPE are reported in normalized yields as used for the neat reactions, while selectivity values are used for NBBM-derived products. The use of selectivity values is possible because the conversion of NBBM was directly measured, and selectivities permit for direct comparison of these results to studies previously conducted employing NBBM.[7] The selectivity value of a product was defined as the ratio of the moles of the species formed to the moles of NBBM converted. The reproducibility of yields for HDPE-derived species was the same as for the neat reactions. The error for the selectivities of NBBM-derived species was ±5% at the lowest reaction time and decreased to ±2% for the 240 minute reactions.

The products observed during binary mixture reactions of HDPE and NBBM were similar to those observed during previous studies in our laboratory for the co-reaction of tetradecane and NBBM. The HDPE-derived products quantified by gas chromatography and identified by mass spectrometry were primarily composed of α-olefins and *n*-alkanes, while

NBBM-derived species were identical to those previously reported.[7] The strong phenyl-carbon bonds in NBBM and the absence of aliphatic gas phase species in the neat NBBM product spectra indicate that the aliphatic products observed during binary mixture experiments are derived solely from HDPE. Trends in product yields revealed that synergistic effects similar to those observed during model compound studies existed. During binary mixture reactions with HDPE, there was an increase in the selectivity to primary products of the coal model compound at higher conversions and also a significant reduction in the formation of unsaturated NBBM species. Though these beneficial interactions were similar to those observed during model compound studies, there were some differences in the underlying feedstock interactions due to the phase behavior of the system. In contrast to the tetradecane/NBBM reactions, aliphatic hydrocarbons were present in significant quantities in the liquid phase during HDPE/NBBM coprocessing.

The conversion of NBBM during neat pyrolysis and binary mixture reactions with tetradecane and HDPE is shown in Figure 8. The data set Bin(2:2) corresponds to binary reactions between 12.3 mg of tetradecane and 20.0 mg NBBM at the same reaction conditions, which were previously reported.[7] It can be seen that the conversion of the coal model compound was slightly reduced during coprocessing with HDPE as compared to the previous studies. This can be explained by noting that during reactions with the polymer, the conversion of NBBM will be reduced due to two main factors. First, the recombination of NBBM-derived radicals in the liquid phase following homolysis of the bibenzyl linkage is enhanced compared to the neat reactions due to "cage" effects which are promoted by the polymer,[18-20] which inhibits NBBM degradation. This explanation is consistent with the observation that the conversion of the coal model compound was independent of the initial reactant ratio or overall reactant loading during

coprocessing since the polymer comprises a significant enough portion of the liquid phase to impart "cage" effects for all reaction sets studied. In addition to the effects of diffusion limitations, there is also a reduction in the overall degradation rate of NBBM since there are fewer NBBM self-interactions as compared to neat pyrolysis or coprocessing with tetradecane due to the increased fraction of aliphatic hydrocarbons in the liquid phase. The combination of these effects results in a slight inhibition in the conversion of the coal model compound when reacted with the polymer.

The calculated conversion values for HDPE, X_{HDPE}, were similar during both the neat and the binary mixture reactions. This is contrary to the significant enhancement of tetradecane reactivity that was observed during previous coprocessing studies.[7] These discrepancies can be explained in part by considering that the overall molecular weight distribution was not characterized during the HDPE studies. During reactions employing tetradecane, the reactant is well defined and it is straightforward to calculate a value for reactant conversion, i.e., the total moles of tetradecane converted during the reaction period normalized by the initial moles charged. For reactions with HDPE, however, the reported conversion values are based on the total extracted products that were quantified and do not reflect other changes in the overall molecular weight distribution of the sample indicative of reaction. Molecular weight distributions for the reacted polyethylene samples could not be obtained in our laboratory due to the specialized solvents and high temperature apparatus needed for this analysis. Although the calculated conversions of HDPE are approximately equal as a function of reaction time during coprocessing, the changes in the NBBM-derived product selectivities which will be discussed below indicate that favorable interactions between NBBM and the polymer do exist.

For NBBM-derived products, an enhancement in the selectivities of primary products was observed at higher reactant conversions, while yields of secondary and tertiary products were significantly reduced over the full range of reaction times studied. The selectivity to toluene, one of the primary products of NBBM, is shown for various reaction sets as a function of reactant conversion and reactant loading in Figure 9. The trends shown for toluene are similar to those observed for 1-methyl-4-(1-naphthylmethyl)benzene, the complimentary product formed from fission of the bibenzyl linkage in NBBM, followed by subsequent hydrogen abstraction. The selectivity to toluene during binary mixture reactions with HDPE was initially similar or lower, depending on the reactant loadings, than that observed during neat NBBM pyrolysis. At conversions greater than about 40%, though, the selectivity was significantly enhanced for all reactions with the polymer. This behavior is opposite of that observed during binary reactions with tetradecane, where the selectivity of primary products was enhanced over the entire range of conversions studied.[7] Because the yields of other NBBM-derived species which were quantified were not significantly enhanced at low reactant conversions, new reaction pathways which initially consume the radicals evolved during homolysis of NBBM and lead to products which are not quantified by gas chromatography were implicated. This hypothesis was supported when phenyl and naphthyl ring balances were calculated for the various reaction products quantified. Though the ring balances were very similar for neat and binary mixture reactions conducted with model compounds, balances obtained for binary mixture reactions with HDPE were initially significantly lower. As conversion increased, though, the ring balances for reactions with the polymer approached those obtained during the model compound studies. This indicates that products are initially formed which are not, or can not be, quantified because either they are not solubilized during extraction or do not elute on the column. However, these species must

undergo degradation as reaction time increases. A plausible explanation for these observations is that the NBBM-derived radicals are undergoing liquid phase, bimolecular reactions with the polymer.

In addition to the increase of the selectivity to primary products at higher conversions, there was a significant reduction in the selectivity of products formed through NBBM-NBBM ipso-substitution reaction pathways during coprocessing with HDPE. These observations are consistent with those observed during coprocessing of the model compounds;[7] however, the reduction was much more pronounced for NBBM-HDPE coprocessing. The selectivities for 1-naphthylphenylmethane, a product formed primarily through ipso-substitution pathways at the 1-naphthyl position,[7,11] are shown in Figure 10. The trends for this species are representative of those observed for all other products formed directly through NBBM-NBBM ipso-substitution pathways, and these indicate that HDPE is more effective than tetradecane at preventing these reactions.

During the model compound studies, it was shown that NBBM was primarily in the liquid phase while tetradecane was selectively partitioned into the gas phase.[7] This phase behavior resulted in favorable interactions when NBBM-derived species entered the gas phase. The same benefits are also realized in the present study since low molecular weight species which form as HDPE decomposes partition into the gas phase, particularly at higher conversions. However, the interactions of NBBM-derived species with the polymer as described above result in reduced NBBM self-interactions throughout the full range of reaction times studied.

The increased interactions between NBBM-derived radicals and the polymer are even more apparent when the selectivities for 1-(2-phenylethenyl)-4-(1-naphthylmethyl)benzene are compared for different reaction conditions, as shown in Figure 11. Although the C-H bond

dissociation energy is lower for a carbon on the bibenzyl linkage of NBBM (≅85 kcal mol^{-1}) than on a secondary carbon on HDPE (≅95 kcal mol^{-1})[21] and thus abstraction is energetically favored at the benzylic sites, reaction path degeneracy and diffusion limitations favor interactions with the polymer. Based on estimates from modeling studies in our own lab[22], the rate of abstraction is still 2-3 times higher from NBBM than from HDPE even with reaction path degeneracy included. The reduction in selectivities to 1-(2-phenylethenyl)-4-(1-naphthylmethyl)benzene, indicating that NBBM- and HDPE-derived radicals are primarily stabilized by interacting with polymeric chains rather than with NBBM, suggest that diffusion limitations are important.

As described above, the yields of products formed through NBBM-NBBM ipso-substitution reactions diminished during coprocessing with both tetradecane and HDPE. Accordingly, there was an increase in the selectivities of NBBM-derived species which are formed through competing pathways. The trends for these products were similar during binary mixture reactions with both tetradecane and HDPE; however, there were some products which had higher overall selectivities when NBBM was coprocessed with the polymer as compared to tetradecane. In particular, there were four minor NBBM-derived species, 1-methylnaphthalene, ethylbenzene, p-xylene, and 4-methylbibenzyl, which showed enhanced selectivities during coprocessing with the polymer. These observations were explained by considering the increased interactions with the polymer in the liquid phase contrary to reactions with tetradecane. Concurrent with the increased yields of 1-methylnaphthalene, a decrease in the selectivity to 1,4-bi-(1-naphthylmethyl)benzene, a species formed through an ipso-substitution reaction of a 1-methylnaphthalene radical at the internal phenyl ring of NBBM, was observed. Since NBBM self-interactions are more effectively reduced during reactions with the polymer, there is an increase in selectivities to species whose precursors would be consumed through such pathways,

which is the case for 1-methylnaphthalene. In addition to stabilization effects, substitution reactions involving HDPE-derived radicals and NBBM in the liquid phase can lead to the enhanced formation of other minor NBBM products contrary to reaction with tetradecane. For instance, substitution reactions at the 1-naphthyl position of NBBM or 1-methyl-4-(1-naphthylmethyl)benzene by an HDPE-derived radical would result in the release of radicals that could ultimately form 4-methylbibenzyl or p-xylene. This would allow for the increased yields of these low molecular weight species and also would support the explanation for the diminished ring balances at short reaction times. Analogously, the formation of ethylbenzene can occur through similar substitution reactions at the internal phenyl ring on NBBM.

The effects of coprocessing on the HDPE-derived product slate were very similar to those observed during binary mixture reactions employing tetradecane.[7] During reactions with model compounds, it was observed that the selectivity to high molecular weight *n*-alkanes increased at the expense of longer α-olefins, ethylene and methane. These trends were also apparent for products of all carbon numbers during coprocessing of HDPE and NBBM. These product trends are shown for 1-pentadecene and *n*-pentadecane as representative members of the product classes in Figures 12 and 13, respectively. As a result, the α-olefin to *n*-alkane ratio, which is presented as a function of carbon number in Figure 14 for reactions conducted for 180 minutes, was significantly reduced during the binary mixture reactions. Overall, the trends of adding NBBM to the system followed those observed as the initial loading of HDPE was increased during neat pyrolysis.

With the addition of NBBM, there is a relative increase in the initiation of HDPE-derived radicals in the system due to favorable feedstock interactions. This results in an increase in the rate of termination for these radicals and also a reduction in the repeated unimolecular

degradation steps of high molecular weight radicals. Consequently, the formation of saturated hydrocarbons is favored over unsaturated species. Therefore, the yields of *n*-alkanes increase at the expense of the corresponding α-olefins and gaseous hydrocarbons.

Both the initial reactant ratio and the overall reactant loading strongly influenced the trends for higher molecular weight HDPE-derived product yields during coprocessing. Representative trends are shown for 1-pentadecene and *n*-pentadecane in Figures 12 and 13, respectively. In order to quantify the effect of increasing the initial NBBM to HDPE ratio, the HDPE(12.3:12.3) and HDPE(12.3:20) reaction sets were compared. As the loading of NBBM was increased, there was a significant decrease in the yields of high molecular weight α-olefins with a concurrent increase in the yields of the corresponding paraffins. This is consistent with the explanation for increased yields of saturated species presented in the preceding paragraph since the total radical population increases with increased NBBM loading. The effect of increasing the HDPE reactant loading on product trends for the aliphatic hydrocarbons was also observed during coprocessing with NBBM, which can be discerned by comparing the HDPE(12.3:20) and HDPE(20:20) reaction sets. The paraffin yields once again increased at the expense of the α-olefins, which is consistent with the trends observed during neat HDPE pyrolysis. Overall the lowest α-olefin and highest paraffin yields for high molecular weight species were observed for the HDPE(20:20) reactions, where both increasing the polymer loading and adding NBBM influenced the degradation pathways of the polymer.

In addition to the changes in the product yields for higher molecular weight species, coprocessing was found to affect the product trends for some of the gaseous hydrocarbons. The resulting alterations to the product yields were similar to those observed during coprocessing studies employing tetradecane.[7] For the gaseous species derived from HDPE, the yields of

olefins of carbon numbers C_2-C_5 and methane were most notably affected during coprocessing. The yields for ethylene during binary mixture reactions are shown in Figure 15 and are representative of those observed for the other unsaturated species. The changes in the trends for these species are similar to those observed as the initial concentration of HDPE in the neat experiments was raised and are consistent with a reduction in repeated unimolecular degradation steps of higher molecular weight radicals. In addition to the reduction in the rates of formation, the unsaturated species are also consumed through bimolecular pathways, such as radical addition reactions, as reaction time proceeds.

Conclusions

Binary mixture reactions employing HDPE and NBBM have shown that the feedstock synergism that was observed during reactions with tetradecane and NBBM was still obtained.[7] In this study, there was an increase in selectivity to primary products of the coal model compound with a significant reduction in the formation of secondary and tertiary products. The major difference in the product trends for reactions with the polymer, though, is that there was initially a minimal enhancement or inhibition in the formation of primary products of NBBM, depending upon reactant loadings, followed by subsequent enhancement. This observation, in addition to the reduced selectivity to secondary and tertiary products of NBBM as compared to the model compound studies, was primarily due to the differences in the phase behavior in the reaction system during coprocessing with HDPE. In this study, the high proportion of HDPE in the liquid phase induced diffusion limitations in the system which resulted in a slight reduction in the rate of NBBM degradation, but also minimized NBBM self-reactions by promoting reactions with the surrounding polymer. However, the HDPE-NBBM interactions initially led to

alternative reaction pathways for the coal-derived radicals to form products which could not be identified and quantified. These products eventually underwent degradation themselves, though, resulting in significantly enhanced selectivities for primary products at longer reaction times. Therefore, the increase in selectivity to primary NBBM products observed during previous studies was still realized, but as an added benefit, there was a significant reduction in the formation of NBBM ipso-substitution products.

The effects of coprocessing on the HDPE-derived product yields were similar to those observed during studies employing tetradecane, where a significant increase in the yields of high molecular weight paraffins at the expense of the full range of α-olefins was observed. The changes were more marked for reactions with the polymer, though, which were attributed to the occurrence of additional bimolecular reactions in the liquid phase which resulted in the formation of *n*-alkanes and consumption of α-olefins. Increasing the relative loadings of the components only slightly altered the product selectivities for NBBM but resulted in enhanced yields of longer alkanes at the expense of α-olefins. These observations were consistent with increasing the overall polymer loading during neat pyrolysis.

Overall, the degradation mechanisms of HDPE and tetradecane are similar for both neat pyrolysis and reaction in the presence of NBBM. By employing the information obtained from previous model compound studies,[7] it was possible to deconvolute the complicated feedstock interactions and identify the relevant reaction pathways during reactions employing the polymer. Therefore, the model compound reactions that were previously carried out provided valuable insight and guidance when reactions with a more complicated feedstock were performed.

Acknowledgment The authors are grateful for financial support from the United States Department of Energy, Grant DE-FG22-96-PC96204.

References

(1) Rowatt, R. J., *Chemtech,* **1993**, *23(1)*, 56-60.

(2) Pett, R. A.; Golovoy, A.; Labana, S. S., In *Plastics, Rubber, and Paper Recycling: A Pragmatic Approach* ; Rader, C. P., Baldwin, S. D., Cornell, D. D., Sadler, G. D., Stockel, R. F., Eds.; American Chemical Society: Washington, DC, 1995; Vol. 609, pp 47.

(3) Graff, G., *Modern Plastics,* **1992**, *69(7)*, 45.

(4) Taghei, M.; Feng, Z.; Huggins, F.; Huffman, G. R., *Energy & Fuels,* **1994**, *8*, 1228-1232.

(5) Joo, H. K.; Curtis, C. W., *Energy & Fuels,* **1997**, *11(4)*, 801-812.

(6) Rothenberger, K. S.; Cugini, A. V.; Thompson, R. L.; Ciocco, M. V., *Energy & Fuels,* **1997**, *11(4)*, 849-855.

(7) De Witt, M. J.; Broadbelt, L. J., *Energy & Fuels,* **1999**, *in press*.

(8) Farcasiu, M.; Smith, C., *Energy & Fuels,* **1991**, *5(1)*, 83-87.

(9) Matson, D. W.; Linehan, J. C.; Darab, J. G.; Buehler, M. F., *Energy & Fuels,* **1994**, *8*, 10-18.

(10) Tang, Y.; Curtis, C. W., *Energy & Fuels,* **1994**, *8*, 63.

(11) Walter, T. D.; Casey, S. M.; Klein, M. T.; Foley, H. C., *Catalysis Today,* **1994**, *19*, 367-380.

(12) Ng, S. W.; Seoud, H.; Stanciulescu, M.; Sugimoto, Y., *Energy & Fuels,* **1995**, *9*, 735-742.

(13) Rice, F. O., *Journal of the American Chemical Society,* **1933**, *55*, 3035-3040.

(14) Rice, F. O.; Herzfeld, K. F., *Journal of the American Chemical Society,* **1934**, *56*, 284-289.

(15) Kossiakoff, A.; Rice, F. O., *Journal of the American Chemical Society,* **1943**, *65*, 590-595.

(16) Wu, G.; Katsumura, Y.; Matsuura, C.; Ishigure, K.; Kubo, J., *Industrial & Engineering Chemistry Research,* **1996**, *35*, 4747-4754.

(17) Ford, T. J., *Industrial & Engineering Chemistry Research,* **1986**, *25*, 240-243.

(18) Moore, J. W.; Pearson, R. G. (1981). Kinetics and Mechanism. New York, John Wiley & Sons, Inc.

(19) Kochi, J. K. (1973). Free Radicals. New York, John Wiley & Sons, Inc.

(20) Stein, S. E.; Robaugh, D. A.; Alfieri, A. D.; Miller, R. E., *J. Am. Chem. Soc.*, **1982**, *104*, 6567-6570.

(21) Stein, S. E. (1994). NIST Structures & Properties Database Version 2.0. Gaithersburg, MD.

(22) De Witt, M. J., Ph.D. Dissertation, Northwestern University, Evanston, IL, **1999**.

Table 1: Representative Experimental Data for Neat HDPE Pyrolysis

Reaction Set	12.3	12.3	12.3	20	20	20	27.8	27.8	27.8
Reaction Time (min)	30	90	150	30	90	150	30	90	150
HDPE Loading (mg)	12.3	12.2	12.3	20.2	20.0	19.9	28.1	27.8	27.6
HDPE Conversion	0.04	0.21	0.34	0.05	0.23	0.36	0.05	0.20	0.32
Normalized Yield [a]									
methane	0.00	11.61	33.88	1.49	14.07	35.46	1.51	11.04	28.90
ethylene	2.81	13.87	31.77	2.79	14.02	27.83	1.93	10.15	20.39
ethane	2.29	14.01	37.96	2.60	16.76	41.71	1.80	13.21	33.85
propylene	5.18	21.93	51.71	5.55	24.84	52.72	3.95	19.62	41.74
propane	3.17	11.50	27.47	3.64	14.61	32.86	2.71	12.30	28.03
1-butene	3.90	11.05	22.80	4.11	12.09	23.09	3.08	9.57	18.30
n-butane	2.50	8.17	16.80	2.78	9.74	19.75	2.02	8.17	16.75
1-pentene	1.03	4.62	11.59	1.07	5.14	11.08	0.75	3.83	8.20
n-pentane	0.85	1.72	7.24	0.88	3.86	8.15	0.66	2.99	6.62
1-octene	0.28	3.35	7.12	0.75	4.36	8.51	0.56	3.56	7.33
n-octane	0.26	2.45	4.65	0.93	3.44	6.24	0.65	3.08	6.07
1-nonene	0.61	3.52	7.00	0.59	4.19	7.41	0.68	3.59	6.68
n-nonane	0.45	2.22	4.11	0.71	3.18	5.55	0.53	2.81	5.60
1-decene	0.73	4.23	7.66	1.02	4.76	7.77	0.99	4.07	6.77
n-decane	0.23	2.12	3.69	0.65	2.97	5.24	0.51	2.73	5.00
1-undecene	0.89	3.71	6.64	0.97	4.19	6.64	0.86	3.74	6.10
n-undecane	0.55	2.54	4.33	0.69	3.08	4.94	0.61	3.02	5.38
1-dodecene	0.76	3.25	5.55	0.41	3.51	5.53	0.70	3.03	4.90
n-dodecane	0.57	2.48	3.99	0.62	2.91	4.62	0.61	2.81	4.70
1-tridecene	0.70	2.87	5.29	0.69	3.07	4.68	0.65	2.66	4.14
n-tridecane	0.50	2.22	3.66	0.55	2.70	4.40	0.55	2.58	4.45
1-tetradecene	0.82	3.13	4.88	0.78	3.00	4.62	0.81	2.76	4.06
n-tetradecane	0.54	2.15	3.52	0.51	2.45	4.09	0.54	2.42	4.17
1-pentadecene	0.84	2.76	4.18	0.79	2.76	3.85	0.72	2.39	3.40
n-pentadecane	0.51	2.08	3.32	0.54	2.47	3.85	0.53	2.36	3.94
1-hexadecene	0.65	2.34	3.49	0.65	2.39	3.23	0.58	2.03	2.77
n-hexadecane	0.53	2.02	3.18	0.51	2.41	3.73	0.51	2.29	3.78
1-heptadecene	0.67	2.10	3.05	0.60	2.04	2.76	0.53	1.77	2.34
n-heptadecane	0.47	1.85	2.89	0.47	2.17	3.39	0.47	2.12	3.42
1-octadecene	0.63	1.96	2.75	0.59	1.93	2.41	0.54	1.64	2.07
n-octadecane	0.48	1.84	2.79	0.44	2.10	3.15	0.44	2.03	3.22
1-nonadecene	0.61	1.70	2.29	0.50	1.67	1.95	0.47	1.41	1.68
n-nonadecane	0.43	1.64	2.62	0.41	1.99	2.90	0.41	1.94	2.98
1-eicosene	0.54	1.60	2.05	0.45	1.49	1.73	0.46	1.23	1.42
n-eicosane	0.45	1.67	2.49	0.37	1.95	2.80	0.42	1.86	2.81
1-heneicosene	0.49	1.40	1.91	0.41	1.32	1.49	0.38	1.06	1.20
n-heneicosane	0.40	1.61	2.37	0.38	2.05	2.72	0.38	1.90	2.80
1-docosene	0.53	1.37	1.58	0.41	1.26	1.34	0.43	0.96	1.04
n-docosane	0.38	1.50	2.15	0.35	1.86	2.65	0.35	1.68	2.54
1-tricosene	0.45	1.25	1.27	0.38	1.08	1.11	0.38	0.84	0.79
n-tricosane	0.31	1.51	2.02	0.15	1.76	2.47	0.35	1.62	2.34
1-tetracosene	0.00	0.93	0.51	0.32	0.93	0.80	0.29	0.62	0.51
n-tetracosane	0.00	1.33	2.46	0.00	1.63	2.28	0.25	1.50	2.29
C25 [b]	0.25	2.16	2.89	0.24	2.43	2.87	0.54	2.11	2.55
C26	0.00	2.25	2.66	0.28	2.19	2.53	0.52	1.94	2.31
C27	0.00	2.09	2.81	0.17	1.98	2.29	0.47	1.79	2.03
C28	0.00	1.98	2.10	0.25	1.78	2.11	0.48	1.63	1.84
C29	0.00	1.88	1.95	0.33	1.66	1.91	0.38	1.53	1.67
C30	0.00	1.67	1.77	0.24	1.53	1.71	0.17	1.39	1.45
C31	0.00	1.48	1.52	0.14	1.15	1.43	0.14	1.25	1.29
C32	0.00	1.37	1.27	0.00	0.52	1.26	0.00	1.11	1.14
C33	0.00	0.00	0.00	0.00	0.52	0.96	0.00	0.89	0.94
C34	0.00	0.00	0.00	0.00	0.00	0.34	0.00	0.00	0.68

(a) Normalized yield defined as (moles species i formed)/(initial moles HDPE).

(b) Ci corresponds to sum of 1-alkene and n-alkane yields for carbon number i.

Table 2: Representative Experimental Data for HDPE-Derived Products During Binary Mixture Pyrolysis with NBBM

Reaction Set	(12.3:12.3) [b]	(12.3:12.3)	(12.3:12.3)	(12.3:20)	(12.3:20)	(12.3:20)	(20:20)	(20:20)	(20:20)
Reaction Time (min)	30	90	150	30	90	150	30	90	150
HDPE Loading (mg)	12.2	12.4	12.2	12.1	12.4	12.3	20.1	20.0	20.0
HDPE Conversion	0.05	0.20	0.33	0.04	0.20	0.32	0.05	0.20	0.32
NBBM Loading (mg)	12.2	12.3	12.2	20.0	20.0	19.9	20.0	19.9	19.9
Normalized Yield [a]									
methane	1.64	15.37	38.07	1.91	12.13	36.34	1.48	13.79	33.01
ethylene	2.69	13.16	26.23	2.39	9.84	21.87	1.98	10.39	18.52
ethane	2.93	18.17	44.25	2.13	15.30	41.24	2.44	17.00	39.00
propylene	5.02	22.28	45.49	4.06	17.91	38.86	4.48	19.81	36.72
propane	3.30	14.20	31.84	2.74	12.24	29.92	3.13	14.21	30.16
1-butene	3.57	10.52	18.88	3.12	8.64	16.93	3.58	9.19	15.68
n-butane	2.57	9.35	18.67	2.16	8.54	18.59	2.41	9.18	18.48
1-pentene	0.86	4.32	8.58	0.55	2.71	7.35	0.67	3.20	6.65
n-pentane	2.36	3.52	7.70	0.61	3.84	5.76	0.79	2.97	6.97
1-octene	0.73	4.45	7.59	0.88	3.62	6.99	0.75	3.87	6.10
n-octane	0.69	3.57	6.15	0.81	3.47	6.97	0.68	3.82	6.57
1-nonene	0.78	3.60	6.60	0.67	3.39	5.75	0.70	3.30	5.56
n-nonane	0.57	2.83	5.42	0.55	2.91	5.86	0.59	3.26	6.43
1-decene	1.13	4.33	6.91	1.04	3.87	5.78	1.07	3.80	5.43
n-decane	0.55	2.49	4.96	0.53	2.68	5.41	0.59	2.97	6.11
1-undecene	0.89	3.49	5.83	0.79	3.10	4.78	0.85	3.17	4.79
n-undecane	0.60	2.81	5.24	0.58	2.92	5.74	0.65	3.08	5.85
1-dodecene	0.72	3.00	4.66	0.63	2.74	4.11	0.68	2.68	3.73
n-dodecane	0.60	2.68	4.81	0.56	2.89	5.42	0.61	2.97	5.45
1-tridecene	0.67	2.93	4.16	0.60	2.67	3.33	0.66	2.52	3.07
n-tridecane	0.52	2.44	4.40	0.50	2.65	4.99	0.56	2.68	5.22
1-tetradecene	0.91	2.70	3.26	0.98	2.20	2.75	0.75	2.20	2.67
n-tetradecane	0.53	2.42	4.14	0.50	2.49	4.68	0.51	2.60	4.86
1-pentadecene	0.77	2.38	3.19	0.72	2.09	2.65	0.68	1.96	2.43
n-pentadecane	0.60	2.33	4.09	0.53	2.52	4.61	0.56	2.60	4.74
1-hexadecene	0.70	2.39	3.23	0.63	2.16	2.52	0.64	2.10	2.21
n-hexadecane	0.60	2.67	4.32	0.59	2.55	4.60	0.59	2.85	4.66
1-heptadecene	0.63	2.07	2.64	0.54	1.92	2.30	0.52	1.75	2.18
n-heptadecane	0.48	2.19	3.66	0.50	2.37	4.15	0.49	2.39	4.20
1-octadecene	0.55	1.65	1.95	0.45	1.43	1.61	0.50	1.40	1.47
n-octadecane	0.48	2.13	3.51	0.43	2.26	3.91	0.47	2.29	3.95
1-nonadecene	0.49	1.39	1.82	0.40	1.22	1.27	0.42	1.28	1.20
n-nonadecane	0.42	1.97	3.45	0.41	2.31	3.97	0.41	2.34	3.91
1-eicosene	0.46	1.19	1.17	0.39	0.93	0.88	0.37	0.88	0.79
n-eicosane	0.47	1.98	3.20	0.45	2.12	3.51	0.43	2.11	3.50
1-heneicosene	-	-	-	-	-	-	-	-	-
n-heneicosane	-	-	-	-	-	-	-	-	-
1-docosene	0.37	0.88	0.78	0.32	0.65	0.65	0.29	0.63	0.61
n-docosane	0.41	1.80	2.83	0.39	1.97	2.65	0.39	2.06	2.79
1-tricosene	0.29	0.75	0.54	0.19	0.67	0.51	0.30	0.62	0.38
n-tricosane	0.34	1.87	3.34	0.49	2.17	3.11	0.37	2.06	3.15
1-tetracosene	0.00	0.51	0.32	0.00	0.37	0.29	0.26	0.47	0.31
n-tetracosane	0.04	1.93	3.12	0.22	2.34	2.79	0.32	2.31	3.08
C25 [c]	0.00	2.11	3.13	0.00	2.44	2.99	0.26	2.31	3.00
C26	0.17	2.35	3.02	0.24	2.46	3.14	0.43	2.31	3.11
C27	0.19	2.05	2.47	0.52	2.05	2.57	0.38	2.09	2.72
C28	0.52	1.57	1.87	0.42	1.51	1.97	0.44	1.64	2.10
C29	0.49	1.17	1.89	0.27	1.65	2.10	0.30	1.60	2.17
C30	0.24	1.40	1.54	0.00	1.35	1.53	0.14	1.49	1.74
C31	0.00	1.38	1.58	0.00	1.35	1.61	0.03	1.36	1.69
C32	0.00	0.00	0.00	0.00	0.00	0.00	0.00	0.14	0.00
C33	0.00	0.00	0.00	0.00	0.00	1.14	0.00	0.73	0.93
C34	0.00	0.00	0.00	0.00	0.00	0.00	0.00	0.14	0.27

(a) Product yield defined as (moles species i formed)/(initial moles HDPE) (b) (a:b) denotes ratio of *a* mg of HDPE to *b* mg of NBBM loaded.

(c) Ci corresponds to sum of 1-alkene and n-alkane yields for carbon number i.

Table 3: Representative Experimental Data for NBBM-Derived Products During Neat and Binary Mixture Pyrolysis with HDPE

Reaction Set	Neat	Neat	Neat	(12.3:12.3) [c]	(12.3:12.3)	(12.3:12.3)	(12.3:20)	(12.3:20)	(12.3:20)	(20:20)	(20:20)	(20:20)
Reaction Time (min)	40	90	120	30	90	150	30	90	150	30	90	150
NBBM Loading (mg)	20.3	19.9	20.3	12.2	12.3	12.2	20.0	20.0	19.9	20.0	19.9	19.9
NBBM Conversion	0.23	0.51	0.65	0.19	0.46	0.63	0.20	0.45	0.62	0.22	0.45	0.63
HDPE Loading (mg)	0.0	0.0	0.0	12.2	12.4	12.2	12.1	12.4	12.3	20.1	20.0	20.0
Product Yield (x10 ^{2}) [a]												
toluene	7.58	16.45	23.14	5.99	18.71	29.91	6.12	17.28	28.06	5.38	18.16	27.30
ethylbenzene	0.00	0.00	0.41	0.20	0.69	2.15	0.17	0.89	1.93	0.21	1.16	2.38
p-xylene	0.00	0.56	1.12	0.12	0.68	2.57	0.10	0.86	2.39	0.13	1.03	2.71
naphthalene	0.23	0.73	1.18	0.19	0.81	2.38	0.19	1.02	3.01	0.17	0.94	2.68
1-methylnaphthalene	0.26	0.87	1.52	0.38	1.37	2.36	0.30	1.23	2.07	0.34	1.42	2.38
bibenzyl	0.09	0.24	0.41	0.00	0.00	0.00	0.00	0.00	0.00	0.04	0.09	0.14
4-methylbibenzyl	1.10	2.40	3.22	1.28	2.98	4.43	1.14	3.16	4.89	1.17	3.13	4.67
1-methyl-4-(2-phenylethenyl)-benzene	0.09	0.53	0.98	0.05	0.21	0.24	0.05	0.21	0.22	0.05	0.20	0.20
1-naphthylphenyl methane	0.81	2.67	4.24	0.45	1.02	1.12	0.38	1.11	1.60	0.31	0.92	1.31
1-methyl-4-(1-*A*)benzene [b]	7.63	15.43	19.75	6.75	18.63	27.54	5.94	16.57	23.88	5.28	15.38	21.60
1-benzyl-4-(1-*A*)benzene	0.33	1.65	2.74	0.09	0.34	0.52	0.10	0.45	0.71	0.09	0.43	0.63
1-(4-methylbenzyl)-4-(1-*A*)benzene	1.37	2.59	2.95	0.89	1.79	2.13	0.92	2.01	2.37	0.97	2.15	2.46
1-(2-phenylethenyl)-4-(1-*A*)benzene	7.18	11.48	11.17	3.93	3.98	2.57	3.84	3.78	2.46	3.47	3.71	2.54
1,4-(bi-1-*A*)benzene	0.83	2.73	4.11	0.00	0.56	0.76	0.00	0.79	1.05	0.15	0.61	0.85

(a) Product yield defined as (moles species i formed)/(initial moles NBBM). (b) Symbol *A* denotes (naphthylmethyl).

(c) (a:b) denotes ratio of *a* mg of HDPE to *b* mg of NBBM loaded.

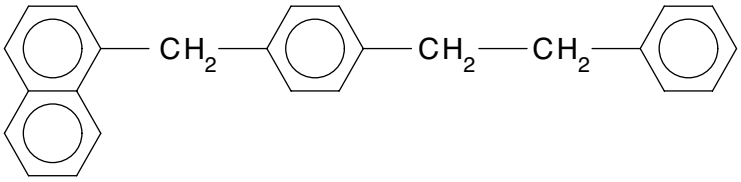

Figure 1: Structure of coal model compound 4-(1-naphthylmethyl)bibenzyl.

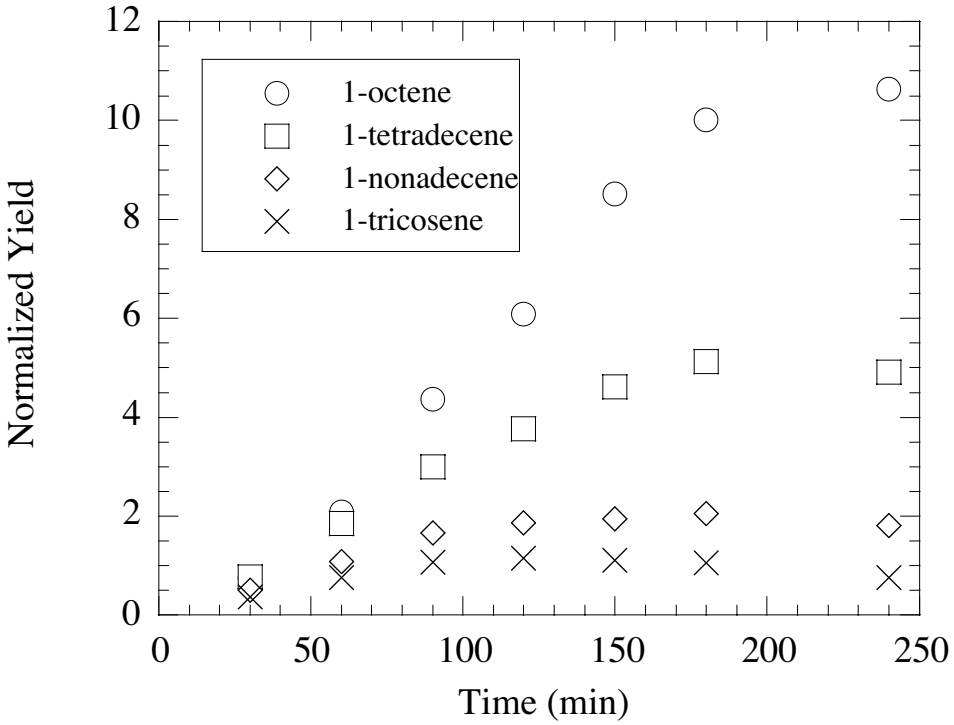

Figure 2: Comparison of normalized yields of selected α-olefins for 20 mg reactant loading of HDPE.

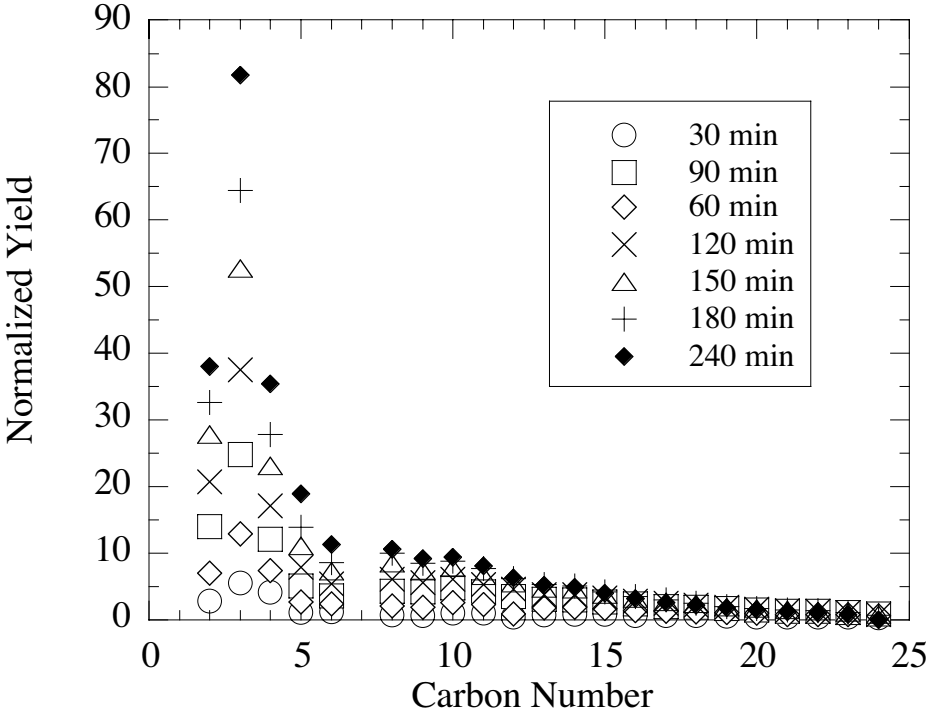

Figure 3: Comparison of normalized yields of α-olefins as a function of reaction time and carbon number for 20 mg reactant loading of HDPE.

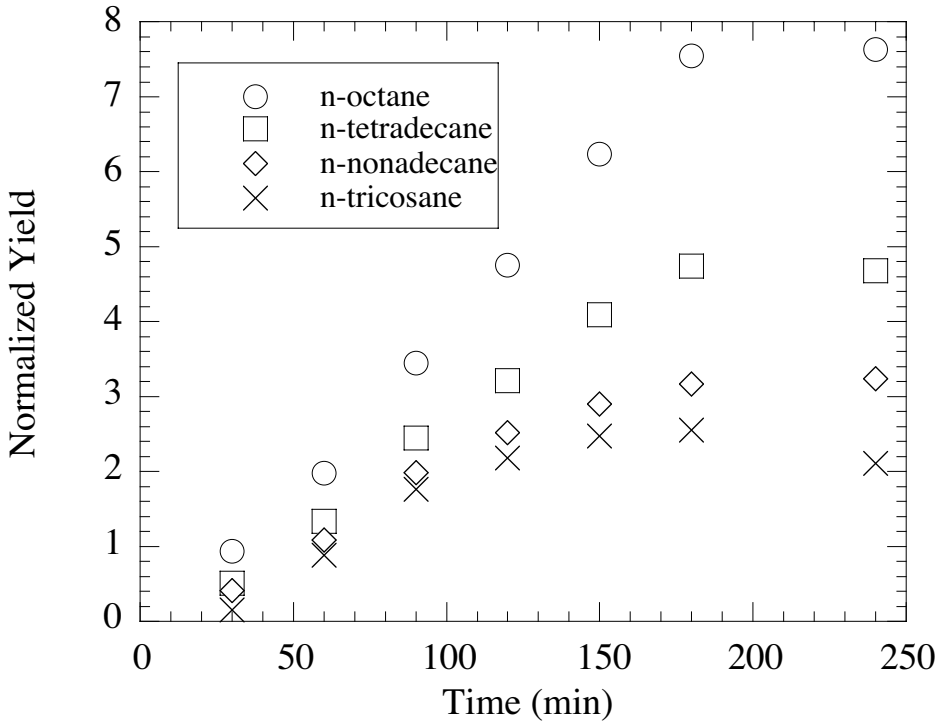

Figure 4: Comparison of normalized yields of selected *n*-alkanes for 20 mg reactant loading of HDPE.

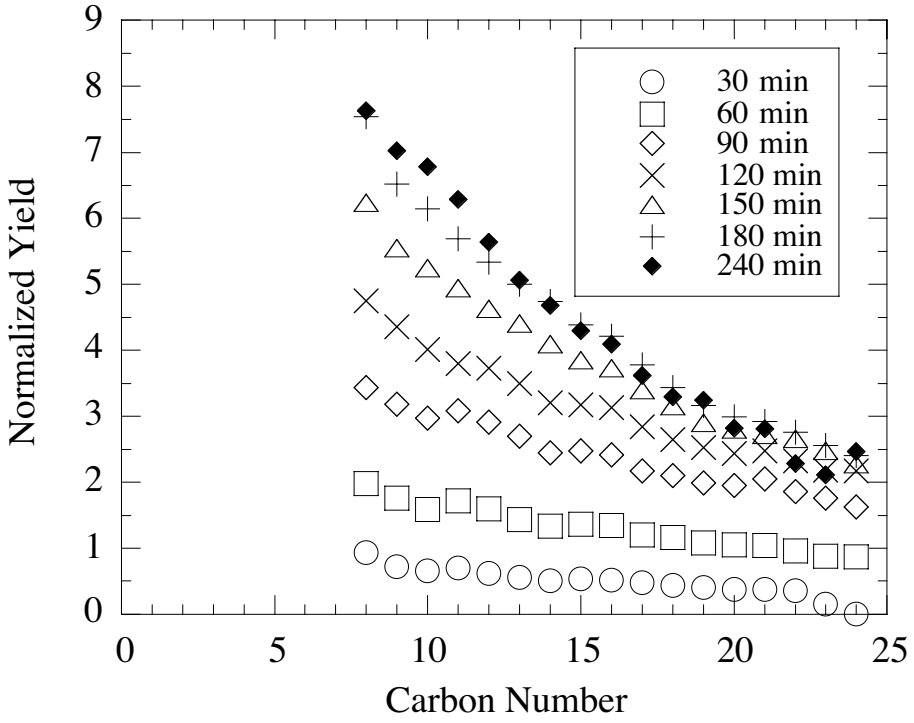

Figure 5: Comparison of normalized yields of *n*-alkanes as a function of reaction time and carbon number for 20 mg reactant loading of HDPE.

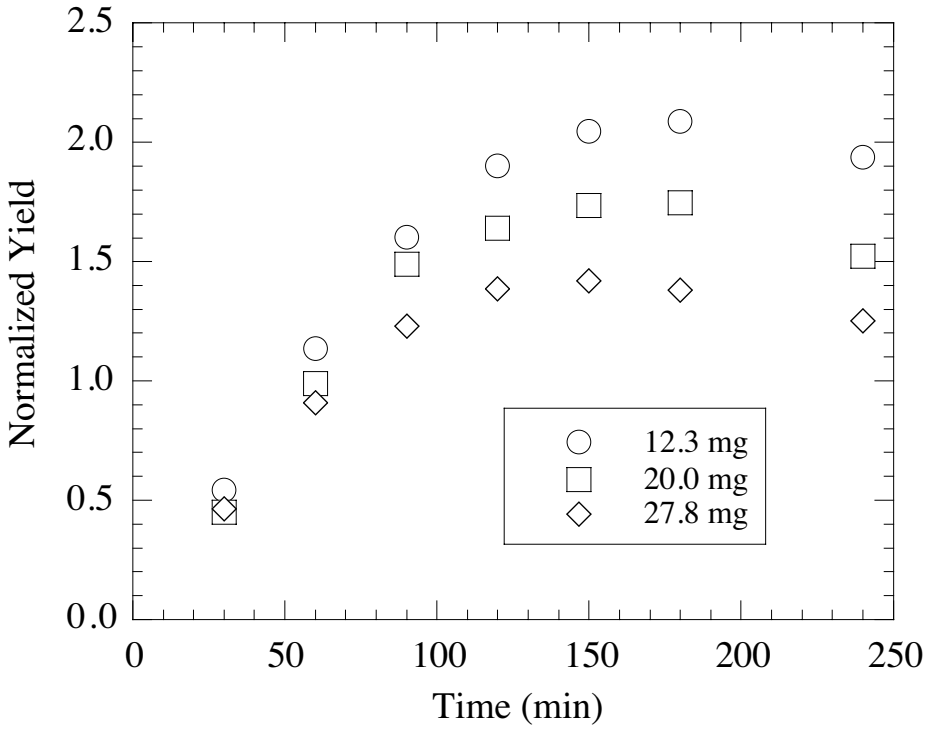

Figure 6: Comparison of normalized yields of 1-eicosene as a function of reaction time and reactant loading for neat pyrolysis of HDPE.

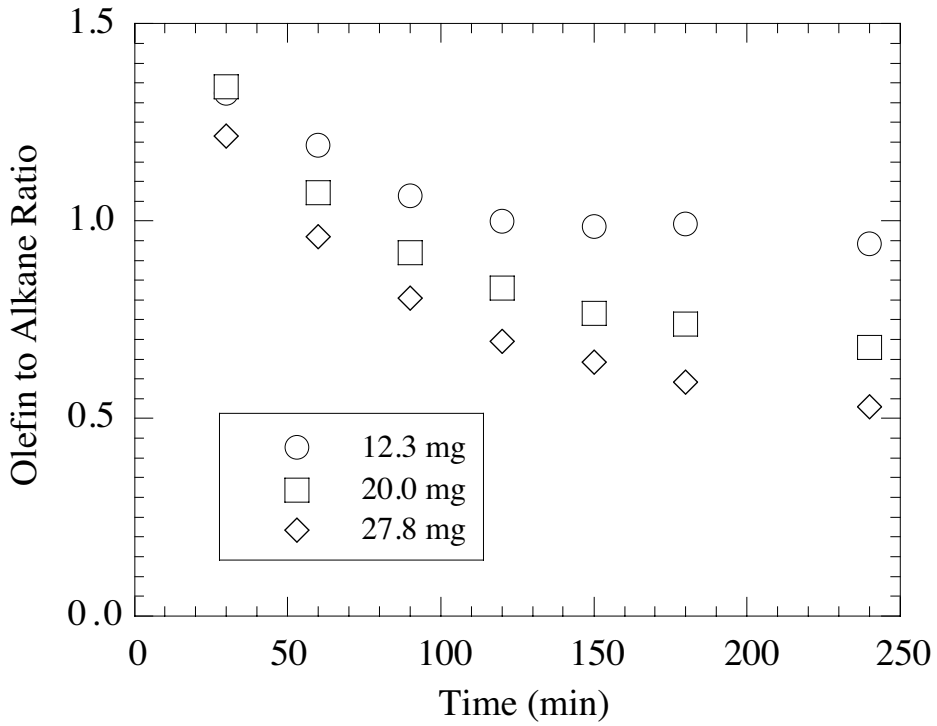

Figure 7: Comparison of α-olefin to *n*-alkane ratio for C_{18} as a function of reaction time and reactant loading for neat pyrolysis of HDPE.

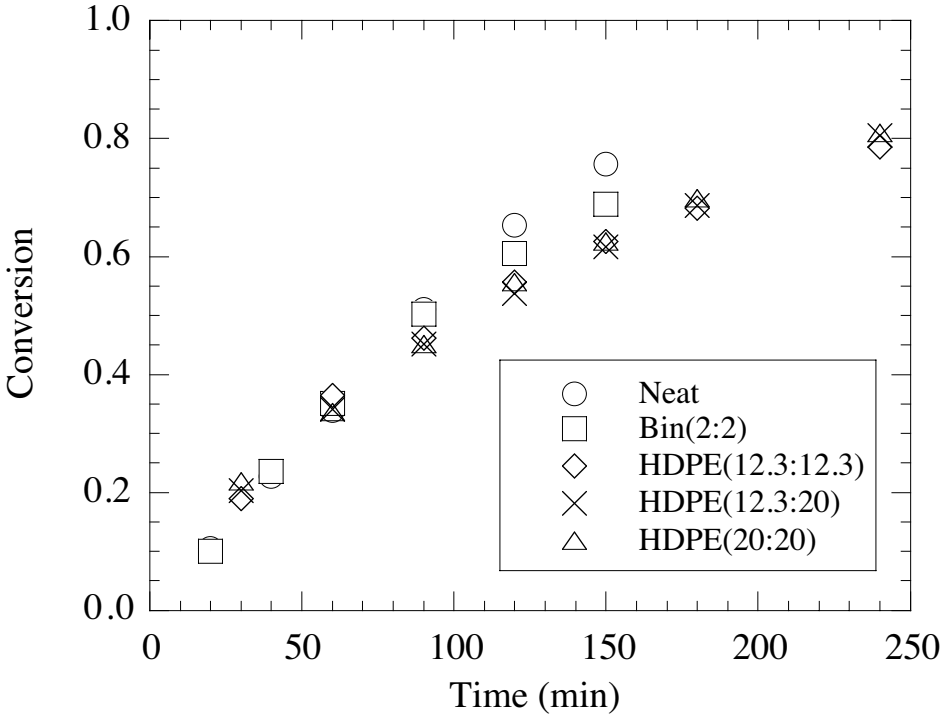

Figure 8: Comparison of the conversion of NBBM during neat pyrolysis and binary mixture reactions with tetradecane and HDPE.

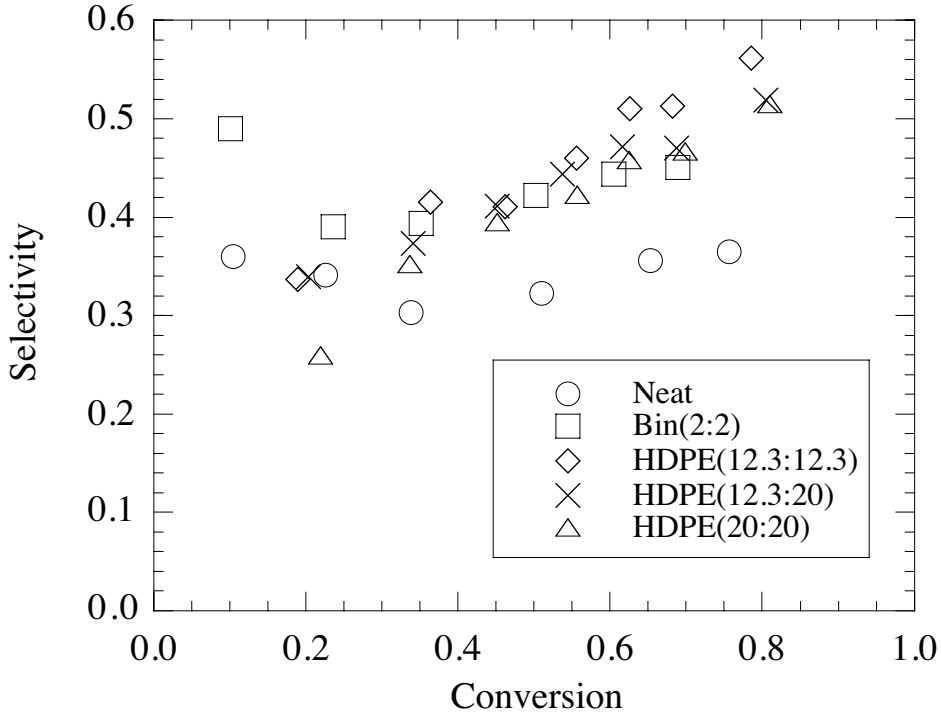

Figure 9: Comparison of toluene selectivities during neat pyrolysis of NBBM and binary mixture reactions with tetradecane and HDPE.

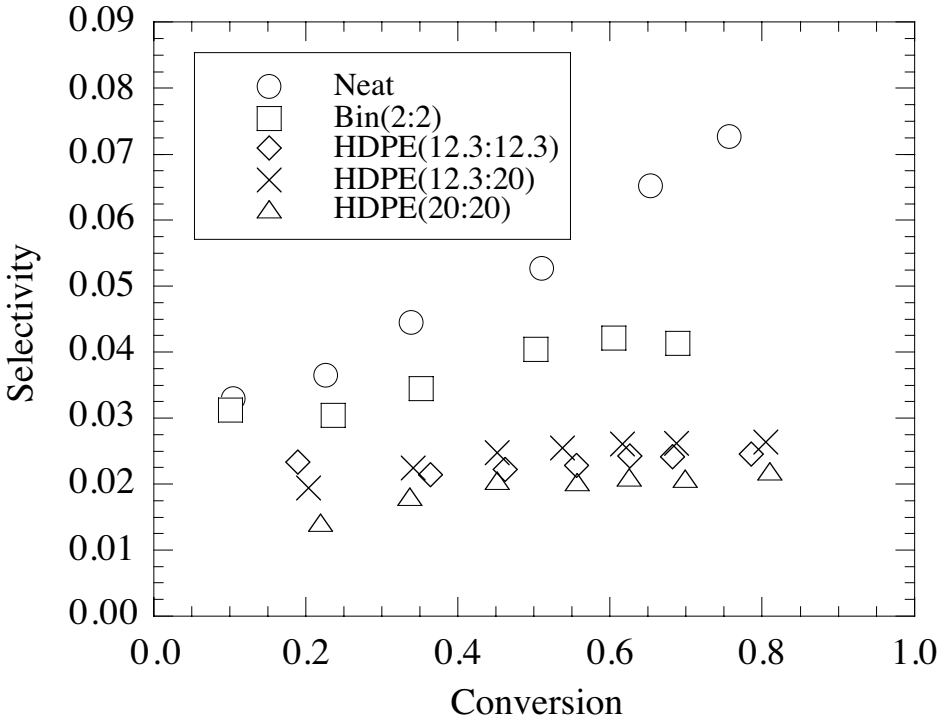

Figure 10: Comparison of 1-naphthylphenylmethane selectivities during neat pyrolysis of NBBM and binary mixture reactions with tetradecane and HDPE.

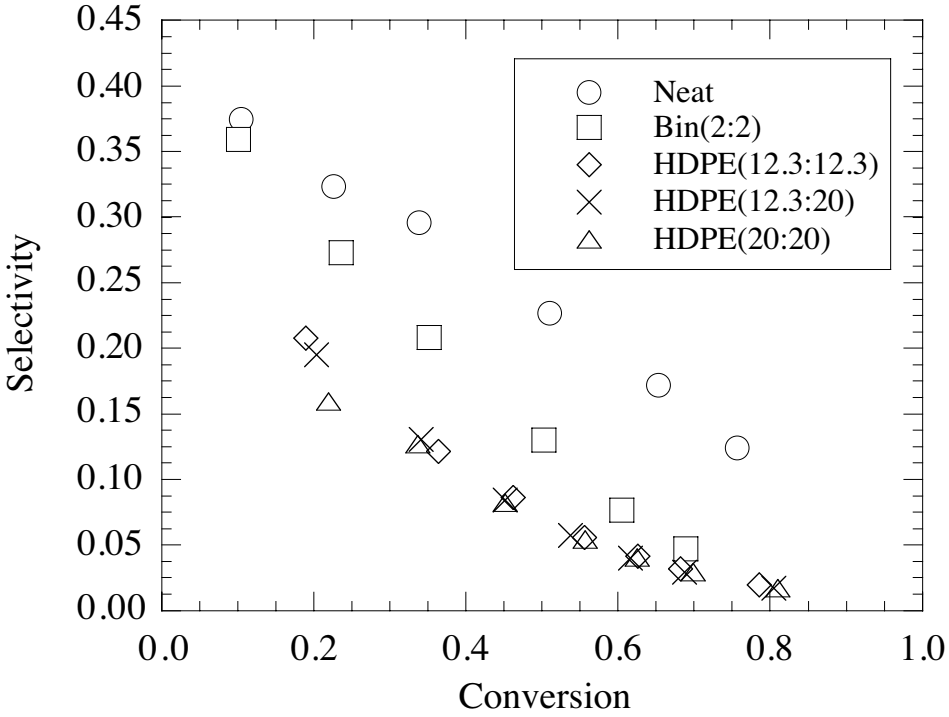

Figure 11: Comparison of 1-(2-phenylethenyl)-4-(1-naphthylmethyl)benzene selectivities during neat pyrolysis of NBBM and binary mixture reactions with tetradecane and HDPE.

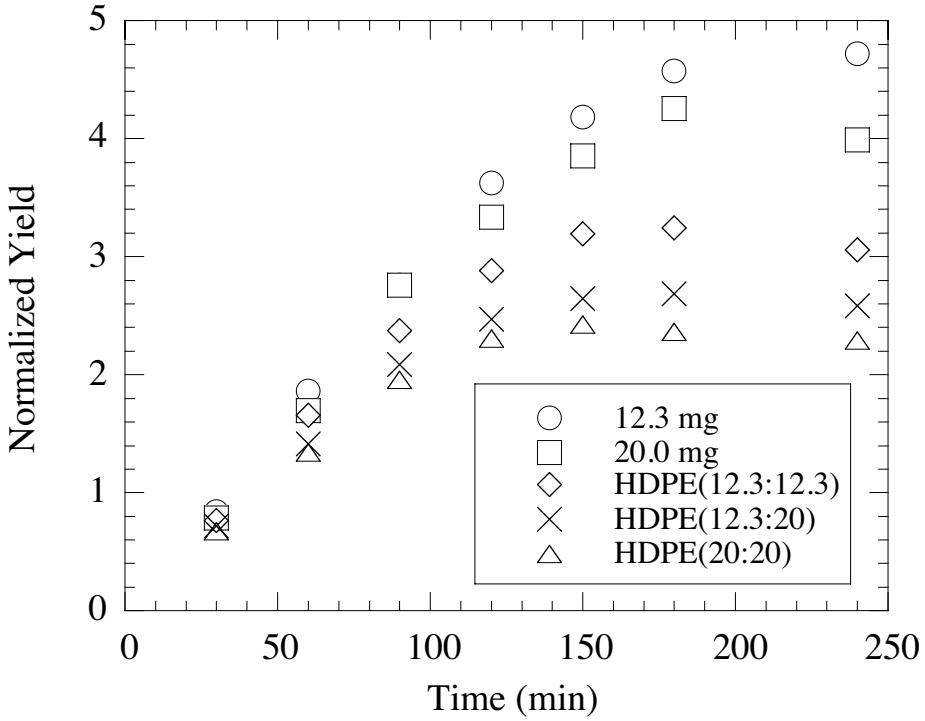

Figure 12: Comparison of normalized yields of 1-pentadecene during neat pyrolysis of HDPE and binary mixture reactions with NBBM.

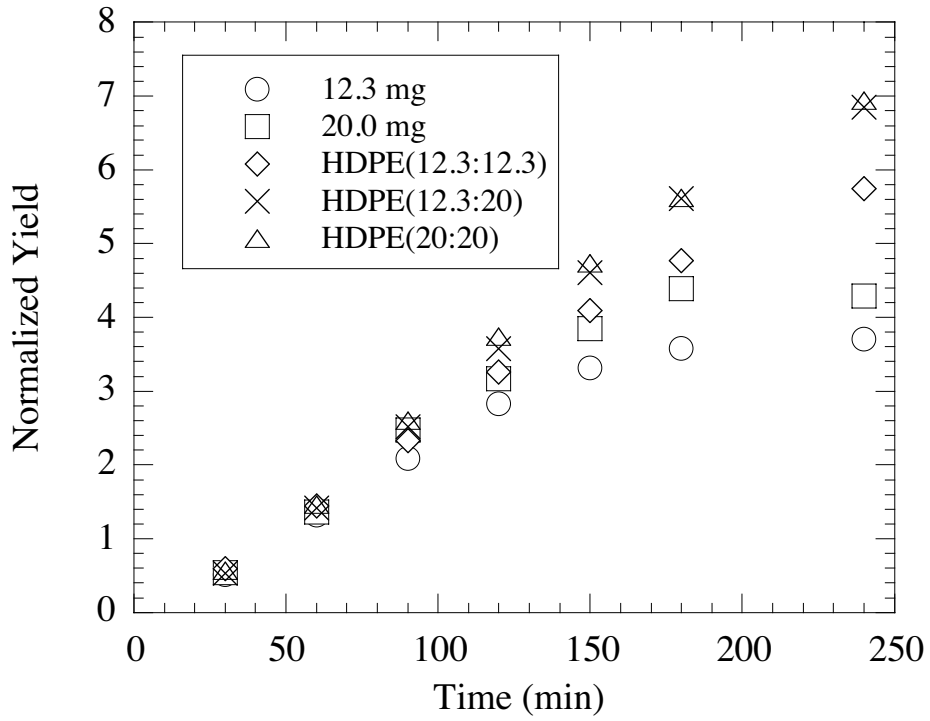

Figure 13: Comparison of normalized yields of *n*-pentadecane during neat pyrolysis of HDPE and binary mixture reactions with NBBM.

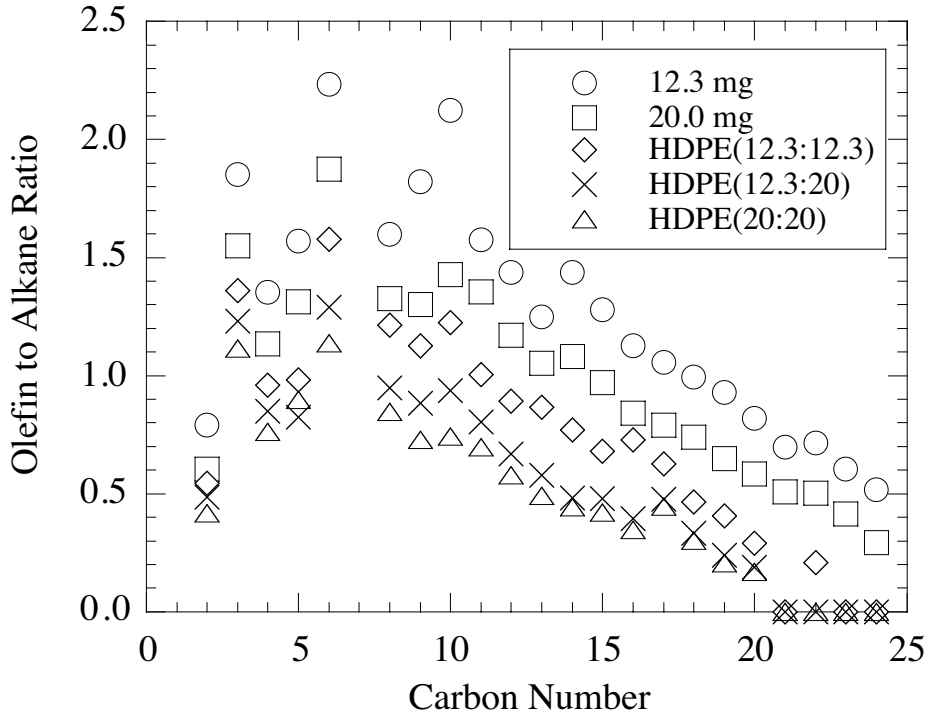

Figure 14: Comparison of the α-olefin to *n*-alkane ratio at a reaction time of 180 minutes for various carbon numbers for neat pyrolysis of HDPE and binary mixture reactions with NBBM.

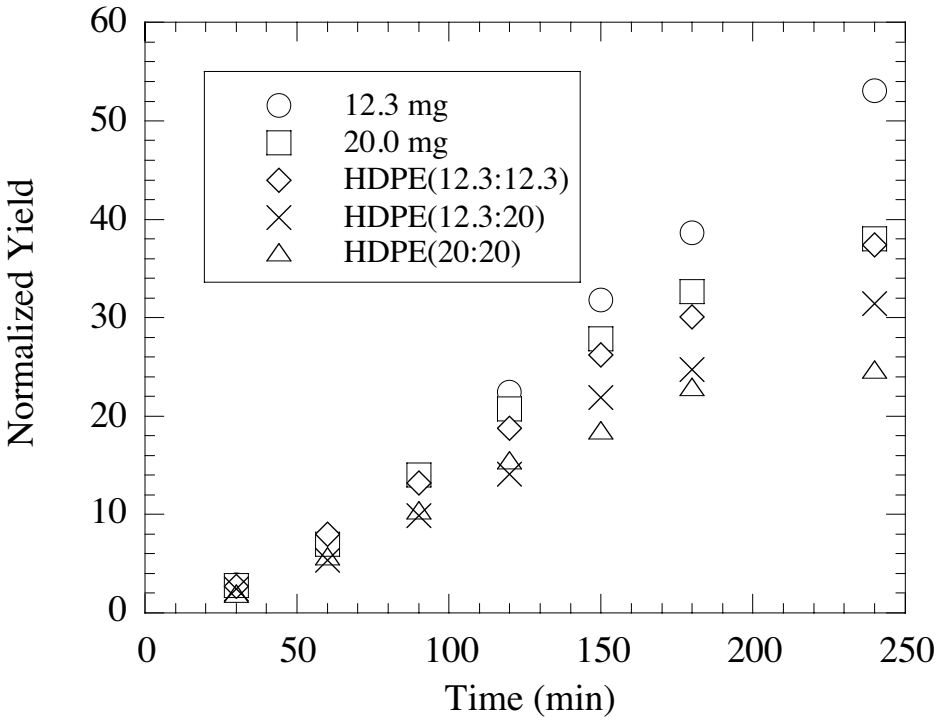

Figure 15: Comparison of normalized yields of ethylene during neat pyrolysis of HDPE and binary mixture reactions with NBBM.

Tertiary Resource Recovery From Waste Polymers Via Pyrolysis: Neat and Binary Mixture Reactions of Polypropylene and Polystyrene

Hsi-Wu Wong and Linda J. Broadbelt*

Department of Chemical Engineering, Northwestern University, 2145 Sheridan Road, Evanston, IL, 60208, USA

(Phone 847-491-5351; FAX 847-491-3728; broadbelt@northwestern.edu)

ABSTRACT

Batch pyrolysis of polypropylene, polystyrene and their binary mixture was carried out at temperatures of 350ºC and 420ºC. Two different loadings were also studied for neat polypropylene and polystyrene to assess the impact of total pressure, which was also a function of reaction time and temperature. For polypropylene neat pyrolysis, total conversion was an order of magnitude higher at 420ºC than at 350ºC. For neat polystyrene pyrolysis, conversion reached approximately 75% at 350ºC, whereas at 420ºC the conversion reached a maximum around 90% after 10 minutes of reaction and decreased to around 70% after 180 minutes. For binary mixture pyrolysis, the overall conversion was higher than the average of the two neat cases. The conversion of polystyrene remained the same, but significant enhancement of the polypropylene conversion was observed. These results suggest that the more facile degradation of polystyrene helped to initiate the less reactive polypropylene.

INTRODUCTION

In recent years, post-consumer wastes have caused increased concern because of the escalation of municipal solid wastes (MSW) generated. Plastics make up a significant portion of MSW (* To whom correspondence should be addressed) of plastics are

manufactured annually, and production is projected to increase to 26.7 million tons in 2005[1]. In 1997, 9.9 weight percent of MSW was comprised by plastics, which was more than 20% by volume[2]. Within the plastic waste stream, 13.0 weight percent was composed of polypropylene (PP), and 9.8 weight percent contained polystyrene (PS)[1].

Tertiary recycling, in which discarded plastic products are converted into high-value petrochemical or fuel feedstocks, has received increased attention in recent years. Two methods of tertiary recycling, chemical recycling and thermal recycling, may be applied, depending on which polymer is involved. Condensation polymers, such as polyesters, nylons and polyurethanes, can undergo decomposition via chemical methods such as glycolysis, methanolysis, and hydrolysis. Addition polymers, such as polystyrene, polyethylene, and polypropylene, are typically broken via thermal or catalytic cracking[3]. Thermal degradation is the simplest form of tertiary recycling of addition polymers and therefore has been studied most extensively.

One of the biggest costs associated with polymer recycling is the sorting of the original polymers. However, the conditions required to break down addition polymers lead to a broad product distribution even for a single component. Therefore, tertiary recycling of addition polymers via processing of a multicomponent polymeric mixture is one potential solution to eliminate the cost of sortation. The economics of fuel or chemical production from a mixed stream of addition polymers may be further improved by optimizing the coprocessing conditions.

Our objective was to investigate the interactions of different polymers during pyrolysis to assess if any synergistic effects are present during coprocessing. Specifically, we have conducted binary mixture pyrolysis of polypropylene and polystyrene as a model

of mixed plastic waste and compared the results to neat pyrolysis of the individual components. Although the neat pyrolysis of both polypropylene[4-8] and polystyrene[9-13] has been extensively studied, and a small number of investigations have been carried out on the pyrolysis of mixed polymers[14-18], very few researchers have focused on the binary system of polypropylene and polystyrene[18]. Furthermore, our investigation placed emphasis on a detailed quantification of the low molecular weight products, which would be useful as fuels and chemicals.

EXPERIMENTAL

Batch pyrolysis experiments were carried out by loading either polystyrene or polypropylene into a 3.1-ml glass ampoule (Wheaton). This simple reactor configuration facilitated product analysis and allowed interactions of the volatile products and the degrading polymer, as would occur in a continuous flow reactor, to be gauged. Two different loadings, 20 mg and 10 mg, were studied. For binary reactions, 10 mg of each polymer were used. The polystyrene (Mw=111,800, Mn=98,100) was prepared in our laboratory by anionic polymerization[16]. Polystyrene synthesized by anionic polymerization does not contain weak links, and therefore, the degradation behavior may be attributed to the regular polystyrene structure. Furthermore, this enabled comparison with our previous work[16,19,20]. The polypropylene was obtained from Aldrich (syndiotactic; Mw=127,000, Mn=54,000) in powder form. After purging with argon for 2 minutes, each ampoule was sealed using an oxygen/propane flame, then the sample was reacted in an isothermal fluidized sand bath. Two reaction temperatures, 350°C and 420°C, were studied. A temperature of 350°C was chosen because it is above the ceiling

temperature of polystyrene but below that of polypropylene, and 420°C was chosen to obtain appreciable conversion of polypropylene and was the same temperature used to study the degradation of polyethylene[21]. The reaction times ranged from 1-180 minutes. These times allowed a large range of conversions to be studied for both polymers. In addition, runs with a reaction time of 18 hours for polypropylene pyrolysis at 420°C were carried out. Upon completion of the reaction, the ampoule was removed from the sand bath and quenched in another sand bath set at ambient temperature. At least two replicates and in most cases three replicates were performed for each reaction time.

Products that were gaseous at room temperature from neat polypropylene and binary pyrolysis were analyzed by placing the ampoule inside a 53-ml flask with a Tygon tube on one end and an injection port on the other. Both ends were then sealed with septa. The flask was purged with helium for 10 minutes and, after the ampoule was broken, the gases were allowed to equilibrate for 30 minutes. Gas samples were taken using a gas-tight syringe and then identified and quantified using a Hewlett Packard 5890 Series II Plus Gas Chromatograph equipped with a thermal conductivity detector (TCD) and a 6 ft stainless steel Porapak Q column (Supelco).

Liquid and solid products were extracted with 1.5 ml HPLC grade methylene chloride. The product solution was first passed through a 0.45-μm polypropylene filter (Alltech) attached to a syringe and then passed through a Waters Gel Permeation Chromatograph (GPC). The molecular weight distribution of the soluble polymer fraction was measured. Polystyrene and its degradation products were completely soluble in methylene chloride, while polypropylene-derived products only up to C_{25} were completely soluble. Products with molecular weights less than ~400 g/mol were collected

using a fraction collector attached to the GPC outlet. An external standard (biphenyl) was added after fraction collection. Product identification and quantification were achieved using a Hewlett Packard 6890 Series Gas Chromatograph-Mass Spectrometer and a Hewlett Packard 6890 Series Gas Chromatograph with a flame ionization detector (FID), each equipped with a Hewlett Packard 30 m crosslinked 5% Ph Me Silicone capillary column.

The percent conversion of the polymer, X, used here was defined according to Equation (1):

$$X = \frac{W}{W_o} \times 100\% \tag{1}$$

where W is the weight of the products analyzed by gas chromatography, which is equal to the sum of the weight of the gaseous products (W_g) and the liquid products (W_l), and W_o is the initial weight loading of polymer. More specifically, W_l is the sum of the weight of non-aromatic liquid products with carbon number less than or equal to 25 and aromatic products with molecular weight less than or equal to 404. In the case of neat polystyrene pyrolysis, less than 1% gaseous products were found even at 420°C for 180 minutes of reaction, and thus W_g was neglected. For binary mixture pyrolysis, the conversion of polystyrene was calculated from the weight of all aromatic products, while the weight of all other products was used to calculate the conversion of polypropylene.

Selectivity, S, of a certain species A was based on Equation (2):

$$S = \frac{W_A}{W} \times 100\% \tag{2}$$

where W_A is the weight of species A. Product yields used for neat polypropylene and binary pyrolysis were normalized by dividing the millimoles (mmol) of each product by

the initial molar loading of polymer repeat units. Finally, error bars shown in the figures represent the standard deviations of experiments that have been at least duplicated.

RESULTS AND DISCUSSION

3.1 Neat Polypropylene Pyrolysis

The overall conversion of polypropylene during neat pyrolysis increased with respect to reaction time for both temperatures and loadings, as illustrated in Figure 1. After 90 minutes of reaction, the conversion at 420°C reached approximately 60%, and no significant change was observed at longer reaction times. This suggests that little additional conversion can be achieved even for very long reaction times at this temperature in a closed batch reactor of 3.1 ml. This was verified by running the reaction for 18 hours, and the conversion was 65.2% and 59.0% for reactant loadings of 10 mg and 20 mg, respectively. The conversion was significantly lower at 350°C, achieving a maximum value of only around 3% after 180 minutes of reaction. The pressure only increased by less than 0.1 atm for both loadings. Clearly, as shown in Figure 1, the effect of temperature on polypropylene pyrolysis is marked, whereas the influence of different loadings is not significant. For 420°C runs, the conversion of the sample with a loading of 10 mg reached 57.5% after 180 minutes of reaction, while the conversion for the 20 mg loading was slightly higher at 62.7%. However, after 18 hours of reaction, the conversion for the 10 mg loading was higher than the conversion for the loading of 20 mg as described above. The slight differences in conversion between the two loadings can be explained by the differences in total pressure between the two systems. While the initial pressure was 2.3 atm for both loadings, the pressure was around 5.8 atm for the higher

loading and 3.9 atm for the lower loading after 180 minutes of reaction. The higher pressure in the 20 mg sample results in an enhancement in bimolecular reactions and a faster rate of conversion. However, the final conversion is dictated by thermodynamics and is higher for the system with the lower total pressure.

If the products were divided into three fractions, C_1-C_4, C_5-C_{10}, and C_{11}-C_{25}, respectively, the yields of these fractions showed different temporal behavior, as shown in Figure 2. At 420°C, the yield of the C_1-C_4 fraction increased monotonically with reaction time, whereas the C_5-C_{10} fraction reached a subtle maximum around 120 minutes with no significant change observed at 180 minutes. Finally, the C_{11}-C_{25} fraction reached a distinct maximum around 60 minutes. No significant difference between the two loadings was observed at this temperature. At 350°C, all three fractions increased with reaction time, with the yield of the C_1-C_4 fraction significantly lower than the other two. Slightly higher yields were found for a loading of 10 mg for the C_5-C_{10} and C_{11}-C_{25} fractions at reaction times of 120 and 180 minutes. The results suggest that as reaction time and temperature increased, the heavier products decompose to lighter ones.

The reaction products of polypropylene pyrolysis consisted of four major categories – alkanes, alkenes, dienes, and aromatic compounds. The yields of alkanes and alkenes are plotted in Figure 3. Lower molecular weight species were found in higher yields, whereas the yields of compounds with carbon numbers greater than ten were notably lower. For alkanes, ethane (C_2), n-pentane (C_5), 4-methylheptane (C_8), C_{11}, C_{14}, and C_{17} were found in high yields. The alkanes were thus dominated by products with carbon numbers C_{3n-1}, with n=1,2,3,4,… The yields of the majority of the alkanes increased with respect to reaction time. For alkenes, propylene oligomers (C_3, C_6, C_9, C_{12},

C_{15}, C_{18}, C_{21}, and C_{24}), i.e., C_{3n}, n=1,2,3,4,…, were dominant products. It is believed that commercial syndiotactic polypropylene made using coordination catalysts would have chains with double bonds on the ends[22], such that the penpenultimate bonds from the chain ends would be weaker than normal carbon-carbon bonds. In addition, olefinic end groups are produced during degradation. Therefore, isobutylene (C_4 alkenes), which can be formed from polypropylene chains with double bonds on the ends, was found in high yield. Dienes, which were found beginning with C_7 and were present in relatively low yields, appeared as C_7, C_{10}, C_{13}, C_{16}, C_{19}, C_{22}, and C_{25}, i.e., C_{3n-2}, n=3,4,5,6… Finally, aromatic compounds were also found as minor products. Their yields were comparable in magnitude to the diene yields.

As noted above, the product distribution revealed that the dominant alkenes were for compounds in the form of C_{3n}, whereas alkanes and dienes appeared in the form of C_{3n-1} and C_{3n-2}, respectively. This product distribution is in agreement with observations reported in the literature[5,6,8,23] and can be explained by the mechanism illustrated in Figure 4, which was based on the reaction types proposed by Tsuchiya et al[5]. We have clarified the mechanistic picture by delineating the pathways that lead to the different observed product classes (alkenes, alkanes, and dienes) with the dominant carbon numbers (C_{3n}, C_{3n-1}, C_{3n-2}, respectively). The initiation step of the free radical mechanism is simply to break any of the polypropylene chains into two shorter end-chain radicals. The end-chain radicals (or mid-chain radicals formed subsequently) may abstract hydrogen from a long polypropylene chain to form a tertiary radical, as shown in Figure 4(a). Upon undergoing β-scission, the tertiary polymer radical is broken into two fragments, one with a double bond on the end (denoted as I), and the other with a

secondary free radical (denoted as II). When the polymer chain I is attacked by another free radical and β-scission occurs, dienes (in the form of C_{3n-2}) and alkenes (in the form of C_{3n}) can be formed, as shown in Figure 4(b). On the other hand, polymer chain II can undergo three kinds of reactions such that alkanes (in the form of C_{3n-1}) and alkenes (in the form of C_{3n}) can be formed, as shown in Figure 4(c). Although other steps not explicitly drawn are possible, the formation of C_{3n} alkenes, C_{3n-1} alkanes, and C_{3n-2} dienes as the dominant products suggests that the mechanism in Figure 4 captures the major reaction pathways.

3.2 Neat Polystyrene Pyrolysis

The overall conversion of neat pyrolysis of polystyrene at both temperatures and loadings is shown in Figure 5. For high temperature (420ºC) reactions, polystyrene degraded completely in 10 minutes, and reactions occurred to form condensed aromatic products at longer times as suggested by a new peak appearing on the gel permeation chromatograms and the increasing yields of naphthalene and 2-phenylmethylnaphthalene after 10 minutes of reaction (not shown). For low temperature (350ºC) reactions, the conversion reached around 75% after 180 minutes of reaction. No significant influence of different loadings on the total conversion at both temperatures was observed.

The major products of neat polystyrene pyrolysis were a function of temperature and were similar to those reported in the literature[10,11,13]. The mechanism of polystyrene decomposition leading to the major products is depicted in Figure 1 of reference 20. At 420ºC, the major products for polystyrene pyrolysis were toluene, ethylbenzene, and styrene. As shown in Figure 6, the selectivity of styrene was around 70% initially and

went down as reaction time increased. However, the selectivities of toluene and ethylbenzene increased monotonically. One possibility is that styrene began to decompose or react with other heavier compounds to form toluene and ethylbenzene. The selectivity of styrene for the 10 mg loading was slightly higher than that for the 20 mg loading, whereas the selectivities of toluene and ethylbenzene were slightly lower with decreasing loading. This behavior is consistent with enhanced decomposition of styrene to form toluene and ethylbenzene at higher total pressures. The pressure after 10 minutes of reaction was around 5.1 atm for the higher loading, and 3.7 atm for the lower loading. At 350°C, the major products of polystyrene pyrolysis were styrene and 2,4-diphenyl-1-butene (styrene dimer). As shown in Figure 7, the selectivities of both compounds were relatively insensitive to reaction time at the 10 mg loading, whereas they decreased slightly with respect to reaction time for the 20 mg loading. As was observed at 420°C, the secondary reactions of the olefinic compounds were enhanced at higher total reaction pressures. This behavior is more marked at longer reaction times, when the pressure difference between the two loadings is more severe. After 180 minutes of reaction, the pressure was near 4 atm for the higher loading and 3.1 atm for the lower loading, while the initial pressure for both loadings was 2.1 atm.

3.3 Pyrolysis of a Binary Mixture of Polypropylene and Polystyrene

The total conversion during binary mixture pyrolysis at 420°C and 350°C is compared to the conversion of neat polystyrene and polypropylene in Figures 8 and 9 for 420°C and 350°C, respectively. For both temperatures studied, the overall conversion for binary mixture pyrolysis was higher than the average of the neat cases represented by the

dashed lines in the figures, which indicate the conversion if there were no interactions between the two polymers. By attributing all aromatic products formed during binary mixture pyrolysis to polystyrene, it was observed that the conversion of polystyrene in binary reactions was similar to that in the neat cases at both temperatures, as shown in Figure 10. In addition, the molecular weight distributions of polystyrene during neat pyrolysis at both loadings and binary mixture pyrolysis were also similar at 350°C (Figure 11). However, the conversion of polypropylene was significantly enhanced during binary reactions, as shown in Figure 12. Although it was prohibitive to do high temperature GPC on all the polypropylene samples, analysis of two different reaction times revealed that the molecular weight of PP was lowest for the binary mixture sample. Furthermore, rheological measurements were also qualitatively consistent with the GPC data.

The normalized yields of polypropylene-derived compounds for representative binary mixture reaction conditions are listed in Table 1. For reactions at 350°C, the yields of both alkanes and alkenes were higher for binary reactions than for neat pyrolysis. At 420°C, the alkane yields were slightly lower in the binary reaction while alkene yields were higher, contributing to the higher total conversion for the binary reactions.

In order to understand the origin of the enhancement of polypropylene's reactivity in the presence of polystyrene, the kinetic coupling formulation developed by LaMarca et al. for binary mixture pyrolysis was used[24]. Although their analysis was restricted to small molecules, their approach provided initial quantitative insights into the interactions between the two polymers. The enhancement or retardation of the rate of disappearance of a component in the coupled system compared to the neat degradation was predicted by

calculating the rate enhancement, which is defined as the rate of disappearance of a given component in the mixture relative to its neat degradation rate. If the rate enhancement for component i is equal to 1, then the addition of the second component has no impact on the rate of decomposition of i. If rate enhancements for both components are greater than 1, this is a clear indication of mutual synergistic effects. In order to obtain the rates of degradation for polypropylene, polystyrene and the binary mixture, rate constants were obtained from the literature when available (see references in 20), and unknown values were estimated using the Evans-Polanyi relationship[25]:

$$k_{ij} = A_i \exp\left(\frac{-(E_{o,i} + \alpha_i \Delta H_j)}{RT}\right) \tag{3}$$

where the rate constant (k_{ij}) depends on the frequency factor (A_i), the intrinsic barrier ($E_{o,i}$), and the transfer coefficient (α_i) for a given reaction type i, and the heat of reaction, ΔH_j, for a particular reaction. Representative values of A_i, $E_{o,i}$, and α_i are listed in Table 2 and are derived from the polystyrene modeling study of Kruse et al.[20] The first six columns of Table 2 are identical to Table 1 in their work. Based on the mechanism in Figure 4, it is clear that the same reaction families govern both polypropylene and polystyrene decomposition. We assumed for this first-order analysis that the A_i, $E_{o,i}$, and α_i values are the same for polypropylene and polystyrene, consistent with the reaction family concept. However, the activation energies will be different for polypropylene and polystyrene for a given reaction family because the heats of reaction are different. The heats of reaction for polystyrene were obtained from Kruse et al.[20], and the heats of reaction for representative polypropylene and cross reactions were calculated from the NIST Structures and Properties Database[26] based on relative radical stabilities.

Using this rate constant information, the binary kinetic coupling model predicted that the rate enhancement for polystyrene was very close to unity, while that of polypropylene was much smaller than one. This result suggests that the overall conversion for polystyrene should remain unchanged in the presence of polypropylene, while polypropylene degradation should be strongly retarded in the binary system. This result is consistent with the fact that the tertiary polystyrene-derived radicals are more stable than tertiary polypropylene-derived radicals by 16.3 kcal/mol. If the two polymers are well mixed, the polystyrene-derived radicals prefer self-interactions, and polypropylene-derived radicals preferentially abstract hydrogen from polystyrene instead of from polypropylene. Clearly, the predicted retardation of polypropylene degradation by the model is in contradiction with the experimental results.

The model developed by LaMarca et al. was based on a binary component system that is homogenous, i.e., the two components are well mixed. In polymer systems, the miscibility of two polymers depends on the Gibbs free energy of mixing. A negative free energy of mixing is one of the necessary conditions for miscibility[27,28]. Several researchers have shown that polypropylene/polystyrene blends are totally immiscible at low temperatures[29-31]. Because the entropy of mixing is negligible for high molecular weight polymers with a degree of polymerization greater than 100[28], the polymers will also be immiscible at the temperature investigated here. Therefore, a homogenous model is an inadequate description of this polypropylene/polystyrene binary mixture pyrolysis.

This analysis suggests that other interactions are responsible for the observed enhancement in the degradation rate of polypropylene. As evidenced by the neat experimental data and supported by the lower carbon-carbon bond dissociation energy for

polystyrene (69.7 kcal/mol) compared to polypropylene (86.0 kcal/mol), polystyrene degrades much more rapidly than polypropylene. It is possible that low molecular weight polystyrene-derived radicals near the polymer interface diffuse into the polypropylene region and initiate the more recalcitrant polypropylene. Detailed kinetic modeling is currently in progress to explore this possibility further.

CONCLUSIONS

Total conversion of polypropylene during neat pyrolysis in a closed batch reactor reached around 60% at 420°C and less than 4% at 350°C. There was a significant influence of reaction temperature but only slight effects of sample loading. Four classes of products appeared during polypropylene pyrolysis – alkanes, alkenes, dienes, and aromatic compounds, with the first two present in significantly greater yields than the latter two. The product distribution also showed that most alkenes appeared in the form of C_{3n}, alkanes in the form of C_{3n-1}, and dienes in the form of C_{3n-2}. This product distribution can be explained by the typical free radical mechanism involving bond fission, hydrogen abstraction, β-scission, intramolecular hydrogen transfer and radical recombination as the dominant steps.

For neat polystyrene pyrolysis, the polymer degraded completely in 10 minutes at 420°C, and condensation products were observed at longer times. At 350°C, the conversion to low molecular weight products reached around 75%. Major products of polystyrene pyrolysis were toluene, ethylbenzene, and styrene at 420°C, and styrene and 2,4-diphenyl-1-butene (styrene dimer) at 350°C.

During binary mixture pyrolysis of the two polymers, the overall conversion was higher than the average of the neat cases at both temperatures. The conversion of polystyrene in binary reactions was similar to that of the neat cases. However, the conversion of polypropylene in binary reactions was enhanced by the presence of polystyrene. The enhancement is likely due to increased initiation through hydrogen abstraction from polypropylene by small polystyrene-derived radicals, which diffused into the polypropylene region as polystyrene degraded separately.

ACKNOWLEDGMENT

The authors are grateful for financial support from the Department of Energy (DE-FG22-96-PC96204), the CAREER Program of the National Science Foundation (CTS-9623741), and the MRSEC program of the National Science Foundation (DMR-9632472) at the Materials Research Center of Northwestern University.

LITERATURE CITED

(1)Frank Associates. *Characterization of Municipal Solid Waste in the United States : 1998 Update* ;United States Environmental Protection Agency, June, 1999.

(2)Rowatt, R. J. The Plastic Waste Problem. *Chemtech* **1993**, *23*, 56-60.

(3)Shelley, S.; Fouhy, K.; Moore, S. Plastics Reborn. *Chemical Engineering* **1992**, *July*, 30-35.

(4)Davis, T. E.; Tobias, R. L.; Peterli, E. B. Thermal Degradation of Polypropylene. *Journal of Polymer Science* **1962**, *56*, 485-499.

(5)Tsuchiya, Y.; Sumi, K. Thermal Decomposition Products of Polypropylene. *Journal of Polymer Science Part A-1* **1969**, *7*, 1599-1607.

(6)Sousa Pessoa de Amorim, M. T.; Comel, C.; Vermande, P. Pyrolysis of Polypropylene : I. Identification of Compounds and Degradation Reactions. *Journal of Analytical and Applied Pyrolysis* **1982**, *4*, 73-81.

(7)Chan, J. H.; Balke, S. T. The Thermal Degradation Kinetics of Polypropylene : Part I. Molecular Weight Distribution. *Polymer Degradation and Stability* **1997**, *57*, 113-125.

(8)Bockhorn, H.; Hornung, A.; Hornung, U.; Schawaller, D. Kinetic Study on the Thermal Degradation of Polypropylene and Polyethylene. *Journal of Analytical and Applied Pyrolysis* **1999**, *48*, 93-109.

(9)Yamaguchi, T.; Watanabe, S.; Shimada, Y. Recover of Monomeric Styrene from Polystyrene. *Chemosphere* **1973**, *1*, 7-10.

(10)Ogawa, T.; Kuroki, T.; Ide, S.; Ikemura, T. Recovery of Indan Derivatives from Polystyrene Waste. *Journal of Applied Polymer Science* **1981**, *27*, 857-869.

(11)Ide, S.; Ogawa, T.; Kuroki, T.; Ikemura, T. Controlled Degradation of Polystyrene. *Journal of Applied Polymer Science* **1984**, *29*, 2561-2571.

(12)Ohtani, H.; Yuyama, T.; Tsuge, S.; Plage, B.; Schulten, H. R. Study on Thermal Degradation of Polystyrenes by Pyrolysis-Gas Chromatography and Pyrolysis-Field Ionization Mass Spectrometry. *European Polymer Journal* **1990**, *26(8)*, 893-899.

(13)Gardner, P.; Lehrle, R. Polystyrene Pyrolysis Mechanisms- I. As Deduced From the Dependence of Product Yields on Film Thickness. *European Polymer Journal* **1993**, *29*, 425-435.

(14)McCaffrey, W. C.; Brues, M. J.; Cooper, D. G.; Kamal, M. R. Thermolysis of Polyethylene/Polystyrene Mixtures. *Journal of Applied Polymer Science* **1996**, *60*, 2133-2140.

(15)Ibrahim, M. M.; Hopkins, E.; Seehra, M. S. Thermal and Catalytic Degradation of Commingled Plastics. *Fuel Processing Technology* **1996**, *49*, 65-73.

(16)Woo, O. S.; Broadbelt, L. J. Recovery of High-Value Products from Styrene-Based Polymers Through Coprocessing : Experiments and Mechanistic Modeling. *Catalysis Today* **1998**, *40*, 121-140.

(17)Madras, G.; McCoy, B. J. Distribution Kinetics for Polymer Mixture Degradation. *Ind. Eng. Chem. Res* **1999**, *38*, 352-357.

(18)Williams, P. T.; Williams, E. A. Interaction of Plastics in Mixed-Plastics Pyrolysis. *Energy and Fuels* **1999**, *13*, 188-196.

(19)Woo, O. S.; Ayala, N.; Broadbelt, L. J. Mechanistic Interpretation of Base-Catalyzed Depolymerization of Polystyrene. *Catalysis Today* **2000**, *55*, 161-171.

(20)Kruse, T. M.; Woo, O. S.; Broadbelt, L. J. Detailed Mechanistic Modeling of Polymer Degradation: Application to Polystyrene. *Chemical Engineering Science* **2001**, *56*, 971-979.

(21)De Witt, M. J.; Broadbelt, L. J. Binary Interactions between High-Density Polyethylene and 4-(1-Naphthylmethyl)bibenzyl during Low-Pressure Pyrolysis. *Energy and Fuels* **2000**, *14(2)*, 448-458.

(22)Dotson, N. A.; Galvan, R.; Laurence, R. L.; Tirrell, M., *Polymerization Process Modeling*; John Wiley and Sons: New York, 1996.

(23)Uemichi, Y.; Kashiwaya, Y.; Tsukidate, M.; Ayame, A.; Kanoh, H. Product Distribution in Degradation of Polypropylene Over Silica-Alumina and CaX Zeolite Catalysts. *Bulletin of Chemical Society Japan* **1983**, *56*, 2768-2773.

(24)LaMarca, C.; Libanati, C.; Klein, M. T. Design of Kinetically Coupled Complex Reaction Systems. *Chemical Engineering Science* **1990**, *45*, 2059-2065.

(25)Evans, M. G.; Polanyi, M. Inertia and Driving Force of Chemical Reactions. *Trans. Faraday Soc.* **1938**, *34*, 11-29.

(26)Stein, S. E.; Lias, S. G.; Liebman, J. F.; Kafafi, S. A. NIST Structure and Properties Users Guide. 1994.

(27)Paul, D. R.; Barlow, J. W. Polymer Blends (or Alloys). *J. Macrmol. Sci.-Rev. Macromol. Chem.* **1980**, *C18(1)*, 109-168.

(28)Eastmond, G. C., In *Advances in Polymer Science : Biomedical Applications/Polymer Blends* , Eds.; Springer: , 1999; Vol. 149, pp 69-79.

(29)Krause, S., *Polymer Blends*; Academic Press: New York, 1978.

(30)Radonjic, G. Compatibilization Effects of Styrenic/Rubber Block Copolymer in Polypropylene/Polystyrene Blends. *Journal of Applied Polymer Science* **1999**, *72*, 291-307.

(31)Fortelny, I.; Michalkova, D.; Mikesova, J. Effect of the Mixing Conditions on the Phase Structure of PP/PS Blends. *Journal of Applied Polymer Science* **1996**, *59*, 155-164.

(32)Deady, M.; Mau, A. W. H.; Moad, G.; Spurling, T. H. Evaluation of the Kinetic Parameters for Styrene Polymerization and their Chain Length Dependence by Kinetic Simulation and Pulsed Laser Photolysis. *Makromol. Chem.* **1993**, *194*, 1691.

(33)Fried, J. R. *Polymer Science and Technology*; Prentice-Hall Inc.: New Jersey, 1995.

(34)Schreck, V. A.; Serelis, A. K.; Solomon, D. H. Self-Reactions of 1,3-Diphenylpropyl and 1,3,5-Triphenylpentyl Radicals - Models for Termination in Styrene Polymerization. *Australian Journal of Chemistry* **1989**, *42*, 375.

(35)Yang, M.; Shibasaki, Y. Mechanisms of Thermal Degradation of Polystyrene, Polymethacrylonitrile, and Their Copolymers on Flash Pyrolysis. *Journal of Polymer Science: Part A: Polymer Chemistry* **1998**, *36*, 2315.

Figure 1. Total conversion of neat polypropylene pyrolysis at 350°C and 420°C.

Figure 2. Weight yields of different product fractions as a function of reaction time: (a) 420°C, (b) 350°C.

Figure 3. Representative normalized yields of polypropylene pyrolysis at 420°C for a 20 mg loading of: (a) alkanes; (b) alkenes.

Figure 4. (a) Formation of two kinds of polymer chains (I and II) through bond fission, hydrogen abstraction and β-scission and proposed reaction mechanisms of polymer chains (b) I and (c) II.

Figure 5. Total conversion of neat polystyrene pyrolysis at 350°C and 420°C.

Figure 6. The selectivities of toluene, ethylbenzene, and styrene during polystyrene pyrolysis at 420°C.

Figure 7. The selectivities of styrene and 2,4-diphenyl-1-butene during polystyrene pyrolysis at 350°C.

Figure 8. Comparison of conversion of a binary mixture of PS and PP to neat pyrolysis at 420°C.

Figure 9. Comparison of conversion of a binary mixture of PS and PP to neat pyrolysis at 350°C.

Figure 10. Comparison of PS conversion during binary mixture pyrolysis to neat pyrolysis.

Figure 11. Changes in the number average (M_n) and weight average (M_w) molecular weight of polystyrene during pyrolysis at 350°C as a function of time.

Figure 12. Comparison of polypropylene conversion during binary mixture pyrolysis to neat cases. Only the 20 mg loading is shown since the neat conversion was insensitive to loading.

Table 1 Representative experimental data for PP/PS binary mixture pyrolysis: (a) alkanes (b) alkenes (c) dienes

(a) Alkanes

Reaction Temperature (°C)	420	420	420	350	350	350
Reaction Time (min)	10	90	180	10	90	180
Total Conversion (%)	68.60	70.76	72.73	1.80	31.06	46.08
Carbon Number	Normalized Yield (mmole/mole)					
C1	1.26	15.55	31.86	0.00	0.00	0.00
C2	2.80	22.89	36.78	0.09	0.27	0.41
C3	0.73	11.30	20.45	0.00	0.00	0.00
C4	0.34	4.01	7.01	0.00	0.00	0.00
C5	12.66	28.88	34.83	0.69	2.15	3.32
C6	0.21	1.73	2.48	0.00	0.00	0.00
C7	0.00	0.00	0.00	0.00	0.00	0.00
C8	1.99	2.53	3.41	0.00	0.92	0.61
C9	0.09	0.21	0.38	0.03	0.00	0.00
C10	0.00	0.00	0.00	0.00	0.00	0.00
C11	1.33	2.80	2.61	0.00	0.41	0.81
C12	0.00	0.00	0.00	0.00	0.00	0.00
C13	0.00	0.00	0.00	0.00	0.00	0.00
C14	0.15	0.28	0.16	0.00	0.00	0.03
C15	0.00	0.00	0.00	0.00	0.00	0.00
C16	0.00	0.00	0.00	0.00	0.00	0.00
C17	0.04	0.10	0.06	0.00	0.00	0.00
C18	0.00	0.00	0.00	0.00	0.00	0.00
C19	0.00	0.00	0.00	0.00	0.00	0.00
C20	0.00	0.00	0.00	0.00	0.00	0.00
C21	0.00	0.00	0.00	0.00	0.00	0.00
C22	0.00	0.00	0.00	0.00	0.00	0.00
C23	0.02	0.00	0.00	0.00	0.00	0.00
C24	0.00	0.00	0.00	0.00	0.00	0.00
C25	0.00	0.00	0.00	0.00	0.00	0.00

(b) Alkenes

Reaction Temperature (°C)	420	420	420	350	350	350
Reaction Time (min)	10	90	180	10	90	180
Total Conversion (%)	68.60	70.76	72.73	1.80	31.06	46.08
Carbon Number	Normalized Yield (mmole/mole)					
C2	1.36	7.75	8.91	0.00	0.09	0.19
C3	22.93	68.23	70.72	0.18	1.89	4.03
C4	5.25	39.16	52.34	0.00	0.25	0.77
C5	0.88	6.13	8.24	0.00	0.00	0.23
C6	13.62	27.03	29.42	0.39	2.46	6.36
C7	1.65	3.81	3.54	0.00	0.00	0.25
C8	1.93	3.52	3.88	0.00	0.00	0.00
C9	31.74	29.25	24.49	0.59	5.22	10.19
C10	1.58	12.03	12.25	0.84	0.54	0.21
C11	0.73	1.87	1.09	0.00	0.00	0.00
C12	6.05	5.77	3.84	0.15	1.49	3.18
C13	3.96	2.53	1.24	0.00	0.48	1.74
C14	1.91	5.51	4.42	0.00	0.00	0.21
C15	10.17	9.09	6.56	0.12	2.19	4.55
C16	0.00	0.00	0.00	0.00	0.00	0.00
C17	0.37	1.38	1.66	0.24	0.16	0.29
C18	3.77	3.28	2.03	0.00	0.39	1.28
C19	0.00	0.00	0.00	0.00	0.00	0.00
C20	0.00	0.00	0.00	0.00	0.00	0.00
C21	2.21	0.50	0.15	0.00	0.49	1.43
C22	0.00	0.00	0.00	0.00	0.00	0.00
C23	0.00	0.00	0.00	0.00	0.00	0.00
C24	0.50	0.16	0.05	0.00	0.14	0.25
C25	0.00	0.00	0.00	0.00	0.00	0.00

(c) Dienes

Reaction Temperature (°C)	420	420	420	350	350	350
Reaction Time (min)	10	90	180	10	90	180
Total Conversion (%)	68.60	70.76	72.73	1.80	31.06	46.08
Carbon Number	Normalized Yield (mmole/mole)					
C7	0.79	3.78	5.41	0.00	0.00	0.00
C8	0.00	0.03	0.00	0.00	0.00	0.00
C9	0.19	0.55	0.41	0.00	0.00	0.00
C10	0.10	6.04	11.86	0.98	0.58	0.00
C11	0.00	0.00	0.00	0.00	0.00	0.00
C12	0.00	0.00	0.00	0.00	0.00	0.00
C13	2.65	4.23	4.35	0.02	0.01	0.08
C14	0.00	0.00	0.00	0.00	0.00	0.00
C15	0.00	0.00	0.00	0.00	0.00	0.00
C16	2.14	1.32	0.40	0.00	0.00	1.34
C17	0.00	0.00	0.00	0.00	0.00	0.00
C18	0.00	0.00	0.00	0.00	0.00	0.00
C19	1.43	0.42	0.00	0.00	0.22	0.58
C20	0.00	0.00	0.00	0.00	0.00	0.00
C21	0.00	0.00	0.00	0.00	0.00	0.00
C22	0.82	0.16	0.00	0.00	0.02	0.36
C23	0.00	0.00	0.00	0.00	0.00	0.00
C24	0.00	0.00	0.00	0.00	0.00	0.00
C25	1.28	0.09	0.00	0.00	0.00	0.08

Table 2. Representative values of kinetic and thermodynamic parameters for reaction types incorporated into binary kinetic coupling model of polystyrene and polypropylene degradation.

Reaction family	Frequency factor, A_i (s^{-1} or l mol^{-1} s^{-1})	Intrinsic barrier, $E_{o,i}$ (kcal mol^{-1})	Transfer coefficient, α_i	Representative heat of reaction for polystyrene, ΔH_j (kcal mol^{-1})	Activation energy for polystyrene (kcal mol^{-1})	Representative heat of reaction for polypropylene, ΔH_j (kcal mol^{-1})	Activation energy for polypropylene (kcal mol^{-1})
Chain fission	7.98×10^{15}	2.3 [b]	1.0	69.7	72.0	86.0	88.3
Carbon-hydrogen bond fission	3.5×10^{15}	0.0	1.0	78.5	78.5	94.8	94.8
Hydrogen abstraction	1.5×10^{8}	13.3	0.70(endo) 0.30 (exo)	-3.1	12.4	-3.1	12.4
Chain-end β-scission	2.62×10^{12} [a]	12.9	0.5	16.4 [b]	21.1	16.7 [b]	21.3
Mid-chain β-scission	2.62×10^{12} [a]	12.9	0.5	19.5	22.7	19.8	22.8
Radical recombination	2.17×10^{9} [b]	2.3 [b]	0.0	-69.7	2.3	-86.0	2.3
Disproportionation[b,c]	1.14×10^{8}	2.3	0.0	---	2.3	---	2.3
Radical addition	9.7×10^{6} [a]	12.9	0.5	-19.5	3.2	-19.8	3.2
1,5-Hydrogen Transfer	2.57×10^{9} [d]	13.3	0.70(endo) 0.30 (exo)	-3.1	12.4	-3.1	12.4

[a] frequency factors from Deady et al. (1993) [32]
[b] parameters obtained from Fried (1995) [33]
[c] disproportionation estimated to be 5% of recombination rate at 350ºC (Schreck et al., 1989 [34])
[d] estimated from data obtained by Yang and Shibasaki (1998) [35]

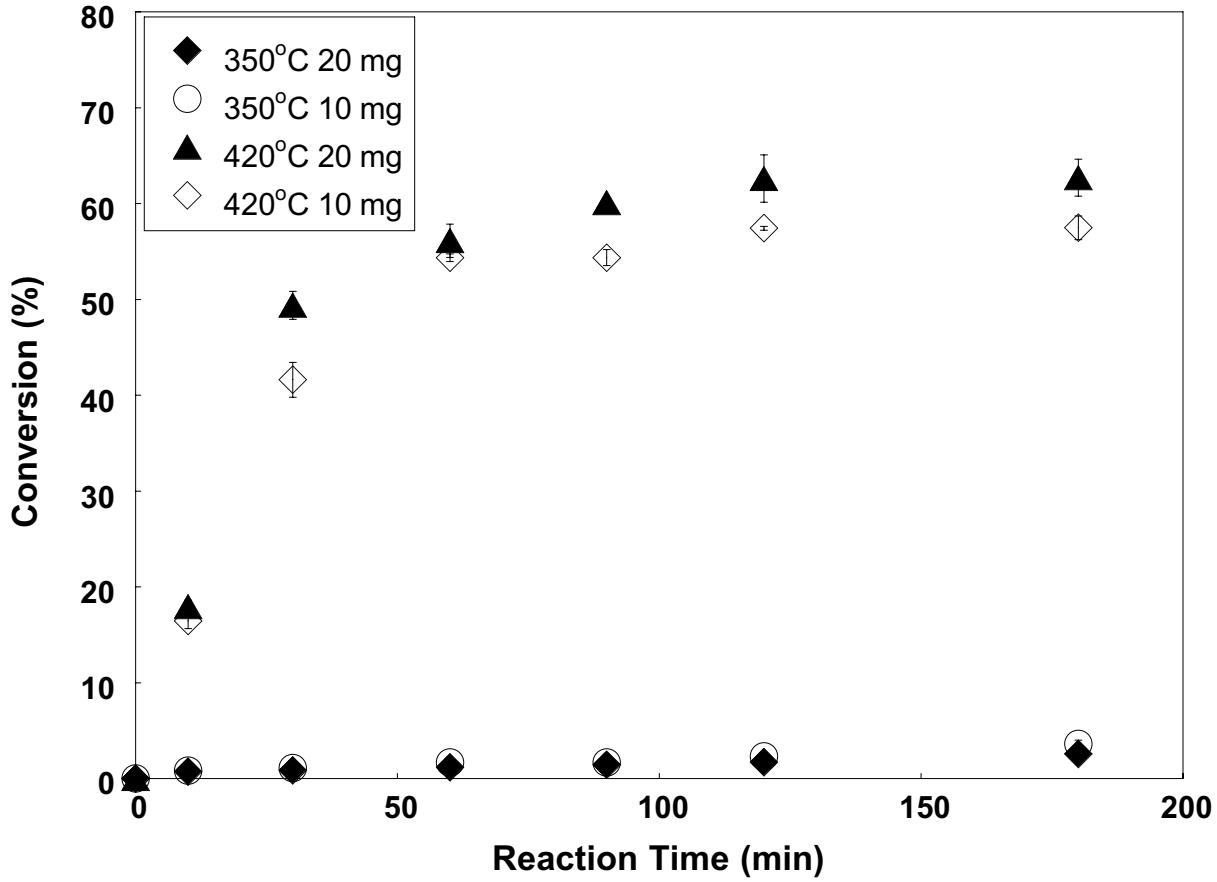
350°C 20 mg
350°C 10 mg
420°C 20 mg
420°C 10 mg
Conversion (%)
Reaction Time (min)
0
10
20
30
40
50
60
70
80
0
50
100
150
200

(a)

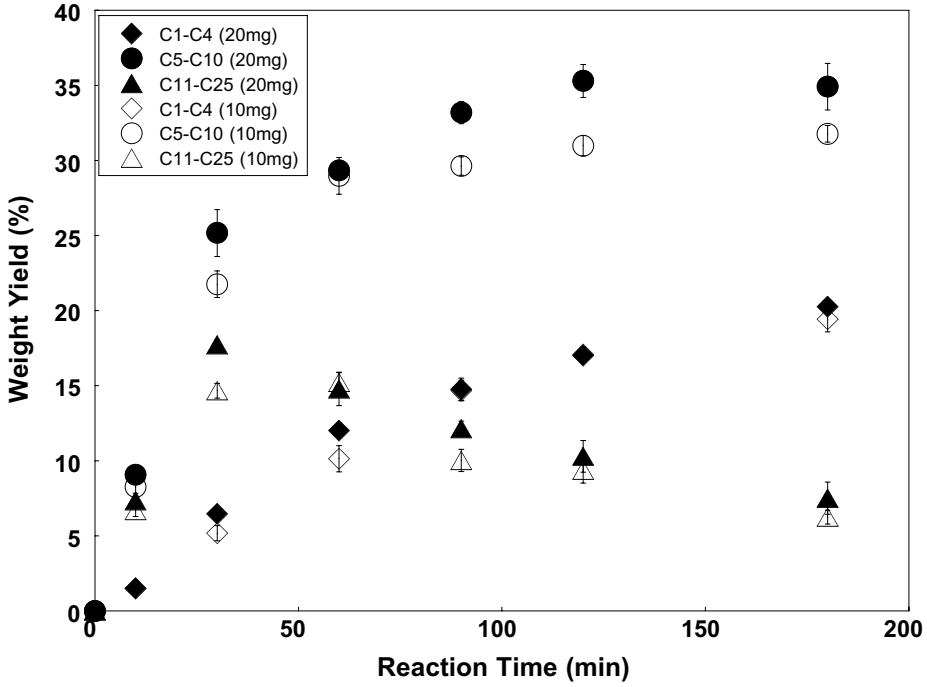
C1-C4 (20mg)
C5-C10 (20mg)
C11-C25 (20mg)
C1-C4 (10mg)
C5-C10 (10mg)
C11-C25 (10mg)
Weight Yield (%)
Reaction Time (min)
0
5
10
15
20
25
30
35
40
0
50
100
150
200

(b)

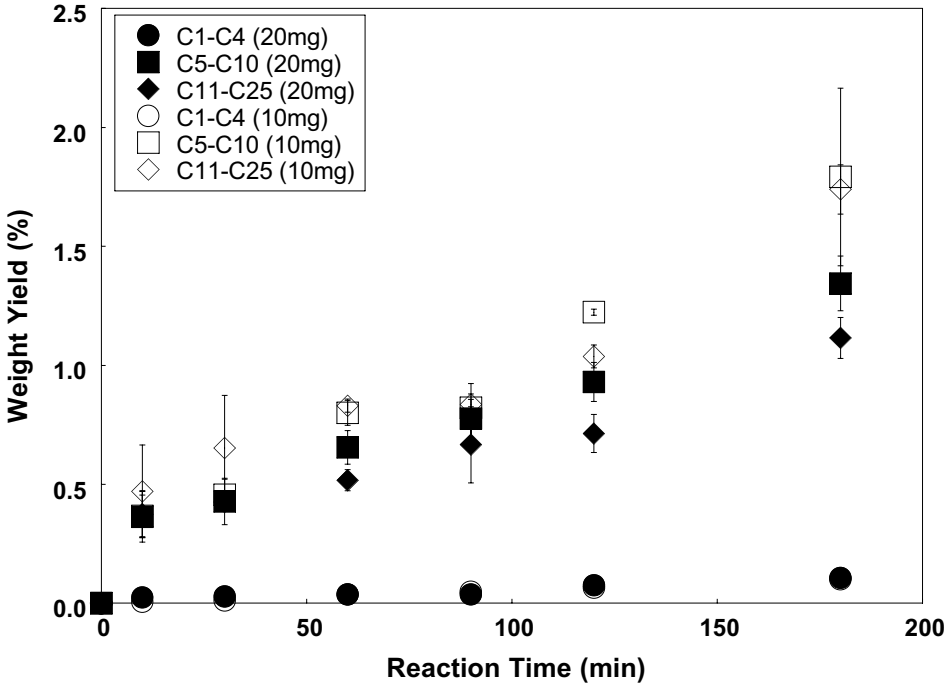
C1-C4 (20mg)
C5-C10 (20mg)
C11-C25 (20mg)
C1-C4 (10mg)
C5-C10 (10mg)
C11-C25 (10mg)
Weight Yield (%)
Reaction Time (min)
0.0
0.5
1.0
1.5
2.0
2.5
0
50
100
150
200

(a)

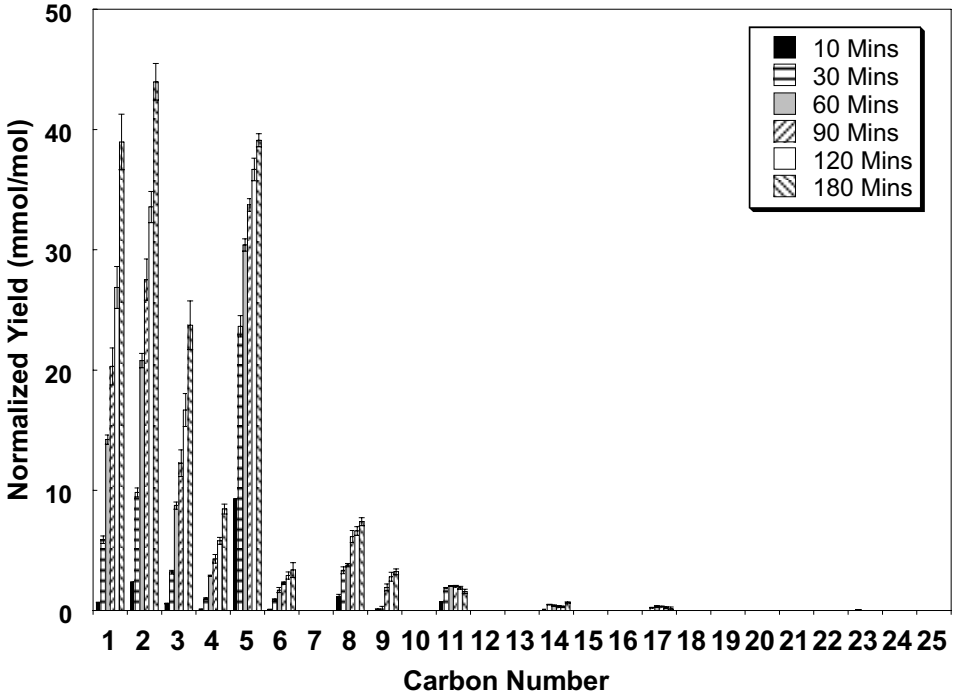
Normalized Yield (mmol/mol)
Carbon Number
10 Mins
30 Mins
60 Mins
90 Mins
120 Mins
180 Mins

(b)

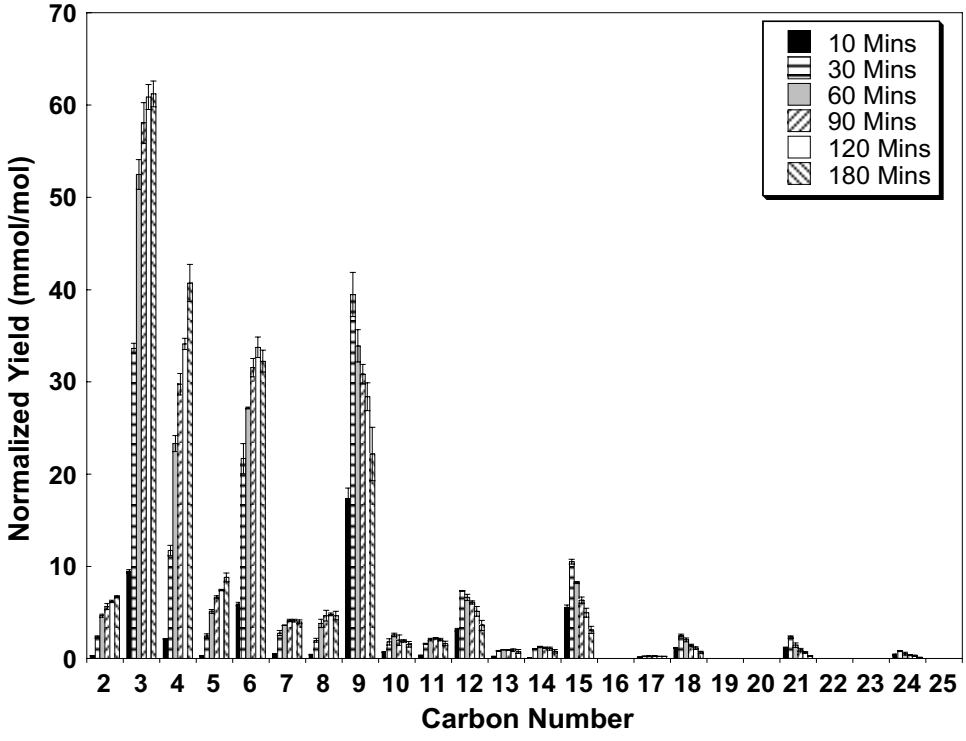
Normalized Yield (mmol/mol)
Carbon Number
10 Mins
30 Mins
60 Mins
90 Mins
120 Mins
180 Mins

(a)

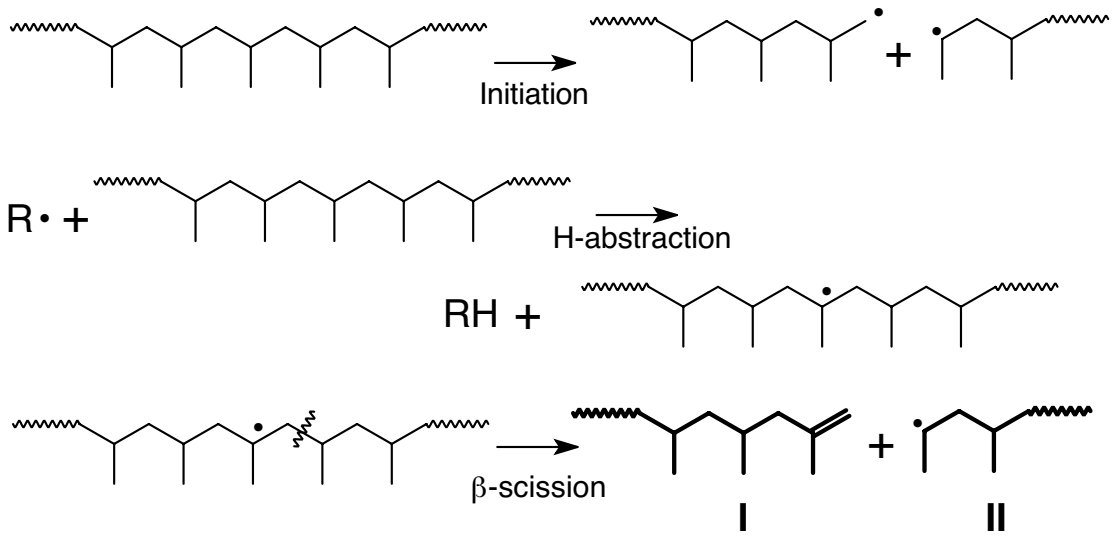
Initiation
R• +
H-abstraction
RH +
β-scission
I
II

(b)

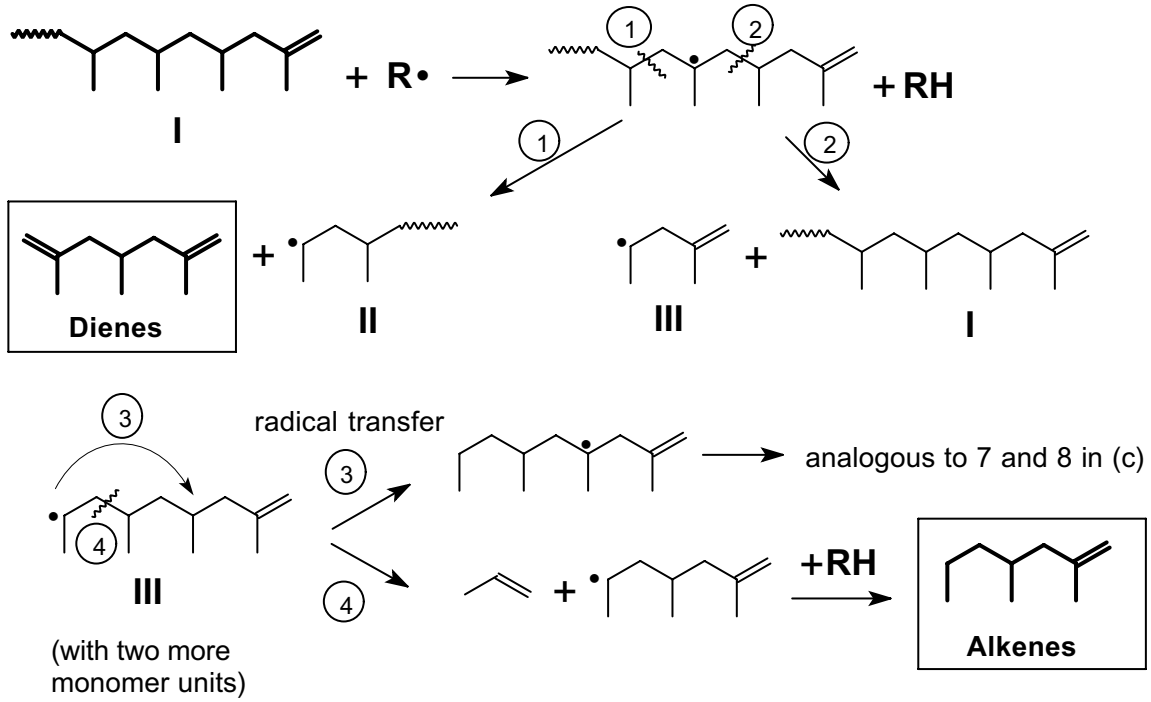
+ R•
+ RH
I
1
2
Dienes
II
III
I
3
4
radical transfer
analogous to 7 and 8 in (c)
+RH
Alkenes
(with two more
monomer units)

(c)

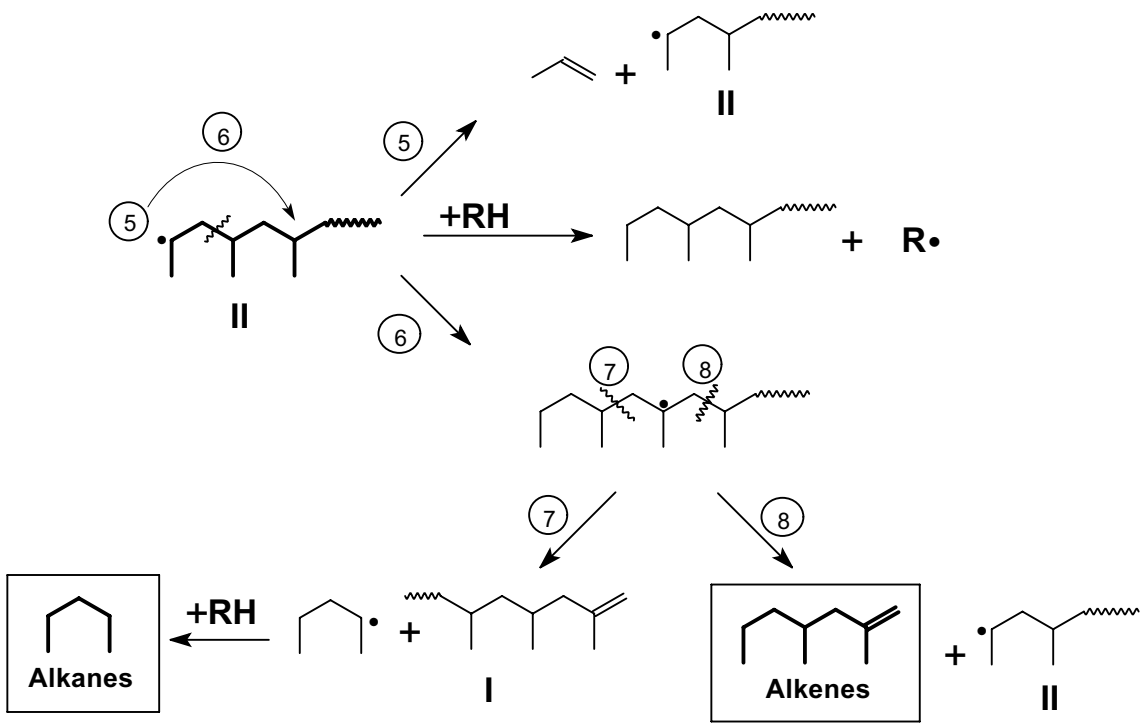

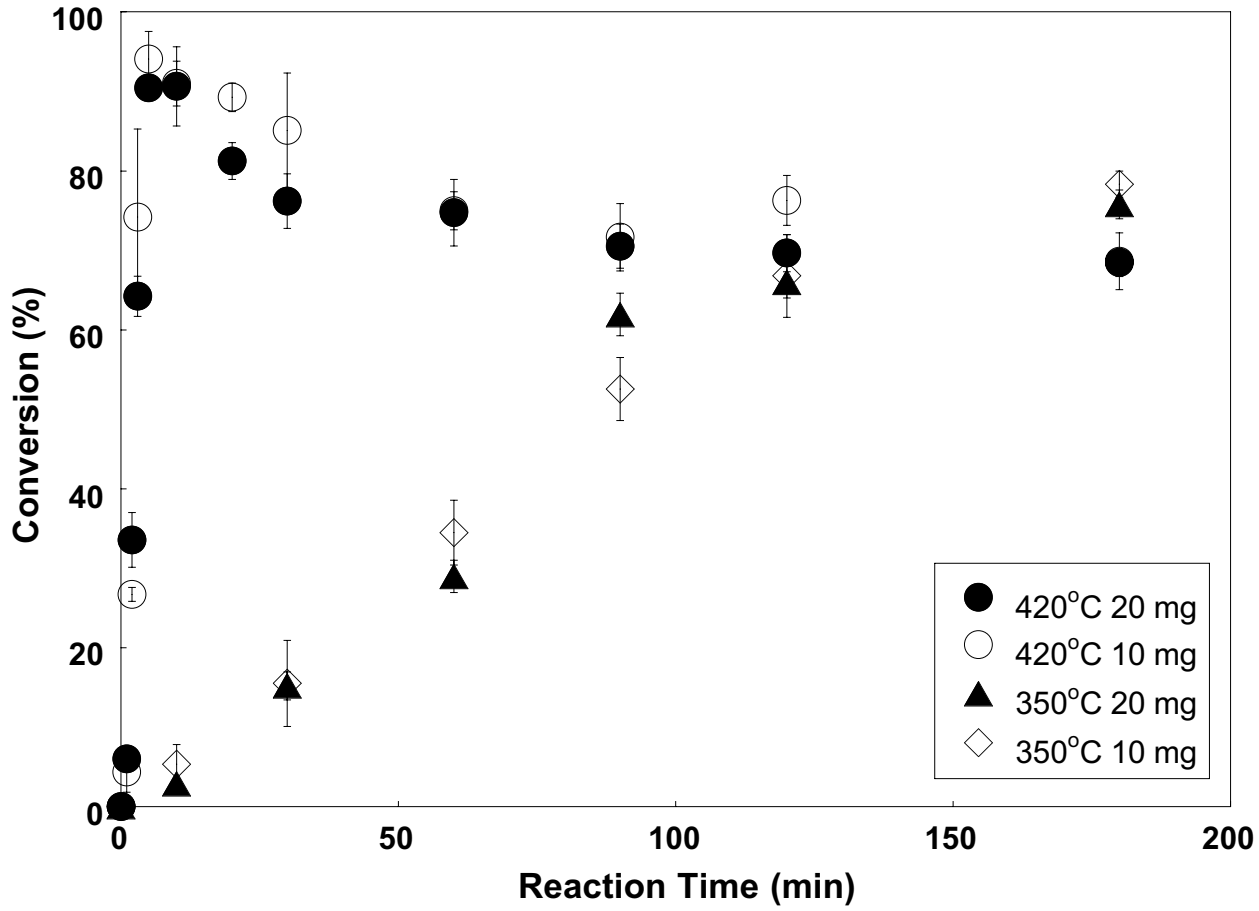
Conversion (%)
Reaction Time (min)
0
20
40
60
80
100
0
50
100
150
200
420°C 20 mg
420°C 10 mg
350°C 20 mg
350°C 10 mg

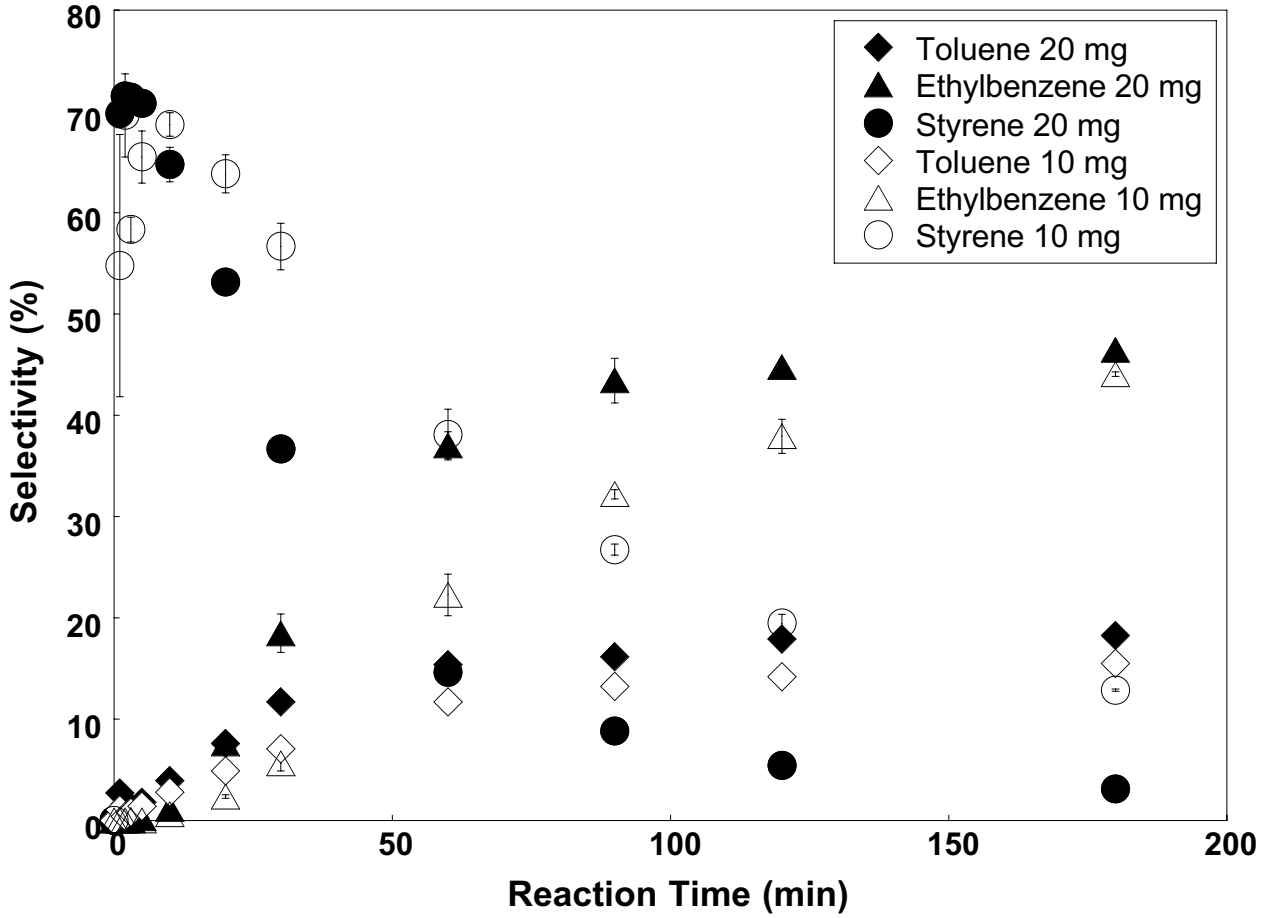
Toluene 20 mg
Ethylbenzene 20 mg
Styrene 20 mg
Toluene 10 mg
Ethylbenzene 10 mg
Styrene 10 mg
Selectivity (%)
Reaction Time (min)
0
10
20
30
40
50
60
70
80
0
50
100
150
200

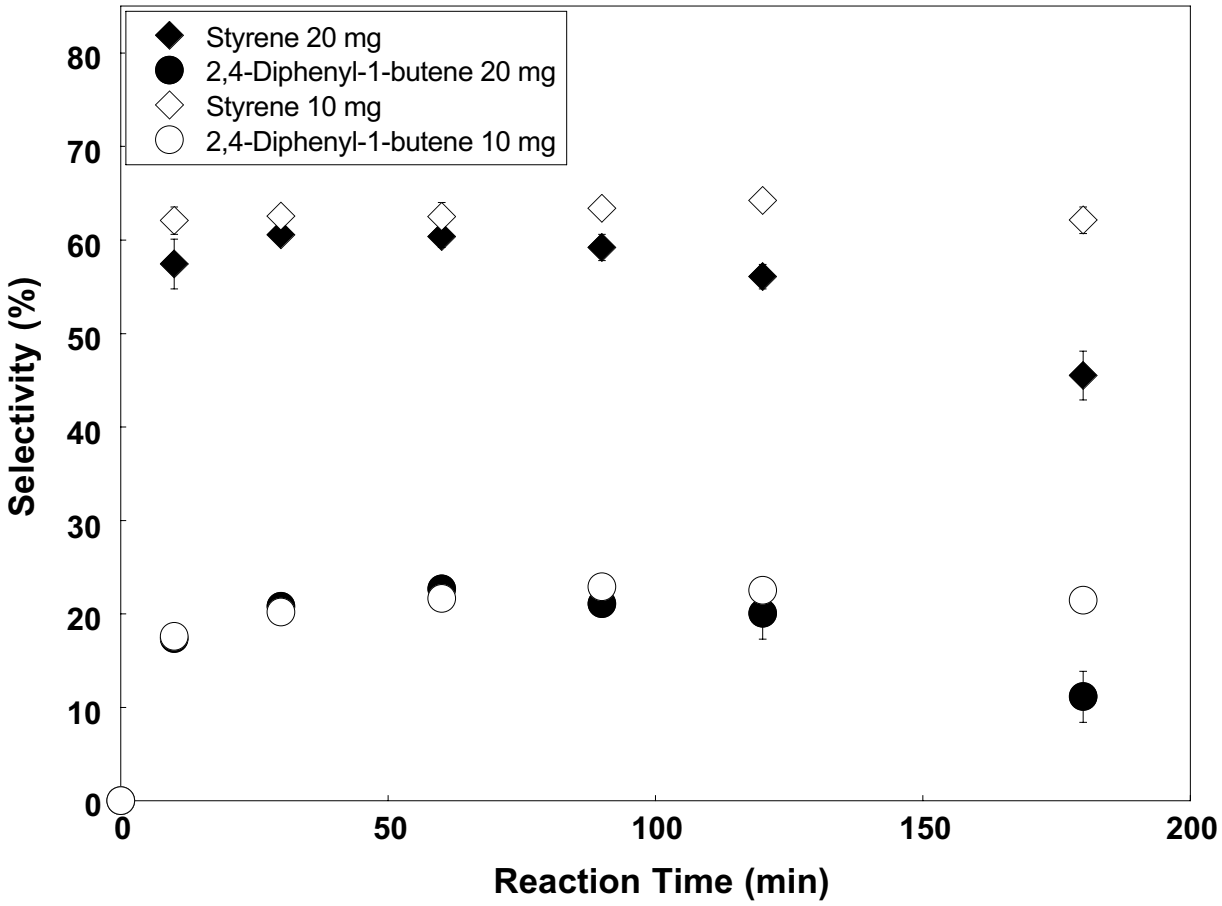
Styrene 20 mg
2,4-Diphenyl-1-butene 20 mg
Styrene 10 mg
2,4-Diphenyl-1-butene 10 mg
Selectivity (%)
Reaction Time (min)
0
10
20
30
40
50
60
70
80
0
50
100
150
200

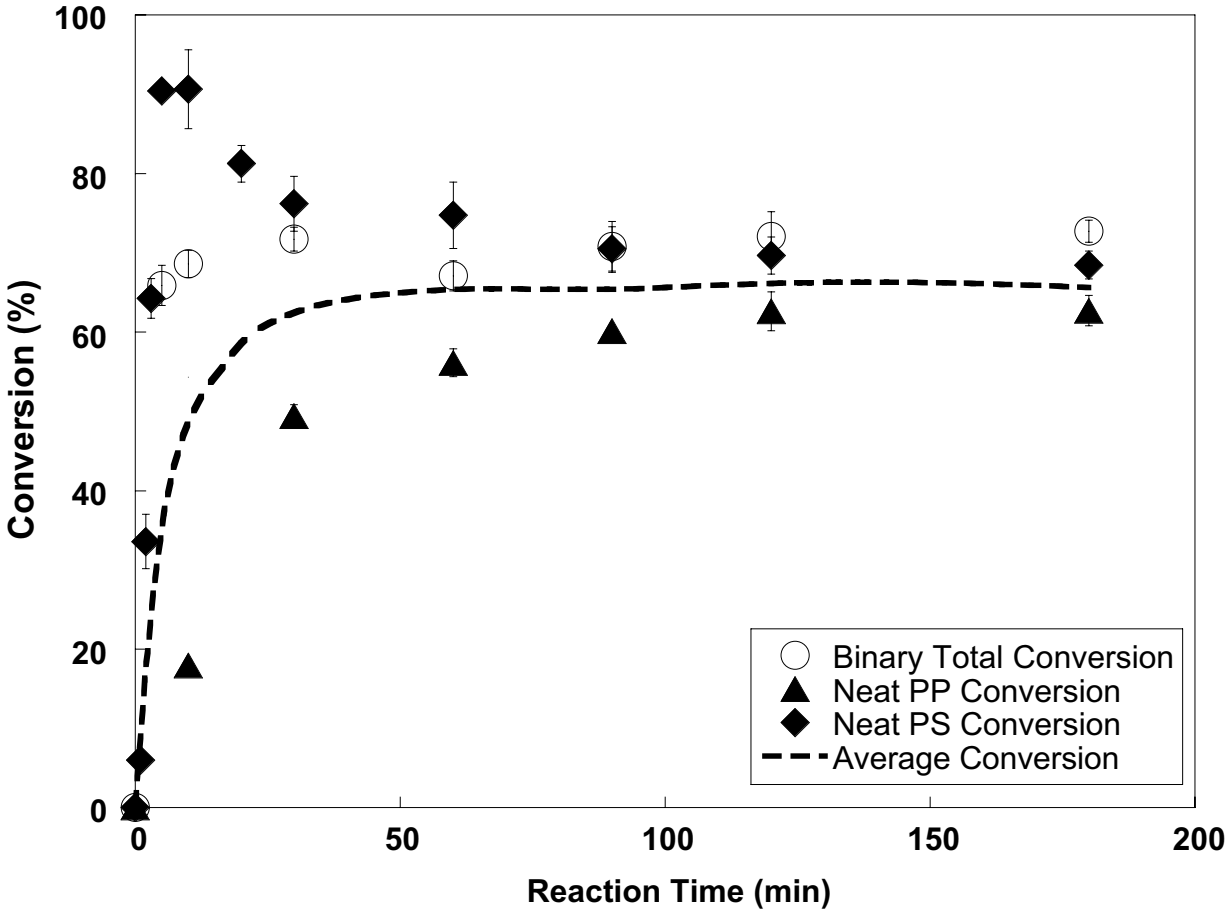
100
80
60
40
20
0
Conversion (%)
0
50
100
150
200
Reaction Time (min)
Binary Total Conversion
Neat PP Conversion
Neat PS Conversion
Average Conversion

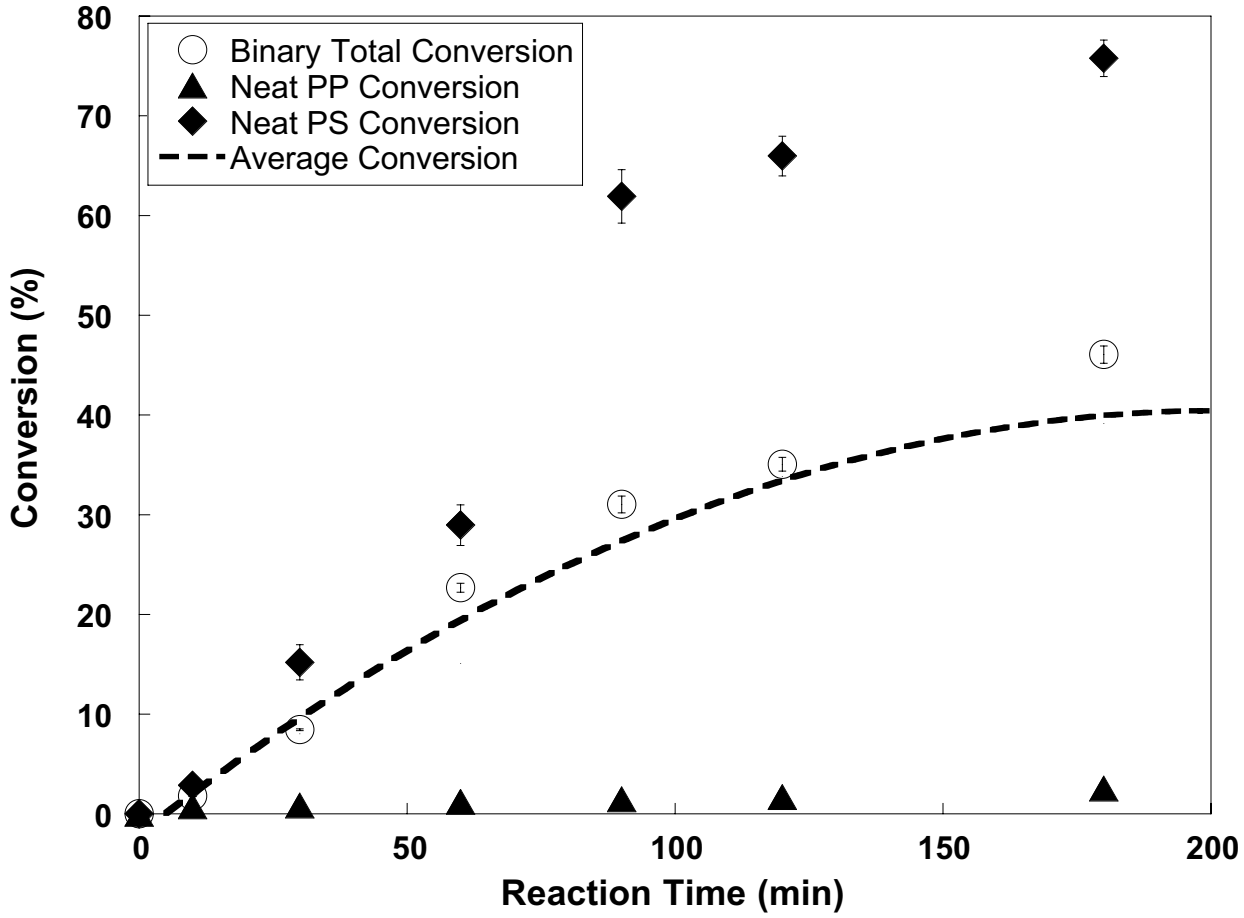
Binary Total Conversion
Neat PP Conversion
Neat PS Conversion
Average Conversion
Conversion (%)
Reaction Time (min)
0
10
20
30
40
50
60
70
80
0
50
100
150
200

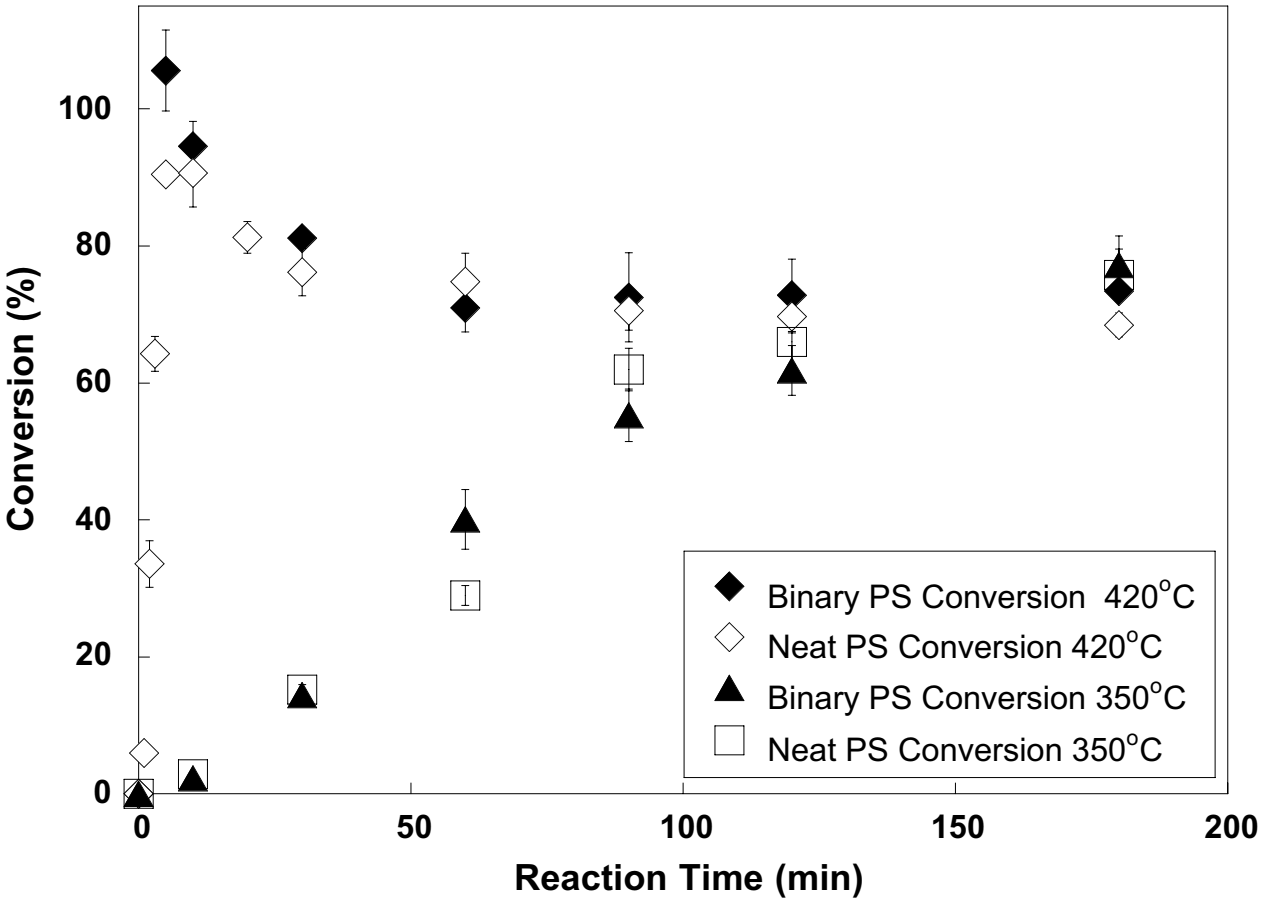
Conversion (%)
100
80
60
40
20
0
0
50
100
150
200
Reaction Time (min)
Binary PS Conversion 420°C
Neat PS Conversion 420°C
Binary PS Conversion 350°C
Neat PS Conversion 350°C

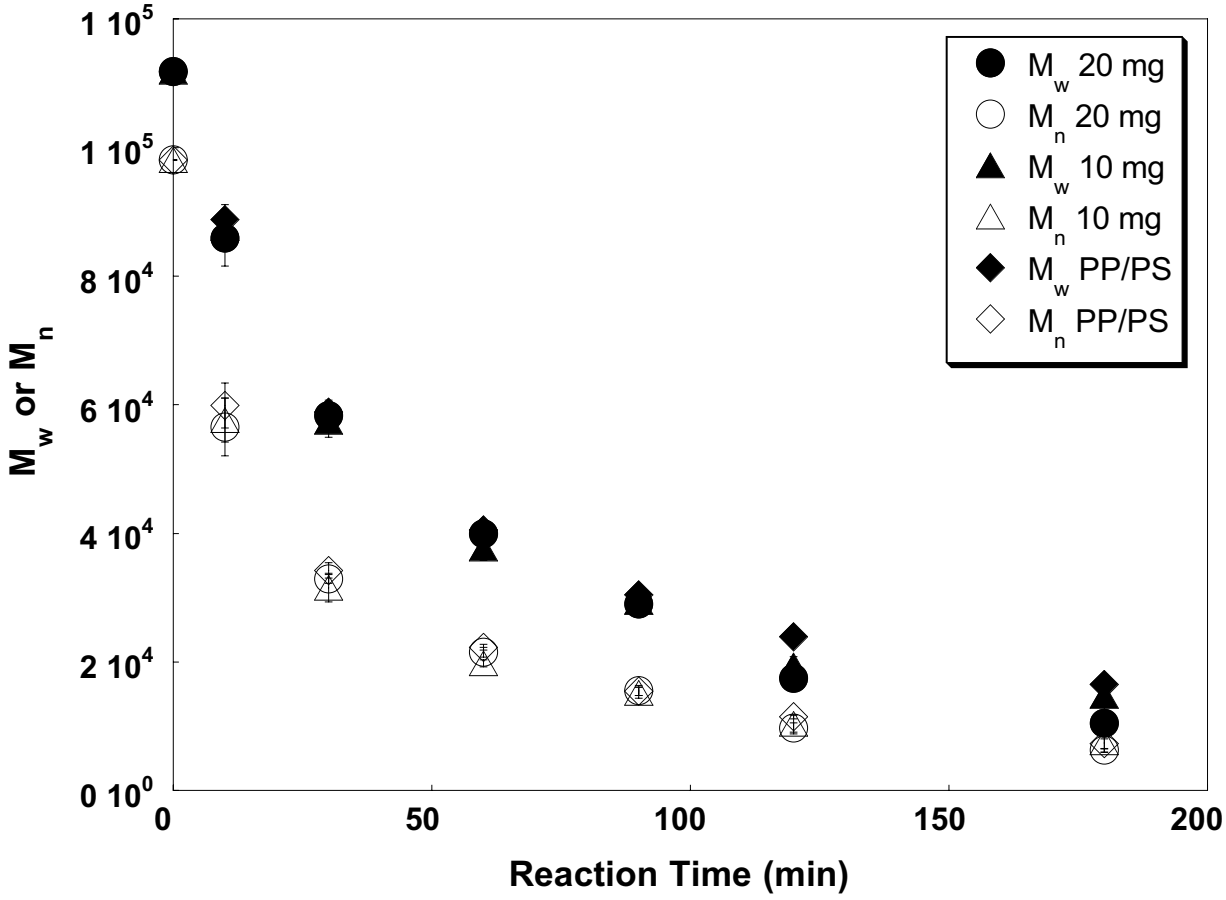
1 10^5
1 10^5
8 10^4
6 10^4
4 10^4
2 10^4
0 10^0
M_w or M_n
0
50
100
150
200
Reaction Time (min)
M_w 20 mg
M_n 20 mg
M_w 10 mg
M_n 10 mg
M_w PP/PS
M_n PP/PS

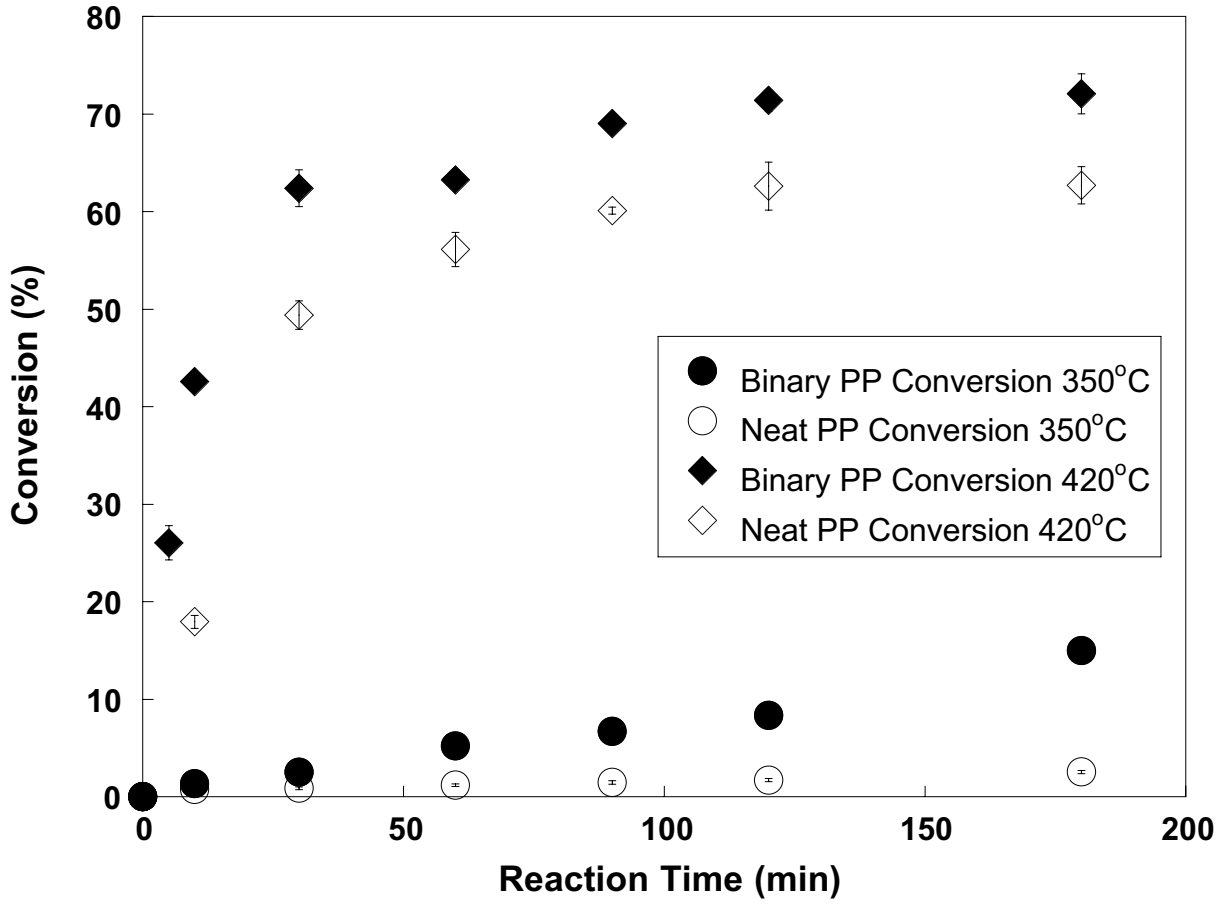
Conversion (%)
Reaction Time (min)
0
10
20
30
40
50
60
70
80
0
50
100
150
200
Binary PP Conversion 350°C
Neat PP Conversion 350°C
Binary PP Conversion 420°C
Neat PP Conversion 420°C

COPROCESSING OF POLYMERIC WASTE WITH COAL: REACTION OF POLYETHYLENE AND COAL MODEL COMPOUNDS

Matthew J. De Witt and Linda J. Broadbelt
Department of Chemical Engineering
Northwestern University
Evanston, Illinois 60208

Keywords: Coprocessing, Coal, Polymeric Waste

ABSTRACT

Environmental and economical concerns over diminishing landfill space and the growing abundance of mixed plastic waste mandate development of viable strategies for recovering high-valued resources from waste polymers. Co-processing of waste polymer mixtures with coal allows for the simultaneous conversion of coal and plastics into high-valued fuels. However, there is limited information about the underlying reaction pathways, kinetics, and mechanisms controlling coal liquefaction in the presence of polymeric materials.

A series of model compound experiments has been conducted, providing a starting point for unraveling the complex, underlying chemistry. Neat pyrolysis studies of model compounds of polyethylene and coal were conducted in batch reactors. Tetradecane ($C_{14}H_{30}$) was used as a polyethylene mimic, and 4-(naphthylmethyl)bibenzyl was used as a coal model compound. Reaction temperatures were 420 and 500˚C, and batch reaction times ranged from 5-150 minutes. Detailed product analysis using gas chromatography and mass spectrometry enabled the reactant conversion and product selectivities to be determined. Reaction of single components and binary mixtures allowed the kinetic coupling between feedstocks to be examined.

INTRODUCTION

Recently, concerns over the inadequacy of current treatment and disposal methods for mixed plastic wastes have driven the exploration of new strategies for viable plastics resource recovery. The emphasis of the recovery is to obtain high-valued, useful products from the waste polymers. Post-consumer waste plastics are a major contributor to the municipal solid waste (MSW) stream, constituting approximately 11% by weight and 21% by volume of waste in landfills[1]. Over 40% of the landfills in the United States were closed in the past decade, and it is estimated that over half of the remaining ones will be full by the end of the century[2]. This poses a significant dilemma since there appears to be no immediate decrease in the usage of plastic products; in fact, due to their versatility, the usage will most likely increase.

The current motivation for the recovery of plastics is due to government mandates, rather than to industrial initiatives. Some states, such as California, Oregon, and Wisconsin, have passed laws which specify that plastic bottles must be manufactured from a minimum of 25% recycled plastics. Germany has dictated that over 80% of all plastic packaging must be recycled by methods other than combustion by 1996[3-5]. Conventional plastics recycling technologies encounter a number of difficulties which range from costly separation to removal of impurities and contaminants. A consequence of these problems is that products manufactured from recycled polymers are of lower quality and higher cost (approximately 10% higher for high-density polyethylene (HDPE)) than those from the corresponding virgin polymer[4]. As a result, in the United States, only about 4% of 30 million tons of total plastics produced each year is recycled[6].

Coprocessing of polymeric waste with other materials may provide potential solutions to the deficiencies of current resource recovery processes, including unfavorable process economics. By incorporating polymeric waste as a minor feed into an existing process, variations in plastic supply and composition could be mediated and as a result, allow for continuous operation. One option for coprocessing is to react polymeric waste with coal under direct liquefaction conditions[2,7,8]. Coprocessing of polymeric waste with coal provides for simultaneous conversion of both feedstocks into high-valued fuels and chemicals.

EXPERIMENTAL

In order to obtain information about underlying reaction pathways, kinetics, and mechanisms without the complicating effects of the macrostructure, experiments were performed using model compounds for both coal and polyethylene, a voluminous component of mixed plastic waste. To mimic the structure of coal, 4-(naphthylmethyl)bibenzyl (NBBM) was used. NBBM contains both condensed and isolated aromatic species connected by short alkyl chains. An added feature is that it contains five different aromatic-aliphatic or aliphatic-aliphatic carbon-carbon bonds. Successful predictions of the relevant primary products for real systems using NBBM confirmed the adequacy of this model compound, and thus, it will be employed in this study[9-12]. The structure of NBBM is depicted in Figure 1. Although numerous hydrocarbons may serve as appropriate model compounds for high density and low density polyethylene, tetradecane, $C_{14}H_{30}$, was chosen as an appropriate compromise in reactant size.

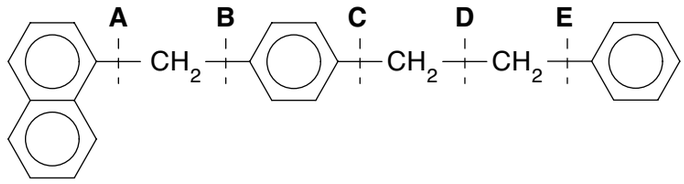

Figure 1: Structure of coal model compound 4-(naphthylmethyl)bibenzyl.

Batch pyrolyses were carried out in an isothermal (±1°C) fluidized sand bath. The experiments were conducted in 2 ml glass cryules charged with ca. 20 mg of reactant for the neat reactions. Equimolar ratios of tetradecane/NBBM were used for the binary experiments, with loadings based on ca. 10 mg of NBBM. After filling, the ampoules were purged with argon, and then sealed using an oxygen/propane flame. Pyrolysis was conducted at both 420 and 500°C, and reaction times ranged from 5-150 minutes. Upon completion of the reaction period, the ampoules were removed from the sand bath and permitted to cool at room temperature. The experiments were replicated a minimum of two times, and conversions and selectivities were reproducible with an error of less than 1%.

Soluble reaction products were extracted from the ampoules using 5 ml of methylene chloride, and an external standard (biphenyl) was added. Product identification and quantification, which enabled reactant conversions and product selectivities to be determined, was achieved using an HP 6890 GC/MS and HP 5890 GC equipped with a flame ionization detector, respectively, each employing a Hewlett Packard 30 m crosslinked 5% Ph Me Silicone capillary column .

RESULTS AND DISCUSSION

The reactant conversions for pyrolysis of tetradecane and NBBM at 500°C were very high, as almost complete conversion was achieved at a reaction time of 10 minutes for all the systems studied. As evidenced by the product spectra and the temporal variations of the major products, secondary and tertiary reactions occurred, making it difficult to deconvolute reaction pathways. Therefore, the reaction temperature was lowered to 420°C, a value still within the range of relevant liquefaction conditions, to achieve lower conversions and isolate primary decomposition pathways. It was noted from the data at 500°C, however, that the conversion of tetradecane was enhanced slightly in the presence of NBBM as compared to the neat reaction.

Reactions carried out at 420°C facilitated identification of the underlying reaction pathways and kinetics. As illustrated in Figure 2, the conversion was significantly lower at a given reaction time as compared to that observed at 500°C. For example, only 37 % of the tetradecane was converted after 150 minutes of reaction time.

The major products observed from the pyrolysis of tetradecane were α-olefins, with minor selectivity to n-alkanes. The highest selectivity, 0.13, was obtained for 1-heptene, and α-olefins with carbon numbers of 6 to 11 were also observed in significantly quantities. As reaction time increased, the selectivity to α-olefins decreased, while that of n-alkanes slightly increased, as observed in Figure 3. This behavior can be explained by noting that hydrogenation of olefins and continued thermal cracking can occur as reaction time increases.

The product distribution was rationalized in terms of the typical free radical Rice-Herzfeld and Rice-Kossiakoff mechanisms[13-16]. The mechanism is initiated by carbon-carbon bond fission along the main chain to form two primary radicals. These primary radicals form secondary radicals through hydrogen abstraction from a secondary carbon or an intramolecular hydrogen rearrangement. These secondary radicals then undergo β-scission to form α-olefins and primary radicals. Termination occurs by recombination of radicals.

Two of the major products from pyrolysis of NBBM, which are formed by carbon-carbon bond fission and subsequent hydrogen abstraction, were toluene and 1-methyl-4-(naphthylmethyl) benzene, each observed with a selectivity of greater than 0.28 at all reaction times studied. The other major product was 1-(2-phenylethenyl)-4-(naphthylmethyl) benzene, with an initial selectivity of approximately 0.35 which decreased linearly with reaction time to 0.11 at 150 minutes. Minor selectivities were observed for a number of products from NBBM pyrolysis. Methyl bibenzyl and 1-(4-(4-methyl)phenylmethyl)benzyl) naphthalene were observed with initial selectivities of 0.055 and 0.070, respectively. Other minor products included 1,4-(binaphthylmethyl) benzene, phenyl methyl naphthalene, naphthalene, methyl naphthalene, 1-(phenylmethyl)-4-(naphthylmethyl) benzene, 1-methyl-4-(2-phenylethenyl) benzene and p-xylene.

Mechanistic interpretation using the ideas put forth by Walter et al. (1994) successfully accounted for the observed product spectra. The products anticipated from scission of the five main bonds of NBBM, labeled A-E, and subsequent hydrogen abstraction and β-scission, are depicted in Figure 4. The formation of high yields of toluene and 1-methyl-4-(naphthylmethyl) benzene is consistent with the proposed mechanism involving bond D fission. This is the weakest bond in the molecule, since the radicals which are formed can be stabilized by the adjacent benzyl substituents. Similarly, the C_2 linkage in NBBM possesses the most easily abstractable hydrogens. Once a secondary radical is formed, it can undergo β-scission to form 1-(2-phenylethenyl)-4-(naphthylmethyl) benzene. This compound could then undergo degradation reactions similar to those observed for NBBM, leading to a reduction in selectivity as reaction time increases.

A comparison of the selectivities of products associated with cleavage of bond A as a function of conversion is shown in Figure 5. If these products were solely formed by bond A scission, it would be expected that the selectivities would be equal for naphthalene and the sum of methyl bibenzyl and its corresponding derivatives. This is clearly not the case. Therefore, another reaction pathway for the formation of these products must exist. Upon examination of other bond scission pairs, a discrepancy between bond C products, phenyl methyl naphthalene, which was

observed, and ethylbenzene, which was not, was noted. Also, as stated, other products which can not be explained by one of the five bond scissions were observed, which leads to investigation of secondary pathways. These observations are consistent with a free radical ipso-substitution scheme for the formation of the various products as proposed by Walter et al. (1994). For example, attack by a benzyl radical of the NBBM molecule at the 1-naphthyl position would afford phenyl methyl naphthalene. This scheme would involve the formation of a mole of naphthalene and phenyl methyl naphthalene for every mole formed of methyl bibenzyl and its derivatives. This comparison is presented in the plot of Figure 6. Likewise, various radical attack at bond C can explain the appearance of 1-(4-(4-methyl)phenylmethyl)benzyl) naphthalene, 1,4-(binaphthylmethyl) benzene, and 1-(phenylmethyl)-4-(naphthylmethyl) benzene. Overall, the main reaction families for NBBM pyrolysis are therefore bond thermolysis, hydrogen abstraction, radical ipso-substitution, β-scission, and radical recombination[12].

Reactions of binary mixtures of tetradecane and NBBM revealed interactions between the reactants and synergistic effects. As observed in Figure 2, tetradecane conversion was increased in the presence of NBBM, which can be rationalized in terms of kinetic coupling[17]. The internal carbon-carbon bonds of tetradecane have a higher bond dissociation energy (90 kcal mol^{-1}) than that of bond D in NBBM (60 kcal mol^{-1})[18]. This has the potential to increase the quantity of radicals in the system with respect to the neat tetradecane experiments at a particular reaction time. The NBBM-derived radicals can easily abstract hydrogen from the secondary carbons of tetradecane, forming a tetradecane-derived radical and converting a tetradecane molecule, enhancing its conversion. Once formed, these tetradecane-derived radicals undergo their own decomposition reactions as observed for neat pyrolysis, and similar product yields are observed.

The interactions between NBBM and tetradecane can be further supported by examining the products derived from NBBM. Since abstraction of hydrogen from tetradecane is facile and has a high reaction path degeneracy of 24, NBBM radicals are capped and stabilized through this abstraction step before undergoing secondary reactions. This effect on the overall product yields can be discerned from Figure 7. The radicals formed from bond D thermolysis abstract hydrogen with higher selectivity and afford higher yields of toluene. Correspondingly, the selectivity to the radical ipso-substitution pathway and formation of phenyl methyl naphthalene is diminished. Therefore, it can be seen that during low pressure pyrolysis, favorable interactions between the two reactants exist. The effective tetradecane conversion is increased, and primary product selectivities are enhanced.

CONCLUSIONS

Recent investigations have demonstrated the feasibility coprocessing of coal with polymers. In this study, feedstock interactions were observed using model compound mimics of both coal and polyethylene. In binary mixtures, the conversion of tetradecane increased while the selectivity to primary products of NBBM pyrolysis was enhanced. These observations were attributed to the stabilization of NBBM-derived radicals through hydrogen abstraction from tetradecane which in turn, increases the rate of tetradecane conversion In order to optimize the interaction between reactants, further experimental and theoretical studies will be conducted at high pressures and in the presence of catalysts in order to delineate the underlying kinetics, pathways, and mechanism controlling coal/polymer coprocessing.

ACKNOWLEDGMENTS

This work was supported by the United States Department of Energy Grant DE-FG22-96-PC96204.

REFERENCES

[1]-Rowatt, R.J., *Chemtech*, 1993, **23**, 56-60.

[2]-Taghei, M., Feng, Z., Huggins, F., and Huffman, G.R., *Energy & Fuels*, 1994, **8**, 1228-1232.

[3]-Menges, G., Emminger, H., and Lackner, G., *International Journal of Materials and Product Technology*, 1991, **6**, 307-330.

[4]-Graff, G., *Modern Plastics*, 1992, **69**, 45.

[5]-Fouhy, K., Kim, I., Moore, S., and Culp, E., *Chemical Engineering*, 1993, **100**, 30-33.

[6]-EPA, *U.S. Environmental Protection Agency*, 1992.

[7]-Anderson, L.L. and Tuntawiroon, W., *American Chemical Society, Division of Fuel Chemistry--Preprints*, 1993, **38**, 816-822.

[8]-Joo, H.K. and Curtis, C.W., *Energy & Fuels*, 1996, **10**, 603-611.

[9]-Farcasiu, M. and Smith, C., *Energy & Fuels*, 1991, **5**, 83-87.

[10]-Matson, D.W., Linehan, J.C., Darab, J. G., and Buehler, M. F., *Energy & Fuels*, 1994, **8**, 10-18.

[11]-Tang, Y. and Curtis, C.W., *Energy & Fuels*, 1994, **8**, 63.

[12]-Walter, T.D., Casey, S.M., Klein, M.T., and Foley, H.C., *Catalysis Today*, 1994, **19**, 367-380.

[13]-Rice, F.O., *Journal of the American Chemical Society*, 1933, **55**, 3035-3040.

[14]-Kossiakoff, A. and Rice, F.O., *Journal of American Chemical Society*, 1943, **65**, 590-595.

[15]-Voge, H.H. and Good, G.M., *Journal of American Chemical Society*, 1949, **71**, 593-597.

[16]-Mushrush, G. W. and Hazlett, R.N., *Industrial & Engineering Chemistry Fundamentals*, 1984, **23**, 288-294.

[17]-LaMarca, C., Libanati, C., and Klein, M.T., *Chemical Engineering Science*, 1990, **45**, 2059-2065.

[18]-Poutsma, M.L., *Energy & Fuels*, 1990, **4**, 113-131.

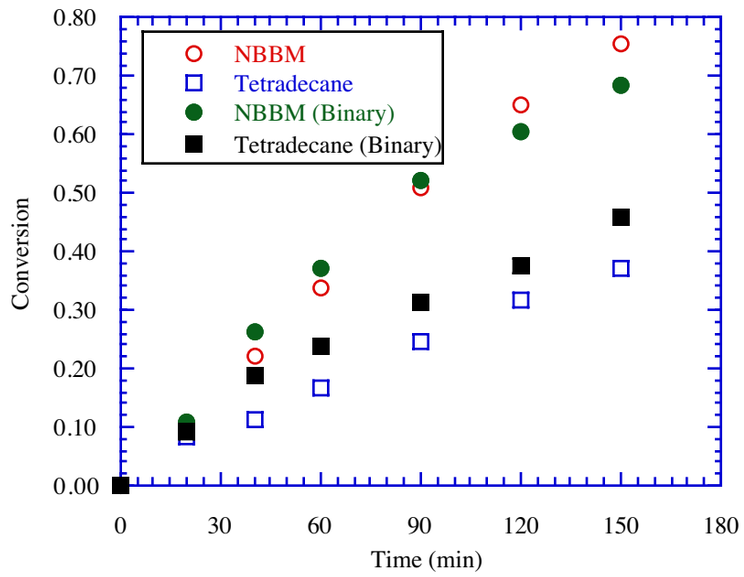

Figure 2: Conversion of tetradecane and NBBM, neat and in binary mixtures, at 420 °C.

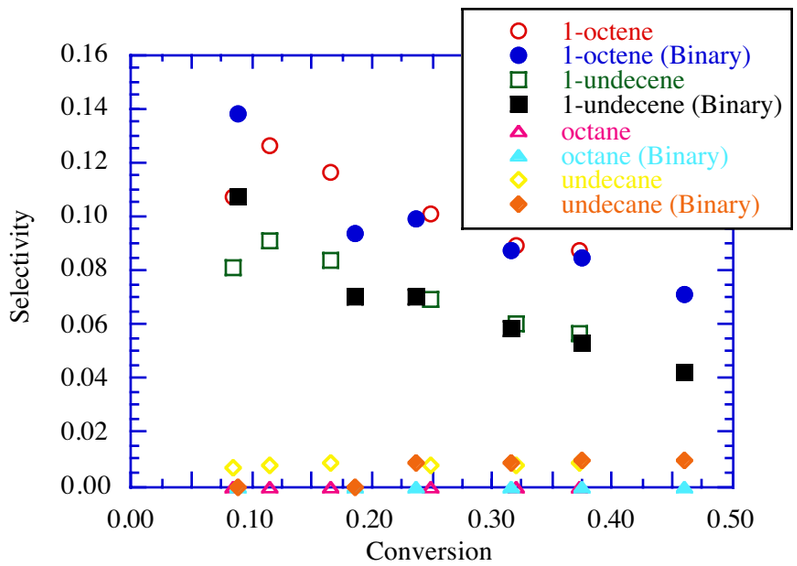

Figure 3: Comparison of alkane/alkene selectivities during neat and binary mixture reactions.

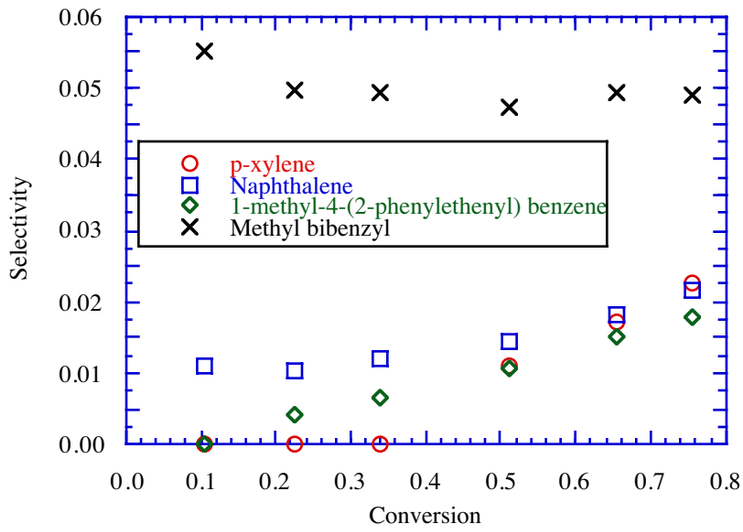

Figure 5: Comparison of selectivities of products associated with cleavage of bond A as a function of conversion.

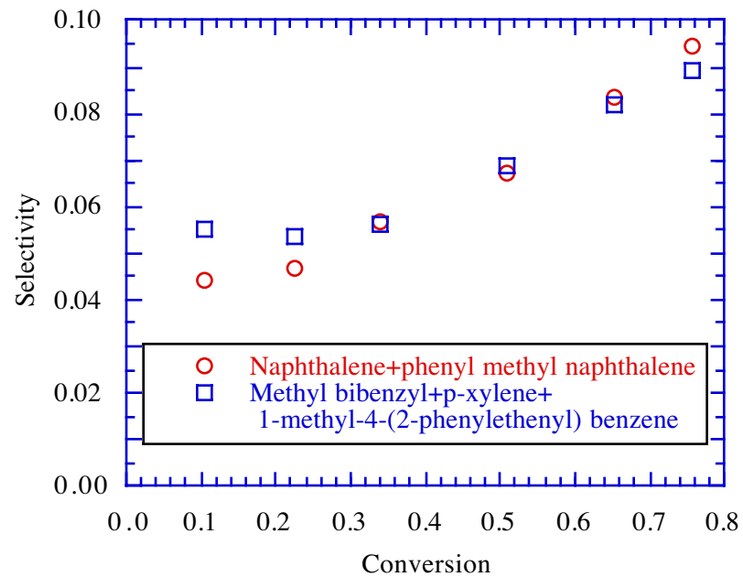

Figure 6: Comparison of products from free radical ipso-substitution reaction which accounts for cleavage of bond A.

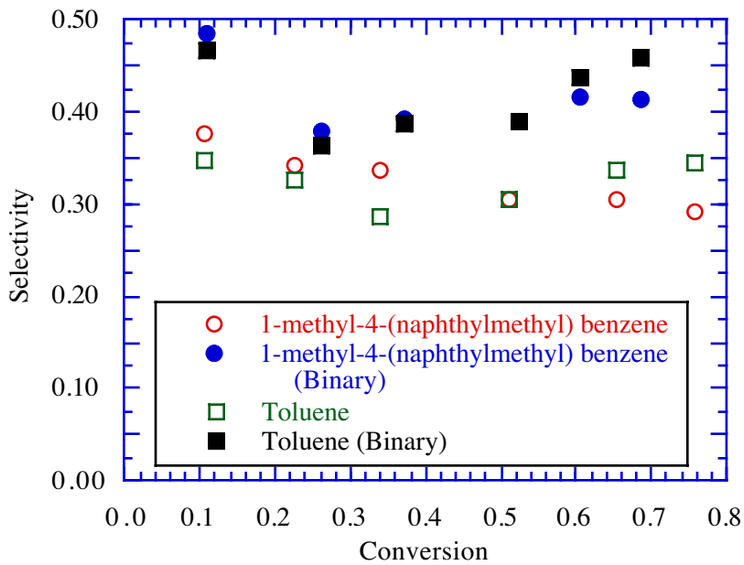

Figure 7: Comparison of products from bond D cleavage during neat NBBM and binary mixture reactions.

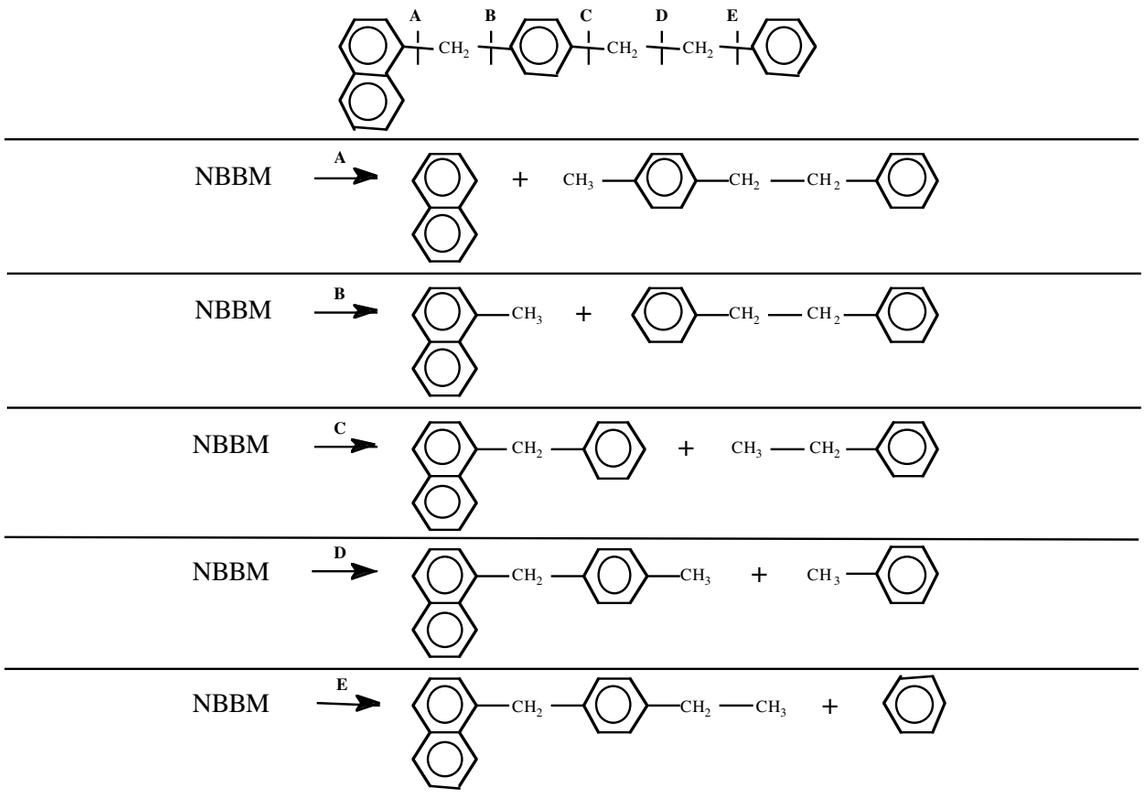

Figure 4: Bond assignment and corresponding products of NBBM pyrolysis, allowing for only bond fission, hydrogen abstraction, and β-scission

TERTIARY RESOURCE RECOVERY FROM WASTE POLYMERS VIA PYROLYSIS: POLYPROPYLENE

Hsi-Wu Wong, Todd M. Kruse, Oh Sang Woo and Linda J. Broadbelt
Department of Chemical Engineering
2145 Sheridan Road, Northwestern University
Evanston, IL 60208

ABSTRACT

Polypropylene is a significant component of mixed plastic waste from which fuels and chemicals can be recovered via thermal or catalytic degradation. Pyrolysis of polypropylene was investigated at a temperature of 420°C and reaction times ranging from 10 to 180 minutes. Total conversion reached approximately 60% at 90 minutes, and no significant change was observed for longer reaction times. The selectivity to monomer, propylene, achieved a plateau at approximately 10% after a reaction time of 90 minutes. The overall product distribution can be explained by the typical free radical mechanism with the dominant products as alkenes in the form of C_{3n}, alkanes in the form of C_{3n-1}, and dienes in the form of C_{3n-2}.

I. INTRODUCTION

In recent years, post-consumer wastes have caused increased concern because of the escalation of municipal solid wastes (MSW) generated. In 1995, 208 tons of MSW were generated, and it increased to 340 tons in 1998, with more than 60% of MSW landfilled. The decreasing availability of landfill space and the inefficient use of post-consumer products through landfilling, have heightened the attention paid to recycling of MSW over the past decade.

Plastics make up a significant portion of post-consumer products. In the United States alone, over 70 billion pounds of plastics are manufactured annually, while only 10% of this amount is recycled or incinerated. In 1995, 9.1 weight percent of MSW was composed of plastics, with a total of 30% by volume. Among the plastic waste, 15.3 weight percent contained polypropylene.

Currently, the recycling of plastics can be divided into four categories – primary, secondary, tertiary, and quaternary. Primary recycling simply reuses the plastics as products that have similar properties to the discarded materials. Secondary recycling, also known as material or mechanical recycling, is achieved by melting, grinding, and reforming plastic waste mixtures into lower value products. Tertiary recycling converts discarded plastic products into high-value petrochemical or fuel feedstocks. Quaternary recycling uses combustion or incineration to recover energy from plastic products. Since primary and secondary recycling have limitations on the properties and uses of the final products, and quaternary recycling is an insufficient use of resources and has a negative public image because of release of CO_2 and airborne particles, tertiary recycling promises the best long-term solution. However, tertiary recycling is not economical at present. One of the biggest costs is the sorting of the original polymers. Therefore, processing of multicomponent polymeric wastes may provide a potential solution. To establish a baseline to which pyrolysis of mixed plastic wastes containing polypropylene can be compared, the thermal degradation of neat polypropylene was examined.

II. EXPERIMENTAL

Batch pyrolysis experiments were carried out by loading 20 mg of polypropylene (PP) into a 3.1-ml glass ampoule (Wheaton). The polypropylene was obtained from Aldrich Chemical (M_w=127,000, M_n=54,000) in powder form. After purging with argon for 2 minutes, each ampoule was sealed using an oxygen/propane flame, and then the sample was reacted in an isothermal fluidized sand bath at 420°C. Reaction times ranged from 10-180 minutes. Upon completion of the reaction, the ampoule was removed from the sand bath and quenched in another sand bath set at ambient temperature. Three replicates were performed for each reaction time.

Gaseous products were analyzed by putting the ampoule inside a 53-ml flask with a Tygon tube on one end and an injection port on the other. Both ends were then sealed with septa. The flask was purged with helium for 10 minutes and, after the ampoule was broken, allowed to equilibrate for 30 minutes. Two ml gas samples for the 10 minute reaction runs and 1 ml samples for the other runs were then taken using a gas-tight syringe. Gaseous products were then identified and quantified against known standards using a Hewlett Packard 5890 Series II Plus Gas Chromatograph equipped with a thermal conductivity detector (TCD) and a 6 ft stainless steel Porapak Q column (Supelco).

Liquid and solid products were extracted with 1.5 ml HPLC grade methylene chloride overnight. The product solution was first passed through a 0.45-μm polypropylene filter (Alltech) attached to a syringe and then passed through a Waters Gel Permeation Chromatograph (GPC). Products with molecular weights less than ~400 g/mol were collected with the fraction collector attached to the GPC outlet. An external standard (biphenyl) was added after fraction collection. Product identification and quantification were achieved using a Hewlett Packard 6890 Series Gas Chromatograph-Mass Spectrometer and a Hewlett Packard 6890 Series Gas Chromatograph with a flame ionization detector (FID), each equipped with a Hewlett Packard 30 m crosslinked 5% Ph Me Silicone capillary column.

The percent conversion of PP, X, was defined according to the equation:

$$X = \frac{W_g + W_l}{W_o} \times 100\%$$

where W_g is the weight of gaseous products, W_l is the weight of liquid products with carbon number less than or equal to 25, and W_o is the initial weight loading of PP. Selectivity, S, of a certain species A was based on the following equation:

$$S = \frac{W_A}{W_g + W_l} \times 100\%$$

where W_A is the weight of species A. Product yields were normalized by dividing the millimoles of each product by the initial molar loading of propylene repeat units. Finally, error bars shown in the figures represent the standard deviations of experiments that have been triplicated.

III. RESULTS

The overall conversion of neat pyrolysis of polypropylene increased with respect to reaction time, as illustrated in Figure 1. After 90 minutes of reaction, the conversion reached approximately 60%, and no significant change was observed at longer reaction times. This suggests that little additional conversion can be achieved even for very long reaction times at this temperature in a closed batch reactor of 3.1 ml. The selectivity of polypropylene monomer, propylene, showed similar behavior, achieving a selectivity of approximately 10% after 90 minutes of reaction as shown in Figure 2.

If the products were divided into three fractions, C_1-C_4, C_5-C_{10}, and C_{11}-C_{25}, respectively, the yields of these fractions behaved differently. As shown in Figure 3, the yield of the C_1-C_4 fraction increased with reaction time, whereas the C_5-C_{10} fraction reached a maximum around 120 minutes and no significant change was observed at 180 minutes. Finally, the C_{11}-C_{25} fraction reached a maximum around 60 minutes. These results suggest that as reaction time increased, the heavier products decompose to lighter ones.

The reaction products of polypropylene pyrolysis consisted of four major categories - alkanes, alkenes, dienes, and aromatic compounds. Lower molecular weight species were found in higher yields whereas there were notable decreases in the yields with carbon numbers greater than ten. For alkanes, the most dominant product was ethane (C_2). In addition, pentane (C_5), 4-methylheptane (C_8), C_{11}, C_{14}, and C_{17} were found in the highest yield; the alkanes were thus dominated by products with carbon numbers C_{3n-1}, with n=1, 2, 3, 4,…, as shown in Figure 4. The yields of the majority of the alkanes increased with respect to reaction time. For alkenes, propylene was the most dominant product with propylene oligomers (C_6, C_9, C_{12}, C_{15}, C_{21}, and C_{24}), i.e., C_{3n}, n=1, 2, 3, 4,…, as the other major olefinic products. As shown in Figure 5, yields of alkenes with carbon numbers greater than five all reached maximum values then decreased when reaction time increased. However, yields of lighter alkenes (with carbon numbers less than five) increased monotonically with reaction time. Dienes, which were found beginning with C_7 and were present in relatively low yields, appeared as C_7, C_{10}, C_{13}, C_{16}, C_{19}, C_{22}, and C_{25}, i.e., C_{3n-2}, n=3, 4, 5, 6,…(not shown). They also appeared to reach maximum values then decrease except for C_7. Finally, aromatic compounds were also found as minor products. Their yields were comparable in magnitude to the diene yields. The yields of aromatic compounds generally increased with respect to reaction time (not shown).

As noted above, the product distribution showed that most alkenes appeared in the form of C_{3n}, whereas alkanes and dienes appeared in the form of C_{3n-1} and C_{3n-2}, respectively. This product distribution is in agreement with observations reported in the literature [1-2] and can be explained by the mechanism illustrated in Figure 6, which was based on the one proposed by Tsuchiya et al. [3]. The initiation step of the free radical mechanism is simply to break any of the PP long chains into two shorter end-chain radicals. The end-chain radicals (or mid-chain radicals formed subsequently) may abstract hydrogen from a PP long-chain to form a tertiary radical, as shown in Figure 6(a). Upon undergoing β-scission, the tertiary polymer radical is broken into two parts, one with a double bond on the end (denoted as I), and the other with a secondary free radical (denoted as II). When the polymer chain I is attacked by another free radical and β-scission occurs, dienes (in the form of C_{3n-2}) and alkenes (in the form of C_{3n}) can be formed, as shown in Figure 6(b). On the other hand, polymer chain II can undergo three kinds of reactions such that alkanes (in the form of C_{3n-1}) and alkenes (in the form of C_{3n}) can be formed. Figure 6(c) shows three possible reaction pathways of polymer chain II. Although other steps not explicitly drawn are possible, the formation of C_{3n} alkenes, C_{3n-1} alkanes and C_{3n-2} dienes as the dominant products suggests that the mechanism in Figure 6 captures the major reaction pathways.

ACKNOWLEDGMENT

The authors are grateful for financial support from the Department of Energy (DE-FG22-96-PC96204), the CAREER Program of the National Science Foundation (CTS-9623741), and the MRSEC program of the National Science Foundation (DMR-9632472) at the Materials Research Center of Northwestern University.

REFERENCES

[1] Uemichi, Y., Kashiwaya, M., Tsukidate, M., Ayame, A., and Kanoh, H., *Bull. Chem. Soc. Jpn.*, 1983, **56**, 2768-2773.

[2] Audisio, G., Silvani, A., Beltrame, P. L., and Carniti, P., *Journal of Analytical and Applied Pyrolysis*, 1984, **7**, 83-90.

[3] Tsuchiya, Y., Sumi, K., *Journal of Polymer Science: Part A-1*, 1969, **7**, 1599-1607.

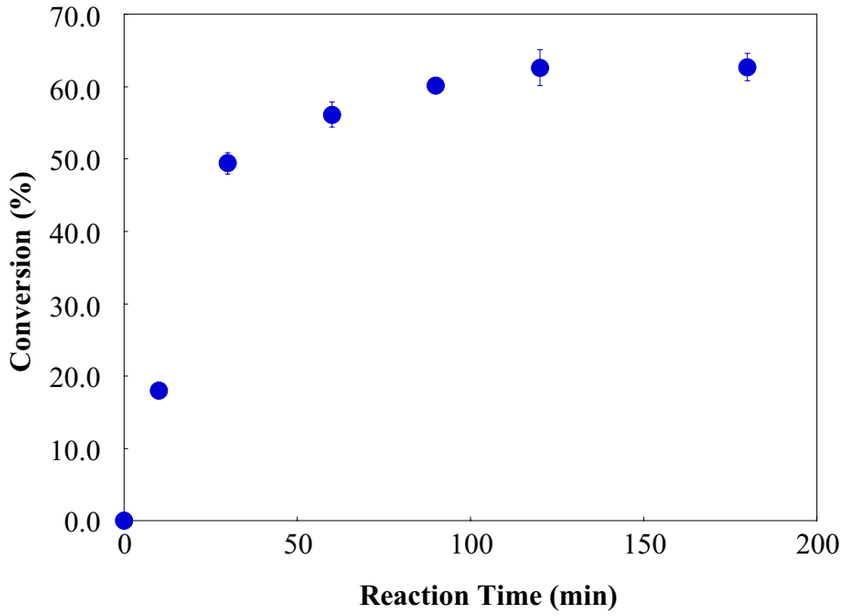

Figure 1 : Conversion of polypropylene as a function of reaction time.

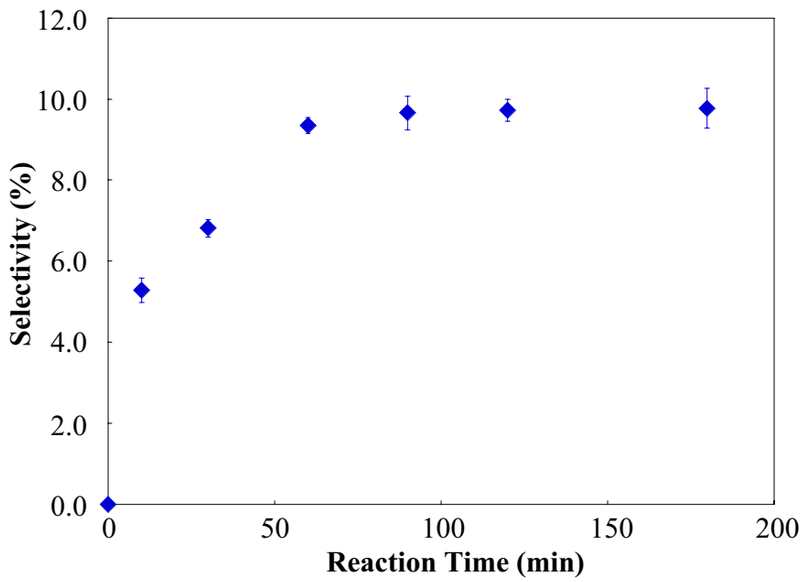

Figure 2 : Selectivity of propylene as a function of reaction time.

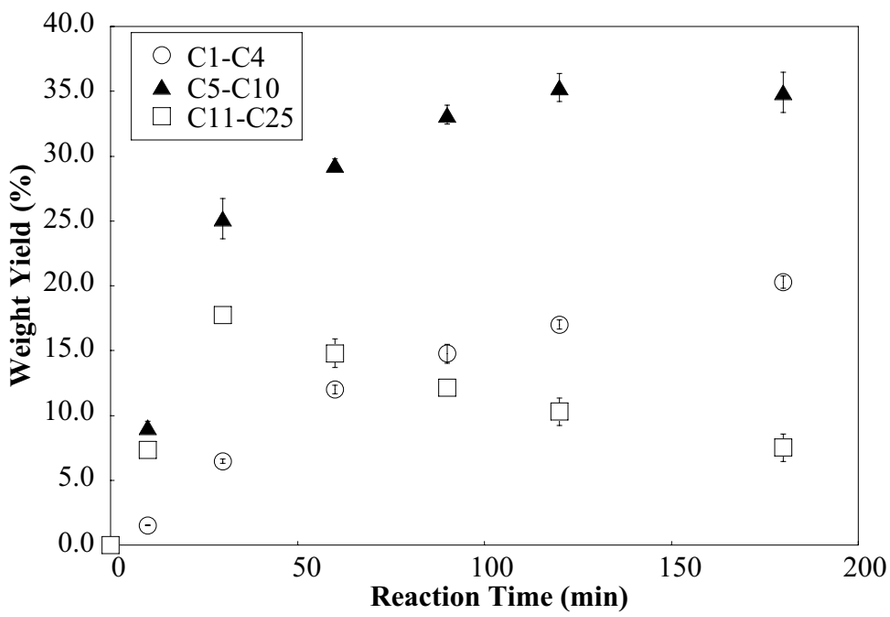

Figure 3 : Weight yields of different product fractions as a function of reaction time.

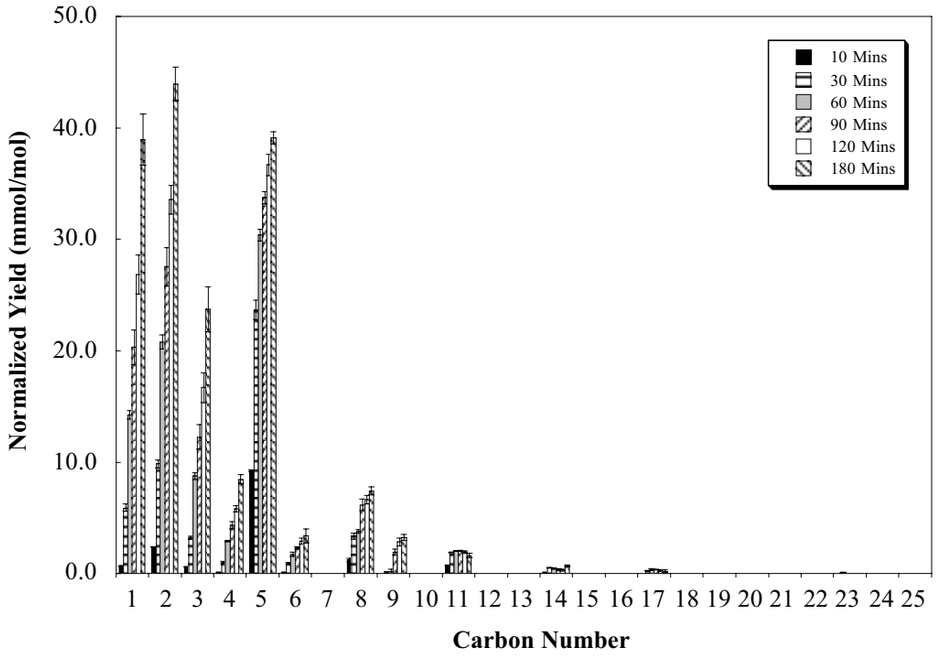

Figure 4 : Comparison of normalized yields of alkanes as a function of reaction time and carbon number.

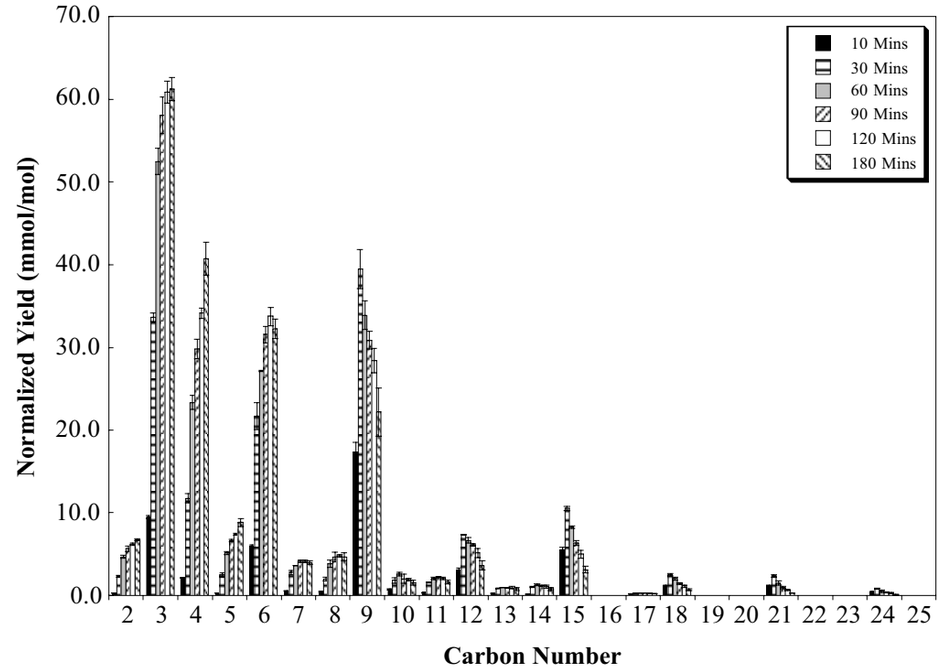

Figure 5 : Comparison of normalized yields of alkenes as a function of reaction time and carbon number.

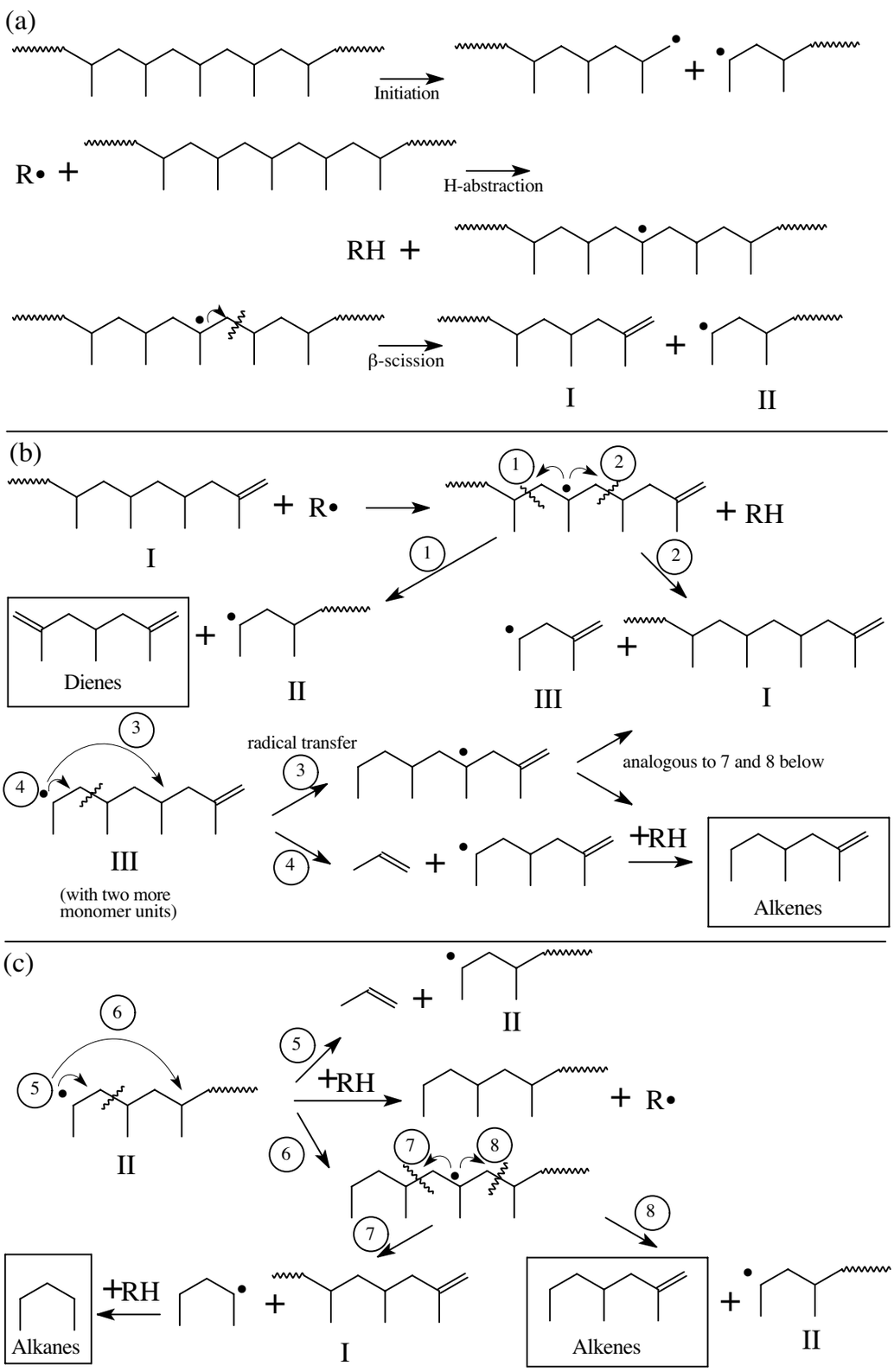

Figure 6: (a) Formation of two kinds of polymer chains (I and II) through bond fission, hydrogen abstraction and β-scission and proposed reaction mechanisms of polymer chains (b) I and (c) II.

Computer Generation of Reaction Mechanisms Using Quantitative Rate Information: Application to Long-Chain Hydrocarbon Pyrolysis

Matthew J. De Witt, David J. Dooling, and Linda J. Broadbelt*
Department of Chemical Engineering
Northwestern University
Evanston, Illinois 60208-3120

Abstract

In recent years, the use of mechanistic modeling to identify the underlying kinetics of complex systems has increased greatly. One of the challenges to kinetic modeling is constructing a model which can capture the essential chemistry of a system while retaining a manageable size. The rate-based generation of mechanistic models is an attractive approach since kinetically significant species can be determined and selectively included in the final mechanism. An algorithm for the rate-based generation of reaction mechanisms developed previously[1] was improved and used to construct a compact mechanistic model for low pressure tetradecane pyrolysis. Though thousands of species and reactions were generated, only a small portion of these (2% of species and 20% of reactions) was deemed necessary and incorporated into the final model. Experimental data were used to determine frequency factors for a subset of the reaction families, while all other kinetic parameters were set based on literature values. With no adjustment to the optimized frequency factors, the mechanistic model was able to accurately predict reactant conversions and product yields for varying reaction conditions and initial reactant loadings. It was also observed that increasing the quantity of species initially seeded resulted in a smaller mechanism that had comparable fitting and predicting abilities as models seeding only the reactant. Subsequent regeneration of the reaction mechanisms using the optimized values for the frequency factors resulted in smaller models with comparable capabilities.

Introduction. The use of kinetic modeling has significantly increased in recent years due to both economic and environmental driving forces. Kinetic modeling allows for the facile and rapid

investigation of various processing conditions while at the same time allowing the modeler to evaluate proposed reaction mechanisms, quantify the underlying reaction kinetics, and interpret complex experimental data. Furthermore, the information obtained from mechanistic modeling can be subsequently used for overall process improvement and optimization.

The major challenge to constructing mechanistic models is the extreme complexity that accounting for all possible reactions, products, and reactive intermediates creates. The pyrolysis of hydrocarbons, for example, can generate thousands of reactive intermediates and products, making tabulation and tracking of all the species very difficult. Manual construction of models for such systems is daunting, and therefore, employing computers to automatically generate and reduce large mechanisms is attractive and is a strategy used by a number of researchers in recent years.[1-18] Although models of significant size can be developed using typical workstations today, there is still a limit to the overall mechanism size that can be solved in a reasonable amount of time. Therefore, there is a driving force to create the smallest mechanism possible which still contains all kinetically significant species and reactions. Hence, the ability to determine necessary and important species with the exclusion of "unreactive" ones is a vital aspect of the automated construction of reaction mechanisms.

The program for automatic mechanism generation of Broadbelt et al., NetGen,[6-8] has been successfully used to generate reaction mechanisms for several distinct reaction chemistries. The original version of NetGen generated reaction mechanisms using a rank-based generation criterion, which limited the addition of a species to the growing network based upon the number of successive reactions necessary to produce it starting from the initial reactant pool. Although adequate models were produced using this approach, many insignificant species of low rank could be included, while truly important "reactive" species of higher rank were omitted. Therefore, recent work has been carried out to improve the ability of the program to consider a larger number of species while retaining only those which influence the kinetics.[1,17] The basic approach is to estimate reaction rate constants during generation and solve the model as it is being constructed, allowing for the determination of important species in the growing mechanism. These studies have

considered a significantly higher number of total species than the rank-based generation criterion, while distilling these species into a more manageable reaction mechanism. The work which will be discussed in this paper expands on the previous studies of Susnow et al.[1] by introducing thermodynamic constraints into the estimation of the controlling rate parameters and a modified approach for determining the species included in the final mechanism. Furthermore, several different models were built by varying the parameters controlling the rate-based generation, and each model's utility was assessed through its ability to capture experimental data for tetradecane pyrolysis collected in our laboratory.[19] Rank-based models were unable to capture the experimental data. Hardware limitations prevented a rank two model from being constructed (> 6000 species), and a rank one model was unable to capture the disappearance of olefin products observed experimentally. The rate-based methodology employed and its application to long-chain hydrocarbon pyrolysis are discussed below.

Details of the Rate-Based Building Algorithm. To generate a reaction mechanism for long-chain hydrocarbon pyrolysis which would be valid over wide ranges of temperature, concentration, and reaction time yet still maintain a manageable size, necessary *reactive* radical intermediates and product molecules (collectively referred to as "species") were determined employing a rate-based generation criterion. The algorithm employed was similar to that of Susnow et al.[1]; however, some key modifications enhanced its capabilities. Thermodynamic constraints were incorporated into the estimation of the rate constants, and reaction time was used as the iteration variable.

The general approach is summarized as follows. Initially, the reactant or reactants for which the mechanism is being generated are specified by the user. These are treated as reactive species and are added to the reactive species list. The temperature, pressure, and reactor type which are to be employed are also specified. The input values for the temperature and pressure should be reasonable for the conditions for which the final model will ultimately be used. However, because the reactions are described at the mechanistic level and the rate constants are temperature dependent, the model is valid beyond the conditions used for its construction. The user then specifies the total

reaction time and the particular types of reactions that the reactive species may undergo. Some reactions will result in the formation of species which are currently not in the mechanism, and these species are not permitted to immediately undergo further reactions. These species are labeled *unreactive* in the growing model. The rate of formation of a particular *unreactive* species, and hence its kinetic significance, is solely dependent upon *reactive* species. It should be noted that although there is distinction between *reactive* and *unreactive* species, all species and reactions which are generated are tracked throughout the entire model construction process.

To quantify the rates of formation of the *unreactive* species and therefore determine which species will be allowed to react next, the species balance equations are combined with the appropriate reactor design equations and the model is solved. To control mechanism growth for batch reaction kinetics, reaction time was used as the controlling iteration variable, and the subinterval used to increment time was adjusted as the time constant of the kinetics changed during reaction. Choice of reaction time as the controlling iteration variable differs from the approach in previous work,[1] where intervals of reactant conversion were used. The current approach is more general in that it can easily be applied to systems with many reactants and, hence, many different reactant conversions, without ambiguity. Furthermore, it more accurately reflects the dynamics of systems in which reactants quickly reach equilibrium or have a very slow rate of conversion.[20]

To determine which species were allowed to react at any given point during mechanism generation, a characteristic rate of the system was defined as:

$$R_{char} = \max\left(\left|r_i\right|\right) \tag{1}$$

where r_i is the net rate of formation of species i, and the function max selects the largest absolute value of r_i from the set of all r_i for *reactive* species over the interval of integration. In our work, R_{char} is based on the most dynamic species in the system instead of on a single reactant that may equilibrate or react slowly as used previously.[1] The minimum rate of formation for a species to be considered *reactive*, R_{min}, is calculated:

$$R_{min} = \varepsilon \cdot R_{char} \quad , \quad \varepsilon > 0 \tag{2}$$

where ε is a user-defined threshold. The list of *unreactive* species is then inspected, and the species with the largest rate of formation, $r_{j,max}$, is selected. If $r_{j,max}$ is greater than R_{min}, species *j* is added to the *reactive* species list. The new *reactive* species is then subjected to the reaction rules, and all of the possible reactions for the new species are generated. The new model, with one more *reactive* species and (possibly) several more *unreactive* species than the previous model, is then solved for the same time subinterval. The R_{char}, R_{min}, and $r_{j,max}$ values are recalculated, and the new $r_{j,max}$ and R_{min} are compared. This iterative procedure continues until $r_{j,max}$ is less than R_{min}. At this point, the algorithm proceeds to the next time subinterval and the entire process is repeated. The process terminates after the last subinterval has been traversed. The user can tailor the model size through the ε parameter and the total reaction time. Decreasing ε will result in larger reaction mechanisms since *unreactive* species will need to be formed at a smaller fraction of the characteristic rate of the system to be considered as *reactive*. Varying the length of the total reaction time allows for the investigation of a wide range of reactant conversions.

Rate Constant and Thermochemical Property Estimation. To employ the rate-based generation criterion during model construction, it is essential to have reliable estimates of the reaction rates in the mechanism. In this work, a hierarchical approach was employed to calculate rate parameters for all reactions generated during the construction of the rate-based mechanism. During model generation, all reactions created were first compared to a user-defined rate constant library containing specific reactions and their respective Arrhenius frequency factors and activation energies. If a generated reaction exists in this library, the appropriate rate constant parameters from the library are assigned within the model. For this investigation, available experimental rate constants for *n*-alkane pyrolysis[21-23] were used.

If experimental data for particular reactions were not available, a combination of literature values, linear free energy relationships (LFERs), and thermodynamic data was used to estimate the rate parameters. Specifically, typical literature values or optimized values of frequency factors and the Evans-Polanyi relationship were used to estimate rate constants for forward reactions, k_f, while

the reverse rate constants were constrained by reaction thermodynamics. The Evans-Polanyi relationship[24] relates the activation energy, E_A, to the heat of reaction, ΔH_{rxn}, through the equation:

$$E_A = E_0 + \alpha \Delta H_{rxn} \tag{3}$$

where E_0 is termed the intrinsic barrier to reaction, and α is the reaction transfer coefficient. E_0, α, and the Arrhenius frequency factor were constant within a particular reaction family. The overall rate constant as a function of temperature for the forward reaction was calculated assuming the Arrhenius relationship is valid.

Once rate constants for forward reactions were calculated, equilibrium constants, K_p, were used to calculate the rate constants for the corresponding reverse reactions, k_r. Also, since the rate constants were on a per event basis, the ratio of the reaction path degeneracy of the forward to the reverse reaction, *rpdratio*, was also included, yielding equation 4:

$$k_r = rpdratio \cdot k_f / K_p \tag{4}$$

K_p was calculated as a function of temperature from the change in Gibbs free energy upon reaction with a third order polynomial chosen for the temperature dependence of $c_{p,i}(T)$ values. This approach differs from previous implementations of NetGen in which thermodynamic consistency was not strictly enforced. This was a critical addition to the routines for rate-based mechanism generation, as the approach relies heavily on accurate quantification of reaction rates.

To obtain the necessary thermodynamic parameters, the NIST Structures and Properties thermochemical database[25] was searched to determine if experimentally-derived properties are tabulated. If experimental values were unavailable, a group additivity method was applied to estimate the species' thermochemical properties.[26] If this approach failed, properties were calculated using MOPAC, a semi-empirical computational chemistry package.[27,28] This approach is consistent with that previously taken.[1,6-8,17]

Application of the Rate-Based Generation Algorithm. A mechanism for low pressure tetradecane pyrolysis was generated to determine the effectiveness of the adapted rate-based generation algorithm. This reaction system was chosen since it complemented experimental work which was conducted in our laboratory.[19] Low pressure batch pyrolysis studies of tetradecane were conducted at 420 and 450°C in 3.1 mL pyrex ampules. Reactant loadings ranged from 6.2 to 27.8 mg (1.01×10^{-2} to 4.53×10^{-2} mol/L) with reaction times varying between 10-150 minutes.

The pyrolysis of tetradecane was observed to follow the typical free radical Rice-Herzfeld and Rice-Kossiakoff mechanisms for low pressure hydrocarbon pyrolysis, and product distributions were consistent with those reported in the literature.[29-33] A summary of experimental conversions and product yields is provided in Table 1. Light gaseous hydrocarbons were formed in the highest yields, with the highest selectivities observed for ethane and propylene. For higher molecular weight species, α-olefins were the major products with minor yields of the corresponding *n*-alkanes. This reaction system served as an adequate test for the rate-based generation criterion since thermolysis of a long chain paraffin can lead to thousands of intermediates and stable products. However, only a small fraction of these are kinetically significant, and thus a mechanism of reasonable size was generated. The mechanism built was then used to determine optimized values of a small subset of the controlling kinetic rate parameters, and the model was then used to predict reactant conversions and product yields for varying reactant loadings without further adjustment of any parameters.

For gas-phase hydrocarbon pyrolysis at moderate temperatures, six important reaction families were identified. Homolytic bond fission, radical recombination and disproportionation, β-scission, radical addition, and hydrogen abstraction reactions, both intramolecular and intermolecular, were incorporated. The reaction mechanism in this study was generated using estimates of the Arrhenius frequency factors, E_0, and α for each reaction family from the literature. The literature values used for each of these parameters are shown in Table 2. The model was constructed using an initial tetradecane concentration of 3.22×10^{-2} mol/L (20.0 mg) and a reaction temperature of 420°C.

During model construction, the primary user-specified parameter that was varied was the threshold, ε. The different models generated were evaluated based on three main criteria: 1) including major experimental products, 2) capturing the yields of the major products, and 3) obtaining physically reasonable values for the subset of frequency factors which were optimized using experimental data. Once a mechanism was obtained that met these modeling goals, additional strategies were examined for reducing the model size further. First, using the initial mechanism constructed as a guide, key reactive intermediates of high rank were identified and "seeded" into the initial reactant pool. Second, the impact of the kinetic parameters on model generation was explored by regenerating the models using the parameters obtained from optimization against experimental data.

Variation of Threshold, ε.

Model Characteristics. The model characteristics as the threshold, ε, was varied are summarized in Table 3. Quantities monitored were the numbers of total and *reactive* species, the numbers of total and *reactive* reactions, and the inclusion of major products and key intermediates. The user-specified threshold was initially set equal to 1.0, which resulted in a model that was generated very quickly, but only included a portion of the species observed during the experimental studies. Therefore, the threshold was slowly reduced to obtain an adequate model while preventing excessive growth. In addition, as the threshold was reduced and the number of *reactive* species in the model increased, the generation time significantly increased, providing impetus to proceed cautiously. As Table 3 shows, all of the species that were observed experimentally were not deemed *reactive* until the threshold was reduced to a value of 5.0×10^{-5}. However, the generated mechanism was unable to capture the underlying chemistry, which was attributed to the absence of other necessary species, which were primarily reactive intermediates. Reducing the threshold to a value of 1.0×10^{-5} resulted in a mechanism that overestimated the yields of long-chain α-olefins at higher reaction times, and the frequency factor for initiation was significantly too high. This was attributed to the inability of the α-olefins to undergo subsequent degradation at longer reaction times due to the absence of their

corresponding allylic and secondary radicals in the mechanism. In particular, 2-propenyl radical was not a *reactive* species. This is one of the products formed during fission of the weakest bond in an α-olefin (allylic bond), and it ultimately results in the formation of high yields of propylene. Since it was believed the olefinic radicals were necessary to generate an adequate model for a wide range of conversions, the threshold was further reduced.

As the threshold was reduced below a value of 1.0×10^{-5}, the number of *reactive* species and overall model construction time became very sensitive to the incremental change of the threshold value, with both quantities increasing significantly with only slight reductions ($\pm 1.0 \times 10^{-6}$) in the specified threshold. Therefore, the threshold was reduced at fine increments until 2-propenyl radical was included as a *reactive* species in the final generated model. This occurred when the threshold was set at a value of 7.0×10^{-6}, which resulted in a manageable model size with essential chemical detail. The overall mechanism, which will be referred to as Mechanism I, included a total of 19,052 species and 479,206 reactions, but the rate-based criterion reduced this to only 289 *reactive* species and 102,257 reactions. Thus, the rate-based criterion reduced the number of reactions by approximately 80% and the number of species by over 98%. It should be noted, however, that the actual number of unique reactions is much lower than the reported quantities imply. The listed values count the forward and reverse of a particular reaction separately, and reaction path degeneracy is accounted for by specifically writing each equivalent site as a unique reaction. Mechanism I required 209 hours to generate on a 633 MHz Alpha, but once constructed, only 45.6 seconds were required to solve it up to 150 minutes of reaction time. In contrast, a rank-based model with products of comparable rank had over 6,000 *reactive* species and could not be solved because of hardware limitations.

Determination of Rate Parameters and Predictive Capabilities. Experimental data from pyrolysis reactions of tetradecane at a loading of 20.0 mg conducted at 420°C and 450°C were used to optimize a subset of the controlling rate parameters. The different parameters which *could* be varied in the mechanism are shown in Table 2. However, only the parameters shown in Table 4 were

optimized using experimental data, while all others were constrained at their literature values in Table 2. As shown in Table 4, only frequency factors were permitted to vary, while all activation energies and transfer coefficients were set. It can be observed that the final optimized values for the frequency factors were reasonably consistent with literature values for the respective reaction families.

A parity plot comparing the fitted model results to the experimentally observed values for the reactant and major and minor products employing the frequency factors in Table 4 is shown in Figure 1. The yield of a particular product was defined as the moles of the species formed normalized by the initial moles of tetradecane charged to the system. The model did an excellent job of fitting the experimental data from the pyrolysis reactions over several orders of magnitude. The majority of the variance was attributed to differences between fitted and experimental values for long chain *n*-alkanes, which were only minor products. Also, major products which were formed in higher yields, including gaseous hydrocarbons and α-olefins, were fit very well. The agreement between the model and the experimental reactant conversions at both temperatures is shown in Figure 2a. A comparison between the experimental and fitted yields for 1-butene, *n*-octane, and 1-decene for tetradecane pyrolysis conducted at 420°C is shown in Figure 2b and is representative of the agreement for most other species. It should be reiterated that although the optimized frequency factors were fit using data from two temperatures, there were no adjustments made to the activation energies.

Once appropriate rate parameters were obtained, the predictive capabilities of Mechanism I were assessed. In particular, the ability of the model to predict reactant conversions and product yields for varying reactant loadings was investigated. The results which follow are truly predictions, i.e., no adjustments were made to the six frequency factors fitted to the 20.0 mg pyrolysis data. A comparison of predicted and experimental conversion values for tetradecane pyrolysis for different initial reactant loadings is shown in Figure 3. The experimental conversions for initial reactant loadings of 6.2 and 27.8 mg of tetradecane are shown as symbols, with each respective model prediction shown as lines. The mechanistic model was able to accurately predict the trends in the

experimental conversions as a function of reactant loading and the actual conversion values very well.

As a representative example of the ability to predict product yields, a comparison of the predicted and experimental evolution of propylene as a function of reactant conversion and reactant loading is shown in Figure 4. The comparison for propylene is shown since it was one of the major products formed during tetradecane pyrolysis. Also, the data are plotted in terms of moles rather than yields to make the different data sets more discernible. The model was able to accurately predict both the trends in the data as well as the actual values over a wide range of conversions and reactant loadings. Note that the best agreement is for the lowest concentration and the shortest reaction times, when higher rank reactions that have not been included in this model potentially become important. The agreement obtained for propylene was consistent with that for other gaseous hydrocarbons and long-chain α-olefins. A comparison of the predicted and experimental evolution of 1-decene is shown in Figure 5. The predictions for *n*-alkanes were also good, but there was more variance for these predictions than for the major products. It should be noted that Mechanism I was able to accurately predict product yields and trends for species regardless of whether their rates of formation were increasing, decreasing, or went through a maximum as the reaction proceeded.

Overall, a mechanistic model for low pressure tetradecane pyrolysis was constructed using a rate-based generation algorithm with only a small number of user-specified variables. The model was able to accurately fit experimental yields for various products over several orders of magnitude at two different reaction temperatures with no adjustments to the corresponding activation energies. The mechanistic model was then able to accurately predict reactant conversions and product yields for varying reactant loadings employing the rate parameters optimized for independent reaction sets. In addition, although it was not discussed in the previous sections, the model was able to predict the correct behavior for product trends for different reaction conditions such as changes in the relative α-olefin/paraffin ratio for varying reactant loadings.

Effect of Varying Initial Reactant Pool. It was observed that the user-specified threshold strongly impacted the resulting mechanistic model for the low pressure pyrolysis of tetradecane. The threshold had to be incrementally reduced until certain intermediates, necessary to accurately capture the underlying chemistry over a wide range of conversions, were included in the mechanism. However, care had to be taken to vary the threshold at small increments to prevent explosive growth since the rate-based construction became very sensitive to the input threshold. As observed, though, it was possible to generate an effective model, provided caution was exercised during the construction process. An alternative approach to varying the threshold until certain species were included in the mechanism was to specify these species in the initial reactant pool, thus deeming them *reactive* from the onset. Placing a particular species in the initial reactant pool can be very helpful, especially if it is known to be an important and necessary species to the mechanism *a priori*. A similar approach used by Joshi[34] for rank-based construction was shown to reduce the overall model size significantly.

During the initial rate-based generation of tetradecane pyrolysis, only tetradecane, the reactant, was specified in the initial reactant pool. As discussed above, Mechanism I could not adequately fit the experimental data until olefinic radicals were included in the model. This only occurred at very low threshold values, potentially resulting in other less important species being included in the mechanism as well. To investigate whether a smaller mechanism could be constructed by selectively placing important reactive intermediates in the initial reactant pool, Mechanism II was generated in a manner identical to Mechanism I, with the exception of the initial reactant pool. In addition to tetradecane, allylic radicals of all α-olefins of carbon numbers 3 to 13 (e.g. 1-penten-3-yl) and one additional non-allylic radical for α-olefins of carbon numbers 5 to 13 were placed in the initial reactant pool. During model construction, the user-specified threshold was reduced until all species observed experimentally were included in the reaction mechanism. This was achieved when the threshold was set at a value of 3.5×10^{-5}. The overall mechanism included a total of 11,530 species and 310,008 reactions, while the rate-based criterion reduced this to a *reactive* mechanism of only 221 species and 64,762 reactions, respectively. Mechanism II took

approximately half as long to generate as Mechanism I, and because it was smaller, shorter model solution and optimization times were realized. In addition, it should be noted that the user-specified threshold necessary to meet the modeling targets was higher than that used in the previous section, and also the model generation was not as sensitive to incremental changes to the threshold.

Frequency factors for selected reaction families in Mechanism II were determined by fitting experimental data in the same manner as for Mechanism I. Final optimized values of the frequency factors for the model with the larger initial species pool are shown in Table 4. It should be noted that these values are consistent with those obtained during optimization of Mechanism I and are comparable to those found in the literature for each reaction family. The different product yields obtained for Mechanism II using the optimized parameters in Table 4 were very similar to those obtained for Mechanism I. A representative comparison of the experimental and fitted yields of 1-octene using Mechanism I and Mechanism II is shown in Figure 6. Overall, the fitted yields for Mechanism I were in slightly better agreement with the experimental values. This observation can be rationalized by noting that when only seeding tetradecane, the mechanism truly grows directly from the reactant. Therefore, if all species of interest are included in the model, then other components which are necessary for their formation must also be present in the model. When seeding reactive intermediates in addition to the reactant, though, it is possible to generate a mechanism which may include the majority, but not all, of the kinetically significant species. However, the differences in the fitted yields and optimized parameters between Mechanisms I and II were very subtle, indicating that both mechanisms performed effectively.

The prediction of the reactant conversions and product yields for different initial reactant loadings were very similar for the two mechanisms, with Mechanism I predicting the experimental values slightly better. This is consistent with the observations made during the fitting of experimental data as discussed above.

Overall, seeding reaction intermediates in addition to the reactant resulted in the generation of a smaller reaction mechanism, which reduced the time required for model construction, solution, and parameter optimization. The optimized frequency factors for the mechanism were consistent

with those for Mechanism I, and the model fit and predicted experimental data very well. Therefore, this study demonstrates that if kinetically important species are known *a priori*, the efficiency of the construction of a mechanistic model using the rate-based generation algorithm can be improved, resulting in a smaller, more easily solvable model.

Regeneration of Reaction Mechanisms Using Optimized Parameters Obtained During Initial Model Construction**.** As discussed in the previous sections, compact mechanistic models for low pressure tetradecane pyrolysis were generated using a rate-based generation criterion. These models were able to both accurately fit experimental data from different reaction temperatures, as well as predict reactant conversions and product yields for different initial conditions. During model construction, several controls had to be specified by the user: the relevant reaction families, estimates of the kinetic parameters, the specified threshold for determination of *reactive* species, and the initial species pool. The effects of varying the user-specified threshold and initial species pool were discussed, and it was observed that both significantly affected the construction process and the final *reactive* mechanism obtained. The estimates provided for the controlling kinetic parameters may also have a significant influence on the generated model. In particular, the values used for the LFER parameters and the Arrhenius frequency factors are very important since the majority of forward reaction rate constants are calculated using this method, while the reverse rate constants are calculated using these forward rate constants and equilibrium information. It is very important to have accurate estimates for these parameters since inaccurate ones will result in the construction of either mechanisms that are unable to capture the underlying chemistry or models that include superfluous species and require longer generation and solution times.

For the construction of Mechanisms I and II, parameters for the frequency factors were set based upon ranges reported in the literature. The specific values chosen may impact the model construction and may alter the list of species in the final mechanism. The optimized parameters obtained above were used to regenerate the reaction mechanisms to determine if improvements were made to the final *reactive* models. Two possible benefits of regenerating a reaction mechanism with

the new parameters are 1) a reduction in the overall size of the mechanism since species that are kinetically insignificant for the particular experimental system being studied can be removed from the model and 2) the model may fit experimental data more accurately and provide better predictive capabilities because it becomes more focused on the particular experimental system of interest rather than the generic construction for which it is initially employed. To explore the effects of the rate parameters on model construction, the mechanisms described in the previous sections were regenerated using optimized parameters. It is also possible to vary the initial species pool during regeneration, but this would not permit for the direct comparison of using optimized rather than literature parameters. Therefore, the same initial reactant pools used to construct the two reaction mechanisms discussed in the previous sections were employed. The user-specified threshold, ε, was once again used to guide mechanism generation toward the established modeling goals.

Regeneration Seeding Only Tetradecane. The optimized parameters of Mechanism I were used to regenerate a model seeding only tetradecane at a concentration of 3.22×10^{-2} M and a reaction temperature of 420°C, as used for the initial construction of Mechanism I. All requisite species were included in the model when a threshold of 1.2×10^{-5} was employed. This regenerated model (Mechanism III) consisted of 253 *reactive* species and 71,707 reactions, and a total of 13,074 species and 378,506 reactions. This model was smaller than Mechanism I and took approximately half the total time to generate, indicating that model reduction could occur during regeneration employing optimized kinetic parameters. Mechanism III was then used to fit the experimental data while permitting the same subset of kinetic parameters to be optimized as for the previous mechanisms. Mechanism III fit the experimental data from both reaction temperatures very well, and the final optimized values for this model are shown in Table 4. It can be seen that the majority of the optimized parameters were very close to those obtained for Mechanism I with the exception of the frequency factor for bond fission; the value for Mechanism III was more consistent with typical literature values. The fitted product yields for Mechanism I and Mechanism III were almost identical over the full range of conversions studied, indicating that the new mechanism was as

effective as the original model. A comparison of the fitted yields of ethylene for the two mechanisms is shown in Figure 7 as a representative example. The predictive capabilities for the two models were also very similar, with almost identical estimates for the product yields for different initial reactant loadings.

Regeneration of the model for tetradecane pyrolysis seeding only the reactant and using previously optimized values resulted in a mechanism that was more compact than the original model, while retaining comparable fitting and predicting capabilities. However, the new mechanism did not require as stringent of a threshold value to meet the desired modeling goals. This was a result of the generation being more "focused" on the particular system of interest.

Regeneration Varying the Initial Species Pool. The effect of varying the initial reactant pool during regeneration was addressed using the same methodology presented previously. The initial pool was identical to that used to construct Mechanism II and consisted of tetradecane, allylic radicals of all α-olefins of carbon numbers 3 to 13, and one additional non-allylic radical for α-olefins of carbon numbers 5 to 13. The mechanism was generated using the optimized parameters for Mechanism I and a threshold of 3.5×10^{-5}, which was the final threshold employed to construct Mechanism II. The regenerated *reactive* mechanism consisted of 166 species and 48,265 reactions, with a total of 7,469 species and 206,946 reactions. This new model (Mechanism IV) was significantly smaller than Mechanism II, which was generated using approximate values from the literature. Similar to the approach for previous models, Mechanism IV was then used to fit the experimental data while permitting the small subset of kinetic parameters to be optimized. The final optimized values for this model are shown in Table 4. It can be seen that the majority of the optimized parameters were very close to those for Mechanism II, while the frequency factor for initiation was reduced, which was also observed during the regeneration while seeding only tetradecane. The abilities of the two models with the larger initial species pools to fit and predict reactant conversion and product yields were equivalent, with only slight differences for a few of the minor products. A comparison for the fitted yields of propylene for the two mechanisms is shown in Figure 8 as a representative example.

Overall, the models had comparable performance, with Mechanism IV being more compact and providing a better estimate for the frequency factor for initiation.

The reduction in the number of *reactive* species from 221 for Mechanism II to 166 for Mechanism IV is primarily due to the absence of methylalkyl radicals in the latter. For instance, 2-ethylhexyl radical, which is primarily formed through radical addition reactions such as those of a 1-butyl radical to 1-butene or an ethyl radical to 1-hexene, was excluded from Mechanism IV because of the smaller radical addition rate constant used during regeneration. The majority of the other species that were not deemed *reactive* were formed through similar reaction pathways. The reduction in the addition rate constant and the absence of these unnecessary species indicated that the generation was more focused on the particular system of interest.

Overall, regeneration with optimized parameters resulted in more compact reaction mechanisms that still captured the experimental data very well. The new models provided estimates for the frequency factor for bond homolysis that were in better agreement with the literature values, with no sacrifice in the fitting or predictive capabilities of the mechanisms. This occurred since the mechanisms had become "tailored" to the particular system of interest, and truly insignificant species were removed. In addition, a higher value for the user-specified threshold could be used when seeding only tetradecane for the same reasons. When also seeding reactive intermediates during regeneration, the rate-based algorithm resulted in the construction of the most compact reaction mechanism which still contained essential chemical information.

Conclusions. A mechanistic model of low pressure tetradecane pyrolysis was constructed using algorithms for automated model construction and a rate-based generation criterion. Novel modifications were made to the core algorithmic components in this work to improve and broaden the rate-based approach. The major alterations were the use of time rather than conversion as the controlling iteration and termination variable, the new definition for the characteristic rate of change in the system, and the use of thermodynamic data to impose thermodynamic consistency between forward and reverse reactions.

For the investigation of low pressure tetradecane pyrolysis, the rate-based model construction was successfully employed to produce a compact model with essential chemical detail. Once constructed, the model was able to accurately fit experimental data from two different reaction temperatures with no adjustment to the activation energies for any reactions. Only frequency factors were permitted to vary, and the final optimized values were consistent with literature values for each respective reaction family. Once rate parameters were determined, the mechanistic model was able to accurately predict reactant conversions and product yields for varying reaction conditions with no adjustments to the optimized rate parameters. Both relative trends and the actual values were predicted correctly over a wide range of reactant conversions and initial reactant loadings.

When kinetically significant species were placed in the mechanism at the onset of generation, the final reactive mechanism became more compact, and comparable fitting and predictive capabilities were obtained. Subsequent regeneration using optimized parameters reduced the model size without compromising the capabilities of the model. The most compact reaction mechanism for tetradecane pyrolysis was obtained when kinetically significant species were "seeded" and optimized rate parameters were used to construct the model. It should be noted, however, it is possible to reduce the mechanism too severely such that the optimized parameters would no longer have physical meaning.

The adapted rate-based generation methodology developed in this work can be used to generate manageable reaction mechanisms for different reactant pools and reaction rules. The user need only specify reactant(s), allowed reaction families, the threshold, and the final reaction time, and the mechanism is generated automatically. This approach allows the user to expend less energy on generating and tracking the species in the reaction mechanism and to focus instead on analyzing model characteristics and performance. Once an adequate model has been generated, the user can predict reactant conversions and product yields for other reaction conditions, facilitating the study of various sets of reaction conditions, thereby reducing the experimental burden.

Acknowledgment. The authors are grateful for financial support from the U. S. Department of Energy, Grant DE-FG22-96-PC96204. Support from the CAREER Program of the National Science Foundation (CTS-9623741) is also gratefully acknowledged.

References

(1) Susnow, R. G.; Dean, A. M.; Green, W. H.; Peczak, P.; Broadbelt, L. J. Rate-Based Construction of Kinetic Models for Complex Systems. *J. Phys. Chem. A* **1997**, *101(20)*, 3731-3740.

(2) Prickett, S. E.; Mavrovouniotis, M. L. Construction of Complex Reaction Systems. 1. Reaction Description Language. *Computers and Chemical Engineering* **1997**, *21*, 1219-1235.

(3) Prickett, S. E.; Mavrovouniotis, M. L. Construction of Complex Reaction Systems. 2. Molecule Manipulation and Reaction Application Algorithms. *Computers and Chemical Engineering* **1997**, *21*, 1237-1254.

(4) Prickett, S. E.; Mavrovouniotis, M. L. Construction of Complex Reaction Systems. 3. An Example: Alkylation of Olefins. *Computers and Chemical Engineering* **1997**, *21*, 1325-1337.

(5) Di Maio, F. P.; Lignola, P. G. KING, A KInetic Network Generator. *Chem. Eng. Sci.* **1992**, *47*, 2713-2718.

(6) Broadbelt, L. J.; Stark, S. M.; Klein, M. T. Computer Generated Pyrolysis Modeling: On-the-Fly Generation of Species, Reactions, and Rates. *Industrial & Engineering Chemistry Research* **1994**, *33(4)*, 790-799.

(7) Broadbelt, L. J.; Stark, S. M.; Klein, M. T. Termination of Computer-Generated Reaction Mechanisms: Species Rank-Based Convergence Criterion. *Industrial & Engineering Chemistry Research* **1995**, *34(8)*, 2566-2573.

(8) Broadbelt, L. J.; Stark, S. M.; Klein, M. T. Computer Generated Reaction Modeling: Decomposition and Encoding Algorithms for Determining Species Uniqueness. *Computers & Chemical Engineering* **1996**, *20(2)*, 113-129.

(9) Ayscough, P. B.; Chinnick, S.J.; Dybowski, R.; Edwards, P. Some Developments in Expert Systems in Chemistry. *Chem. Ind.* **1987**, *15*, 515-520.

(10) Dente, M. E.; Ranzi, E. M., In *Pyrolysis: Theory & Industrial Practice*, Albright, L.F.; Crynes, B.L.; Corcoran, W.H., Eds.; Academic Press: San Diego, 1983; pp 133-175.

(11) Ranzi, E.; Dente, M.; Pierucci, S.; Biardi, G. Initial Product Distributions from Pyrolysis of Normal and Branched Paraffins. *Ind. Eng. Chem. Fundam.* **1983**, *22*, 132-139.

(12) Dente, M.; Pierucci, S.; Ranzi, E. New Improvements in Modeling Kinetic Schemes for Hydrocarbons Pyrolysis Reactors. *Chem. Eng. Sci.* **1992**, *47(9-11)*, 2629-2634.

(13) Tomlin, A. S.; Pilling, M. J.; Merkin, J. H.; Brindley, J.; Burgess, N.; Gough, A. Reduced Mechanisms for Propane Pyrolysis. *Ind. Eng. Chem. Res.* **1995**, *34*, 3749-3760.

(14) Chevalier, C.; Warnatz, J.; Melenk, H. Automatic Generation of Reaction Mechanisms for Description of Oxidation of Higher Hydrocarbons. *Ber. Bunsen-Ges. Phys. Chem.* **1990**, *94*, 1362-1367.

(15) Tomlin, A. S.; Turanyi, T.; Pilling, M. J., In *Low Temperature Combustion and Autoignition*; Pilling, M. J., Hancock, G., Eds.; Elsevier: Amsterdam, 1997; pp 293-437.

(16) Bounaceur, R.; Warth, V.; Glaude, P. A.; Battin-Leclerc, F.; Scacchi, G.; Come, G. M.; Faravelli, T.; Ranzi, E. Chemical Lumping of Mechanisms Generated by Computer. Application to the Modeling of Normal Butane Oxidation. *J. Chim. Phys.* **1996**, *93*, 1472-1491.

(17) Klinke, D. J.; Broadbelt, L. J. Mechanism Reduction during Computer Generation of Compact Reaction Models. *AIChE Journal* **1997**, *43(7)*, 1828-1837.

(18) Domine, F.; Dessort, D.; Brevart, O. Towards a New Method of Geochemical Kinetic Modelling: Implications for the Stability of Crude Oils. *Org. Geochem.* **1998**, *28(9/10)*, 597-612.

(19) De Witt, M. J.; Broadbelt, L. J. Binary Interactions Between Tetradecane and 4-(1-Naphthylmethyl)Bibenzyl During Low and High Pressure Pyrolysis. *Energy & Fuels* **1999**, *13(5)*, 969-983.

(20) Swihart, M. T.; Broadbelt, L. J. AICHE National Meeting, Miami Beach, FL, 1998.

(21) Allara, D. L.; Shaw, R. A Compilation of Kinetic Parameters for the Thermal Degradation of n-Alkane Molecules. *Journal of Physical and Chemical Reference Data* **1980**, *9(3)*, 523-559.

(22) Dominé, F.; Marquaire, P. M.; Muller, C.; Come, G. M. Kinetics of Hexane Pyrolysis at Very High Pressures. 2. Computer Modeling. *Energy & Fuels* **1990**, *4(1)*, 2-10.

(23) Song, C.; Lai, W. C.; Schobert, H. H. Condensed-Phase Pyrolysis of n-Tetradecane at Elevated Pressures for Long Duration. Product Distribution and Reaction Mechanisms. *Industrial & Engineering Chemistry Research* **1994**, *33*, 534-547.

(24) Evans, M. G.; Polanyi, M. Inertia and Driving Force of Chemical Reactions. *Trans. Faraday Soc.* **1938**, *34*, 11-29.

(25) Stein, S. E., *NIST Structures & Properties Database Version 2.0*; Gaithersburg, MD, 1994.

(26) Benson, S. W., *Thermochemical Kinetics*; Wiley-Interscience: New York, 1976.

(27) Stewart, J. J. P., *MOPAC Reference Manual and Release Notes*; Frank J. Seiler Research Laboratory: United States Air Force Academy, CO, 1990.

(28) Stewart, J. J. P., In *Reviews in Computational Chemistry*; Lipkowitz, K. B., Boyd, D. B., Eds.; VCH Publishers, Inc.: New York, 1990.

(29) Rice, F. O. The Thermal Decomposition of Organic Compounds from the Standpoint of Free Radicals. *Journal of the American Chemical Society* **1933**, *55*, 3035-3040.

(30) Rice, F. O.; Herzfeld, K. F. The Thermal Decomposition of Organic Compounds from the Standpoint of Free Radicals. VI The Mechanism of Some Chain Reactions. *Journal of the American Chemical Society* **1934**, *56*, 284-289.

(31) Kossiakoff, A.; Rice, F. O. Thermal Decomposition of Hydrocarbons, Resonance Stabilization and Isomerization of Free Radicals. *Journal of the American Chemical Society* **1943**, *65*, 590-595.

(32) Voge, H. H.; Good, G. M. Thermal Cracking of Higher Paraffins. *Journal of American Chemical Society* **1949**, *71*, 593-597.

(33) Mushrush, G. W.; Hazlett, R. N. Pyrolysis of Organic Compounds Containing Long Unbranched Alkyl Groups. *Industrial & Engineering Chemistry Fundamentals* **1984**, *23*, 288-294.

(34) Joshi, P. Molecular and Mechanistic Modeling of Complex Process Chemistries: A Generic Approach to Automated Model Building. Ph.D. Dissertation, 1998, Newark, DE, University of Delaware,

Table 1: Summary of experimental conversions and product yields for tetradecane pyrolysis at 420°C and 450°C.

Reaction Set	6.2	6.2	12.3	12.3	20	20	27.8	27.8	20-450	20-450
Reaction Time (min)	40	120	40	120	40	120	40	120	5	20
$C_{14}H_{30}$ Loading (mg)	6.4	6.2	12.3	12.2	19.7	20.2	27.6	27.7	19.9	20.0
$C_{14}H_{30}$ Conversion	0.10	0.24	0.11	0.32	0.11	0.32	0.14	0.35	0.11	0.30
Temperature (°C)	420	420	420	420	420	420	420	420	450	450
Product Yield (x10 ^{2})[a]										
methane	2.55	6.98	2.46	6.98	2.23	6.60	1.97	5.78	1.18	6.50
ethylene	4.04	9.77	3.92	9.33	3.58	8.00	3.05	6.35	2.75	9.10
ethane	4.05	10.27	4.61	12.14	4.89	12.64	4.61	11.69	3.05	10.78
propylene	3.43	10.00	4.21	12.60	4.75	13.32	4.56	12.30	2.75	11.04
propane	1.49	4.36	2.47	7.10	3.33	8.87	3.54	9.22	1.82	6.65
1-butene	1.71	4.59	2.04	5.66	2.35	6.03	2.24	5.77	1.37	5.09
n-butane	0.18	1.34	0.73	2.58	1.17	3.68	1.34	4.22	0.51	2.32
1-pentene	1.22	3.18	1.45	3.92	1.66	4.04	1.50	3.80	0.94	3.37
n-pentane	0.05	0.45	0.11	0.95	0.42	1.45	0.49	1.71	0.18	0.86
1-hexene	1.43	3.12	1.73	4.13	2.43	5.21	2.53	5.39	1.43	4.58
n-hexane	0.00	0.00	0.00	0.18	0.16	0.42	0.28	0.71	0.13	0.46
1-heptene	0.82	1.80	1.18	2.68	1.78	3.62	1.67	3.35	1.03	3.34
n-heptane	0.00	0.00	0.00	0.26	0.20	0.57	0.25	0.69	0.09	0.33
1-octene	0.93	2.16	1.22	2.84	1.51	2.99	1.54	3.02	0.85	2.67
n-octane	0.00	0.00	0.00	0.25	0.08	0.42	0.19	0.57	0.06	0.25
1-nonene	0.96	2.07	1.08	2.49	1.30	2.51	1.38	2.60	0.76	2.30
n-nonane	0.00	0.00	0.00	0.21	0.00	0.34	0.15	0.47	0.05	0.18
1-decene	0.94	1.91	1.03	2.29	1.22	2.27	1.28	2.31	0.74	2.13
n-decane	0.00	0.04	0.00	0.07	0.11	0.28	0.15	0.38	0.05	0.15
1-undecene	0.82	1.65	0.90	1.93	1.04	1.93	1.08	1.93	0.66	1.85
n-undecane	0.00	0.09	0.00	0.15	0.09	0.25	0.14	0.33	0.05	0.14
1-dodecene	0.79	1.54	0.86	1.75	0.97	1.78	1.00	1.75	0.61	1.72
n-dodecane	0.00	0.00	0.00	0.00	0.00	0.05	0.04	0.08	0.00	0.03
1-tridecene	0.18	0.36	0.19	0.40	0.21	0.40	0.22	0.40	0.15	0.42
n-tridecane	0.00	0.00	0.00	0.00	0.00	0.00	0.03	0.04	0.00	0.02

(a) Product yield defined as: (moles species i formed)/(initial moles tetradecane).

Table 2: Parameters used for initial rate-based generation of mechanism for low pressure tetradecane pyrolysis.

Reaction Family	**A**[a]	$\mathbf{E_0}$[b]	α
Bond Fission	1.0×10^{16}	0.0	1.0
β-Scission	1.0×10^{14}	14.24	0.76
Radical Addition	1.0×10^{8}	14.24	0.24
Radical Recombination	1.0×10^{9}	0.0	0.0
Intermolecular H-Abstraction			
R•	1.0×10^{8}	13.3	0.7/0.3
H•	1.0×10^{11}	13.3	endo/exo
Intramolecular H-Abstraction			
1,4-shift	2.0×10^{11}	21.0	0.5
1,5 or 1,6-shift	2.0×10^{10}	12.0	0.5
Disproportionation	1.0×10^{9}	0.0	0.0

(a) The units of the frequency factor, A, are 1/s for unimolecular reactions and L/(mol•s) for bimolecular reactions.
(b) The units of the intrinsic barrier to reaction, E_0, are kcal/mol.

Table 3: Effect of variation of user-specified threshold on characteristics of constructed reaction mechanisms for tetradecane pyrolysis using the rate-based generation algorithm.

User-specified Threshold	Number of Total Species	Number of Reactive Species	Number of Total Reactions	Number of Reactive Reactions	Comments
1.0×10^{0}	1,174	73	31,610	5,150	only alkanes C_1-C_7
1.0×10^{-1}	1,387	76	36,094	5,981	only alkanes C_1-C_8
1.0×10^{-2}	1,991	87	56,086	10,849	only alkanes C_1-C_{11}
1.0×10^{-3}	2,894	97	77,686	13,214	no *n* -tridecane
1.0×10^{-4}	3,005	98	80,298	13,230	no *n* -tridecane
7.0×10^{-5}	3,113	99	82,910	13,236	no *n* -tridecane
5.0×10^{-5}	3,180	101	87,652	16,638	no allylic radical
1.0×10^{-5}	4,842	128	131,506	30,250	no allylic radical
8.0×10^{-6}	6,692	153	178,950	36,289	no allylic radical
7.0×10^{-6}	19,052	289	479,206	102,257	all species of interest

Table 4: Optimized Arrhenius frequency factors[a] for low pressure tetradecane pyrolysis mechanisms constructed using rate-based generation algorithm.

Reaction Family	**Mechanism I**	**Mechanism II**	**Mechanism III**	**Mechanism IV**
Bond Fission	1.5×10^{17}	1.3×10^{17}	5.9×10^{16}	6.9×10^{16}
β-Scission	3.6×10^{12}	1.9×10^{12}	1.9×10^{12}	2.0×10^{12}
Radical Recombination	3.9×10^{7}	1.0×10^{7}	1.8×10^{7}	1.0×10^{7}
Intermolecular H-Abstraction: R•	5.2×10^{7}	3.9×10^{7}	4.5×10^{7}	4.9×10^{7}
Intramolecular H-Abstraction 1,5 or 1,6-shift [b]	5.0×10^{9}	3.3×10^{9}	4.7×10^{9}	5.8×10^{9}
Disproportionation	1.0×10^{7}	5.6×10^{7}	1.0×10^{7}	3.8×10^{7}

(a) The units of the frequency factors, A, are 1/s for unimolecular reactions, and L/(mol•s) for bimolecular reactions.
(b) The frequency factor for 1,4-intramolecular hydrogen abstraction is optimized as $(10 \bullet A_{1,5\text{-shift}})$.

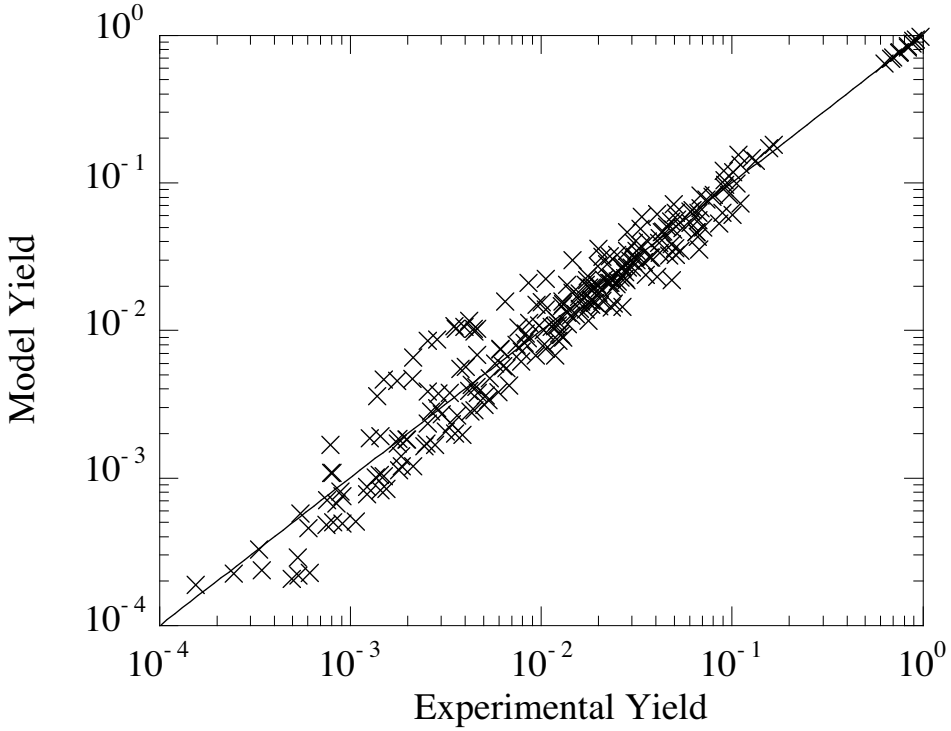

Figure 1: Comparison of fitted and experimental reactant conversions and yields of major and minor products using Mechanism I and the Arrhenius frequency factors listed in Table 4.

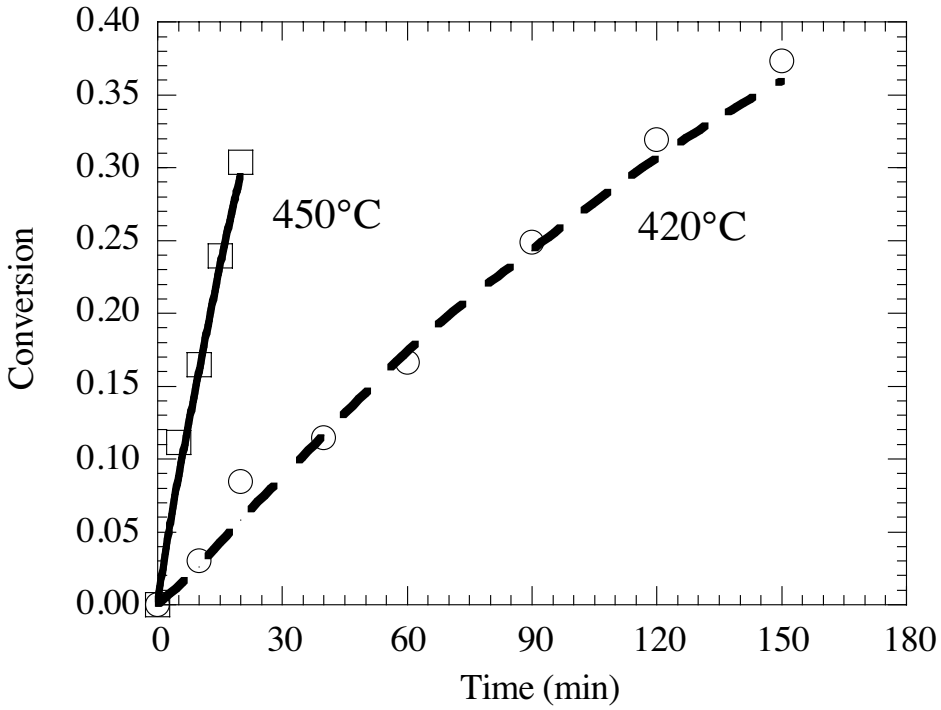

(a)

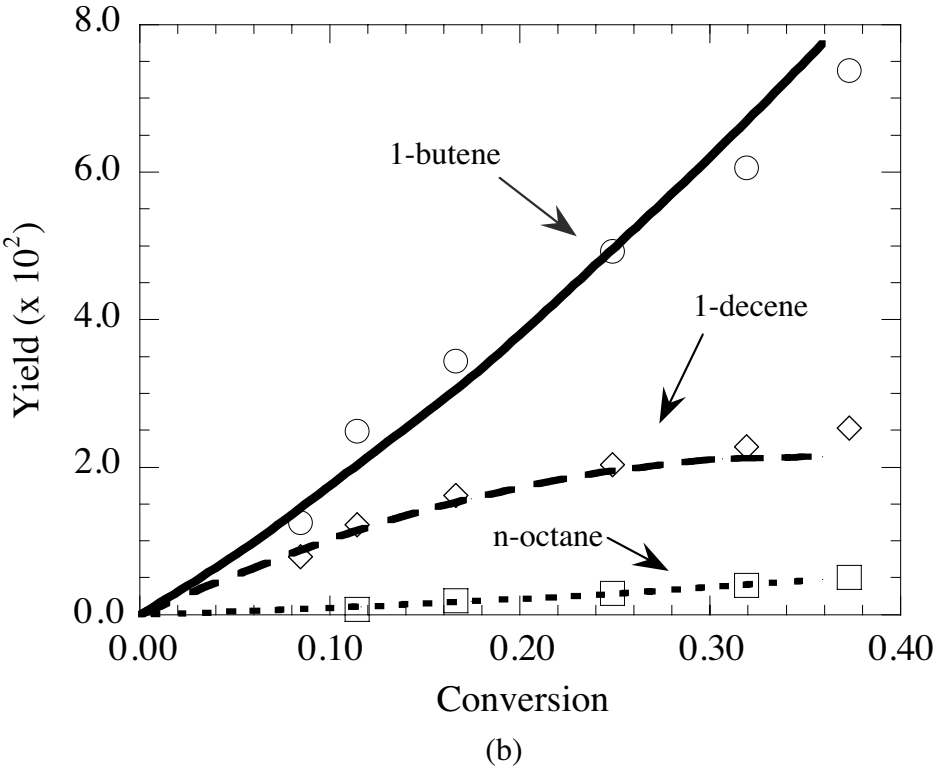

(b)

Figure 2: Comparison of fitted model results (lines) and experimentally observed values (symbols) of (a) reactant conversion at 420°C and 450°C and (b) representative products from tetradecane pyrolysis conducted at 420°C.

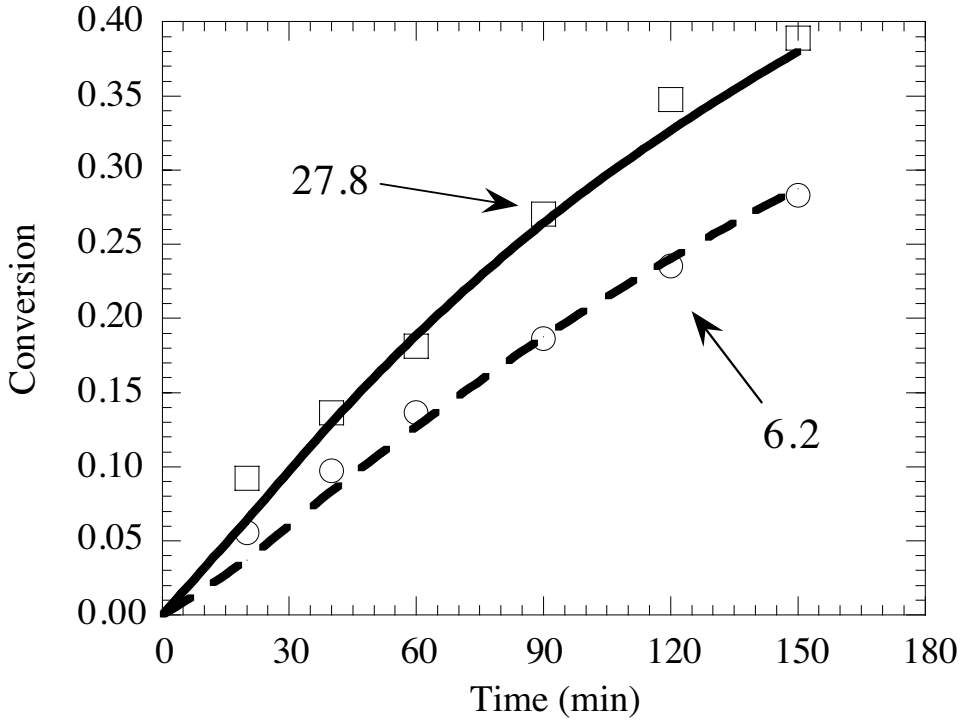

Figure 3: Comparison of experimental (symbols) and predicted (lines) conversion of tetradecane for initial tetradecane loadings of 6.2 and 27.8 mg using Mechanism I.

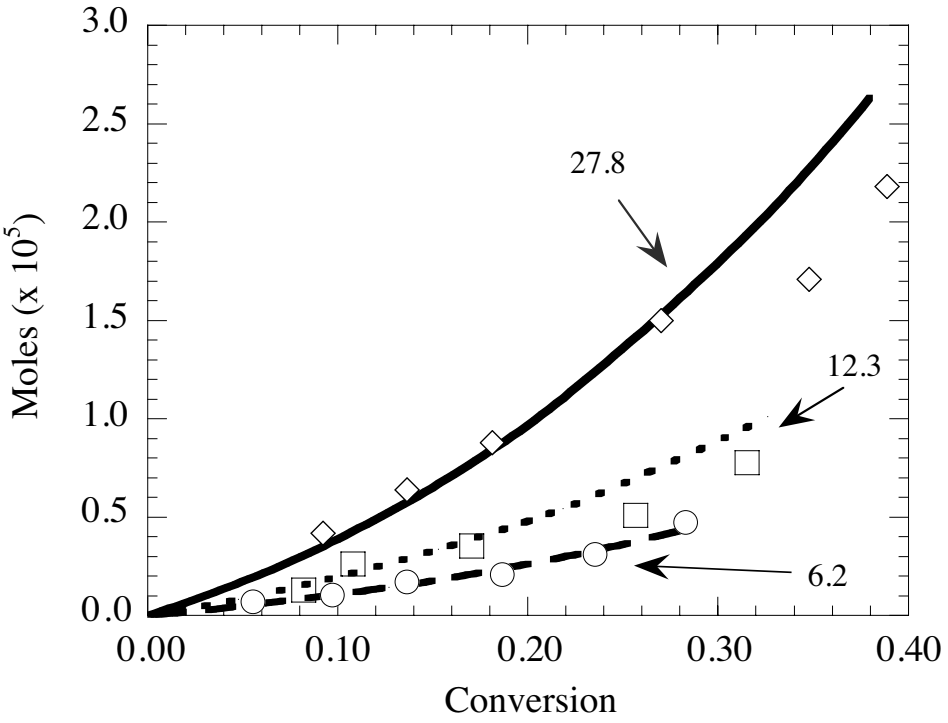

Figure 4: Comparison of the experimental (symbols) and predicted (lines) evolution of propylene for initial tetradecane loadings of 6.2, 12.3, and 27.8 mg using Mechanism I.

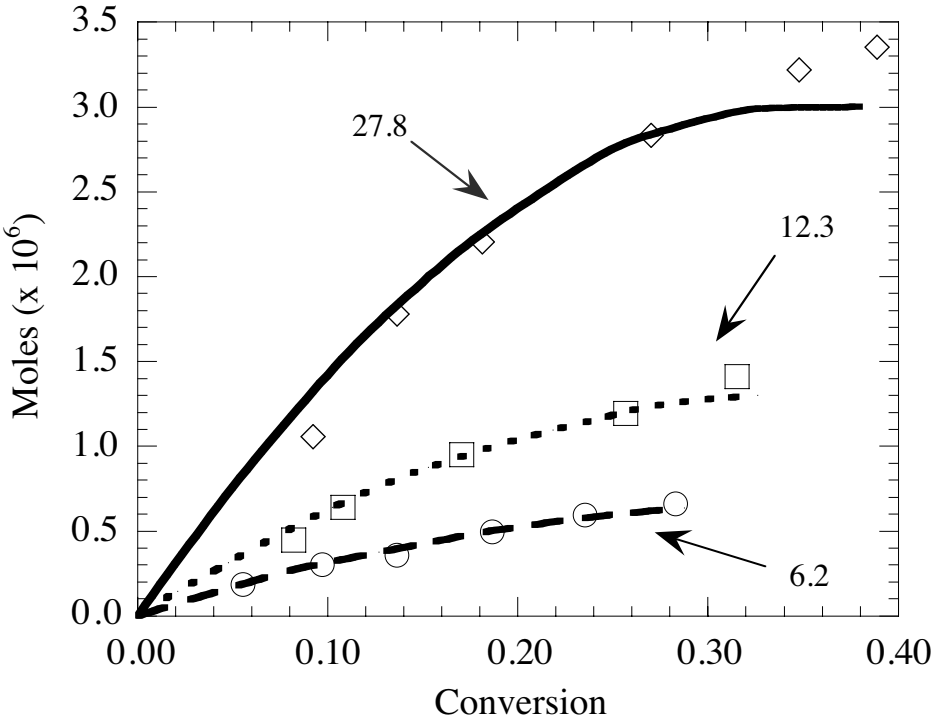

Figure 5: Comparison of the experimental (symbols) and predicted (lines) evolution of 1-decene for initial tetradecane loadings of 6.2, 12.3, and 27.8 mg using Mechanism I.

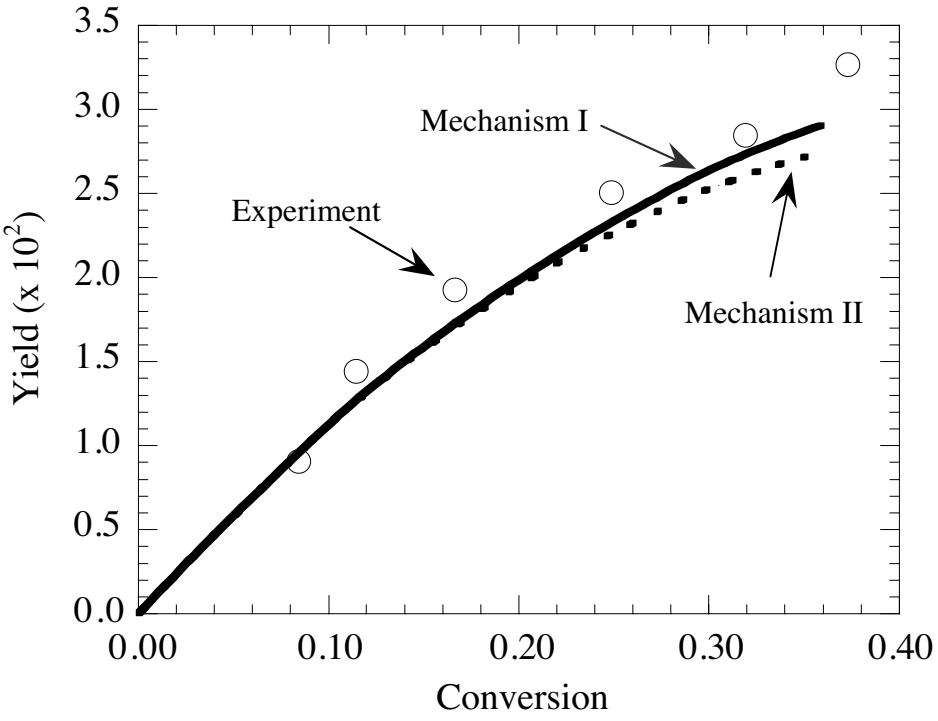

Figure 6: Comparison of the experimental (symbols) and fitted (lines) yields of 1-octene for tetradecane pyrolysis conducted at 420°C using Mechanisms I and II.

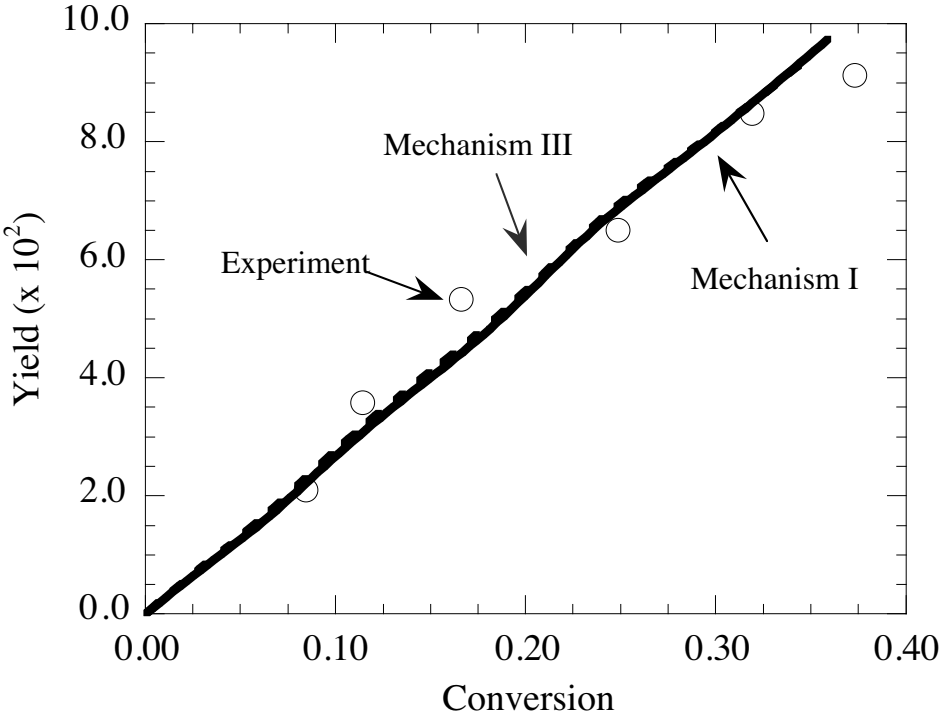

Figure 7: Comparison of the experimental (symbols) and fitted (lines) yields of ethylene for tetradecane pyrolysis conducted at 420°C using Mechanisms I and III.

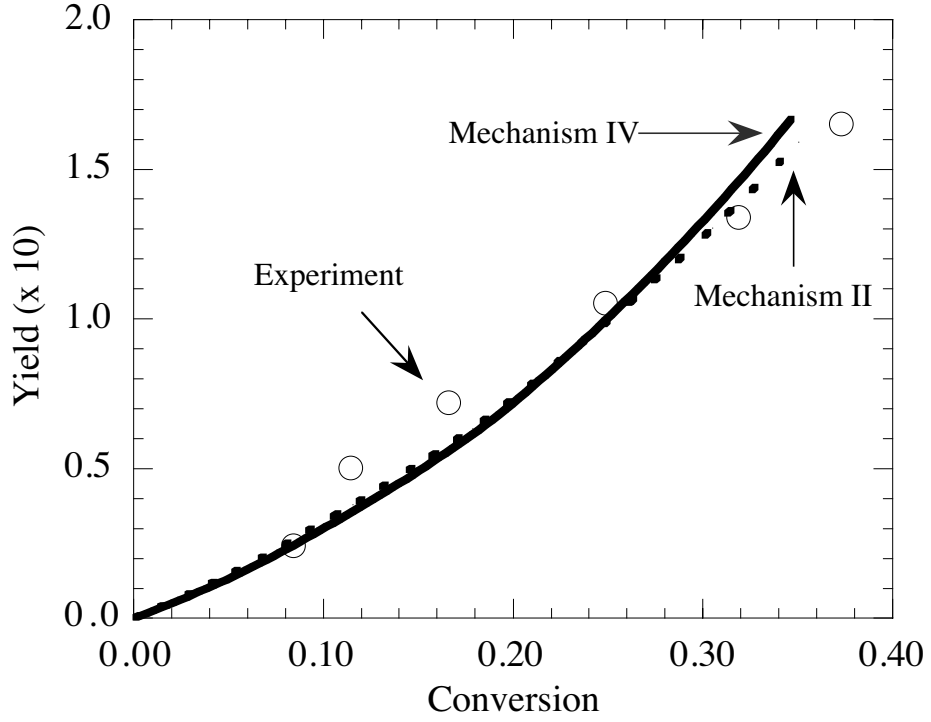

Figure 8: Comparison of the experimental (symbols) and fitted (lines) yields of propylene for tetradecane pyrolysis conducted at 420°C using Mechanisms II and IV.

APPLICATION OF COMPUTER GENERATION OF REACTION MECHANISMS USING QUANTITATIVE RATE INFORMATION TO HYDROCARBON PYROLYSIS

Matthew J. De Witt, David J. Dooling and Linda J. Broadbelt
Department of Chemical Engineering
2145 Sheridan Road, Northwestern University
Evanston, IL 60208

ABSTRACT

Novel modifications were made to the core components of the algorithms for rate-based generation of reaction mechanisms[1], including introducing thermodynamic constraints into the estimation of the controlling rate parameters and an alternative approach for determining the species included in the final mechanism. Once implemented, the adapted rate-based building criterion was successfully employed to construct a compact mechanistic model for low-pressure tetradecane pyrolysis. Though thousands of species and reactions were generated, only a small portion of these were deemed necessary and incorporated into the final model. Experimental data were used to determine frequency factors for a subset of the reaction families, while all other kinetic parameters were set based on the literature. The final optimized values for the frequency factors were consistent with literature, and the model was able to accurately fit experimental data from different reaction conditions. With no adjustment to the optimized frequency factors, the mechanistic model for tetradecane pyrolysis was able to accurately predict reactant conversions and product yields for varying reaction conditions. Both relative trends and the actual values were predicted correctly over a wide range of reactant conversions and initial reactant loadings.

I. INTRODUCTION

The advent of tools for computer generation of reaction mechanisms has dramatically reduced the time for the development of complex reaction models and increased the level of detail they may include. One of the challenges in building reaction mechanisms using algorithms for automated model construction, however, is to describe the essential chemistry and enable prediction of experimental data over wide ranges of reaction conditions while maintaining a manageable model size. For example, hydrocarbon pyrolysis is a chemistry in which molecular weight growth reactions may be important, and a mechanism generated automatically would therefore grow to infinite size without the application of external termination criteria. Implementation of a species rank criterion, which restricts those species capable of undergoing reaction based on the order in which they appear in the mechanism, overcame this obstacle[2]. However, this criterion is usually not restrictive enough since insignificant species must also be included to capture the important ones.

This limitation motivated development of an alternative strategy for computer generation of reaction mechanisms that includes important reactions based on quantitative evaluation of reactivity[1]. This approach exploits the capability to estimate rate constants as the mechanism is generated, allowing it to be solved at any point. The mechanism is built iteratively, as a growing reaction mechanism is alternatively generated and solved. Quantitative evaluation of the formation rates of all species during the mechanism building process determines the next set of species allowed to undergo reaction. The formation rates are compared to a characteristic rate of the current system, and a weighting factor, ε, is used to adjust the characteristic rate to allow more or fewer species to be included in the mechanism.

The work that will be described builds upon the previous work[1] but includes several important improvements. The first implementation of the rate-based approach used the disappearance rate of a single reactant to define a characteristic rate in the system to which all of the other rates were compared, and the conversion of this reactant was used as the marker of the completeness of the mechanism. If the reactant quickly equilibrated, the mechanism building process would not advance. In the new implementation, time is used as the independent variable, and the rates of all of the species in the system are used to determine the overall characteristic rate. Secondly, since the mechanism building process requires on-the-fly kinetic information, a lookup capability was implemented to allow experimental rate information to be incorporated. Finally, equilibrium information was obtained through on-the-fly calculation of heat capacity, enthalpy and entropy values. By marking reversible pairs of reactions, the rate constant for the reverse reaction could be calculated from the forward rate constant and the value of the equilibrium constant. This latter capability represents a substantial advance in our ability to generate complex reaction mechanisms via the computer.

II. PROCEDURE

A mechanism for low pressure tetradecane pyrolysis was generated to determine the effectiveness of the adapted rate-based generation algorithm. This reaction system serves as an adequate test for the rate-based generation criterion since thermolysis of a long chain paraffin can lead to thousands of intermediates and stable products. However, only a small fraction of these is actually kinetically significant. Furthermore, experimental information collected in our laboratory[3] was available to test the ability of the model generated to capture the reactant conversion and product selectivities over a wide range of reaction conditions. Low pressure batch pyrolysis reactions were conducted using initial loadings of tetradecane ranging from 0.01 to 0.045 M for times ranging from 10-150 minutes at temperatures of 420 and 450°C.

The reaction mechanism was built by implementing six reaction families deemed important for gas-phase hydrocarbon pyrolysis at moderate temperatures: bond fission, radical recombination, β-scission, radical addition, disproportionation and hydrogen abstraction (intermolecular and intramolecular through 1,4-, 1,5- and 1,6-hydrogen shift reactions). Estimates of the Arrhenius frequency factors and the parameters of an Evans-Polanyi relationship[4], E_o and α, for each reaction family were obtained from the literature. The model was constructed using an initial tetradecane concentration of 0.0322 M and a reaction temperature of 420°C. The weighting factor, ε, was varied from 1.0 to 5×10^{-5}. The total number of species, the reactive species, the total number of reactions and the number of reactive reactions were tabulated as a function of the weighting factor. Each individual elementary step is specifically tallied; the numbers of reactions reported are not consolidated according to the known reaction path degeneracies nor are reverse and forward pairs lumped as a single reaction.

III. RESULTS

The model characteristics as a function of weighting factor are summarized in Table 1. As the weighting factor decreased, all quantities reported increased. However, the growth in the total number of species was more dramatic than the moderate growth observed for the number of reactive species. Thus, using rate-based building and the weighting factor as a "tuning" parameter, the size of the mechanism solved was easily controlled. The adequacy of the reaction mechanism was assessed by monitoring two key characteristics: whether all of the major products observed experimentally were included and if secondary reactions of olefins were described. For example, at a weighting factor of 1.0, only C_1-C_7 alkane products were included in the model, while C_1-C_{13} alkanes were detected experimentally. It was necessary to decrease the weighing factor to 5×10^{-5} before tridecane, the major product observed in the lowest yield, was included in the mechanism as a reactive species.

The mechanism generated employing a weighting factor of 5×10^{-5} was therefore used to capture the experimental behavior. Experimental data from 20 mg pyrolysis reactions of tetradecane conducted at 420°C and 450°C were used to determine controlling rate parameters. There were 27 parameters which could be varied, a frequency factor, an E_o and an α value for each reaction family. However, only four parameters, $A_{\text{bond fission}}$, $A_{\beta\text{-scission}}$, $A_{\text{H-abstraction by R}\cdot}$ and $A_{\text{1,5-hydrogen shift}}$, were fit against the experimental data. All other parameters were set constant at values obtained from the literature. Note that only frequency factors were permitted to vary, while all intrinsic barriers and transfer coefficients were fixed.

A parity plot comparing the fitted model yields to the experimentally observed yields for major and minor products is shown in Figure 1. The model did an excellent job of fitting the experimental data from the pyrolysis reactions over several orders of magnitude. Reactant conversions for both temperatures were fit extremely well, even though no activation energies were used as fitting parameters. Gaseous hydrocarbons and liquid α-olefins were also fit very well.

The predictive capabilities of the model were then assessed by solving for the product yields and conversion at other reactant loadings with no further adjustment to any of the model parameters. A comparison of predicted and experimental yields of undecene as a function of reactant conversion and reactant loading is shown as a representative example of the predictive capability of the model in Figure 2. The model was able to predict accurately the trends in the data and the actual values over a wide range of conversions and reactant loadings. Similar predictive capabilities were observed for gaseous hydrocarbons and other long chain α-olefins.

ACKNOWLEDGMENT

The authors are grateful for the financial support from the Department of Energy (DE-FG22-96-PC96204).

REFERENCES

(1) Susnow, R.G., Green, W.H., Dean, A., Peczak, P.K. and Broadbelt, L.J. "Rate-Based Construction of Kinetic Models for Complex Systems", *J. Phys. Chem. A*, **1997**, *101*, 3731-3740.

(2) Broadbelt, L.J., Stark, S.M. and Klein, M.T., "Termination of Computer Generated Reaction Mechanisms: Species Rank-Based Convergence Criterion", *Ind. Eng. Chem. Res.*, **1995,** *34*(8), 2566-2573.

(3) De Witt, M.J. and Broadbelt, L.J., "Binary Interactions Between Tetradecane and 4-(1-Naphthylmethyl) Bibenzyl During Low and High Pressure Pyrolysis", *submitted to Energy & Fuels*, **1999**.

(4) Evans, M.G. and Polanyi, M. "Inertia and Driving Force of Chemical Reactions", Trans. Faraday Soc., **1938**, *34*, 11-29.

Table 1. Summary of model characteristics as a function of the weighting factor used to direct rate-based building.

Weighting factor	Number of total species	Number of reactive species	Number of reactions	Number of reactive reactions
1	1908	103	57116	15605
0.1	2401	107	65866	17633
0.01	3349	120	98286	26116
0.001	4676	130	132450	30436
0.0001	11158	236	319408	63004
0.00005	16269	302	477566	98240

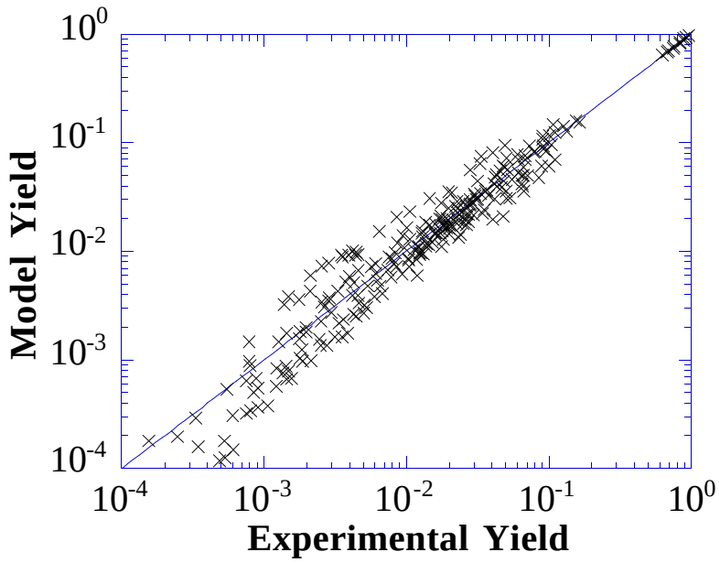

Figure 1. Comparison of fitted model yields and experimentally observed yields for major and minor products of tetradecane pyrolysis.

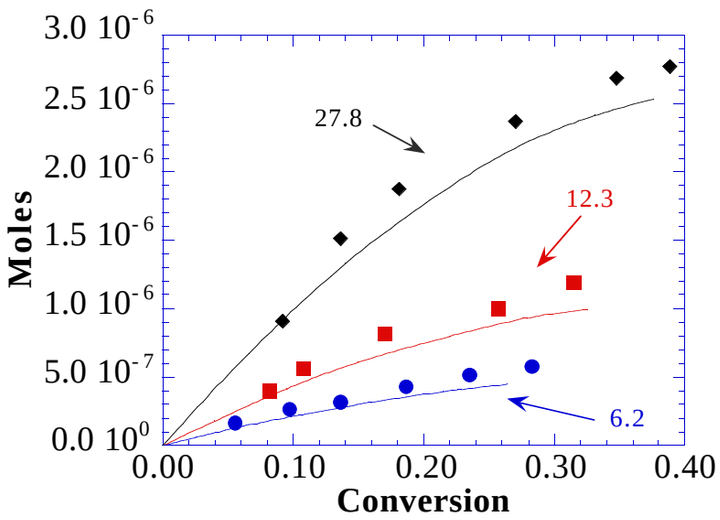

Figure 2. Comparison of the experimental (symbols) and predicted (lines) evolution of undecene for initial tetradecane loadings of 6.2, 12.3 and 27.8 mg.

Computer Generation of Reaction Mechanisms Using Quantitative Rate Information: Application to Long-Chain Hydrocarbon Pyrolysis

Matthew J. De Witt, David J. Dooling, and Linda J. Broadbelt

Department of Chemical Engineering
Northwestern University
Evanston, Illinois 60208-3120

Key words: Automatic generation of reaction mechanisms, pyrolysis, hydrocarbons, tetradecane

Prepared for presentation at the 1999 Spring Meeting, Houston, TX, March 14-18

Abstract

One of the challenges to kinetic modeling is constructing a robust model which can capture the essential chemistry of a system while retaining a manageable size. The rate-based generation of mechanistic models is an attractive approach since kinetically significant species can be determined and selectively included in the final mechanism. In previous work, an algorithm for the effective rate-based generation of reaction mechanisms was developed.[1] Novel modifications were made to the core components of the algorithm in our study, which included introducing thermodynamic constraints into the estimation of the controlling rate parameters and an alternative approach for determining the species included in the final mechanism. Once implemented, the adapted rate-based building criterion was successfully employed to construct a compact mechanistic model for low pressure tetradecane pyrolysis. Though thousands of species and reactions were generated, only a small portion of these were deemed necessary and incorporated into the final model. Experimental data were used to determine frequency factors for each reaction family, while all other kinetic parameters were set based on the literature. With no adjustment to the optimized frequency factors, the mechanistic model for tetradecane pyrolysis was able to accurately predict reactant conversions and product yields for varying reaction conditions.

Introduction. In recent years, the use of kinetic modeling has increased significantly due to both economical and environmental driving forces. Kinetic modeling allows for the facile and rapid investigation of various processing conditions while at the same time allowing the modeler to evaluate proposed reaction mechanisms, quantify the underlying reaction kinetics, and interpret complex experimental data. The major challenge to constructing mechanistic models is the extreme complexity that accounting for all possible reactions, products, and reactive intermediates creates. The pyrolysis of hydrocarbons, for example, can generate thousands of reactive intermediates and products, making tabulation and tracking of all the species very difficult. Although models of significant size can be developed using typical workstations today, there is still a limit to the overall mechanism size which can be solved in a reasonable amount of time. Therefore, there is a driving force to limit the size of reaction mechanisms, while ensuring these compact mechanisms still contain all kinetically significant species and reactions. Hence, the ability to determine necessary and important species with the exclusion of "unreactive" ones is a vital aspect of the automated construction of reaction mechanisms.

Recent work has been carried out to improve the ability of the program for automatic mechanism generation, NetGen,[1-5] to consider a larger number of species while retaining only those species which influence the kinetics. The basic approach is to estimate reaction rate constants during generation and solve the model as it is being constructed, allowing for the determination of important species in the growing mechanism. The work which will be discussed in this paper expands on these previous studies[1] by introducing thermodynamic constraints into the estimation of the controlling rate parameters and an alternative approach for determining the species included in the final mechanism. Furthermore, the

different models built by varying the parameters controlling the rate-based generation were assessed in terms of their ability to capture experimental data collected in our laboratory for tetradecane pyrolysis.

Details of the Rate-Based Building Algorithm. To generate a reaction mechanism for long-chain hydrocarbon pyrolysis which would be valid over ranges of temperature, concentration, and reaction time yet still maintain a manageable size, necessary reactive species were determined employing a rate-based generation criterion. The algorithm employed was similar to that of Susnow et al.[1]; however, some key modifications enhanced its capabilities as described below. As in the previous studies, the rate-based generation algorithm exploits the capability of NetGen to estimate rate constants as the mechanism is generated, thereby allowing the growing mechanism to be solved during construction, affording species concentration versus time profiles.[1] This quantitative information is then used to determine which species that have not yet reacted are most significant in the growing mechanism by comparing each species' rate of formation to a minimum specified rate. Species whose rates of formation exceed this minimum rate are next allowed to react.

In order to quantify the rates of formation of the unreactive species and therefore determine which species will be allowed to react next, the species balance equations must be combined with the appropriate reactor design equations and the model must be solved. It is likely that the rates of formation of unreactive species will change dramatically as reaction proceeds. Therefore, an approach that iterates over the independent variable of the reactor of interest has been adopted. The following discussion will focus on a batch reactor in which the controlling variable is time. First, the user-specified total reaction time is divided into smaller subintervals. The total reaction time is not divided evenly; rather, greater weighting is given to early times where species concentrations and rates of formation change rapidly. Choice of reaction time as the controlling iteration variable differs from the approach in previous work,[1] where intervals of reactant conversion were used. The current approach is more general in that it can easily be applied to systems with many reactants and, hence, many different reactant conversions, without ambiguity. Furthermore, it more accurately reflects the current dynamics of systems in which reactants quickly reach equilibrium or which have a very slow rate of reactant conversion.

Once the total reaction time has been discretized, the model equations are integrated to the end of the first subinterval, and a characteristic rate of change for the system, R_{char}, is calculated. In previous work, R_{char} was based upon the amount of the reactant converted over the time required to achieve that conversion.[1] However, this approach does not necessarily capture the rate of change of the most dynamic species in the system and, again, is not easily applied to systems with more than one reactant. In this work, the characteristic rate of the system was defined as:

$$R_{char} = \max\left(\left|r_i\right|\right)$$

where r_i is the net rate of formation of species i, and the function max selects the largest absolute value of r_i from the set of all r_i for *reactive* species over the full interval of integration.

Once R_{char} has been calculated, the minimum rate of formation for a species to be considered reactive, R_{min}, is calculated:

$$R_{min} = \varepsilon R_{char} \quad , \quad \varepsilon > 0$$

where ε is a user-defined threshold. The list of unreactive species is then inspected, and the species with the largest rate of formation, $r_{i,max}$, is selected. If $r_{i,max}$ is greater than R_{min}, species i is added to the reactive species list. The new reactive species is then subjected to the reaction rules, and all of the possible reactions for the new species are generated. The new model is solved, and the R_{char}, R_{min}, and $r_{i,max}$ values are recalculated. This iterative procedure continues until $r_{i,max}$ is less than R_{min}. At this point, the algorithm proceeds to the next time subinterval and the entire process is repeated. The process terminates after the last subinterval has been traversed.

As noted above, this procedure is similar to that employed by Susnow et al.,[1] with two major differences: 1) time, rather than reactant conversion, is used to control model building and 2) the

characteristic rate of change in the system, R_{char}, is defined more broadly. As noted above, the discretization of time is a more generally applicable approach. Furthermore, by basing R_{char} on the most dynamic species in the system rather than on the rate of disappearance of a single reactant, there is a reduction in the quantity of species which are deemed reactive, and thus the overall size of the mechanism can be more easily controlled.

Rate Constant and Thermochemical Property Estimation. To employ the rate-based generation criterion during model construction, it is essential to have reliable estimates of the reaction rates in the mechanism. In this work, a hierarchical approach is employed to calculate rate parameters for all reactions generated during the construction of the rate-based mechanism. During model generation, all reactions created are first compared to a user-defined rate constant library containing specific reactions and their respective Arrhenius parameters. If a generated reaction exists in this library, the appropriate rate constant parameters from the library are assigned within the model. If experimental data for particular reactions are not available, a combination of linear free energy relationships (LFERs) and thermodynamic data is used to estimate the rate parameters. In particular, the Evans-Polanyi relationship, a specific LFER, is used to estimate rate constants for forward reactions, while the reverse rate constants are constrained by reaction thermodynamics. The Evans-Polanyi relationship relates the activation energy, E_a, to the heat of reaction, ΔH_{rxn}, through a linear relationship, where E_0 (intercept) is an intrinsic barrier to reaction, and α (slope) is the reaction transfer coefficient. E_0 and α are assumed to be constant within a particular reaction family. Once the activation energy has been estimated, the overall rate constant as a function of temperature for the reaction is calculated assuming the Arrhenius relationship. It is assumed that each reaction family has a single Arrhenius frequency factor.

Once rate constants for forward reactions, k_f, are calculated, equilibrium data and the definition of the equilibrium constant, K_p, are used to calculate the rate constants for the corresponding reverse reactions, k_r. This approach differs from previous implementations of NetGen in which thermodynamic consistency was not strictly enforced. K_p can be calculated from the change in Gibbs free energy upon reaction, ΔG_{rxn}, using the definition of the equilibrium constant. As a new species is generated within the reaction mechanism, the NIST Structures and Properties thermochemical database[6] is searched to determine if experimentally-derived properties are tabulated. If experimental values are unavailable, a group additivity method is applied to estimate the species' thermochemical properties.[7] If this approach fails, properties are calculated using MOPAC, a semi-empirical computational chemistry package.[8,9]

Application of the Rate-Based Generation Algorithm. A mechanism for low pressure tetradecane pyrolysis was generated to determine the effectiveness of the adapted rate-based generation algorithm. This reaction system was chosen since it would compliment experimental work which has been conducted in our laboratory.[10] Low pressure batch pyrolysis studies of tetradecane were conducted at 420°C in 3.1 ml pyrex cryules. Reactant loadings ranged from 6.2 to 27.8 mg (1.01×10^{-2} to 4.53×10^{-2} M) with reaction times varying between 10-150 minutes. This reaction system would serve as an adequate test for the rate-based generation criterion since thermolysis of a long chain paraffin can lead to thousands of intermediates and stable products. However, only a small fraction of these are actually kinetically significant. The final mechanism generated was used to determine a measure of the controlling kinetic rate parameters, and then this information was subsequently used for model predictions of reactant conversions and product yields for varying reactant loadings.

For gas-phase hydrocarbon pyrolysis at moderate temperatures, six important reaction families, as summarized in Table 1, were identified. The reaction mechanism in this study was generated using estimates of the Arrhenius frequency factors, E_0, and α for each reaction family from the literature. The model was constructed using an initial tetradecane concentration of 3.22×10^{-2} M (20.0 mg) and a reaction temperature of 420°C. The most robust model constructed using rate-based building was obtained when $\varepsilon = 5.0 \times 10^{-5}$ and included a total of 16,269 species with 477,566 reactions. The rate-based criterion reduced this to only 302 reactive species with 98,240 reactions.

Determination of Rate Parameters and Predictive Capabilities. Experimental data from 20.0 mg pyrolysis reactions of tetradecane conducted at 420°C and 450°C were used to determine controlling rate

parameters. The different parameters which *could* be varied in the mechanism are shown in Table 1. However, only the parameters in bold type were fit using experimental data, while all other variables were set constant. As can be seen in the table, only frequency factors were permitted to vary, while all activation energies and transfer coefficients were set based upon literature values. It should be noted that final optimized values for the frequency factors were consistent with literature values for the respective reaction families.

A parity plot comparing the fitted model yields to the experimentally observed yields for major and minor products employing the parameters in Table 1 is shown in Figure 1. The model did an excellent job of fitting the experimental data from the pyrolysis reactions over several orders of magnitude. The majority of the variance was attributed to differences between fitted and experimental values for long chain *n*-alkanes, which were only minor products. It is not easily discernible in Figure 1, but reactant conversions for both temperatures were fit extremely well using this mechanism. Also, major products which were formed in higher yields, including gaseous hydrocarbons and α-olefins, were fit very well. It should be reiterated that the parameters used were fit using data from two temperatures, but there were no adjustments made to the activation energies.

Once appropriate rate parameters were obtained, the predictive capabilities of the model were assessed. In particular, the ability of the model to predict reactant conversions and product yields for varying reactant loadings was investigated. The results which follow are truly predictions, i. e., no adjustments were made to the rate parameters fitted to the 20.0 mg pyrolysis reactions. A comparison of predicted and experimental conversions for tetradecane pyrolysis for different initial reactant loadings is shown in Figure 2. The experimental conversions for initial reactant loadings of 6.2 and 27.8 mg of tetradecane are shown as symbols, while each respective model prediction is shown using lines. The mechanistic model was able to accurately predict the trends in the experimental conversions and estimate the actual conversion values reasonably well.

As a representative example of the ability to predict product yields, a comparison of the predicted and experimental evolution of propylene as a function of reactant conversion and reactant loading is shown in Figure 3. The model was able to accurately predict both the trends in the data as well as the actual values over both a wide range of conversions and reactant loadings. These observations were consistent with those for other gaseous hydrocarbons and long chain α-olefins.

Overall, the mechanistic model was able to accurately predict reactant conversions and product yields for varying reactant loadings employing rate parameters optimized to independent reaction sets. The model was able to predict the correct behavior for product trends for different reaction conditions such as the relative α-olefin/paraffin ratio for varying reactant loadings.

Acknowledgment. The authors are grateful for financial support from the United States Department of Energy, Grant DE-FG22-96-PC96204.

References

(1) Susnow, R. G.; Dean, A. M.; Green, W. H.; Peczak, P.; Broadbelt, L. J., *Phys. Chem. A,* **1997**, *101(20)*, 3731-3740.
(2) Broadbelt, L. J.; Stark, S. M.; Klein, M. T., *I. & E. C. Res.* **1994**, *33(4)*, 790-799.
(3) Broadbelt, L. J.; Stark, S. M.; Klein, M. T., *I. & E. C. Res.,* **1995**, *34(8)*, 2566-2573.
(4) Broadbelt, L. J.; Stark, S. M.; Klein, M. T., *Comp. & Chem. Eng.,* **1996**, *20(2)*, 113-129.
(5) Klinke, D. J. I.; Broadbelt, L. J., *AIChE Journal* , **1997**, *43(7)*, 1828-1837.
(6) Stein, S. E. (1994). NIST Structures & Properties version 2.0. Gaithersburg, MD.
(7) Benson, S. W. (1976). Thermochemical Kinetics. New York, Wiley-Interscience.
(8) Stewart, J. J. P. (1990). MOPAC Reference Manual and Release Notes. Frank J. Seiler Research Laboratory: United States Air Force Academy, CO.
(9) Stewart, J. J. P., In *Reviews in Computational Chemistry* ; Lipkowitz, K. B., Boyd, D. B., Eds.; VCH Publishers, Inc.: New York, 1990.
(10) De Witt, M. J.; Broadbelt, L. J., *Energy & Fuels,* **1999**, *Submitted*.

Table 1: Input parameters for model of low-pressure tetradecane pyrolysis
(values in bold type were optimized using experimental data).

Reaction Family	**A**	**E_0**	α
Bond Fission	**4.8×10^{16}**	0.0	1.0
β-Scission	**5.8×10^{12}**	14.24	0.5
Radical Addition	**1.0×10^{7}**	14.24	0.5
Radical Recombination	**1.0×10^{7}**	0.0	0.0
Intermolecular H-Abstraction			
R•	**5.0×10^{7}**	13.3	0.7/0.3
H•	1.0×10^{11}	13.3	endo/exo
Intramolecular H-Abstraction			
1,4-shift	**4.9×10^{10}**	21.0	0.5
1,5 or 1,6-shift	**4.9×10^{9}**	12.0	0.5
Disproportionation	1.0×10^{9}	0.0	0.0

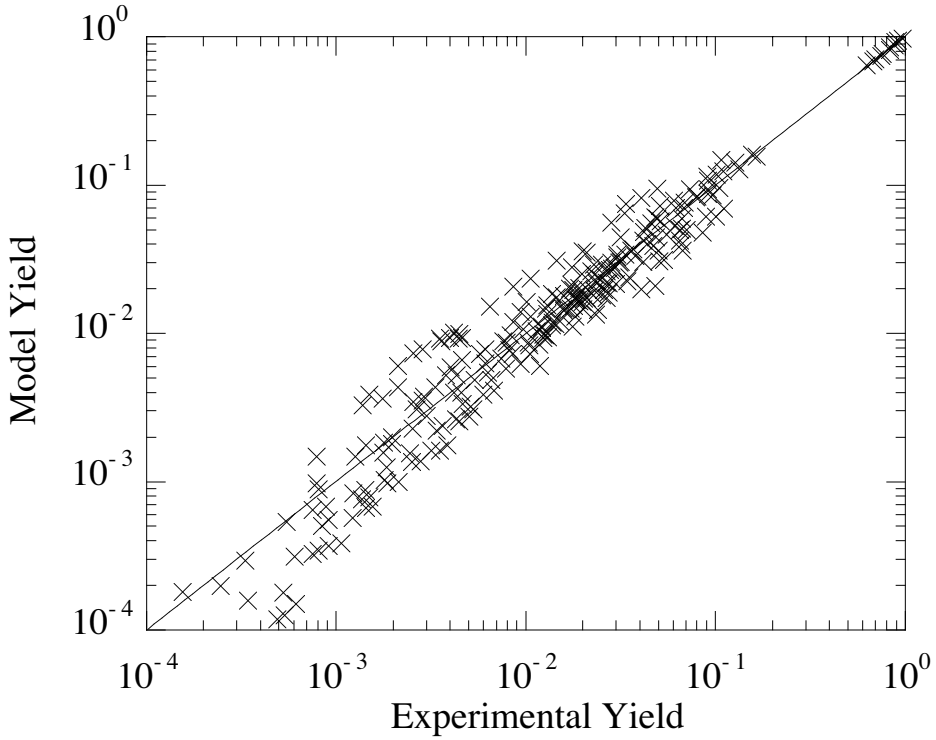

Figure 1: Comparison of fitted model yields and experimentally observed yields for major and minor products of tetradecane pyrolysis employing the parameters listed in Table 1.

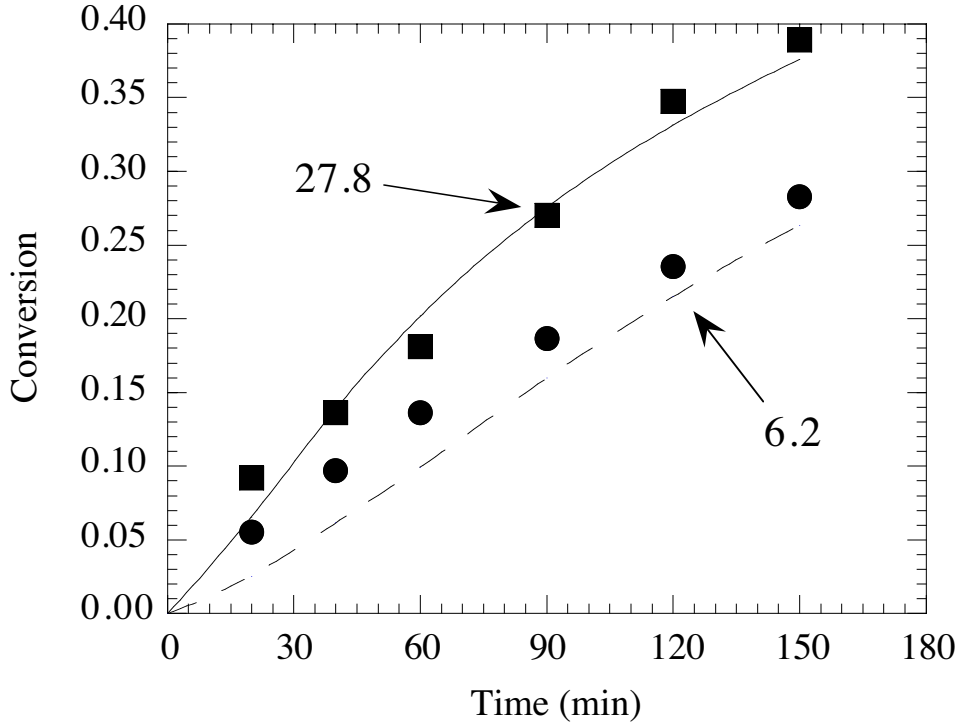

Figure 2: Comparison of experimental (symbols) and predicted (lines) conversions of tetradecane for initial tetradecane loadings of 6.2 and 27.8 mg.

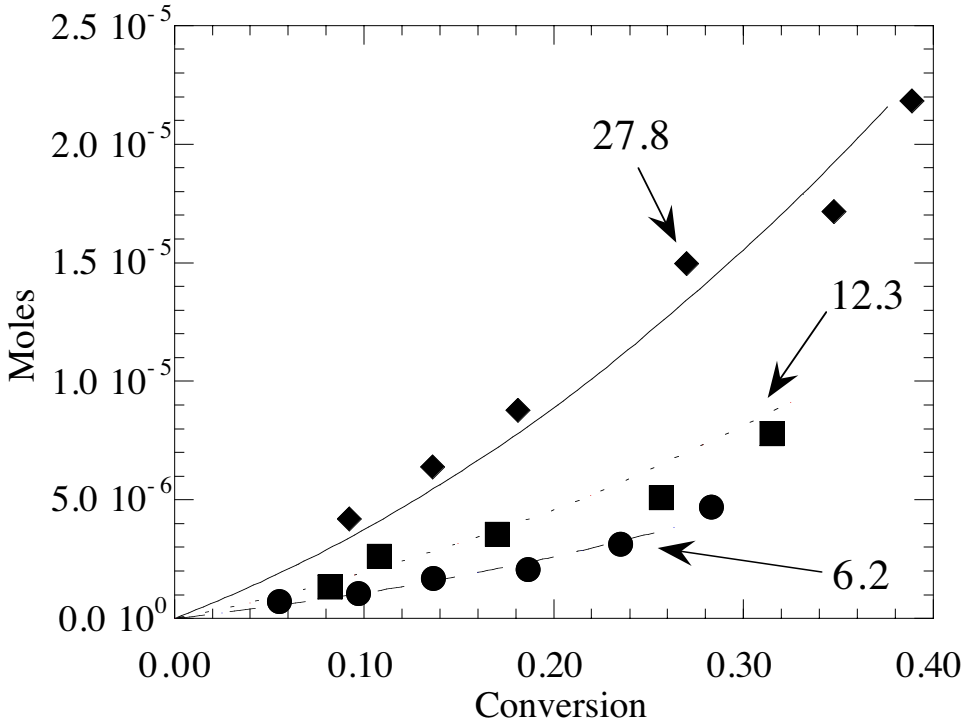

Figure 3: Comparison of the experimental (symbols) and predicted (lines) evolution of propylene for initial tetradecane loadings of 6.2, 12.3, and 27.8 mg.